Role of HtrA2 and its Domains in Regulating its Specificity and Functions

By

Lalith Kumar Chaganti

[LIFE09200804004]

TATA Memorial centre

Mumbai

A thesis submitted to the

Board of Studies in Life Sciences
In partial fulfillment of requirements for the Degree of

DOCTOR OF PHILOSOPHY
of
HOMI BHABHA NATIONAL INSTITUTE
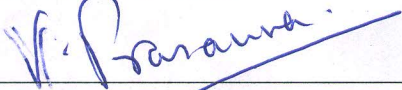

March, 2016

Homi Bhabha National Institute

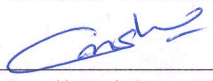## Recommendations of the Viva Voce Committee

As members of the Viva Voce Committee, we certify that we have read the dissertation prepared by Mr. Lalith Kumar Chaganti entitled "Role of HtrA2 and its Domains in Regulating its Specificity and Functions" and recommend that it may be accepted as fulfilling the thesis requirement for the award of Degree of Doctor of Philosophy.
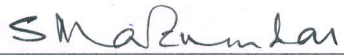
Chairman – Dr. Vinay Kumar   Date: 11/3/2016

Guide / Convener – Dr. Kakoli Bose   Date: 11/8/2016

Examiner- Dr. Patrick D` Silva   Date: 11/03/2016

Member 1 –Dr. Prasanna Venkatraman   Date: 11/03/2016

Member 2- Dr. Murali Krishna Chilakapati   Date: 11/3/2016

Invitee - Dr. Shyamalava Mazumdar   Date: 11/3

Final approval and acceptance of this thesis is contingent upon the candidate's submission of the final copies of the thesis to HBNI.

I hereby certify that I have read this thesis prepared under direction and recommend that it may be accepted as fulfilling the thesis requirement.

Date: 11/03/2016

Place: Navi Mumbai

Dr. Kakoli Bose

Guide

STATEMENT BY AUTHOR

This dissertation has been submitted in partial fulfillment of requirements for an advanced degree at Homi Bhabha National Institute (HBNI) and is deposited in the Library to be made available to borrowers under rules of the HBNI.

Brief quotations from this dissertation are allowable without special permission, provided that accurate acknowledgement of source is made. Requests for permission for extended quotation from or reproduction of this manuscript in whole or in part may be granted by the Competent Authority of HBNI when in his or her judgment the proposed use of the material is in the interests of scholarship. In all other instances, however, permission must be obtained from the author.

Date: 11/3/2016

Lalith Kumar Chaganti

Place: Navi Mumbai

DECLARATION

I, hereby declare that the investigation presented in the thesis has been carried out by me.

The work is original and has not been submitted earlier as a whole or in part for a degree /

diploma at this or any other Institution / University.

Date: 11/3/2016   Lalith Kumar Chaganti

Place: Navi Mumbai

List of Publications arising from the thesis

Journal

1. Intricate structural coordination and domain plasticity regulate activity of serine protease HtrA2. **Chaganti LK**, Kuppili RR, Bose K. *FASEB J* 2013; 27(8):3054-66
2. Allosteric regulation of serine protease HtrA2 through novel non-canonical substrate binding pocket. Bejugam PR, Kuppili RR, Singh N, Gadewal N, **Chaganti LK**, Sastry GM, Bose K. *PLoS ONE* 2013;8(2):e55416. doi: 10.1371

Chapters in books

1. Cathepsins and HtrAs – Multitasking Proteases in Programmed Cell Death. In *Proteases in Apoptosis: Pathways, Protocols and Translational Advances*. **Chaganti LK,** Singh N, Bose K. Ed. Kakoli Bose. Switzerland. **Springer International Publishing, 2015. 95-141**

2. Proteases in Apoptosis: Protocols and Methods. In Proteases in Apoptosis: Pathways, Protocols and Translational Advances. Acharya S, Kuppili RR, **Chaganti LK,** Bose K. Ed. Kakoli Bose. Switzerland. **Springer International Publishing**, 2015. 143-202.

Conferences

- Presented poster entitled "Role of structural plasticity and inter domain contacts in regulating HtrA2 function" by 31st annual convention Indian association of cancer research and international symposium in cancer genomics and its impact in the clinics. Organized by Organized by Advanced Centre for Treatment Research and Education in Cancer, Tata Memorial Centre, Kharghar, Navi-Mumbai, and Maharashtra, India. January 26-29, 2012
- Presented poster in National Symposium on "FRONTIERS OF BIOPHYSICS, BIOTECHNOLOGY & BIOINFORMATICS" & 37th ANNUAL MEETING OF INDIAN BIOPHYSICAL SOCIETY (IBS).Organized by Department of Biophysics & Centre for Excellence in Basic Sciences, University Of Mumbai, Mumbai. January 13-16, 2013
- Presented poster in International Symposium on Conceptual Advances in Cellular Homeostasis Regulated by Proteases and Chaperones the Present, the Future and Impact on Human Diseases. Organized by Advanced Centre for Treatment Research

and Education in Cancer, Tata Memorial Centre, Kharghar, Navi-Mumbai, and Maharashtra, India. December 3-6, 2013

- Presented poster at Biophysics-Pashchim V meeting organized by Tata Institute of Fundamental Research, Mumbai, India
- Presented poster and short talk in Biophysics-Pashchim VI meeting organized by IISER, Pune, India

Others

- Received special prize for best poster presentation by young scientist entitled "Role of structural plasticity and inter domain contacts in regulating HtrA2 function" by 31st annual convention Indian association of cancer research and international symposium in cancer genomics and its impact in the clinics held during Jan 26-29, 2012
- Awarded Professor. K.S. Korgaonkar for the best poster entitled 'Role of Structural Plasticity and Interdomain Crosstalk in Regulating HtrA2 Specificity and Functions' during National Symposium on "FRONTIERS OF BIOPHYSICS, BIOTECHNOLOGY & BIOINFORMATICS" & 37th ANNUAL MEETING OF INDIAN BIOPHYSICAL SOCIETY (IBS) at University of Mumbai, Mumbai, January 13-16, 2013
- Interviewed by Indiabioscience.org for the FASEB J publication, 2013, entitled "Discerning the structure, function and dynamics of proapoptotic protein HtrA2". http://indiabioscience.org/news/discerning-structure-function-and-dynamics-proapoptotic-protein-htra2

Date: 11/3/2016   Lalith Kumar Chaganti

Place: Navi Mumbai

Acknowledgements

I would like to take this opportunity to thank everybody who has supported and guided me through the entire tenure of PhD work.

Foremost, I would like to express my sincere gratitude to my mentor, Dr. Kakoli Bose, for giving me the chance to work on this very interesting project and for all the trust she had in me. Ma'am without your support my Ph.D would have been just remained a dream. In hard times you stood beside me and supported me like a family member. Your persistent guidance, caring, valuable suggestions, critical evaluation helped to maintain stimulation and momentum throughout my PhD tenure. Thanks for being so patient with me and tolerating my ample number of mistakes and correcting me again and again to make me a better researcher and a better person.

I sincerely thank Dr. S. Chiplunkar (Director, ACTREC), Prof. Rajiv Sarin (former Director, ACTREC), Dr. Surekha Zingde (former Dy. Director, ACTREC) for providing me an opportunity to work in this institution. Without your support and encouragement I would have never accomplished my dream.

I owe my sincere thanks to my doctoral committee (DC) members, Dr. Vinay Kumar (BARC), Dr. Prasanna Venktraman (ACTREC), Dr. Murali Krishna Chilakapati (ACTREC), Dr. Shymalava Mazumdar (TIFR), and Dr. Rita Mulherkar (ACTREC, former DC member) for their support, critical analysis of results, insightful comments and valuable suggestions which has helped me to mature into a better researcher.

Dedicated to my beloved parents

CONTENTS

Homi Bhabha National Institute

SYNOPSIS of Ph.D. THESIS

1. Name of the Student: Lalith Kumar Chaganti

2. Name of the Constituent Institution: TMC-ACTREC

3. Enrolment No. LIFE09200804004

4. Title of the Thesis: Role of HtrA2 and its Domains in Regulating its Specificity and Functions

5. Board of Studies: Life Science

Title: Role of HtrA2 and its Domains in Regulating its Specificity and Functions

1. Introduction:

HtrA2 (High Temperature Requirement Protease A2) is a proapoptotic mitochondrial serine protease conserved from prokaryotes to humans (1). The full-length human HtrA2/Omi is a 50 kDa protein with a mitochondrial targeting signal (MTS) at its N-terminal end, a transmembrane domain(TM), Inhibitor of Apoptosis Proteins (IAPs) binding motif, a serine protease domain and a PDZ domain (2). The N-terminal 133 residues are cleaved after its release from mitochondria, there by generating a 36 kDa active form (3-6).

HtrA2 plays an important role in intrinsic apoptotic pathway by binding and cleaving IAP proteins thus relieves the inhibition on caspases (2). HtrA2, via its serine protease activity, induces caspase independent pathway by regulating the antiapoptotic proteins such as FLIP (7), Ped/Pea15 (8) and Hax1(9). This unique property has made it an interesting therapeutic target where caspase activation is prevented or inhibited.

Crystallographic data of mature substrate unbound from of HtrA2 provided only the broad overview of its structural organization (10). It has a trimeric pyramidal architecture with the short N-terminal region form the top and the PDZ domains are located at the bottom of the structure. The core serine protease domains (SPD) are surrounded by C-terminal PDZ domains which restrict entry of the substrates to the active-site leading to a low basal activity. PDZ is attached covalently to the SPD through a flexible interface linker sequence and it is believed that the PDZ-protease dynamics and their relative orientation modulate HtrA2 activity and hence functions. These observations led to development of an activation model, which highlights the

role of PDZ in substrate binding and subsequent protease activation (10). The model states that upon substrate binding, the PDZ that otherwise falls on the protease domain opens up allowing the substrate to enter the binding pocket. Although the model provides a basic understanding of HtrA2 activation, it could neither satisfactorily define the roles of trimerization and N-terminal region in HtrA2 functions nor decipher the dynamics of PDZ-protease crosstalk as electron density for both the linker and part of the N-terminal is not available in the structural data. Therefore, to understand mode of HtrA2 activation, intricate dissection of its structure with functional correlation is required.

Aims and Objectives:-

1. Characterization of structural properties and conformational stability of HtrA2 and the role of its different domains in protein function and specificity. Aim 1 is further divided into the following sub headings

a) Importance of trimerization for HtrA2 activity

b) Role of different domain coordination, critical residues involved and interdomain dynamics in regulating substrate specificity and activity

2. To understand the interaction of proapoptotic serine protease HtrA2 with antiapoptotic binding partner cum substrate–Pea 15

2. Materials and methods:

Using structure-guided design, molecular biology and protein biochemistry various combinations of HtrA2 and Pea15 mutants were obtained. Recombinant proteins were expressed and purified using different chromatography techniques including affinity and size-exclusion, and their percentage purity was determined using SDS-PAGE. Conformational changes and stability were

characterized using spectroscopic tools, while functional studies were delineated using enzymology studies.

Results and discussion:

3.1 Characterization of structural properties and conformational stability of HtrA2 and the role of its different domains in protein function and specificity

3.1.1. Importance of trimerization for HtrA2 activity:

i. Construction of different HtrA2 variants

Different mutants and variants of HtrA2 were generated to understand the role of critical residues and contributions from different domain combinations in maintaining its overall structural integrity and functions. N-SPD (trimeric protein without PDZ inhibition), SPD (without N-terminal and PDZ domain), monomeric HtrA2(F16D) (which is reported monomeric in the literature), N-SPD(F16D) (monomeric mutant without PDZ inhibition) and SPD-PDZ (should mimic monomeric mutant without N-terminal) have been cloned and purified. Since HtrA2 protein sequence does not contain any tryptophan residue, single tryptophan mutants were generated one in the protease domain (N48W) and another in the PDZ domain (Y295W) respectively to monitor and compare the environment surrounding the tryptophan in these proteins spectroscopically. HtrA2(M190R) mutant was introduced in serine protease domain, which is supposed to negatively affect the activity by disrupting the interdomain contacts as suggested by existing activation model of HtrA2 (10).

ii. Requirement of N-terminal for oligomerisation

Oligomeric properties of HtrA2 variants were determined using gel filtration chromatography. HtrA2 (wild type) and N-SPD are trimers with intact N-terminal region. HtrA2(F16D), N-SPD(F16D) and SPD-PDZ represents monomers highlighting the importance of N-terminal and F16 in particular for homotrimerization of HtrA2 as suggested by the literature (10).

iii. Protease assays

Protease activity of HtrA2, its variants and mutants was studied to understand the role of different domains in regulating HtrA2 activity and specificity using β-casein (known substrate of HtrA2) and FITC-labeled β casein-fluorogenic substrate. Wild type, N-SPD, HtrA2(M190R) cleaved β casein while monomeric mutants showed less activity than trimers. This highlights the importance of trimerization in HtrA2 activity. SPD and SPD-PDZ that do not have N-terminal region showed lesser activity compared to their full-length monomeric counterparts. This highlights the importance of N-terminal in formation of proper active-site conformation. HtrA2 and HtrA2(M190R) showed similar substrate binding affinity (K_m) however, the catalytic efficiency for HtrA2(M190R) is ~4 folds higher than the wild-type suggesting presence of a more catalytically competent active-site. In N-SPD variant, slight decrease in K_m value, which is representative of increase in substrate affinity, suggests greater substrate accessibility that might be due to absence of the surrounding PDZ domains. However, N-SPD showed 3.5 folds less k_{cat} than wild type, this highlights the importance of PDZ in initial substrate binding and mediating conformational changes around the active-site that positively influences the rate of catalysis.

3.1.2. Role of different domain coordination, critical residues involved and interdomain dynamics in regulating substrate specificity and activity

---

i. Protease activity as a function of temperature

Literature suggests heat activation of HtrA2 is associated with considerable plasticity at the PDZ-protease interface, which is similar to substrate binding (11). Thus, quantitative analysis of activity of HtrA2 and its variants was performed as a function of temperature to understand how change in activity correlates with conformational changes and dynamic behaviour of HtrA2. Initial velocities were calculated for HtrA2, HtrA2(F16D) and N-SPD domain using FITC β-casein as substrate in the temperature range of 37-65 °C. For HtrA2, initial velocity increased linearly up to 55 °C. Activity of HtrA2 was approximately 5-fold higher at 55 °C than that at 30 °C. Monomeric mutant HtrA2(F16D) and trimeric N-SPD show maximum activity at 50 °C. In both these proteins, increase in activity was observed although the change is not significant (~ 1.7and ~1.2 fold higher than that at 37 °C. This decrease in protease activity for N-SPD and might be due to loss of PDZ-protease movement. HtrA2(F16D), which is a monomer with intact PDZ, no significant change in enzyme activity, was observed as a function of temperature hinting the role of intermolecular PDZ-protease crosstalk in HtrA2 activation.

ii. Secondary and tertiary structural properties of HtrA2 variants

Far UV CD studies were performed to understand the effect of deletions and mutations on HtrA2 secondary structure and stability. All proteins except N-SPD and N-SPD(F16D) showed decrease in α helical character, which might be due to PDZ deletion.

Fluorescence emission studies were performed for all the tryptophan mutants (Y296W and N48W) of HtrA2 to characterize the tertiary structural changes at the PDZ-protease interface, and near the active-site region. The two monomeric variants HtrA2(F16D,Y295W), SPD-PDZ(Y295W) and packing mutant M190R(Y295W) showed red-shifted emission maxima (by

2nm) compared to trimeric HtrA2(Y295W) demonstrating that PDZ of the same molecule might not be completely collapsing on the SPD domain as suggested by the model (3).

iii. Fluorescence quenching studies

Steady state acrylamide quenching studies were performed with tryptophan mutants (Y296W and N48W) to understand the conformational dynamics at the PDZ-protease interface, and the region surrounding the active-site. Stern Volmer quenching constant (K_{SV}) values were calculated for these tryptophan mutants in the temperature range of 30 °C to 60 °C. For HtrA2(Y295W) and HtrA2(M190R,Y295W), increase in K_{SV} values were observed with temperature till 60ºC. This increase in K_{SV} values suggest that PDZ might be moving away from serine protease domain, making the protease more accessible to the substrate thus increasing the protease activity.

   K_{SV} values for HtrA2(N48W) decreased gradually with temperature while for monomeric HtrA2(F16D) and N-SPD(F16D) as well as trimeric N-SPD, it remained unchanged. In both trimeric and monomeric N-SPD, similar observation emphasizes the importance of intermolecular PDZ-protease interactions in HtrA2 activation. All these observations point toward requirement of trimeric architecture of the protease for structural plasticity as well as accentuate the role of intermolecular PDZ-protease interaction in regulating HtrA2 activity.

vi. Intramolecular and intermolecular FRET studies

Förster rresonance energy transfer experiments (FRET) were done using IAEDANS (fluorescent molecule) as acceptor and tryptophan (296W) as donor to validate our hypothesis that intramolecular PDZ-protease collapse is not significant in HtrA2. IAEDANS is an

organic fluorophore where its absorption spectrum overlaps well with the emission spectrum of tryptophan making it useful as an acceptor in FRET experiments. Structure guided mutation, F208C was done in the serine protease domain on HtrA2(Y295W) template. These FRET pairs were chosen such that they face each other and reside near the PDZ-protease linker region. Energy transfer in HtrA2(F208C,Y295W) is more than HtrA2(F16D,F208C,Y295W) and HtrA2(M190R,F208C,Y295W). This suggests that distance between F208C and Y295W is less in HtrA2 compared to HtrA2(F16D) and HtrA2(M190R) thus supporting our hypothesis. With increase in temperature distances 'R' between the acceptor and donor for HtrA2(F208C,Y295W) and M190R(Y295W) increased, suggesting PDZ might be moving away from serine protease domain.

Based on all these observations we propose a comprehensive working model of HtrA2 activation. In full length trimeric HtrA2, initial substrate binding or increase in temperature leads to movement of PDZ from other sub unit move towards SPD of adjacent molecule. This intermolecular movement along with simultaneous N-terminal rearrangement leads to subtle reorganization of the loops to form an active protease.

3.2. To understand the interaction of proapoptotic serine protease HtrA2 with antiapoptotic binding partner cum substrate–Pea 15

Pea15 is a 15 kDa ubiquitously expressed cytosolic protein with an N-terminal death effector domain (DED) and a C-terminal tail having irregular structure (12). Pea15 by virtue of its DED binds to other DED-containing proteins such as FADD and FLICE, and inhibits Fas/TNFR1-induced apoptosis (8). Stress induced activated HtrA2 interacts with the cytosolic Pea15 and promotes its degradation which leads to triggering of apoptosis (8). Therefore, characterizing this

HtrA2-Pea15 interaction will provide better understanding of HtrA2 proapoptotic property and also its complex mechanism of action.

i. HtrA2 protease domain preferably interacts with α -5 and -6 helices of Pea15

To determine the minimal binding region of HtrA2-Pea15 interaction, pull down studies were performed with MBP fused recombinant Pea15 as bait and HtrA2 inactive (S173A) variants as prey. HtrA2 variants used for these studies were HtrA2 full length, N-SPD (PDZ deleted variant) and PDZ domain (protease domain deleted variant). From these pull down experiments we analyzed that serine protease domain of HtrA2 interacted with Pea15. Further to define the region responsible for the interaction of Pea15 with HtrA2, different deletion constructs of Pea15 were used for pull down studies. From these data, we determined that HtrA2 protease domain preferably interacts with α-5 and -6 helices of Pea15 DED domain. Interestingly DED, which has the tendency to interact with several proteins showed very weak interactions with HtrA2, highlighting the importance of C-terminal region in addition to DED for binding. Taking clues from our pull down experiments and Cluspro docking results, we further carried out series of mutations on α-5 and -6 helices of DED and C- terminal region of Pea15. We identified that E68, R71, R83 residues are important in mediating interaction with HtrA2.

ii. Cleavage of Pea15 is independent of HtrA2 PDZ domain

Protease activity of HtrA2 and its variant N-SPD was studied to understand the role of different domains in regulating HtrA2 activity and specificity using Pea15 as a substrate. It was observed that N-SPD cleaved pea15 more competently than full length HtA2. These results suggest that lower protease activity for HtrA2 wild-type might be due to inhibitory effect of PDZ domain on

its protease activity, probably through restriction of substrate accessibility to the active-site. Protease assays were also performed with the deletion constructs of Pea15 and, we observed that HtrA2 and N-SPD cleaved all deletion constructs except Δα(5,6). These protease assay results very well corroborates with the pull down studies where Δα(5,6) did not show any interaction with HtrA2. Further to understand the pattern of pea15 cleavage, time course protease degradation was performed. It was observed that Pea15 which is of ~ 17 kDa is proteolytically degraded into two 8.5 kDa fragments. One of these 8.5 kDa is subsequently degraded to 6.5 kDa and other in to shorter peptides, which were not detected on tristricine gel.

iii. Mapping HtrA2 cleavage sites on Pea15

The pea15 fragments (8.5 and 6.5 kDa) generated by HtrA2 proteolysis were subjected to N-terminal sequencing by Edman degradation. Two preferred cleavage sites were identified in α-5 and -6 helices of DED domain respectively. The preferred scissile peptide bonds are between I63-E64 of -5 helix and V79-D80 of -6 helix.

vi. HtrA2 has broad specificity toward residues neighboring the peptide cleavage site

The literature regarding the HtrA2 substrate specificity is limited to only two published reports, one by combinatorial peptide library (11) and other proteome analysis (13) however, both the results do not match each other in full. To determine whether the specificity of the HtrA2 corresponds with the reported literature, we generated several mutants of P2, P1, P1' and P2' cleavage site residues. Our results based on the N-terminal sequencing and mutational analysis of cleavage site residues showed HtrA2 displays relatively broad specificity towards the P1 site. Although both the reports suggests HtrA2 has preference towards aliphatic residues in P1

position, our studies indicated that polar (D) and aromatic (F) are also equally preferred at P1. In contrast to the previous reports for selectivity for A and S at P1', our results from N-terminal sequencing demonstrate striking preference for E and D at the P1'. Literature suggests P2 prefers basic (R) and aliphatic (L) residues while P2' position displays preference for aromatic (F) residues. In contrast, our data indicates acidic residues (D), are also preferred equally at P2 and P2'.This apparent ambiguity in cleavage site specificity between peptide and protein substrates of HtrA2 may reflect the involvement of additional structural elements in the protein substrates that might interact with the protease and influence its topological targeting and enzymatic activity.

4. Concluding remarks:

Our findings highlight importance of N-terminal region, oligomerization and intricate intermolecular PDZ-protease interaction in proper formation, enzyme-substrate complex stabilization, and hence HtrA2 functions. These observations redefine the existing activation model and provide new insights into HtrA2 structure, function and dynamics.

In this study we also provided the first comprehensive binding and specificity studies on HtrA2-Pea15 interaction. Our i*n vitro* pull down and *in silico* docking studies showed that Pea15 interacts with serine protease domain of HtrA2 and *NOT* the conventional PDZ domain. Protease activity studies delineated allosteric activation of HtrA2 might be required by adaptor proteins in the cell to relieve the inhibitory effect of PDZ domain.

References

1. Lipinska, B., Fayet, O., Baird, L., and Georgopoulos, C. (1989) Identification, characterization, and mapping of the Escherichia coli htrA gene, whose product is essential for bacterial growth only at elevated temperatures. *J Bacteriol* **171**, 1574-1584.

2. Wu, G., Chai, J., Suber, T. L., Wu, J.-W., Du, C., Wang, X., and Shi, Y. (2000) Structural basis of IAP recognition by Smac/DIABLO. *Nature* **408**, 1008-1012

3. Suzuki, Y., Imai, Y., Nakayama, H., Takahashi, K., Takio, K., and Takahashi, R. (2001) A serine protease, HtrA2, is released from the mitochondria and interacts with XIAP, inducing cell death. *Mol. Cell.* **8**, 613-621.

4. Hegde, R., Srinivasula, S., Zhang, Z., Wassell, R., Mukattash, R., Cilenti, L., DuBois, G., Lazebnik, Y., Zervos, A., Fernandes-Alnemri, T., and Alnemri, E. (2002) Identification of Omi/HtrA2 as a mitochondrial apoptotic serine protease that disrupts inhibitor of apoptosis protein-caspase interaction. *J Biol Chem* **277**, 432-438.

5. Martins, L., Iaccarino, I., Tenev, T., Gschmeissner, S., Totty, N., Lemoine, N., Savopoulos, J., Gray, C., Creasy, C., Dingwall, C., and Downward, J. (2002) The serine protease Omi/HtrA2 regulates apoptosis by binding XIAP through a reaper-like motif. *J Biol Chem* **277**, 439-444.

6. Verhagen, A., Silke, J., Ekert, P., Pakusch, M., Kaufmann, H., Connolly, L., Day, C., Tikoo, A., Burke, R., Wrobel, C., Moritz, R., Simpson, R., and Vaux, D. (2002) HtrA2 promotes cell death through its serine protease activity and its ability to antagonize inhibitor of apoptosis proteins. *J Biol Chem* **277**, 445-454.

7. Bhuiyan, M. S., and Fukunaga, K. (2007) Inhibition of HtrA2/Omi ameliorates heart dysfunction following ischemia/reperfusion injury in rat heart in vivo. *European Journal of Pharmacology* **557**, 168-177

8. Trencia, A., Fiory, F., Maitan, M., Vito, P., Barbagallo, A., Perfetti, A., Miele, C., Ungaro, P., Oriente, F., Cilenti, L., Zervos, A., Formisano, P., and Beguinot, F. (2004) Omi/HtrA2 promotes cell death by binding and degrading the anti-apoptotic protein ped/pea-15. *J Biol Chem.* **279**, 46566-46572.

9. Cilenti, L., Soundarapandian, M., Kyriazis, G., Stratico, V., Singh, S., Gupta, S., Bonventre, J., Alnemri, E., ., and AS., Z. (2004) Regulation of HAX-1 anti-apoptotic protein by Omi/HtrA2 protease during cell death. *J Biol Chem.* **279**, 50295-50301.

10. Li, W., Srinivasula, S., Chai, J., Li, P., Wu, J., Zhang, Z., Alnemri, E., and Shi, Y. (2002) Structural insights into the proapoptotic function of mitochondrial serine protease HtrA2/Omi. *Nat. Struct. Biol.* **9**, 436-441.

11. Martins, L., Turk, B., Cowling, V., Borg, A., Jarrell, E., Cantley, L., and Downward, J. (2003) Binding specificity and regulation of the serine protease and PDZ domains of HtrA2/Omi. *J Biol Chem.* **278**, 49417-49427.

12. Hill, J., Vaidyanathan, H., Ramos, J., Ginsberg, M., and Werner, M. (2002) Recognition of ERK MAP kinase by PEA-15 reveals a common docking site within the death domain and death effector domain. *EMBO J.* **21**, 6494-6504.

13. Vande Walle, L., Van Damme, P., Lamkanfi, M., Saelens, X., Vandekerckhove, J., Gevaert, K., and Vandenabeele, P. (2007) Proteome-wide Identification of HtrA2/Omi Substrates. *Journal of Proteome Research* **6**, 1006-1015

Publication in Refereed Journal:

a. **Published:**

1. **Chaganti LK**, Kuppili RR, Bose K, Intricate structural coordination and domain plasticity regulate activity of serine protease HtrA2. *FASEB J* 2013; 27(8):3054-66

2. Bejugam PR, Kuppili RR, Singh N, Gadewal N, **Chaganti LK**, Sastry GM, Bose K, Allosteric regulation of serine protease HtrA2 through novel non-canonical substrate binding pocket *PLoS ONE* 2013;8(2):e55416. doi: 10.1371

b. **Accepted**: NA

c.**.** **Communicated**: NA

d. **Other Publication**: NA

e. **Conference presentations:**

1. Presented poster entitled "Role of structural plasticity and inter domain contacts in regulating HtrA2 function" by 31st annual convention Indian association of cancer research and international symposium in cancer genomics and its impact in the clinics held during Jan 26-29, 2012

2. Presented poster entitled 'Role of Structural Plasticity and Interdomain Crosstalk in Regulating HtrA2 Specificity and Functions' during National Symposium on "FRONTIERS OF BIOPHYSICS, BIOTECHNOLOGY & BIOINFORMATICS" & 37th ANNUAL MEETING OF INDIAN BIOPHYSICAL SOCIETY (IBS) at University of Mumbai, Mumbai, January 13-16, 2013

3. Presented poster entitled "Discerning the molecular mechanism of HtrA2-Pea15 interaction" in International Symposium on Conceptual Advances in Cellular Homeostasis Regulated by Proteases and Chaperones the Present, the Future and Impact on Human Diseases. Organized by Advanced Centre for Treatment Research and Education in Cancer, Tata Memorial Centre, Kharghar, Navi-Mumbai, and Maharashtra, India. December 3-6, 2013

Signature of Student *Ch. Lalithkumar*   Date: 6/4/15

Doctoral Committee:

S. No.	Name	Designation	Signature	Date
1.	Dr. Vinay Kumar	Chairman		7/4/2015
2.	Dr. Kakoli Bose	Guide & Convener		6/4/15
4.	Dr. Prasanna Venkatraman	Member		9/4/15
5.	Dr. Murali Krishna Chilakapati	Member		6/4/15
7.	Dr. Shyamalava Mazumdar	Technology Adviser/ invitee		7/4/015

Forwarded through:

S. Chiplunkar
6/5/15

Dr. S.V. Chiplunkar
Director ACTREC
Chairperson,
Academic & Training Programme

Dr. S. V. Chiplunkar
Director
Advanced Centre for Treatment, Research &
Education in Cancer (ACTREC)
Tata Memorial Centre
Kharghar, Navi Mumbai 410210.

Dr. K. Sharma
Director, Academics
T.M.C.

PROF. K. S. SHARMA
DIRECTOR (ACADEMICS)
TATA MEMORIAL CENTRE
PAREL, MUMBAI

LIST OF ABBREVIATIONS

APAF1   Apoptotic protease-activating factor 1

BIR   Baculoviral IAP repeat BPV Bovine papillomavirus

CD   Circular dichroism

cFLIP   Cellular FLICE-like inhibitory protein

DD   Death domain

DED   Death effector domain

DISC   Death-inducing signaling complex

DMSO   Dimethyl sulfoxide

E.coli   Escherichia coli

EDTA   Ethylene diamine tetraacetic acid

FADD   Fas associated death domain

FITC   Fluorescein isothiocyanate

GST   Glutathione S-transferase

HEK   Human embryonic kidney

HtrA   High temperature requirement A

IAP   Inhibitor of apoptosis protein

IBM   IAP-binding motif

IGFBP   Insulin growth factor binding domain

IMS   Intermembrane space

IPTG   Isopropyl β-D-1-thiogalactopyranoside

KI   Kazal-type S protease inhibitor domain

MBP   Maltose binding protein

MRE   Mean residual ellipticity

NES   Nuclear export signal

OMP   Outer membrane porins ORF Open reading frame

PCR   Polymerase chain reaction

PDB   Protein Data Bank

PDZ   Postsynaptic density protein 95-Discs large-Zona occuldens 1

PEA-15   Phosphoprotein enriched in astrocytes-15

SDS   Sodium dodecyl sulphate

PAGE   Polyacrylamide gel electrophoresis

List of figures

List of tables

Chapter 1

Introduction

Programmed cell death or apoptosis plays a critical role in the development and homeostasis of normal tissues (14). It contributes in selective clearance of unwanted or infected cells to maintain the healthy balance between cell survival and cell death (15-21). Alteration of this process may lead to the deadly disease conditions such as cancer and neurodegenerative disorder (16, 22-27). During apoptosis, activation of specific proteases results in breakdown of cellular machinery, which finally culminates into characteristic morphological and biochemical changes, and hence death (28, 29). For many years, it was believed that caspases were the key effectors responsible for the proteolytic cascade in apoptosis (30). However, accumulating evidences indicate that cell death can occur in a programmed manner independent of caspase activation (31). Recently, HtrAs (high temperature requirement protease A), have drawn attention as key players in initiation and execution of the apoptotic cascade. HtrA family proteins are serine proteases (S1, chymotrypsin family) that are conserved from prokaryotes to humans (32, 33). They are described as potential modulators of programmed cell death and chemotherapy-induced cytotoxicity (34, 35). To date, four human HtrA homologs (HtrA1-HtrA4) have been identified of which, HtrA2/Omi has proapoptotic activity, while very little information is available on other human HtrAs (32, 36-40).

This thesis focuses on HtrA2, a mitochondrial proapoptotic serine protease with multitasking ability. It is involved in several critical biological functions such as protein quality control, unfolded protein response (UPR), cell growth, apoptosis, arthritis, cancer and neurodegenerative disorders (41-44). It was first identified as an inhibitor of apoptosis (IAP) binding protein due to its IAP recognizing reaper-like motif (AVPS) (3, 4). HtrA2 is expressed as a 49 kDa pro-enzyme that is predominantly localized to the intermembrane space (IMS) of mitochondria (3). Upon maturation, the N-terminal 133 residues get cleaved and the mature protein resides in

mitochondria. During apoptotic stimulation, is the mature 36 kDa mature protease is released from mitochondria into the cytosol (3-6). HtrA2 plays an important role in intrinsic apoptotic pathway by binding and cleaving IAP proteins thus relieving their inhibition on caspases (3). Moreover, HtrA2, via its serine protease activity, induces caspase independent pathway by regulating the antiapoptotic proteins such as FLIP, Ped/Pea15 and Hax1 (7-9). Additionally, based on the chaperoning ability of its bacterial counterpart DegP, and a few evidences from the literature, it has been reported that HtrA2 might also play a protective role in the mitochondria under normal conditions (5, 45, 46). Therefore, regulating HtrA2 activity might give rise to therapeutic possibilities in various diseases it is associated with (35). In order to modulate HtrA2 functions with desired characteristics, its structural dynamics, mechanism of activation, and mode of substrate recognition needs to be elucidated.

Crystallographic data of mature unbound from of HtrA2 provided only the broad overview of its structural organization (10). The three dimensional structure reveals that HtrA2 has a trimeric pyramidal architecture with the short N-terminal region forming the top and PDZ domains at the base of the pyramid respectively. The core serine protease domains (SPD) are surrounded by C-terminal PDZ domains, which restrict entry of the substrates to the active-site thus leading to a low basal activity. PDZ is attached covalently to the SPD through a flexible interface linker sequence, and it is believed that the PDZ-protease dynamics and their relative orientation modulate HtrA2 activity and hence functions. These observations led to development of an activation model, which highlights the role of PDZ in substrate binding and subsequent protease activation. The model states that upon substrate binding, the PDZ that otherwise falls on the protease domain opens up allowing the substrate to enter the binding pocket. Although the model provides a basic understanding of HtrA2 activation, it could not define the role of N-terminal

region, trimerisation and PDZ-protease cross-talk which is a prerequisite for delineating its role in various biological pathways and diseases. Although PDZ acts as a regulatory domain in all the HtrA family proteins, uniqueness of HtrA2 is manifested by its ability to the IAPs, through its N-terminus and subsequently cleaves them. This phenomenon emphasizes multiple modes of HtrA2 activation and regulation, the precise mechanism for which remains to be elucidated. Therefore, to understand the mode of HtrA2 activation, substrate recognition and cleavage, intricate dissection of its structure with functional correlation is required. Hence, we delineated the role of different domains, their combinations, oligomerization, and critical residues in modulating HtrA2 specificity and functions. Furthermore, to understand its proapoptotic property and its complex mechanism of action, we performed a comprehensive binding analysis with Pea15.

Our studies highlight the importance of N-terminal region, oligomerization and intricate intermolecular PDZ-protease interaction in proper formation and hence HtrA2 functions. It establishes the role of PDZ domain in not only interface dynamics and initial substrate binding but also in intermolecular contacts in the trimeric protease architecture leading to efficient substrate catalysis. Our interaction studies with Pea15 provide first mechanistic insight into the substrate recognition and specificity of HtrA2. Binding studies with Pea15 define a bipartite mode of interaction between HtrA2 and Pea15. Enzymology studies with Pea15 suggest allosteric activation of HtrA2 might be required by adaptor proteins in the cell to relieve the inhibitory effect of PDZ domain. Substrate specificity studies reveal that HtrA2 has broad substrate specificity toward the residues near the cleavage site. These observations redefine the existing activation model and provide new insights into HtrA2 structure, function, and dynamics.

Chapter 2

Review of literature

2.1 Apoptosis

Apoptosis is a Greek term meaning 'dropping of', and refers to the falling of leaves from trees in autumn (14). It is an evolutionary conserved, tightly regulated process of cell death (47). It is a fundamental biological process that occurs normally during development and aging (15-21). It is essential for cellular homeostasis i.e. to maintain a delicate balance between cell proliferation and cell death (15-21). Insufficient apoptosis leads to accumulation of unwanted or damaged cells, which may ultimately result in malignancy (16, 22-27). In contrast, excessive apoptosis has been associated with autoimmune disease, atherosclerosis and neurodegenerative disorders (11-16). Apoptosis is just one form of cell death, cells may be eliminated by a number of alternative mechanisms such as necrosis or 'nonspecific' form of cell death, which occurs in response to inflammation, ischemic or toxic injury (48). In contrast, apoptosis is an active, highly selective, metabolic, genetically encoded and evolutionarily selected death pathway. Furthermore, apoptotic cell death is the consequence of a series of precisely regulated events that include shrinkage of cell, DNA fragmentation, blebbing of the plasma membrane, condensation of chromatin and appearance of intracellular inclusions or 'apoptotic bodies' (28, 29). The basic differences between these two cell death processes emphasize the reason why apoptosis represents the most desirable target mechanism for the induction of cell death in tumor cells without damage to normal cells (49).

There has been tremendous progress in identifying the key components of apoptotic signaling cascade. Caspases regulates the apoptotic machinery, although several other less prominent players are also involved such as cathepsins granzymes, calpains and HtrAs (31). Classical apoptotic pathway include two major pathways, extrinsic and intrinsic cell death path way.

2.1.1 Extrinsic cell death pathway

The extrinsic or death receptor pathway initiates apoptosis when death ligands bind to the death receptors (50, 51). These death receptors are members of the tumor necrosis factor (TNF) receptor gene super family. Members of the TNF receptor family share similar cyteine-rich extracellular domains for recognition of their specific ligands **(Figure 2.1)**. They also comprise an cytoplasmic domain of about 80 amino acids known as 'death domain' (52, 53). This death domain plays a critical role in transmitting the death signal from the cell surface to the intracellular signaling pathways through homotypic protein-protein interactions. To date, the best-characterized ligands and corresponding death receptors include FasL/FasR (CD95L/ CD95R), TNF-α/TNFR1, TNF-related apoptosis-inducing ligand-receptor 1 (TRAIL-L1/TRAIL-R1) Apo3L/DR3, Apo2L/DR4 and Apo2L/DR5 (54). The sequences of events that define the extrinsic signaling cascade of apoptosis are best characterized with the FasL/FasR and TNF-α/TNFR1 models. Binding of cognate ligands to these monomeric death receptors result in receptor trimerization. The trimeric death receptors then interact with the cytosolic adapter proteins such as TNF receptor-associated death domain (TRADD) and Fas-associated death domain (FADD) through homotypic interactions by their respective death domain (DD) (55). This interaction recruits upstream procaspase-8 to these preassembled adaptor molecules to form a death-inducing signaling complex (DISC) (56-58). Oligomerization of caspase-8 upon DISC formation drives its auto-catalytic activation through self-cleavage (59). Thus, activated caspase-8 induces apoptosis by activating other downstream or executioner caspases such as caspase-3 and -7.
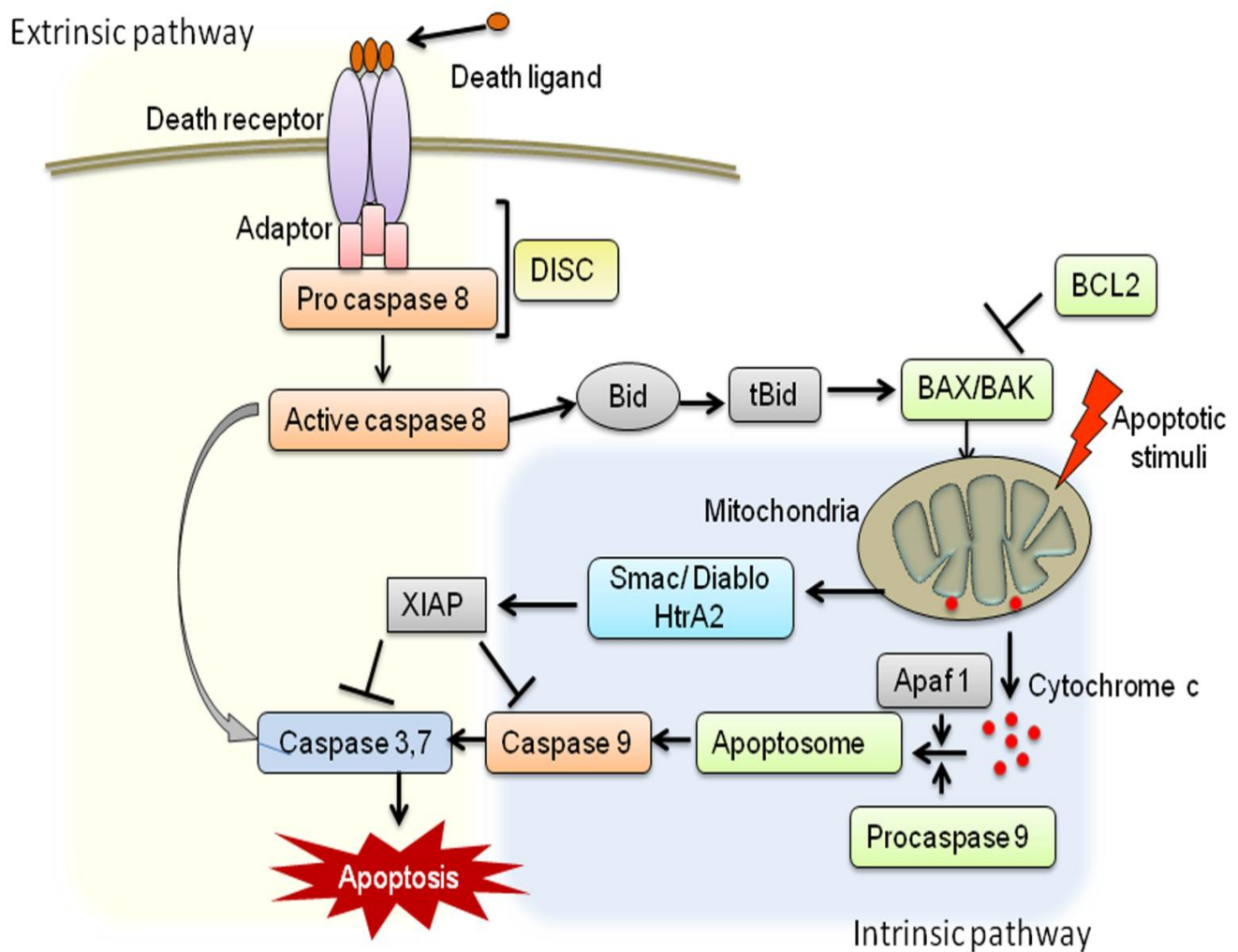
Figure 2.1 Apoptotic pathways. *A) The extrinsic apoptotic pathway is initiated by the ligation of death receptors with their cognate ligands, leading to the recruitment of adaptor molecules such as FAS-associated death domain protein (FADD) and then caspase 8. This results in the dimerization and activation of caspase 8, which can then directly cleave and activate caspase 3 and caspase 7, leading to apoptosis. B) Intrinsic apoptotic stimuli, such as DNA damage, activate B cell lymphoma 2 (BCL-2) homology 3 (BH3)-only proteins leading to BCL-2-associated X protein (BAX) and BCL-2 antagonist or killer (BAK) activation and mitochondrial outer membrane permeabilization (MOMP). Anti-apoptotic BCL-2 proteins prevent MOMP by binding BH3-only proteins and activated BAX or BAK. Following MOMP, release of various proteins from the mitochondrial intermembrane space (IMS) promotes caspase activation and apoptosis. Cytochrome c binds apoptotic protease-activating factor 1 (APAF1), inducing its oligomerization and thereby forming a structure termed the apoptosome that recruits and activates an initiator caspase, caspase 9. Caspase 9 cleaves and activates executioner caspases, caspase 3 and caspase 7, leading to apoptosis. Mitochondrial release of second mitochondria-derived activator of caspase Smac/Diablo and HtrA2 neutralizes the caspase inhibitory function of X-linked inhibitor of apoptosis protein (XIAP). C) Crosstalk between the extrinsic and*

intrinsic pathways occurs through caspase 8 cleavage and activation of the BH3-interacting domain death agonist (BID), the product of which (truncated BID; tBID) interacts with BAX and BAX and induces MOMP.

2.1.2 The intrinsic cell death pathway

In the intrinsic or mitochondrial pathway of apoptosis, caspase activation is closely linked to permeabilization of the outer mitochondrial membrane by numerous stress inducing stimuli and proapoptotic signal-transducing molecules (BCL family proteins). Stimuli for intrinsic pathway include calcium overload, endoplasmic reticulum stress, DNA damage, altered redox potential, growth factor deprivation, oncoproteins, viral virulence factors and chemotherapeutic agents (50, 60). BCL-2 proteins, which regulate mitochondrial membrane potential (MOMP) are categorized under three sub-groups: anti-apoptotic (BCL-2, BCL-W, BCL-xL, a-1 and MCL-1), proapoptotic effectors (BAX, BAK, and BOX) and proapoptotic BH3 only proteins (BID, BIM, BAD, etc.). Oligomerization of BAX-BAK complex at the outer membrane of the mitochondria results into membrane permeabilization, thereby resulting in efflux of cytochrome-c and other anti-apoptotic proteins such as HtrA2 and Smac/Diablo into the cytosol **(Figure 2.1)**. In the presence of ATP/dATP, cytochrome c binds apoptotic protease-activating factor 1 (APAF1) monomer, leading to formation of heptameric wheel-like structure called the apoptosome (61, 62). This protein complex, apoptosome later recruits and activates initiator procaspase-9. Other mitochondrial proteins Smac/Diablo and HtrA2 present in the cytosol cleave 'Inhibitor of Apoptosis Proteins' (IAPs) and relieve their inhibition on caspase -9. Consecutively, active caspase-9 in turn activates other executioner caspases, caspase-3, -6 and -7. These caspases cleave key substrates in the cell to produce many of the cellular and biochemical events of apoptosis.

Both the intrinsic and extrinsic pathways interconnect with the proapoptotic protein Bid, a member of the BH3 family of proteins (63, 64). Bid is processed into tBid by caspase-8 of the extrinsic pathway. Truncated, tBid translocates to the mitochondria where it interact with BAX and BAK, thereby promotes the release of cytochrome c from the mitochondria (65).

 Tremendous progress in apoptotic research in the past decade has identified caspases to be the key players responsible for the proteolytic cascades in apoptosis. However, accumulating evidences suggest that cell death can occur in a programmed fashion in absence of caspase activation. For example, other proteases, such as cathepsins, Granzymes and HtrAs (high temperature requirement protease A), are also involved in the initiation and execution of the apoptosis. These proteases are capable of triggering mitochondrial dysfunction with subsequent caspase activation and cellular demise.

2.2 Human HtrA proteases

HtrA (high-temperature requirement protease A), belongs to the family of S1B class of serine proteases identified in *E. coli* as a heat shock-induced envelope-associated serine protease (1, 32, 33). It generally acts as a molecular chaperone at low temperatures and exhibits its proteolytic activity with increase in temperature (66). In humans, HtrAs are involved in numerous cellular processes, ranging from maintenance of mitochondrial homeostasis to cell death in response to stress-inducing agents (43). Interestingly, despite diversity in functions and low sequence identity, HtrAs share a common structural integrity that comprises a trypsin like protease domain and one or more C-terminal Postsynaptic density protein 95-Discs large-Zona occuldens 1 (PDZ) or protein-protein interaction domains. In recent years, human HtrAs have drawn attention as key effectors in multiple pathways of programmed cell death and are described as potential

modulators of chemotherapy-induced cytotoxicity (33, 36). This multifaceted ability associates them with different pathological conditions such as cancer, neurodegenerative disorders and arthritis including myocardial ischemia/reperfusion injury hence making them therapeutically important (34, 35, 43).

Based on their domain architecture that comprise an N–terminal signal peptide (SP), an insulin growth factor binding domain (IGFBP) and a kazal-type S protease inhibitor domain (KI), a serine protease domain and PDZ domain, four human HtrAs have been identified **(Figure 2.2).** These are HtrA1 (L56, PRSS11), HtrA2 (Omi), HtrA3 (PRSP) and HtrA4 (32, 36-40). Among the HtrA homologs, HtrA1 and HtrA2 are well characterized, while very little information on HtrA3 and HtrA4 are currently available. Interestingly, of the four human HtrAs, HtrA2 has evolved into a mitochondrial proapoptotic molecule with ability to induce apoptosis via multiple pathways.
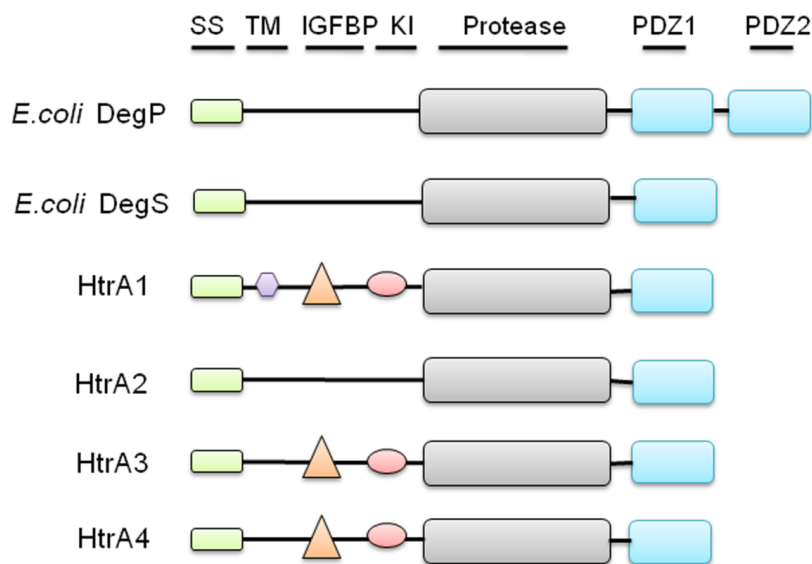
Figure 2.2 Schematic representation of domain organization of HtrA family of proteases. *The protease domain is in grey rectangles, PDZ1 and PDZ2 domains in blue rectangles, SS (signal sequence) in green rectangles, TM (transmembrane domain) in purple triangle, IGFBP (Insulin-like growth factor binding) in orange triangles, and KI (Kazal protease inhibitor domain) in pink oval. Here, E. coli represents Escherichia coli and HtrA represents high temperature requirement protease A*

2.2.1 HtrA2

HtrA2 was originally isolated as an interactor of Mxi2, the alternatively spliced form of the p38 stress activated kinase. HtrA2 is ubiquitously expressed in all tissues, while the alternatively spliced form, lacking exons 3 and 7, is expressed only in the kidneys, thyroid, and colon (67). It is predominantly localized in the mitochondria where transmembrane region of HtrA2 is anchored in the inner mitochondrial membrane while the protease and PDZ domains are exposed into the mitochondrial intermembrane space (IMS). The full length protein is expressed as a 49 kDa pro-enzyme where the first 133 amino acids from the N-terminus get cleaved upon maturation (3). During triggering of apoptotic the mature form (36 kDa) is released from the IMS into the cytosol (3-6, 68). This cleavage exposes an internal tetrapeptide motif (AVPS) that binds to IAPs and relieve their inhibition on caspases (2). Mature HtrA2 is composed of a short N-terminal region and well-defined serine protease and PDZ domains (3, 4).

2.2.1.1 Structural assembly

Crystallographic structure of substrate-unbound form of mature HtrA2 (134-458) was solved at 2.1Å, which provides a broad overview of its structural organization (10). It has trimeric pyramidal architecture with short N-terminal on the top and PDZ domain residing at base. Mature HtrA2 with 7 α-helices and 19 β-sheets forms well defined protease and PDZ domains. Trimerisation is mediated by extensive intermolecular hydrophobic and van der Waals interactions mainly involving three aromatic residues (Y14, F16 and F123). The core serine protease is gated by C-terminal PDZ domains. This, along with its trimeric structural arrangement, restricts HtrA2's accessibility to substrate molecules, thus leading to its low basal activity. The protease domain adopts chymotrypsin fold, comprising of two six-stranded β-

barrels. The active-site pocket consisting of the amino acid triad H65-D95-S173 is located at the interface of the two perpendicularly arranged β-barrels, buried 25Å above the base of the pyramid. Moreover, the active-site is surrounded by several regulatory loops that are named according to the chymotrypsin nomenclature, LA (residues, 37-41), L1 (residues, 169-173), L2 (residues, 190-196), L3 (residues, 142-162), and LD (residues, 126-140). PDZ is attached covalently to SPD through a flexible linker sequence which regulates HtrA2 activity though subtle conformational changes.
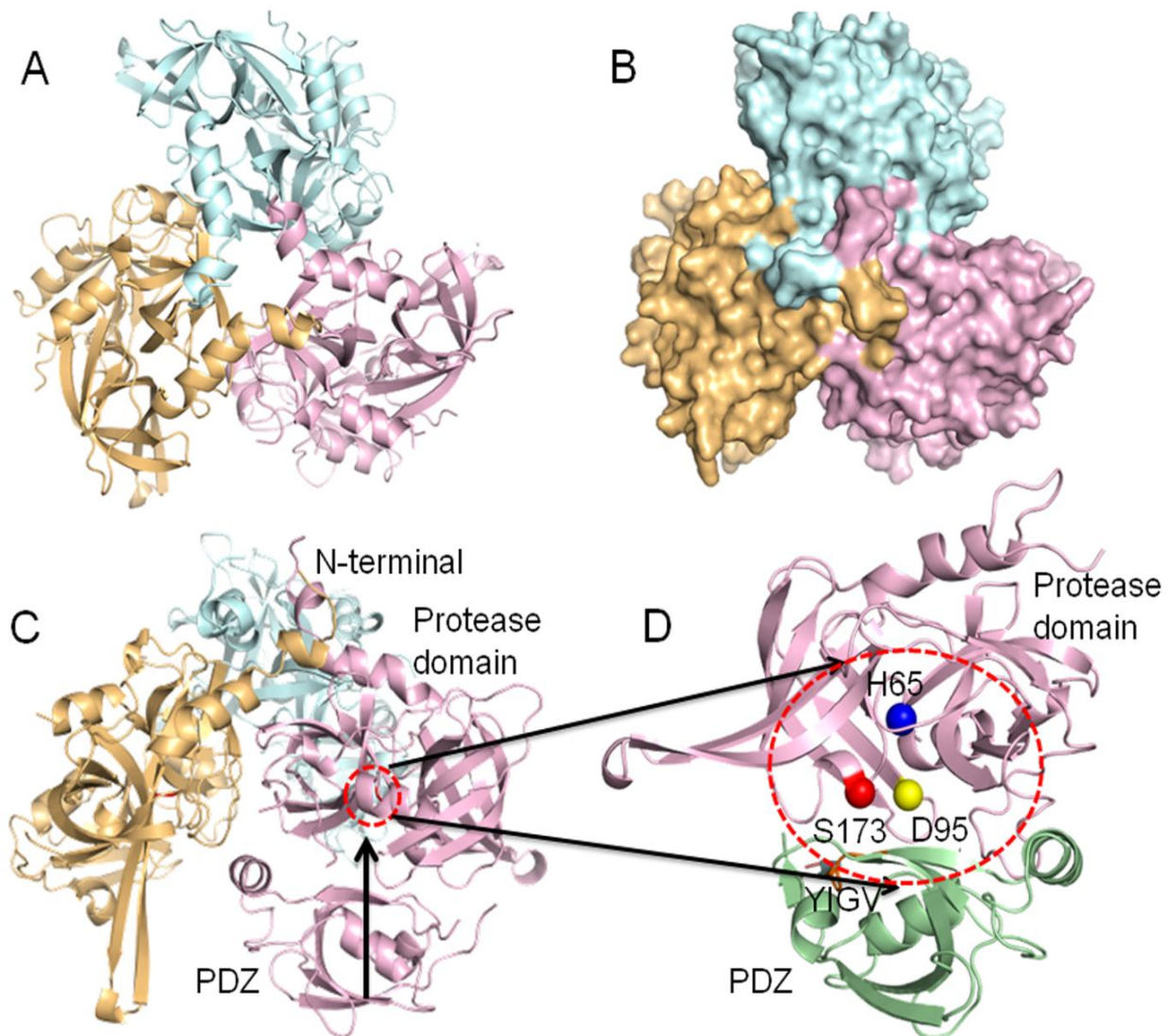
Figure 2.3 Crystal structure of HtrA2. A) Schematic representation of HtrA2 trimer (PDB entry 1LCY). Each monomeric subunit is represented in blue, orange and pink. B) Surface representation of the HtrA2 structure. C) side view of trimeric HtrA2. Trimerization is mediated exclusively by the serine protease domain. The N-terminal IAP-binding tetrapeptide motif is located at the top of the pyramid, and the PDZ domain is at the base. D) Cartoon representation of HtrA2 monomer. Serine protease and PDZ domains are colored in pink and green respectively. The position of catalytic triad residues: H65 (blue), D95 (yellow) and S173 (red) are shown as spheres. The position of canonical peptide binding groove 'YIGV' is represented in orange. The figures are generated using PyMOL (DeLano Scientific, USA).

PDZ domains are well characterized protein-protein interaction domains known to recognize specific hydrophobic residues in the C-termini of binding partners (69, 70). These domains are of 80–100 amino-acid residues, present in many metazoan genomes. HtrA2 PDZ domains comprise five β-strands and two α-helices, similar to the other canonical PDZ domains. Typical PDZ domains have a canonical binding site comprising highly conserved 'G-Φ-G-Φ motif', where Φ denotes hydrophobic residues (70). The first G residue is highly variable among PDZ domains, while the second and fourth residues are hydrophobic (V, I, L, or F). This recognition sequence is substituted by 'YIGV' in HtrA2, which is highly buried in the intimate interface between the PDZ and the protease domains. The PDZ domain packs against the protease domain through van der Waals contacts. On one end of the interface hydrophobic residues on β14 and helix α5 (M365, L367, I373 and L377) of the PDZ domain interact with the hydrophobic residues on β11 and β12 (M323, V325, I329 and F331) of the protease domain (10). Moreover, this peptide binding groove is also loosely occupied by two hydrophobic residues, P225 and V226 that are located between β5 and β6 strands of the protease domain. These rearrangements strongly suggest that the peptide binding groove is unavailable for interaction with other proteins in this 'closed' conformation.

2.2.1.2 Activation mechanism

From the structural insights, Li and co-workers proposed a working model for HtrA2 activation (10), where the relative intra-molecular PDZ-protease movement was considered the primary regulatory factor. According to this model, in the basal state, the PDZ domains keep the protease activity of HtrA2 in check. Substrate or ligand binding at 'YIGV' groove induces a large conformational change at the PDZ-protease interface which removes the inhibitory effect of PDZ from the . This structural rearrangement leads to significant increase in activity thus emphasizing intra-molecular PDZ-protease crosstalk to be pivotal in HtrA2 activation. Since the YIGV groove is deeply embedded within the hydrophobic core where the residues are intertwined with each other through several intra-molecular interactions, accessibility of ligands to this site seems to be limited. Recently our group characterized allosteric activation of HtrA2, where the signal is relayed *via* a distal non-canonical substrate binding site with subsequent opening up of the YIGV (71). The allosteric switch propagated by PDZ domain might lead to a disorder-to-order transition of important regulatory loops (L1, L2, L3, and LD) in protease domain. This intrinsic allosteric regulation mechanism is initiated by sensor loop L3 and subsequently a cascade of conformational changes occurs along L3→LD→L1/L2, enabling the remodeling and activation of the proteolytic site **(Figure 2.4)**. This general mechanism of allosteric regulation is conserved in other bacterial homologs (13, 72). However, the activation signal detected by sensor loop L3 is different.

Basal state
(low activity)

Binding to target protein

Active state
(high activity)
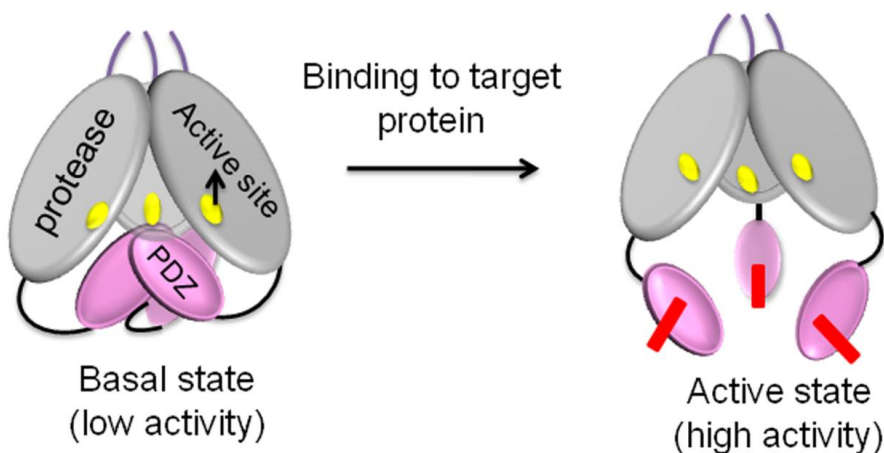
Figure 2.4. Proposed working model for HtrA2 activation. In the basal state, the PDZ domains keep the protease activity of HtrA2 in check. Upon binding to the target proteins, the PDZ domains moves away from the protease to make the catalytic serine accessible to the substrate

In addition to the PDZ-domain-mediated activation, protease activity of HtrA2 is also modulated by binding to IAPs, through its N-terminus (73). It was observed that HtrA2 incubated with XIAP showed increase proteolytic activity toward its substrates, H2-Opt peptide (synthetic substrate of HtrA2) and β-casein (generic substrate for all proteases) (73). This phenomenon emphasizes involvement of multiple modes of HtrA2 activation and regulation, involving PDZ as well as other regions of the protein

2.2.1.3 Catalytic mechanism

Active-site cleft of HtrA2 comprise a conserved catalytic triad with S173, D95 and H65. It shares a common catalytic mechanism with other endogenous serine proteases. The general catalytic mechanism of serine proteases is based on the chymotrypsin model (74). The mechanism for hydrolysis of the peptide bond is an addition-elimination reaction involving two tetrahedral intermediates. During the first step of the peptide bond hydrolysis, side chain of the substrate at the residue N-terminal to the scissile bond, binds to the specificity pocket. This is followed by a nucleophilic attack by S173, which is facilitated by H65. An acyl-enzyme intermediate is formed by the covalent bond between the C-atom of substrate and hydroxyl group of the S173. The intermediate with the carbonyl atom in a tetrahedral state is stabilized by the 'oxanion hole,' where G171 and S173 donate backbone hydrogens for hydrogen bonding to the

negatively charged oxygen of the substrate. Further, a proton is transferred from H65 to the amide of peptide to release the C-terminal of the substrate. In the final step, the acyl-intermediate is deacylated by forming a tetrahedral intermediate state with water. This step is followed by a nucleophilic attack by the hydroxyl group of a water molecule that is hydrogen bonded to H65. This releases the carboxylic acid product from enzyme restoring the protease in its initial state.

2.2.1.4 Functions

The primary function of HtrA2 is the maintenance of mitochondrial homeostasis. Under normal physiological conditions, it acts as a quality control factor and promotes cell survival. In response to apoptotic stimuli such as cellular stresses, UV exposure, oxidative stress, and death receptor activation, it transforms from being protective to a proapoptotic. The following section highlights both these signaling mechanisms in detail.

i) Apoptosis

Although caspases are recognized as the main players in the initiation and execution of apoptosis, several reports have substantiated the role of HtrA2 in the apoptotic cascade. Apoptotic insults trigger the translocation of mature HtrA2 into the cytosol, where it contributes to apoptosis through both caspase-dependent and independent pathways (**Figure 2.5**).

a) Caspase-dependent mechanism

Proteolytic maturation of HtrA2 exposes the internal tetrapeptide motif (AVPS), which mediates interaction with the IAPs (6). These IAPs such as XIAP (X-linked inhibitor of apoptosis protein), cIAP1 (cellular inhibitor of apoptosis protein-1), cIAP2, Apollon/BRUCE are endogenous inhibitors of caspase-3, -7 and -9 (**Table 2.1**). Upon apoptotic stimulation, mature HtrA2 is released into the cytosol, where it interacts with IAPs and relieves caspase inhibition

thus promoting apoptotic signaling cascade and hence cell death. The homotrimeric HtrA2 may also interact via its PDZ domain with a trimeric assembly of TNFR1 or Fas (10, 65). The Fas ligand-induced trimerization activates the 'death domain' present in the cytoplasmic region of each Fas monomer thereby initiating caspase-8-dependent apoptotic pathways.
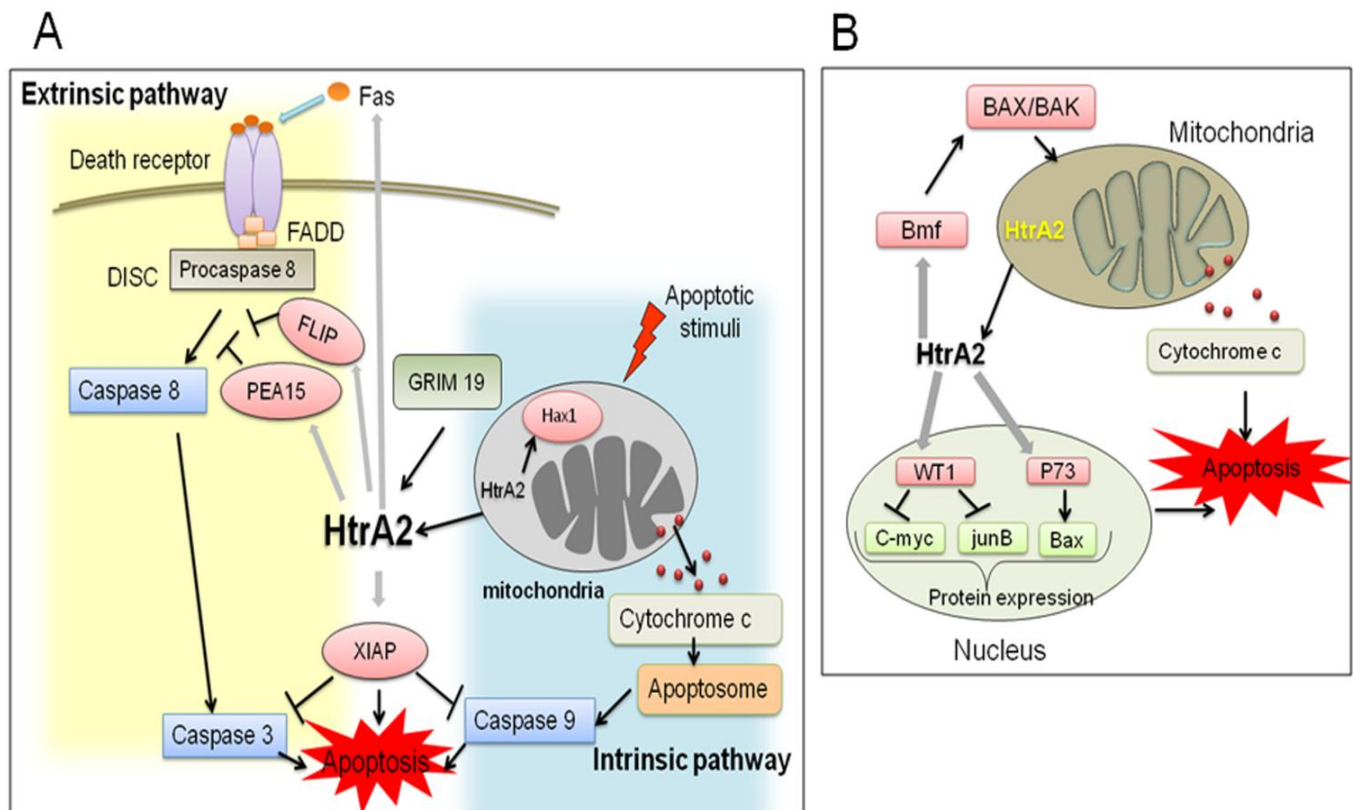
Figure 2.5. HtrA2 mediated apoptotic pathway. *A) Upon apoptotic stimuli, mature HtrA2 is released from the mitochondrial intermembrane space into the cytosol. HtrA2 interacts with anti-apoptotic protein, XIAP thus relieving its inhibitory action on caspases, thereby facilitating caspase-dependent apoptosis. Homotrimeric HtrA2 via its PDZ domain interacts with a trimeric assembly of Fas, thus initiating death-receptor pathway of apoptosis. HtrA2 through its serine protease activity also induces caspase-independent cell death by binding and cleaving anti-apoptotic proteins FLIP, PEA15 and HAX1. Grim 19 modulates HtrA2 protease activity. B) HtrA2 promotes apoptosis by proteolytic activation of proapoptotic p73 and WT1 (Wilms tumor suppresor1) proteins. The proteolytically degraded p73 and WT1 result in elevated expression of BAX, c-myc and JunB. HtrA2 regulates the translocation of BAX into mitochondria by cleaving Bmf*

b) Caspase-independent mechanism

HtrA2 contributes to apoptosis through additional mechanisms that are independent of caspase activation (4). This mechanism is independent of its AVPS motif, and instead relies primarily on its protease activity (75, 76). It was observed that, HtrA2 over-expression-induced cell death was neither inhibited by the synthetic caspase inhibitors (zVAD-fmk or Boc-D-fmk) nor accompanied by detectable caspase activity. HtrA2 promotes cell death specifically by binding to and cleavage of the death effector domains (DED) of FLIP (7) and anti-apoptotic Ped/Pea-15 (8). It was speculated that HtrA2 may interact with the death receptors (Fas and TNFR) or other components of the death-inducing signaling complex (DISC) to activate a caspase-9-independent apoptotic pathway (65). This hypothesis was supported by an increased FasL expression after myocardial ischemia/reperfusion (65). HtrA2 can induce apoptosis without being released from mitochondria by cleaving mitochondrial antiapoptotic HS1-associated protein X-1 (Hax-1) (9). Hax-1 is believed to participate in regulation of mitochondrial membrane potential. Proteolytic degradation of HAX-1 by HtrA2 might be an early event and defines a new proapoptotic pathway initiated in the mitochondria. Furthermore, caspase-independent proapoptotic property is manifested by its ability to cleave important cytoskeletal proteins such as actin, α-, β-tubulin, and vimentin (13). Apart from cleaving several antiapoptotic proteins, HtrA2 promotes apoptosis by proteolytic activation of proapoptotic p73, a member of the p53 family, which functions as a transcription factor. During apoptotic stimuli, HtrA2 is translocated to the nucleus where it cleaves p73 (77). Proteolytically modified p73 thereby stimulates transcription of the proapoptotic BAX gene. In addition, HtrA2 indirectly regulates the translocation of BAX into mitochondria by cleaving Bmf, an endogenous inhibitor of BAX (65).

Recently, it was demonstrated that the cytotoxic drugs such as etoposide or staurosporine induced HtrA2 to cleave Wilms tumor suppressor protein (WT1), a transcriptional regulator of genes controlling apoptosis, cell growth and differentiation (78). The proteolytically degraded WT1 resulted in elevated expression of c-*myc* and *JunB* and subsequent apoptosis of human osteosarcoma cells treated with staurosporine. There is also evidence that HtrA2 is involved in p53-dependent apoptosis. Jin *et al*. showed that HtrA2 gene expression is regulated by p53 protein (79). Human thymocytes and HeLa cells treated with etoposide, an agent that triggers p53-dependent apoptosis showed increased gene expression of HtrA2. Under these conditions HtrA2 degraded IAPs and thus potentiated apoptosis.

ii) Other functions

Under normal physiological conditions, HtrA2 acts as a quality control factor facilitating cell survival rather than cell death. Alteration in the HtrA2 proteolytic activity leads to the accumulation of unfolded proteins in mitochondria, dysfunction of the mitochondrial respiration, generation of reactive oxygen species and also loss of mitochondrial competence (5, 45, 46). The mnd2 (motor neuron degeneration 2) mice carrying missense mutation S276C, as well as the knockout mice carrying a homologous deletion of the HtrA2 gene results in the loss of the HtrA2 proteolytic activity. Both these strains exhibit phenotypes of neurodegenerative disorder with features typical for the Parkinsonian syndrome (45, 80). Moreover, phophorylation of HtrA2 by serine/threonine kinase PINK1 amplifies its protease activity in mitochondria, thereby contributing to an increased protection in mitochondria under stress conditions (81). In agreement with these findings, decreased HtrA2 phophorylation was observed in brains of Parkinson's disease patients, carrying mutations in the PINK1 kinase. Moreover, two different point mutations in HtrA2, G399S (82) and A141S (83) were identified in a group of German

Parkinson's disease patients. These mutations demonstrated reduced proteolytic activity of HtrA2 *in vitro.* Overall, these findings suggest that mutations abolishing HtrA2 protease activity may cause increased susceptibility to mitochondrial stress and neuronal death, thereby increasing the risk of developing Parkinsonian disease.

HtrA2 has a protective role against the development of Alzheimer's disease (AD), which is characterized by the presence of aggregates of the amyloid β, a major element of neurotoxic deposits in brains of AD patients. HtrA2 chaperoning function prevents the aggregation of amyloid β-peptides (Aβ40 and Aβ42), keeping the peptide in monomeric state (84). Furthermore, HtrA2 is involved in processing of mitochondrial amyloid precursor protein (APP), to generate a 28-kDa APP fragment that is apparently released in to cytosol (85). Accumulation of APP disrupts the basic functions of mitochondria and impair energy metabolism. In accordance with APP processing activity, the generation of APP fragment was greatly reduced in brain extracts of *mnd2* mice leading to the death of the HtrA2 deficient neuronal cells.

HtrA2 is involved in maintaining the levels of Mulan (Mitochondrial ubiquitin ligase activator of NF-kB) protein under normal conditions as well as during oxidative stress (86). Upregulation of Mulan, in the absence of HtrA2, leads to the degradation and removal of Mfn2 (mitofusin 2) protein leading to mitochondrial dysfunction and mitophagy in muscle cells. This mechanism of maintaining the levels of Mulan defines a new function of HtrA2 in mitochondrial homeostasis (86). Mitochondrial proteomic analysis from HEK 293 cells identified two potential substrates of HtrA2 that impact metabolism and ATP production (13). Two substrates are the key proteins of Kreb's cycle, PDHB (Pyruvate dehydrogenase E1 component beta subunit) and IDH3A (Isocitrate dehydrogenase [NAD] subunit alpha). This implicates a new regulatory role of mitochondrial HtrA2 in a novel mechanism relating to metabolism.

2.2.1.5 Alterations in cancer

Microarray analysis of HtrA2 expression levels delineated that it was down-regulated in some tumors and up-regulated in others (35). HtrA2 expression was down-regulated in ovarian cancer, metastatic prostate cancer and adult male germ cell tumor (87, 88). Down-regulation of HtrA2 expression reduced cell death mediated by integrin α7 (ITGA7) in prostate cancer cell lines (89). ITGA7 acts as a proapoptotic factor and enhances the HtrA2 protease activity both *in vitro* and *in vivo*. A similar inhibitory effect was exerted by the HtrA2 inactive variant. In breast cancer, HtrA2 expression was reduced with the increasing tumor staging.

HtrA2 expression was up-regulated in lung adenocarcinoma, superficial or invasive transitional cell carcinoma of bladder, oligodendroglioma (brain) and squamous cell carcinoma of head and neck, B-cell acute lymphoblastic and T-cell lymphoblastic leukemia (43). HtrA2 expression was also up-regulated in Wilm's tumors compared to normal fetal kidney or clear cell sarcoma (90). Collectively altered expression levels HtrA2 highlight its importance in cancer progression and, provide a rationale for targeting this protein for cancer therapy

Protein	Functions	Endogenous substrates in apoptosis	Other endogenous substrates
HtrA2	Apoptosis, caspase and Fas activation, mitochondrial homeostasis, protein quality control	XIAP, cIAP1, cIAP2, Pea15, HAX1, FLIP, Fas, actin, α-, β-tubulin, vimentin, p73, Bmf, WT1	Mulan, WARTS kinase, PDHB, IDH3A, HSPA8, Amyloid β,

Table 2.1. *Functions and substrates of HtrA2*

.

2.3 Pea15

Ped/Pea15 (Phosphoprotein enriched in diabetes/Phosphoprotein enriched in astrocytes) is a highly conserved ubiquitously expressed cytosolic protein (91). It was first identified as an abundant phosphoprotein in brain astrocytes (92). Pea15 is a multifunctional protein, which regulates cell proliferation, autophagy, glucose metabolism and apoptosis (93). It exists *in vivo* as three isoforms, un-, mono and di-phosphorylated forms (91). Pea15 functions are regulated by multiple calcium-dependent phosphorylation pathways. It has been reported that unphosphorylated Pea15 acts as a tumor-suppressor and that phosphorylation modulates its interaction with binding partners to promote tumor development (94).

2.3.1 Structure

Pea15 is a 130 amino-acid protein with a predicted molecular mass of 15 kDa. It has a leucine-rich nuclear export sequence (NES), which is required for localizing in the cytoplasm (95). The three dimensional structure of Pea-15 was determined using NMR spectroscopy (96) **(Figure 2.6)**. Its structure consists of a canonic N-terminal death effector domain (DED), followed by 40 amino acids long irregularly structured C-terminal tail. DED is a conserved small protein recognition domains that mediates homotypic interactions required for signal transduction in programmed cell death (97). Pea15 DED is comprised of six amphipathic α-helices closely packed around a central hydrophobic core. The α-helices in the DED are connected by short loops, two of which contain β-turns (between α2–α3 and α4–α5). The α-helices are arranged in a 'Greek key' topology, where helices α1 and α2 are centrally located, α-3 and α-4 is on one side and α5 and α6 on the other. The α5–α6 loop contains a conserved RxDLf motif (x: any amino acid, f: any hydrophobic residue) similar to other DED-containing proteins. Pea15 C-terminal

region has two phosphorylation sites. The first one, Ser104, located within the motif LTRIPSAKK, which is phosphorylated by PKC (Protein kinase C) (98). The second site, Ser116, is present in the motif DIRQPSEEEIIK, and is the target of the CaMKII (Calmodulin dependent kinase II) (98, 99).
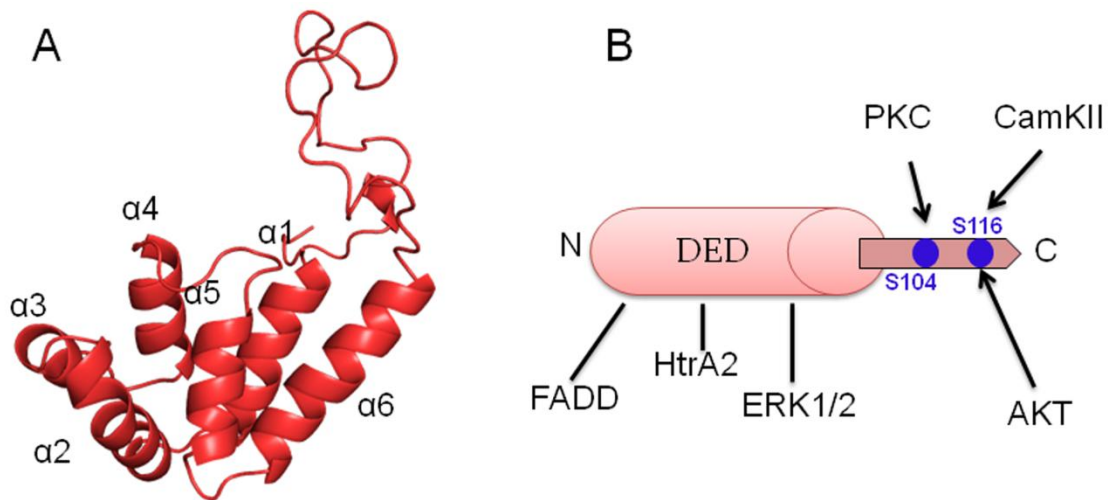
Figure 2.6. Structure of Pea15. A) *NMR* **structure** *of Pea15 (PDB ID 1N3K). B) Domain organization of Pea15, showing interaction with different proteins. Blue circles are the phosphorylation sites in Pea15 A and B*

2.3.2 Functions

Pea15 functions as a tumor suppressor by regulating cellular proliferation mediated by extracellular signal-regulated kinase (ERK) pathway (100) **(Figure 2.7).** The RAS–RAF–MEK–ERK signaling cascade is a core regulatory cascade governing the fundamental cellular processes of cell proliferation, migration and invasion. The inactive or unphosphorylated ERK1/2 is essentially localized in the cytosol, its phosphorylation by MEK1 leads to its translocation into the nucleus. Activated ERK1/2 phosphorylate cytosolic substrates and also an array of critical targets in the nucleus to promote proliferation and differentiation. Pea15 regulates ERK dependent transcription by preventing its translocation into the nucleus and thereby restricts ERK

to the cytoplasm. Inhibition of ERK signaling cascade by Pea15 impaired tumour cell invasion, and promoted Ras induced cell senescence.
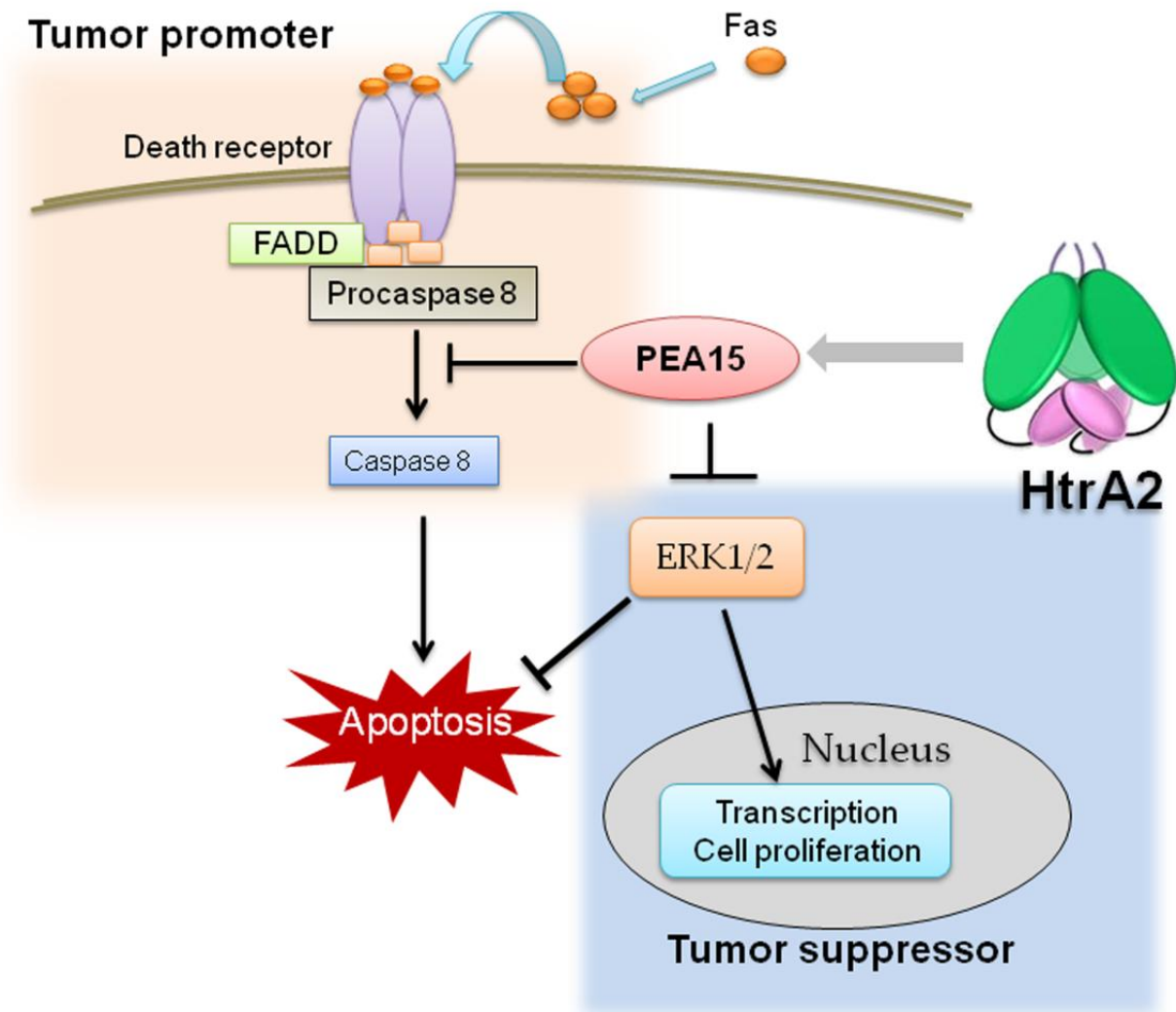
Figure 2.7. Role of Pea15 as tumor suppressor and tumor promoter. *Pea15 interacts with FADD and inhibits DISC (death inducing signaling complex) formation, thereby inhibits apoptosis cascade. Pea15 binds ERK and sequesters to the cytoplasm thereby inhibits ERK dependent cell proliferation*

Pea15 has a survival function in the astrocytes by regulating TNFα mediated apoptosis. Apoptois of neurons and oligodendrocytes has been extensively documented in several pathological conditions. On the contrary, the astrocytes respond to any brain injury in a process called

reactive gliosis (101). They appear to be relatively resistant to central nervous system damage and are at the core of tissue repair and regeneration at the site of injury. Reactive astrocytes feature upregulation of both tumor necrosis factor (TNF)α and apoptosis-signaling receptors of the TNF receptor superfamily, including TNR receptor 1 and Fas. Pea-15 DED interacts with other DED containing proteins like FADD, FLICE. This iteration prevents the recruitment of procaspase-8 into the DISC and blocks TNFα-mediated apoptosis pathway (102). Astrocytes lacking Pea15, and exposed to TNF rapidly exhibited apoptosis while, re-expression of Pea15 after transfection restored protection and survival.

2.3.3 Pathophysiological implications

Pea15 tumor-promoting effects were described by its ability to interfere with apoptotic signaling through its death effector domain. Through interference with apoptosis, Pea 15 showed increased susceptibility to chemically induced skin cancer in transgenic mice and also mediated chemo-resistance in human breast cancer cells. Furthermore, Pea15 protected human glioblastoma cells from glucose deprivation-induced apoptosis. Thus, it acts as a survival factor for cancer cells in microenvironments with low glucose levels.

Pea15's regulation of the MAPK/ERK pathway has been associated with anti-tumor outcomes. Pea15 blocked tumor development in a breast cancer xenograft model and it has been shown to induce cellular senescence in human fibroblasts by preventing oncogenic transformation. Pea15 was shown to be a good prognostic marker in ovarian cancer, where higher expression levels correlated with prolonged patient survival. In contrast, Pea15 expression levels were inversely correlated with the tumor stage in astrocytoma.

It was demonstrated that increased expression of Pea15 in cultured skeletal muscles and adipose cells showed resistance to insulin action in glucose uptake. This abnormality depends largely on Pea15-induced dysfunction of the PKC signaling system (103). It was hypothesized that, Pea15 binds phospholipase D (PLD) isoforms, increases their stability and intracellular diacylglycerol levels, and thereby activates the dyacylglycerol-sensitive PKCα isoform. These studies also revealed that the active PKCα in Pea**15**-overexpressing cells and tissues prevents insulin induction of the PKCζ isoform. This is distinct from PKCα and serves as a major activator of glucose transporter 4 (GLUT4) vesicle translocation toward the plasma membrane. Thus, studies in isolated muscle and adipose cells have shown that the overexpression of Pea**15** may determine peripheral resistance to insulin action by deregulating the signaling of PKC.

Aims and objectives

1. Characterization of structural properties and conformational stability of HtrA2 and the role of its different domains in protein function and specificity. Aim 1 is further divided into the following sub headings

    c) Importance of trimerization for HtrA2 activity

    d) Role of different domain coordination, critical residues involved and interdomain dynamics in regulating substrate specificity and activity

2. To understand the interaction of proapoptotic serine protease HtrA2 with antiapoptotic binding partner cum substrate–Pea 15

Chapter 3

Materials and Methods

3.1 MATERIALS

3.1.1 Bacterial strains

Host/ Strain	Genotype	Origin
E. coli DH5α (Cloning host)	*fhuA2 Δ(argF-lacZ)U169 phoA glnV44 Φ80 Δ(lacZ)M15 gyrA96 recA1 relA1 endA1 thi-1 hsdR17*	New England Biolabs (NEB), Ipswich, USA
E. coli BL21 (DE3) (Expression host)	*fhuA2 [lon] ompT gal (λ DE3) [dcm] ΔhsdS*	NEB
E. coli BL21 (DE3) pLysS (Expression host)	*F⁻ ompT hsdS*$_B$(r$_B^-$ m$_B^-$) *gal dcm* (DE3) *pLysS (Cam^R)*	NEB

3.1.2 Plasmids used for cloning

Plasmid / Vector	Tag	Source
pET 20b	C- terminal His$_6$ tag	Addgene (Cambridge, MA, USA)
pMAL c5E-TEV	N-terminal MBP tag (Maltose binding protein) with TEV protease site	NEB

3.1.3 Resins used for protein purification

Resin	Tag	Source
Ni-IDA	His$_6$ tag	Biotex, Houston, USA
Amylose	MBP tag	NEB
Superdex 200	For gel filtration	GE healthcare, Healthcare, Bjorkgatan, Uppsala, Sweden

3.1.4 Kits used

Kit	Purpose	Source
Plasmid miniprep kit	Plasmid isolation	Sigma chemicals, St. Louis, MO
Gel extraction kit	DNA extraction from agarose gel	Sigma
pJET 2.1 blunt end cloning kit	Blunt end cloning	Fermentas, Waltham, Massachusetts, USA
Quick change site directed mutagenesis kit	Mutagenesis	Stratagene, Cedar Creek, TX, USA

3.1.5 Specialized instruments

Instrument	Purpose	Source
Jasco J815 CD spectrophotometer	Secondary and tertiary structure of proteins	JASCO, Easton, MD, USA
Fluorolog-3 spectrofluorimeter	Fluorescence emission studies, enzyme kinetics, quenching, FRET	HORIBA scientific, Edison, NJ, USA
Mithras multiwell plate reader	Enzyme kinetics	Berthold technologies, Wildbad, Germany
AKTA purifier	Gel filtration	GE Healthcare, Buckinghamshire, United Kingdom

3.2 Buffers and Reagents

3.2.1 Antibiotics

a) Ampicillin sodium salt (Sigma)

Stock concentration: 100 mg/ml (Filter sterilized using 0.22 μm membrane), dissolved in water

and stored at -20 $^{\circ}$C

Working concentration: 100 µg/ml, stored at 4 °C

b) Chloramphenicol (MP Biomedical)

Stock concentration: 34 mg/ml (Filter sterilized using 0.22µm membrane), dissolved in ethanol and stored at -20 °C

Working concentration: 34 µg/ml, stored at 4 °C

3.2.3 Bacterial culture media

a) Luria-Bertani (LB) medium (for 1 L)

25 g of LB powder (Himedia, Mumbai India) was dissolved in 1 L of Milli Q (MQ) water and autoclaved.

b) LB- Agar Plates (for 1 L)

25 g of LB agar powder (Himedia) was dissolved in 1 L of MQ water and autoclaved. It was cooled to about 55 °C and 1 ml of respective antibiotic was added from stock. The media was poured into petri dishes (~25 ml/100 mm plate).

3.2.4. For cloning and site directed mutagenesis

a) Primers

PCR primers were commercially synthesized from Sigma as a lyophilized pellet. The primer pellet was centrifuged at 10,000 rpm for 1 min and then reconstituted in autoclaved deionized water to obtain final concentration of 500 µg/ml. A working dilution of 125 ng/µl was prepared for further experiments.

b) Restriction Digestion and Ligation

Fast Digest DpnI, BamHI, EcoRI, NdeI, XhoI enzymes along with 10X fast digest buffer were obtained from Fermentas. T4 DNA ligase and 10X ligase buffer were supplied from NEB.

c) 0.5 M EDTA, pH 8 (for 1 L)

To 148 g of EDTA ~30-40 g of NaOH pellets were added, pH was adjusted to 8 and volume was made to 1 L

 Note: pH adjusted by NaOH is essential for solubility.

d) Tris-EDTA (TE) Buffer (for 50 ml)

Tris   60.66 mg (10 mM)

EDTA   14.62 (1 mM)

pH was adjusted to 7.5 with 10 N NaOH and autoclaved.

e) Tris Acetate EDTA (TAE) running buffer for agarose gel electrophoresis (for 1 L)

Stock concentration: 50X TAE (2 M Trisacetate, 50 mM EDTA, pH 8)

Working concentration: 1X TAE (0.04 M Trisacetate, 1 mM EDTA, pH 8)

Tris base   242 g

Glacial acetic acid   57.1 ml

0.5 M EDTA (pH 8.0)   100 ml

f) 6X Gel Loading Buffer for DNA (for 100 ml)

(0.25% Xylenecynol, 0.25% bromophenol blue, 30% glycerol)

Xylene Cyanol FF   0.25 g (migrates at 4160 bp with TAE)

Bromophenol blue   0.25 g (migrates at 370 bp with TAE)

Glycerol   30 ml

Autoclaved Milli Q   70 ml

g) Ethidium Bromide (EtBr)

Stock concentration: 10 mg/ml (20000X)

Working concentration: 0.5 µg/ml

3.2.5 Buffers for protein expression and purification

a) 1M Isopropyl-β-D-thiogalactopyranoside (IPTG) (for 5 ml)

IPTG   1.19 g

Autoclaved Milli Q   5 ml

Filter sterilized (0.2µm) and stored at -20 ^{o}C.

b) Phosphate buffer, pH 8

Stock concentration: 10X (200 mM NaH_2PO_4/Na_2HPO_4, 1000 mM NaCl, pH 8)

Working concentration: 1X (20 mM NaH_2PO_4/Na_2HPO_4, 100 mM NaCl, pH 8)

Monobasic or monosodium phosphate (NaH_2PO_4)   59.99 g for 500 ml (1M)

Dibasic or disodium phosphate (Na_2HPO_4)   70.98 g for 500 ml (1M)

NaCl   35.6 g for 1L (1M)

To 200 ml of 1M dibasic solution, 1M monobasic solution was added and pH was adjusted to 8. Later 1M NaCl was added, volume was made to 1L using Milli Q. Buffer was filtered using 0.2 µm filter and autoclaved.

3.2.5.1 Ni -IDA Column Purification buffers

a) Lysis buffer (for 1 L)

(20 mM NaH_2PO_4/Na_2HPO_4, 100 mM NaCl, pH 8, 0.1% triton X 100)

10X Phosphate buffer pH 8   10 ml (1X)

1M imidazole   10 ml (10 mM, reduces non-specific binding of proteins)

TritonX-100   10 ml (0.1%)

10X Protease inhibitor   1X

BME (14.3 M)   0.34 ml (5 mM)

b) Ni-IDA Binding/Washing Buffer (for 1 L)

(20 mM NaH_2PO_4/Na_2HPO_4, 100 mM NaCl, 10 mM imidazole, pH 8)

10X stock Phosphate buffer pH 8   10 ml (1X)

1M Imidazole stock   10 ml (10 mM, reduces non-specific binding of proteins)

14.3M BME stock   0.14 ml (2 mM)

pH was adjusted to 8 , filtered (0.22 μm) and autoclaved

c) Ni-IDA Elution Buffer (for 100ml)

(20 mM NaH_2PO_4/Na_2HPO_4, 100 mM NaCl, 20-250 mM Imidazole, pH 8, 2 mM BME)

10X stock Phosphate buffer pH 8   10 ml (1X)

1M Imidazole stock   2ml (20 mM), 10ml (100 mM), 25ml (250 mM)

BME (14.3 M)   0.14 ml (2 mM)

pH was adjusted to 8, total volume was made to 100 ml, filtered (0.22 μm) and autoclaved.

3.2.5.2 Amylose column purification buffers

a) Binding buffer or column equilibration buffer

1X phosphate buffer

b) Elution buffer for 100 ml

(20 mM NaH_2PO_4/Na_2HPO_4, 100 mM NaCl, pH 8, 10 mM maltose, 2 mM BME)

10X stock Phosphate buffer pH 8   10 ml (1X)

0.5 M Maltose (stock)   2 ml (10 mM)

Miili Q   88 ml

Note: Filtered using 0.22 μm

3.2.5.3 5X SDS sample loading buffer (10 ml)

(250 mM Tris-HCl pH 6.8, 10% SDS, 0.5% BME, 30% glycerol)

1M Tris-HCl pH 6.8   2.5 ml from stock 1M

SDS   10g

Glycerol   3 ml

BME   0.5 ml from stock 14.3M

Bromophenol blue   0.02 g

Milli Q   4 ml

3.2.5.4 30% acrylamide

 (29.2% Acrylamide, 0.8 % N'N'-bis-methylene-acrylamide)

Acrylamide   29.2 g (29.2%)

N'N'-bis-methylene-acrylamide   0.8 g (0.8%)

3.2.5.5 SDS-PAGE Running Buffer (for 1 L)

(25mM Tris, 192mM glycine, pH 8.3, 1% SDS)

Tris Base   3.02 g (25mM)

Glycine   14.4 g (192mM)

Miili Q   1 L

No need to adjust pH

3.2.5.6 Staining / Destaining solution (for 1L)

(50% water, 40% methanol, 10% acetic acid, 0.1% Coomassie blue R-250)

Methanol   400 ml

 Acetic Acid (glacial)   100 ml

Milli Q   500 ml

Coomassie blue R-250   1g

Destaining solution is the same, minus the Coomassie blue.

3.2.5.7 Tris-Tricine SDS-PAGE buffers

a) 10X cathode Buffer (upper buffer)

(1 M Tris, 1 M Tricine, 10% SDS)

Tris base   121.1 g

Tricine   179.2 g

SDS   10 g

Milli Q   1 L

b) 10X anode buffer (lower tank buffer)

(2 M Tris-HCl, pH 8.9)

Tris base   242.2 g

pH was adjusted to 8.9 and volume made to 1 L with Milli Q

c) Tris-Tricine gel buffer

(3M Tris-HCl, 0.3% SDS, pH8.45)

Tris base	182 g
SDS	0.9 g

pH was adjusted to 8.9 and volume made to 300 ml with Milli Q

3.2.5.8 1X Transfer Buffer (for 1 L)

(25 mM Tris, 192 mM glycine, pH 8.3, 20% methanol)

Glycine	14.4 g (192 mM)
Tris Base	3.02 g (25 mM)
Milli-Q	0.8 L
Methanol	200 ml (20%)

Note: No need to adjust pH

3.3 Methods

3.3.1 Primer reconstitution

All the primers used were synthesized from Sigma and were received as a lyophilized nucleic acid pellets (not visible with naked eyes). The primer pellet was centrifuged at 10,000 rpm for 1 min. Primers were suspended in 10 mM Tris, pH 7.5 or autoclaved Milli Q water, pH 7 to obtain stock concentration of 500 µg/ml. Reconstituted primers were stored at -20° C. The working concentration of 125 ng/µl was prepared. Detailed lists of primers used in this thesis are provided in **table 3.3.1**.

HtrA2 domains	Primer sequence 5'-3'
Serine protease domain (SPD)	Forward (F)-**CATATG**GGATGTGGTGGAGAAGAC Reverse (R)-**CTCGAG**AAACTCTCGAAGACG
Serine protease + PDZ domain (SPD-PDZ)	F- **CATATG**GGATGTGGTGGAGAC R-**CTCGAG**CTCAGGGGTCAC
N-terminal + serine protease domain (N-SPD)	F-**CATATG**GCCGTCCCTAGCCCG R-**GAATTC**TCAAACTCTCGAAG
PDZ domain	F- **CATATG**CGGCGCTACATTGGGGT R-**CTCGAG**CTCAGGGGTCAC

HtrA2 mutants	Primer sequence 5'-3'
Y295W	GAAGATGTT**TGG**GAAGCTGTTCG
N48W	CCTATCTCG**TGG**GGCTCAGGATTC-
F16D	GTCAGTACAAC**GAC**ATCGCAGATGTG
M190R	GAACACCAGG**AAG**GTCACAGC
F208C	TCTTCGAGAG**TGT**CTGCATCGTG
S173A	CAGCTATTGATTTTGGAAACTCT

Pea15 deletion constructs	Forward primer sequence 5'-3'
Δα (1- 3)	GATATCGTCGACGGATCCGAGATCACTACAGGCAGTG
Δα (1- 4)	GATATCGTCGACGGATCCAACAAGCTGGACAAAG
Δα (1- 5)	GAT ATCGTCGACGGATCCTCCCGCCGTCCTGACCT
Δα (1- 6)	GATATCGTCGACGGATCCTCAGAGGAGGATGAGCTG

Δα (5,6)	CTGGACAAAGACAACTCAGAGGAGGATGAG
DED (ΔC-terminal)	GAACCCGTGTGCTGCACCACCACTGAG
Pea15 cleavage site mutants	**Forward primer sequence 5'-3'**
V80D	CTATGGTG**GAC**GACTACAGAA C
V80F	CTA TGGTG**TTT**GACTACAGATTCCGTGTGC
D81A	CTATGGTGGTT**GCC**T ACAGAACC
E63A	TCCTACATT**GCG**CACATCTTTG
Y62D	CAACCTCTCC**GAC**ATTGAGCAC
V79D	CTCACTATG**GAC**GTTGACTAC
H65D	CTACATTGAG**GAC**ATCTTTGAG
Y82D	GACGTTGAC**GAC**AGAACCCG
	Pea15 binding site mutants
E68A, R71A	CATCTTT**GCT**ATATCC**GCC**CGTCCTGAC3
D93A, D96A	CAGAGGAG**GCT**GAGCTG**GCC**ACCAAGC
R83A	GGTTGACTAC**GCA**ACCCGTGT

Table 3.3.1 *List of HtrA2 and Pea15 primers. Restriction sites and mutations are highlighted in bold. Reverse primer is the complementary of the forward primer*

3.3.2 Determination of DNA concentration

The absorbance of the DNA samples at 260 nm was measured with a micro-volume UV-Vis spectrophotometer (NanoDrop, Model-ND 1000) and the concentration was calculated according

to the Lambert Beer Law. The ratio of absorptions at 260 nm versus 280 nm was used to assess the purity of the sample with respect to protein contamination. For a pure nucleic acid sample, the 260:280 ratio should be around 1.8-2.0.

3.3.3 Polymerase chain reaction (PCR)

All PCR amplifications were done using pfu turbo polymerase (Stratgene kit) with proofreading activity. For sub cloning, the gene of interest was PCR amplified using gene specific forward and reverse primers. For site directed mutagenesis (SDM) plasmid with gene of interest was amplified using the forward and reverse primer with the desired mutation. In all SDMs, reverse primer was complementary sequence of the forward primer. The primers were designed using '*primer-X*' software and '*oligoanalyser*' tools. The parameters taken under consideration for designing primers are primer length: 18-24 nucleotides, GC content: 40-60%, Tm: 50-65 °C. A typical PCR reaction composition is as follows:

Reagents	Volume (µl)
Autoclaved Milli Q water, pH 7.0	15.5
10 X Pfu buffer	2
10 mM dNTPs	0.5
Template DNA (60 ng)	1
Forward primer (125 ng/µl)	0.5
Reverse primer (125 ng/µl)	0.5
Pfu enzyme (1unit)	0.5
Total Volume	20

Typical cycling steps for the PCR are

Initial denaturation	95 °C, 5 min
denaturation	95 °C, 30 sec
Annealing temperature	53 °C, 55 sec
Elongation	71 °C, 10 min (elongation time depends on size of the DNA and processivity of polymerase)
Final extension	72 °C, 10 min
Repeat step 2 to 4 for 25 cycles	for gene specific amplification 25 cycles, and for SDM 18 cycles were considered

For SDM, amplified PCR products were treated with DpnI enzyme (Fermentas) at 37 °C to degrade the parental template. DpnI is an endonuclease which would specifically target the methylated parental DNA strands. The digested PCR product was then transformed in *E. coli* DH5α cells. Plasmids were isolated from colonies and sequence of the desired mutation was confirmed using the automated DNA sequencing facility at ACTREC.

3.3.4 Agarose gel electrophoresis of DNA

0.8 – 1 % agarose was prepared in 1X TAE and boiled using microwave oven. Solution was allowed to cool to ~50-60 °C and ethidium bromide (0.5 µg/ml) was added to enable fluorescent visualization of the DNA fragments under UV light. The agarose solution was mixed thoroughly and poured in a gel casting tray with comb. The gel was allowed to polymerize for 20-30 mins. The DNA samples as well as DNA size-ladder in the range of 250–10,000 bp (Fermentas) were

loaded along with the 1X DNA loading dye. The samples were resolved at 100 volts for 30-50 min. The DNA bands were analyzed under UV 365 nm followed by documentation (UVP, Bioimaging Systems) and visualization (LaunchVision Works LS software) fo gel.

3.3.5 Restriction digestion reaction

Restriction digestion was performed using desired enzymes to prepare the vectors and inserts for cloning. All restriction digestion reactions were carried out at 37 °C for 1-4 hours using the supplied buffers (Fermentas). After successful restriction digestion of the insert and the vector, both were purified by gel extraction (Gel Extraction Kit, Sigma). A typical restriction digestion reaction conditions are:

10X buffer (Tango/FD)   2µl (1X)

DNA template   10 µl (2-4 µg)

Restriction enzyme 1 unit   1 µl

Autoclaved MQ water pH, 7.0   7 µl

Final Reaction Volume   20 µl

3.3.6 Cloning/Ligation

Ligation was set up using T4 DNA ligase supplied with 10X ligation buffer (Fermentas). For cloning blunt end PCR products, pJET cloning kit (Fermentas) was used and ligation was carried out according to the manufacture's protocol. The vector and PCR product were mixed in 1:3 molar ratios and ligated at 22 °C for 30 min. For cohesive-end cloning, restriction digested vector and insert were gel eluted and mixed in molar ratios of 1:3 or 1:6 and ligated using T4 DNA ligase at 22 °C for 3 hrs or 16 °C for 12 hrs.

Vector to insert molar ratio was calculated using formula:

$$\frac{\text{Vector concentration (ng)}}{\text{Vector size (bp)}} = \frac{\text{Insert concentration (ng)}}{\text{Insert size (bp)}}$$

$$\text{Insert concetration (ng)} = \frac{\text{Vector concentration (ng) X Insert size (bp)}}{\text{Vector size (bp)}}$$

The above equation is for 1:1 molar ratio of vector: insert concentration. For 1:3 molar ratio, 3 times the insert concentration was taken.

Composition for the ligation reaction is as follows:

Vector DNA concentration	60-80 ng
Insert concentration	Calculated from the above formula
10X T4 DNA ligase buffer	2 μl
T4 DNA ligase	1μl
Autoclaved water	Adjusted to total volume of 20 μl

3.3.7 Plasmid construction

3.3.7.1 HtrA2 constructs

Clone of mature HtrA2 construct (Δ133) comprising residues 134-458 in bacterial expression vector (pET-20b) with a C-terminal His_6-tag was obtained from Addgene **(Figure 3.1)**. Different HtrA2 domains, such as serine protease domain (SPD, residues 19–210), serine protease + PDZ domain (SPD-PDZ, residues 19–210) and PDZ (residues 226-325) domain were sub-cloned between Nde-1 and Xho-1 restriction sites of pET-20b vector. N-SPD, comprising N-terminal and serine protease domains (residues 1–210) of HtrA2 was sub cloned between Nde-1 and EcoR1 site of pMAL-c5E-TEV vector (NEB) **(Figure 3.1)**. For the ease of purification, His_6 was

introduced into the C-terminal of pMAL-c5E-TEV-(N-SPD) clone using site-directed mutagenesis. Several mutants of HtrA2 (S173A, N48W, Y295W, F208C, M190R) were generated using site-directed mutagenesis. Sequences of all HtrA2 variants were confirmed by automated DNA sequencing facility at ACTREC.
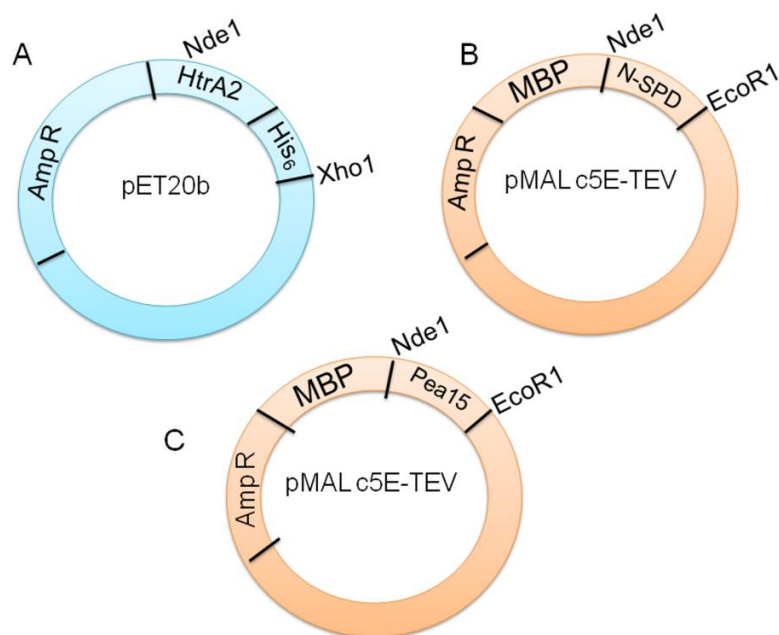
Figure 3.1. HtrA2 and Pea15 constructs. *A) HtrA2 construct in pET20b Vector with C-terminal His6 tag. B) N-SPD construct in pMAL c5E Vector with N-terminal MBP (maltose binding protein) tag. C) Pea15 construct in pMAL c5E Vector with N-terminal MBP (maltose binding protein) tag*

3.3.7.2 Pea15 constructs

Full length Pea15 (1-130 amino acids) from pGEX 2T was sub cloned in to the BamH1 and EcoR1 restrictions sites of pMALc5E- TEV vector (**Figure 3.1**). A C-terminal His-tag was introduced in this vector by site-directed mutagenesis, to facilitate protein purification. Different deletion constructs of Pea15 such as DED (ΔC- terminal, residues 1-86 aa), Δα(1-3), residues Δα(1-4), Δα (1-5), Δα(5,6) and C-terminal region (ΔDED, residues 86-130aa) were generated

with the Quick change site-directed mutagenesis kit (Stratagene). Several mutants of Pea15 (E68A, R71A, R83A, D93A, D96A, Y62D, I63A, E64A, H65D, RV79D, V80D, V80F, D81A, Y82D) were generated using site-directed mutagenesis. The resulting mutations were confirmed by DNA sequencing.

3.3.8 Transformation

The ultra-competent E. *coli* DH5α cells from -80 °C were thawed on ice. 10 µl of the ligation mixture or 5 ng of plasmid DNA was added to an aliquot of competent cells and incubated in ice for 30 min. The cells were given heat shock at 42 °C for 90 sec and incubated immediately in ice for 2-3 min. After heat shock, 750 µl of LB medium was added to the tube and incubated at 37 °C for 45 min with vigorous shaking (200-250 rpm). After 45 min cells were centrifuged at 5000 rpm for 3 min. The supernatant was discarded and 100 µl of fresh LB was added to the tube. Pellet was re-suspended, plated on LB plate with appropriate antibiotic and incubated overnight (16 hrs) at 37 °C.

3.3.9 Bacterial protein expression and purification

3.3.9.1 Sterilization

Bacterial culture media and solutions were sterilized by autoclaving by heating at 120 °C with a pressure of 120 lbs for 20 min. Heat sensitive solutions were sterile filtered with a 0.22 µm filter.

3.3.9.2 Growth conditions

 All recombinant proteins were expressed either in *E. coli* BL21 (DE3) or BL21 (DE3) pLysS. These strains lacks the Lon and OmpT proteases and carries a chromosomal copy of the T_7 RNA

polymerase under the control of lacUV5 promoter (inducible by IPTG) and therefore can conveniently express genes driven by the T7 promoter. Additionally, BL21 (DE3) pLysS was used for expression of toxic genes. The strain contains a chloramphenicol resistant pLysS plasmid which encodes for T7 lysozyme to prevent basal or leaky expression.

A single, transformed, isolated colony of expression host was inoculated in 10 ml LB medium and grown overnight at 37 °C with constant shaking at 200-250 rpm. 10 ml inoculum was further inoculated in 1 litre LB broth in a ratio of 1:100. The culture was grown till the $O.D_{600}$ reached 0.6-0.8. Cells were then induced with 0.3 mM isopropyl-D-thiogalactoside (IPTG) and incubated at 18 °C for 16 hrs. Culture was harvested by centrifugation at 5,000 rpm for 10 min at 4 °C. The bacterial pellets were stored at -80 °C until further use.

3.3.9.3 Ni-IDA agarose affinity chromatography

Ni–IDA affinity purification method was used to purify His_6 tagged proteins. Ni–IDA agarose beads (Biotex) of 2 ml were taken in 1X 10 cm econo column (Millipore). Beads were washed with 1X washing/equilibration buffer with at least three column volumes under native conditions. Equilibrated Ni-IDA beads were then incubated with protein lysate at room temperature (22 °C) for about 30 min. After incubation, unbound lysate (flow through) was collected separately. Beads were washed with 3 column volumes of washing buffer. His_6 tagged proteins were eluted with elution buffer containing imidazole gradient (20-500 mM).

3.3.9.4 Amylose affinity chromatography

Amylose affinity purification method was used to purify the protein tagged with MBP. Amylose beads (Novagen) of 2 ml were taken in 1X 10 cm econo column (Millipore). Beads were washed

with 3 column volumes of 1X washing/column equilibration buffer. Equilibrated Amylose beads were incubated with protein lysate at room temperature (22 °C) for about 30 min on rocker with gentle agitation. After 30 min, flow through was collected and beads were washed with 3 column volumes of wash buffer. Bound proteins were eluted using elution buffer containing 10 mM maltose.

3.3.10. General protocol for protein purification

3.3.10.1 Purification of HtrA2 variants

Mature HtrA2 with C-terminal His$_6$-tag in pET-20b was expressed in *E. coli* strain BL21 (DE3) pLysS. Protein expression was induced by culturing cells at 18 °C for 20 hrs in presence of 0.2 mM IPTG. Cells were lysed by sonication and the centrifuged supernatants of HtrA2 variants were incubated with pre-equilibrated Ni-IDA beads for 1 hr at room temperature. Flow through was collected and beads were washed with 3 column volumes of wash buffer. Elution was performed using an imidazole gradient (20–300 mM) in elution buffer. Eluted protein was further purified using gel permeation chromatography. N-SPD was purified using amylose resin where the bound protein was eluted using 10 mM maltose and was subjected to TEV protease cleavage to remove maltose binding protein (MBP). N-SPD was further separated from MBP using Ni-affinity chromatography. All purified proteins were analyzed by SDS-PAGE for purity. The fractions with >95% purity were dialyzed against phosphate buffer and stored in aliquots at −80 °C until use.

3.3.10.2 Purification of Pea15

Pea15 constructs with N-terminal MBP and C-terminal His$_6$ tags in pMALc5E- TEV vector were expressed in *E. coli* strain BL21 (DE3) pLysS. Protein expression was induced by culturing cells

at 18 °C for 20 hr in presence of 0.3 mM isopropyl-1-thio-D-galactopyranoside. Cells were lysed by sonication and centrifuged at 10,000 rpm for 30 min. Pea15 supernatant was then incubated with pre-equilibrated amylose resin at 4 °C for 1hr. Beads were washed with 3 column volumes of wash buffer. Elution was performed using 10 mM maltose and was subjected to TEV protease cleavage to remove MBP. Pea15 was further separated from MBP using Ni-IDA affinity chromatography. All purified proteins were analyzed by SDS-PAGE for purity.

3.3.10.3 Gel filtration chromatography of HtrA2 variants

Gel filtration or size exclusion chromatography is a separation technique based on size and volume of macromolecules. Relatively small molecules can diffuse into the pores of column matrix whereas large molecules will be prevented by their size from diffusing into the pores thus migrate faster. Gel filtration displays a method that can be applied to purify proteins and also to determine the molecular mass of proteins.

Molecular weights of HtrA2 variants were estimated by size exclusion chromatography. 1 ml aliquots of protein samples (2-3mg) were run on a Superdex 200 10/300 HR column (GE Healthcare) pre-equilibrated with phosphate buffer comprising 20 mM Na_2HPO_4/NaH_2PO_4, 100 mM NaCl, pH 8. Proteins were eluted with the same buffer at a flow rate of 0.5 ml/min. The standards used for calibration were Alcohol dehydrogenase (ADH), Bovine serum albumin (BSA), Lysozyme and Maltose binding protein (MBP). All standards except for MBP that was lab purified were purchased from Sigma. Elution volume (Ve) / void volume (V_0) versus log of molecular weights of standards were plotted to generate the calibration curve from which molecular weights of HtrA2 variants were calculated.

3.3.11 Determination of Protein concentration

Two distinct methods have been used to measure the protein concentration of a given sample.

3.3.11.1 Bradford protein assay

The Bradford protein assay is a spectroscopic analytical procedure used to measure the concentration of protein in a solution (104). The assay is based on the observation that the absorbance maximum for an acidic solution of coomassie brilliant blue G-250 shifts from 465 nm to 595 nm when binding to protein occurs. 5 μl of the BSA standards (1, 0.5, 0.25, and 0.125 mg/ml) were mixed with 200 μl of Bradford reagent (1:4 diluted, Bio-Rad) in triplicates in a 96-well plate. Readings were taken with ELISA plate reader (Spectra Max 790) at 595 nm using SoftMaxPro 4.6 software. Standard graph was plotted by taking absorbance on Y-axis and concentration of protein on X-axis. Concentration of protein of interest was extrapolated from the standard curve.

3.3.11.2 Absorbance at 280 nm

The Absorbance of a protein sample at 280 nm was measured with a Nanodrop. The concentration was calculated according to the Beer-Lambert law: $A = \varepsilon \times c \times l$, where A is the absorption at 280 nm, 'ε' is the molar exctinction coefficient, 'c' the molar concentration of the protein solution and 'l' is the cell length of the cuvette. Molar extinction of proteins was calculated according to the Edelhoch method (105). The equations to calculate the protein concentration are as provided below:

1) Protein concentration (mg/ml) = Absorbance $_{280}$/ ε X Molecular weight of protein (Daltons)

2) Protein concentration (μM) = Absorbance $_{280}$/ ε X 1000000

3.3.12 SDS polyacrylamide gel electrophoresis (SDS-PAGE)

SDS-PAGE was used for the electrophoretic separation of proteins according to the method of Laemmli. The stacking and the separating gel were prepared as described below (table 3.8). The protein samples were mixed with 5x sample buffer, boiled for 5 min and loaded onto the gel. The electrophoresis was performed at 100 V for about 60 min. The gel was stained with coomassie brilliant blue for 10-15 min. The gel was then destained overnight in the destainer and finally preserved in 10% acetic acid and documented.

3.4. Biophysical studies

Biophysical techniques those have been used in this thesis to structurally characterize a given protein are:

3.4.1 Circular Dichroism (CD) spectroscopy

CD spectroscopy is used to determine the secondary and tertiary structural properties of biomolecules. Circular dichroism is the property of chiral molecules to absorb the right and left components of circularly polarized light to a different extent. Far UV CD spectra in the range (260-190 nm) was used to analyze different secondary structural components of the protein such as alpha helix, parallel and antiparallel beta sheet, turn, and others. Absorption minima at 208 and 222 nm indicate α-helical structure, whereas a minimum at 218 nm is a characteristic of β-sheets. Proteins with greater disordered secondary structural elements or random coil regions are characterized by a low elipticity at 210 nm and negative band near 195 nm.

Far-UV CD scans of HtrA2 and Pea15 variants were acquired using a JASCO J 815 spectropolarimeter (JASCO) using a quartz cell with 1-mm path length. Far-UV CD spectrum (260-190 nm) was recorded using a bandwidth of 1 nm and an integration time of 1s, with proteins of 10 µM concentrations. Each spectrum was an average of 5 scans, with a scan rate of 20 nm/min. Thermal stability of proteins were assessed by monitoring the CD spectrum with increasing temperature. A Far-UV CD spectrum was collected in a temperature range of 20 ℃-90 ℃ with an increment of 2 ℃/min. At each data point, the sample was equilibrated for 3 mins. Elipticity corresponding to 222 nm at different temperatures was obtained for calculation of melting temperature (Tm).

Data analysis

The CD data was represented in the form of the mean residual elipticity (MRE or [θ]) given as deg.cm^2.mol^{-1}. Elipticity obtained from the CD spectra was converted to mean residue elipticity using the formula (106):

$$[\theta]MRE = (\theta \times MRW)/ (10 \times c \times d) \tag{1}$$

Where, MRW (Mean residue weight) = Molecular weight / (N–1)

'c' is concentration of protein (mg/ml), 'd' is the path length in cm and 'N' is the number of amino acids.

3.4.2 Fluorescence spectroscopy

Fluorescence is a phenomenon in which a molecule absorbs a lower wavelength photon, undergoes electronic excitation, and then emits longer wavelength. Fluorescence spectroscopy is used for studying dynamics, protein unfolding and biomolecular interactions. The intrinsic

fluorescence of a folded protein is a combination of the signal from individual aromatic residues (Phe, Tyr, Trp) with the major contribution from tryptophan residue.

Fluorescence emission of HtrA2 and Pea15 variants (2 µM) were measured by Fluorolog-3 spectrofluorometer (Horiba Scientific) using a quartz cell with 3 mm path length cuvette. Fluorescence spectra of 2 µM protein solutions were recorded with 295 nm excitation followed by emission between 310-400 nm using a 5 nm excitation and emission slit widths with an integration time of 0.1s.

3.4.3 Acrylamide quenching

Fluorescence quenching is a process which decreases the intensity of the fluorescence emission in presence of a quencher. The accessibility of fluorophores in a protein molecule can be measured by extent of quenching. Fluorescence quenching studies are useful to obtain information about the conformational and dynamic changes of proteins. Different type of quenchers used for these studies are acrylamide (neutral), KI (negatively charged) and CsCl (positively charged).

Steady state fluorescence quenching measurements were carried out using a Fluorolog-3 spectrofluorometer that is attached to a water bath. Stock protein solutions were dialyzed against 20 mM phosphate buffer, 100 mM NaCl, pH 8. A stock solution of 5 M acrylamide (external quencher) was prepared in the same buffer. Fluorescence quenching experiments were performed between 30-65 $^{\circ}$C at 5 ºC interval. Protein solutions (2µM) were diluted from the stock, and 5M acrylamide was added to the final concentration as shown in **table 3.2**. Protein was pre-incubated for 15 min at each respective temperature and fluorescence emission scans were taken after addition of quencher with excitation at 295 nm. The values of fluorescence intensity were

corrected for dilution effects, residual emission, Raman scattering, and absorption of light by acrylamide (107).

Concentration of acrylamide required (M)	Total volume of protein solution (μl)	Volume added from 5M acrylamide stock (μl)	Final concentration of acrylamide (M)	Total volume after adding acrylamide (μl)
0	200	0	0	200
0.05	200	2	0.049	202
0.10	200	2	0.098	204
0.15	200	2	0.145	206
0.20	200	2	0.192	208
0.25	200	2	0.238	210
0.30	200	2	0.283	212
0.35	200	2	0.327	214
0.40	200	2	0.370	216
0.45	200	2	0.412	218
0.50	200	2	0.454	220

Table 3.2. Protocol for acylamide quenching

Data analysis

Fluorescence emission maxima of respective proteins were used for data analysis. Data were then analysed using the Stern–Volmer relationship as shown in equation 2.

$$F_0 / F = 1 + K_{SV} [Q], \tag{2}$$

For graph with upward curvature, modified Stern–Volmer relationship was used:

$$F_0/F = (1 + K_D[Q]) \exp([Q]VN/1000) \tag{3}$$

where, F_0 and F, are fluorescence intensities in absence and presence of quencher respectively,

[Q] is concentration of quencher (molar), K_{SV} is the Stern–Volmer quenching constant, K_D is dynamic quenching constant, 'V' is volume of sphere and 'N' is the Avogadros number.

The procedure to fit these equations in Kaleidgraph is as follows:

a) Go the gallery and select the scatter

b) Plot the graph

c) Go to curve fit and type the formula as shown below:

For linear equation:

$$(1 + m1 * m0); m1 = 10 \text{ (m1=any variable form 1-1000)} \tag{4}$$

m1= K_{SV} value for dynamic quenching constant

For upward curve:

$$(1 + m1 * m0) * \exp(m0 * m2 * 25.2 * 10 \wedge 20); m1 = 1000; m2 = 10 \wedge -30 \tag{5}$$

 m1= K_{SV} value for dynamic quenching

m2= K_{SV} value for static quenching

3.4.4 Förster resonance energy transfer (FRET)

FRET is a distance-dependent interaction between the electronic excited states of two fluorophores in which excitation is transferred from a donor molecule to an acceptor molecule without emission of a photon. FRET efficiency depends on physical parameters such as distance and spectral overlap between donor and acceptor. FRET is an important technique for investigating a variety of biological phenomena such as structure and dynamics of proteins, and receptor/ligand interactions.

The donor and acceptor pair chosen for our FRET studies were tryptophan (Y295W mutants) and 5-((((2-Iodoacetyl) amino) ethyl) amino) Naphthalene-1-Sulfonic Acid (IAEDANS), a

sulfhydryl (SH)-specific fluorescent probe respectively. To 50 μM protein solutions (Y295W, F208C mutants) in phosphate buffer and 5 fold molar excess of IEADANS (Sigma) were added and incubated in dark for 16 hrs at 4 °C. To remove unbound label, protein was passed through Ni-IDA affinity column and labelled protein was eluted using imidazole. Labelling efficiency was assessed using equation:

$$A/\varepsilon \times M/c = \text{Labelling efficiency (LE)} \tag{6}$$

where 'A' is the absorbance of IAEDANS at 336 nm, ε is the molar extinction coefficient of the IAEDANS ($5700\ M^{-1}cm^{-1}$), M is molecular weight of protein, and 'c' is the protein concentration. Fluorescence emission was measured over a temperature range of 30-65 °C at 5 °C intervals. 2 μM proteins were excited at 295 nm, and emission was measured over a wavelength range of 310-575 nm with an excitation and emission slits at 5 nm.

Data analysis

Fluorescence resonance energy transfer efficiency was calculated using the following equation (108):

$$E = 1-(F_{DA}-F_D(1-f_A))/F_D f_A \tag{7}$$

Where, E is the calculated efficiency, F_{DA} and F_D are blank corrected emission of donor (tryptophan) in presence and absence of acceptor (IAEDANS) respectively, and f_A is fractional occupancy (labelling efficiency calculated from equation 1) of the acceptor site. Donor-Acceptor (D-A) separation was obtained using the following relationship,

$$R = (E^{-1}-1)^{1/6} R_0 \tag{8}$$

where, R is the D-A separation and R_0 is the Förster critical distance. The value for R_0 was taken as 22 Å (109).

3.5 Biochemical studies

3.5.1 Affinity pull down studies

Affinity pull down studies help to understand protein-protein interaction in *in vitro* and *in vivo*. Recombinant MBP-fused Pea15 was lysed in a lysis buffer containing (20 mM Na_2HPO_4/NaH_2PO_4, 100 mM NaCl, pH 8, 0.1% Triton X100). 10 µg of Pea15 lysate was incubated with 10 µl of amylose beads (Invitrogen) for 1hr at 4 °C. Beads were then washed extensively with the phosphate buffer. After washes, 100 µg of purified recombinant HtrA2 variants were incubated with amylose bound MBP fused Pea15 proteins (~10 µg), in a final volume of 200 µl in wash buffer. After overnight incubation under agitation at 4 °C, beads were extensively washed for four times with wash buffer and boiled in 30 µl Laemmli buffer. Samples were then analyzed by 15% SDS-PAGE and coomassie blue staining.

3.5.2 *In silico* Docking studies

In silico docking studies are computer assisted programme used to predict the binding interface in protein–protein interactions. Docking studies between the HtrA2 (receptor) and Pea15 (ligand) were performed using the *ClusPro* 2.0, fully automated web server for the prediction of protein–protein interactions (110). First, it runs PIPER, a rigid body docking program, based on a novel Fast Fourier Transform (FFT) docking method with pair-wise potentials. Second, by using a clustering technique for the detection of near native conformations and by eliminating some of the non-native clusters, the 1000 best energy conformations were clustered, and the 30 largest clusters were retained for refinement. Third, by short Monte Carlo simulations, stability of these clusters is analyzed, and by the medium-range optimization method SDU (Semi-Definite programming based Underestimation), the structure refinement was done. Total 40 docked

models based on several parameters such as electrostatic, hydrophobic, van der Waal-electrostatic and balanced interactions were generated (10 docked conformations for each type of interaction). The structures based on the balanced type of interaction were studied, as it favors electrostatic, hydrophobic and electrostatic interactions which were preferred for docking. The interactions observed in these docked conformations were visually examined using the software *PyMol*. The binding interface residues were evaluated using the PDBsum generate server with the default cut-offs (111).

3.5.3 Protease assays with β-casein as substrate

Protease activity of different HtrA2 constructs was determined using substrate β-casein (Sigma), a generic substrate of serine proteases. For each 30 μl reaction mixture, 2 μg of respective protein was incubated with 6 μg of β-casein in assay buffer (20 mM Na_2HPO_4/NaH_2PO_4, pH 8.0, 100 mM NaCl, 0.1 mM DTT) at 37 °C for 2.5 hrs and results were analyzed by SDS-PAGE. For all quantitative studies, FITC (fluorescein isothiocyanate) labelled β-casein (Sigma) was used. Fluorescent substrate cleavage was determined by incubating 200 nM of enzymes with increasing concentration (0–25 μM) of β-casein at 37 °C in assay buffer. Proteolytic cleavage was assessed by monitoring increase in fluorescence intensity of unquenched FITC β-casein in a multi-well plate reader (Berthold Technologies) at 485 nm excitation and 535 nm emission wavelengths **(Figure 3.2)**.

Protease activities of HtrA2 variants over a temperature range of 30-65 °C were determined using Fluorolog-3 Spectrofluorometer (HORIBA Scientific). For each 200 μl of reaction mixture, 0.5 μM protein was incubated with 0.6 μM of FITC labelled β-casein substrate in enzyme assay buffer. Prior to the addition of substrate, enzyme was pre-incubated at each respective

temperature for 15 mins and proteolytic cleavage was monitored with excitation at 485 nm followed by 535 nm emission. Initial velocities were calculated at each respective temperature using linear regression analysis. Assays are representative of at least three independent experiments done in triplicate.

Note: FITC β-casein is photosensitive

Data analysis

Graph was plotted by taking time (min) on X-axis and increase in fluorescence intensity on Y-axis. Slope value for each substrate concentration was determined using linear regression analysis. Reaction rates v_0 (μM/min) of unquenched FITC at respective substrate concentration were determined by dividing the slope with 19422 (slope of free FITC standard curve).

The steady-state kinetic parameters were obtained from the reaction rates by fitting data to Michaelis-Menten equation using nonlinear least squares subroutine in *KaleidaGraph* program (Synergy software).
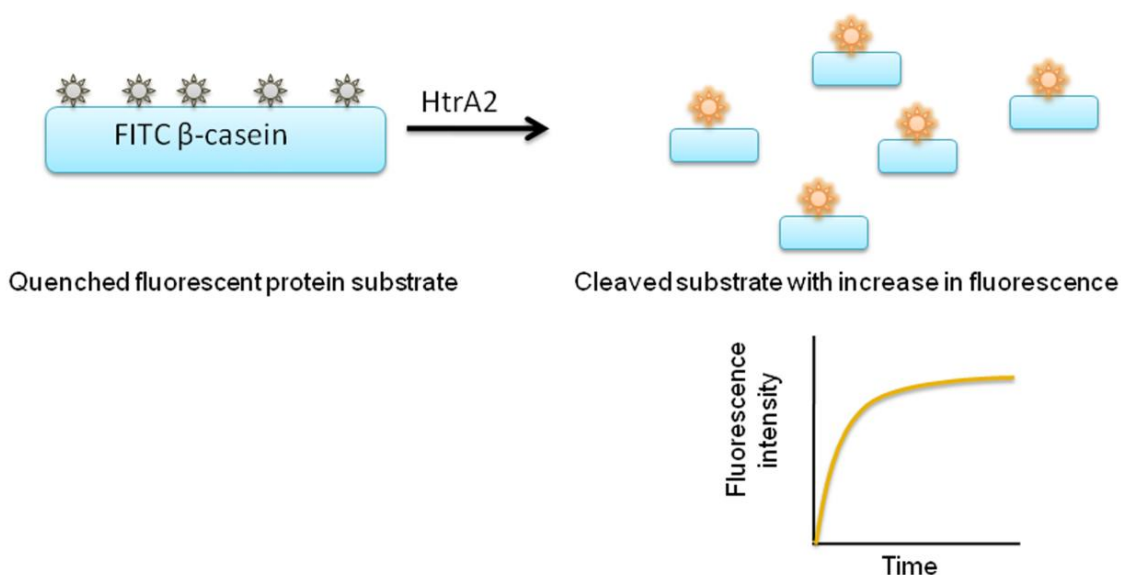
Figure 3.2. Protease assay of HtrA2 using FITC β-casein as substrate*. Proteolytic cleavage of quenched FITC β-casein substrate results in increase in fluorescence intensity*

3.5.4 Protease assays with Pea15 as substrate

HtrA2 protease activity was assayed by incubating 4 μg of recombinant HtrA2 variants with 2μg of recombinant pea-15 constructs in an assay buffer (20 mM Na_2HPO_4/NaH_2PO_4, pH 8, 100 mM NaCl, 0.1 mM DTT) for 0-12 hrs at 37 °C. The reactions were stopped with SDS-sample buffer and boiled for 5 min. The reaction products were analyzed be Tris-Tricine SDS-PAGE at a constant voltage of 90 V followed by coomassie Blue staining. Substrate remaining at 7 hr was quantified by GelQuant.NET by *biochemLabSolutions.com*. All data were normalized relative to the uncleaved Pea15. The obtained values were plotted using the *GraphPad Prism 5* software.

3.5.5 N-terminal sequencing

The proteolytically degraded Pea15 bands were transferred electrophoretically onto a polyvinylidene difluoride (PVDF) membrane (pore size 0.45 μm, Millipore Corporation, Billerica, MA, US) using wet transfer apparatus in 1X transfer buffer at a constant voltage of 20V for 10 hrs. Transferred proteins were stained with 0.2% amido black in 50% methanol, followed by destaining in 50% methanol. The stained fragments were excised from the membrane and were air-dried. The N-terminal five amino acid residues of each fragment were identified using ABI 494 Protein sequencer, Tufts university core facility, Boston.

Chapter 4

Results and Discussion

Chapter 4.1

Characterization of structural properties and conformational stability of HtrA2 and the role of different domains in protein function and specificity

4.2.1 Introduction

High resolution crystal structure of mature unbound form of HtrA2 provides a broad overview of its structural organization and mechanism of activation (10). The trimeric protease has a pyramidal architecture where N–terminal is at the top and PDZ at the base. The core serine protease domains (SPD) are surrounded by C-terminal PDZ domains, which along with the trimeric architecture restrict entry of the substrates to the leading to a low basal activity. It is believed that the PDZ-protease dynamics and their relative orientation modulate HtrA2 activity and hence functions. These observations led to development of an activation model which highlights the role of PDZ in substrate binding and subsequent protease activation (10). The model states that upon substrate binding, PDZ that otherwise shields the protease domain opens up allowing the substrate to enter the binding pocket. While, in the monomeric mutant of HtrA2, PDZ completely collapses on SPD thus restricting substrate entry to the and subsequently rendering it inactive. Although the model provides a basic understanding of HtrA2 activation, it could neither satisfactorily define the roles of trimerization and N-terminal domain in HtrA2 functions nor decipher the dynamics of PDZ-protease crosstalk as electron-density for both the linker and a part of N-terminal region is unavailable in the structural data. Unlike other HtrAs, the substrate binding YIGV (GLGF motif) groove of PDZ domain is buried deep within the protein interior and is blocked by Pro225 and Val226 of SPD in the closed protease conformation (10, 112). Therefore, initial binding at YIGV pocket would demand either an extremely stringent structural signature such as partial substrate unfolding or there might be an alternative mechanism. With a closer look at different biological roles of HtrA2, its wide substrate specificity and putative binding sites on its known available substrates, the former possibility seems unlikely (113). Alternatively, it was shown earlier that activation of HtrA2

occurs allosterically where the signal is relayed via a distal non-canonical substrate binding site with subsequent opening up of the YIGV pocket (71). Here, with an aim at understanding the subtle structural reorganizations and intrinsic conformational dynamics that lead to HtrA2 activation, we dissected its various domains to decipher their roles individually as well as in combination in mediating HtrA2 specificity and functions.

4.1.2 Results

4.1.2.1 Importance of trimerization for HtrA2 activity

4.1.2.1.1 Construction of different HtrA2 domains and variants

Different mutants and variants of HtrA2 were generated to understand the role of critical residues and contributions from different domain combinations in maintaining its overall structural integrity and functions **(Figure 4.1.1A).** It was reported in the literature that N-terminal aromatic residues (Y14, F16 and F123) are crucial for maintaining its trimeric architecture through intermolecular van der Waals interactions (10). One such residue (F16) when mutated to aspartate was found to disrupt these interactions and render the protein monomeric (10, 73). We made the same mutation for our studies to understand the role of trimerization in HtrA2 structure and function. At the same time, this mutant along with N-terminal deleted SPD-PDZ (ΔN-terminal 18 residues) variant was thought to be helpful in understanding the contribution of N-terminal region in structure, stability and formation.

To understand the intimate regulation of protease activity by PDZ domain, we generated a trimeric N-SPD (ΔPDZ) variant that was expected to retain its oligomeric property (intact N-terminal trimerization domain) but with no PDZ interference. M190, a residue at the PDZ-protease interface has been implicated to have a detrimental effect on PDZ plasticity upon

mutation to an arginine due to negative inter-subunit packing. Thus M190R mutant was made to demonstrate the role of this interface residue in relative PDZ-protease orientation, interdomain contacts and its subsequent effect on HtrA2 activity. A monomeric version of N-SPD that is N-SPD(F16D) was generated to understand the importance of N-terminus in HtrA2 structure and stability. This protein upon comparison with N-SPD, mature HtrA2, SPD-PDZ and HtrA2(F16D) would highlight the importance of PDZ in the trimeric HtrA2 structure and role of interdomain interaction if any. SPD (ΔN-terminal + ΔPDZ) was cloned and purified separately to understand the roles of N-terminal region and PDZ domain in proper active-site formation, protein stability and maintaining its structural integrity. It would also demonstrate whether PDZ inhibition might be the sole reason for HtrA2 inactivation.

The subtle structural changes in the protein can be monitored based on the spectral properties of the side chains of aromatic amino acids. In particular, tryptophan has been shown to be a useful probe for studying protein structure and dynamics. Since HtrA2 is devoid of tryptophans, single tryptophan mutants were strategically generated in SPD and PDZ domains (N48W and Y295W) so as to understand and compare spectroscopically the environments surrounding the and PDZ-protease interface respectively **(Figure 4.1.1B)**. N48W was introduced on β2 strand of SPD, in the vicinity of L1 and LD regulatory loops in the region. This tryptophan was expected to be in proximity to F170 of SPD which is an important component of oxyanion hole. The positioning of W48 was chosen in such a way that it reflects the environment of the , the regulatory loops surrounding the pocket as well as the α5 of PDZ which is close to PDZ* of the neighbouring subunit. This tryptophan mutant was thus expected to delineate subtle conformational changes near the region and interdomain cross-talk during HtrA2 activation. Y295W was introduced on α7 of PDZ at the interface between SPD and PDZ domain such that

this tryptophan faces SPD of the same monomer and is very close to the canonical peptide binding (YIGV) groove. It is also in the vicinity of intersubunit linker and is positioned in such a way that PDZ movement away from SPD would expose the tryptophan which will be reflected in its fluorescence emission maxima towards longer wavelength. Thus, these two strategically positioned tryptophans would aid in understanding the conformational changes at the PDZ-protease interface. A cysteine mutation was introduced at SPD, HtrA2(F208C) to examine the distance between PDZ and protease domains by pairing with W295 residue using Förster resonance energy transfer (FRET) studies.
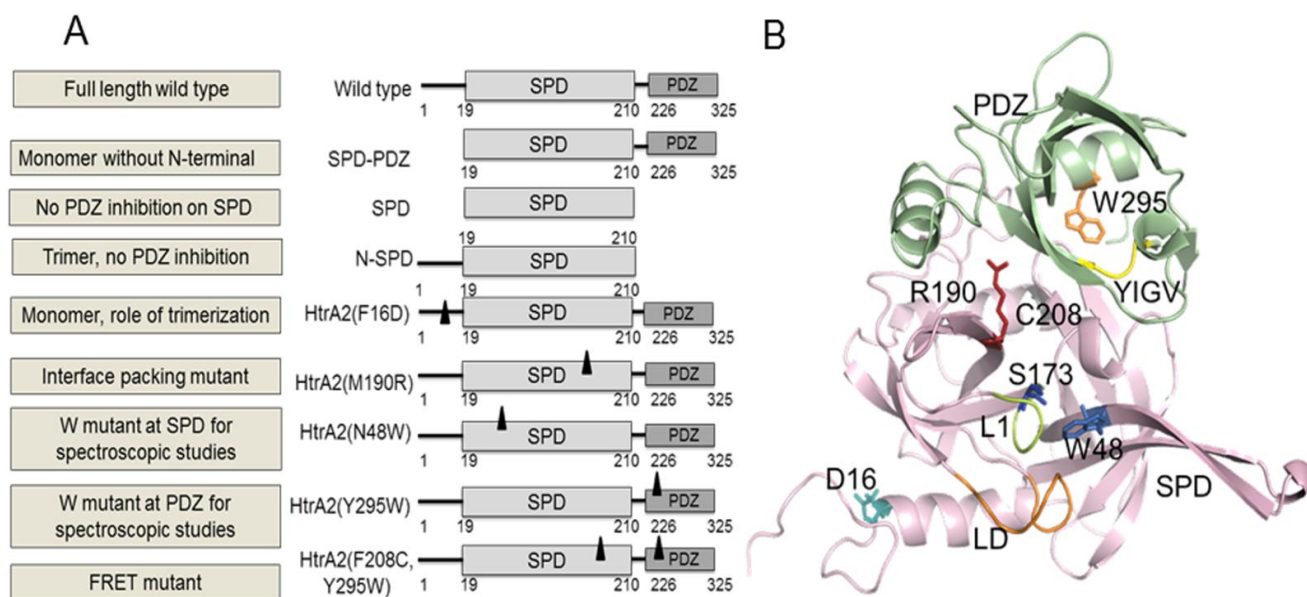
Figure 4.1.1. Representation of different domains and mutants of HtrA2. *A) Schematic representations of different HtrA2 constructs generated for the present study. Light grey boxes indicate protease domain (19-210 residues) and dark grey boxes PDZ (226-325 residues) domain, (—) lines indicate N-terminal region (1-18 residues) and linker region (211-225 residues), and (▲) indicates the position of mutation on the respective domains. B) Ribbon diagram of the crystal structure of HtrA2 (PDB accession number 1LCY). Amino acid substitutions in HtrA2 protease and PDZ domains are shown in stick models. The ribbon diagram was drawn using PyMOL (DeLano Scientific, USA).*

4.1.2.1.2 Role of N-terminal region in oligomerization

Oligomeric properties of HtrA2 variants were estimated to understand the role of N-terminal region mainly F16 in maintaining its trimeric architecture. Elution profile of all HtrA2 variants were monitored using superdex 200 gel filtration column and their respective molecular weights were calculated from the calibration curve generated from protein standards **(Figure 4.1.2A and B)**. The estimated molecular weights of the proteins are shown in **Table 4.1.1** which demonstrates that HtrA2 (wild type) and N-SPD are trimers with intact N-terminal regions. HtrA2(F16D), N-SPD(F16D) and SPD-PDZ represent monomers reiterating the importance of N-terminal F16 in homotrimerization as suggested within the literature. Further gel filtration of HtrA2 tryptophan mutants, HtrA2(Y295W) and HtrA2(N48W) as well as HtrA2(M190R) were performed to look into the effect of these mutations on HtrA2 oligomerization. Estimated molecular weights of tryptophan mutants and HtrA2(M190R) from gel filtration were comparable to the wild-type suggesting the mutations did not affect oligomeric status of the protease.
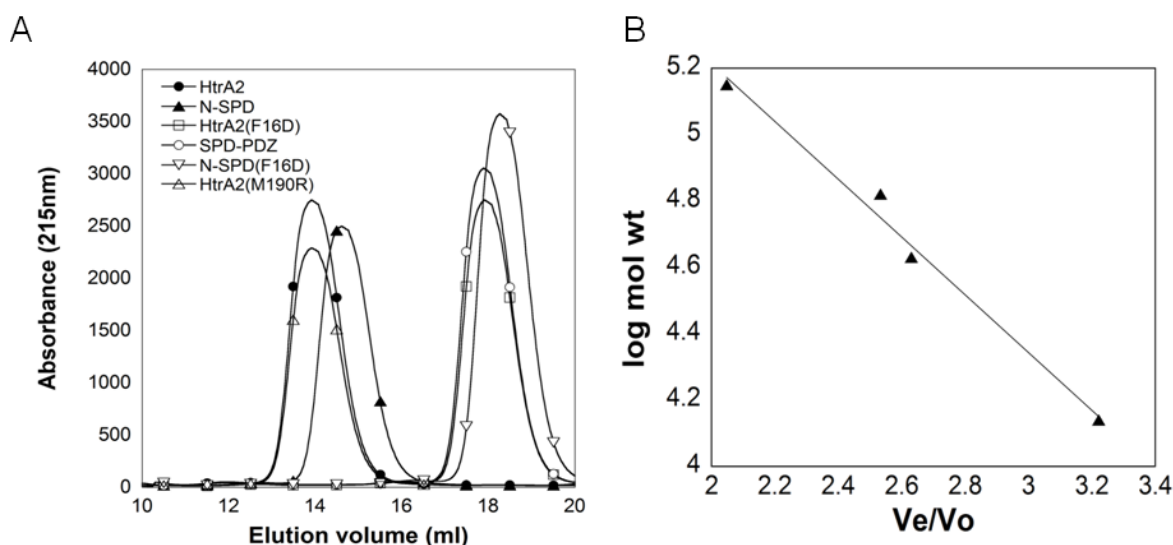
Figure 4.1.2. Oligomeric properties of HtrA2. *A) Elution profile of HtrA2 variants using superdex 200 gel filtration column. B) Calibration curve generated using the protein standards BSA, ADH, MBP, Lysozyme*

Protein	Theoretical molecular weight (kDa) (protparam)	V_e/V_o	Calculated molecular weight (kDa)
ADH	141.00	2.042	
BSA	66.00	2.532	
MBP	43.00	2.631	
Lysozyme	14.40	3.221	
HtrA2(F16D)	36.20	2.722	37.950 (Monomer)
N-SPD	70.30	2.401	73.618 (Trimer)
N-SPD(F16D)	23. 29	2.634	25.456 (Monomer)
SPD-PDZ	34.20	2.732	36.899 (Monomer)
HtrA2 wild type	109.60	2.203	108.798 (Trimer)
HtrA2(M190R)	109.73	2.205	110.796 (Trimer)
HtrA2(N48W)	109.40	2.205	109.797 (Trimer)
HtrA2(Y295W)	109.50	2.206	110.295 (Trimer)

Table 4.1.1. ***Oligomeric properties of different HtrA2 constructs***. *Molecular weights of HtrA2 and its variants were calculated from calibration curve generated using different standard protein molecules (ADH, BSA, MBP and Lysozyme) as described under materials and methods*

4.1.2.1.3 Role of oligomerization and different domains in protease activity

Protease activity of HtrA2, its variants and mutants was studied to understand the role of different domains and critical residues in regulating HtrA2 activity and specificity using a generic serine protease substrate β-casein in both gel and fluorescence based assays. These studies have been designed to reflect protease activity as a consequence of conformational changes due to initial substrate (here β-casein) binding at PDZ domain. In all protease activity studies, mutant, HtrA2(S173A) was used as a negative control. It was observed that HtrA2, N-SPD and HtrA2(M190R) cleaved β-casein but monomeric HtrA2(F16D) showed very less cleavage and other monomeric variants such as SPD and SPD-PDZ variants did not show any protease activity **(Figure 4.1.3A),** thus highlighting the importance of trimerization and also the

N-terminal region in HtrA2 activity. For more quantitative analysis, enzyme kinetics was studied fluorometrically with FITC-labeled β-casein as a substrate and initial velocities (v_0) were calculated **(Figure 4.1.3B)**. Monomeric mutants and variants such as HtrA2(F16D), SPD, N-SPD(F16D) and SPD-PDZ showed very less activity compared to wild type. Tryptophan mutants, HtrA2(Y295W) and HtrA2(N48W) have enzyme activity comparable to the wild-type suggesting the mutations did not affect the active conformation of the protease. Interestingly, contrary to the existing literature report, SPD was found to be completely inactive while HtrA2(M190R) was enzymatically more active than the wild-type. Interestingly, the M190R variant was expected to negatively affect SPD-PDZ packing leading to PDZ collapse on SPD and subsequent loss of activity. These observations suggest that PDZ collapse on protease domain might not be the sole reason for HtrA2 inactivity as proposed by Shi and co-workers in 2002 (10).
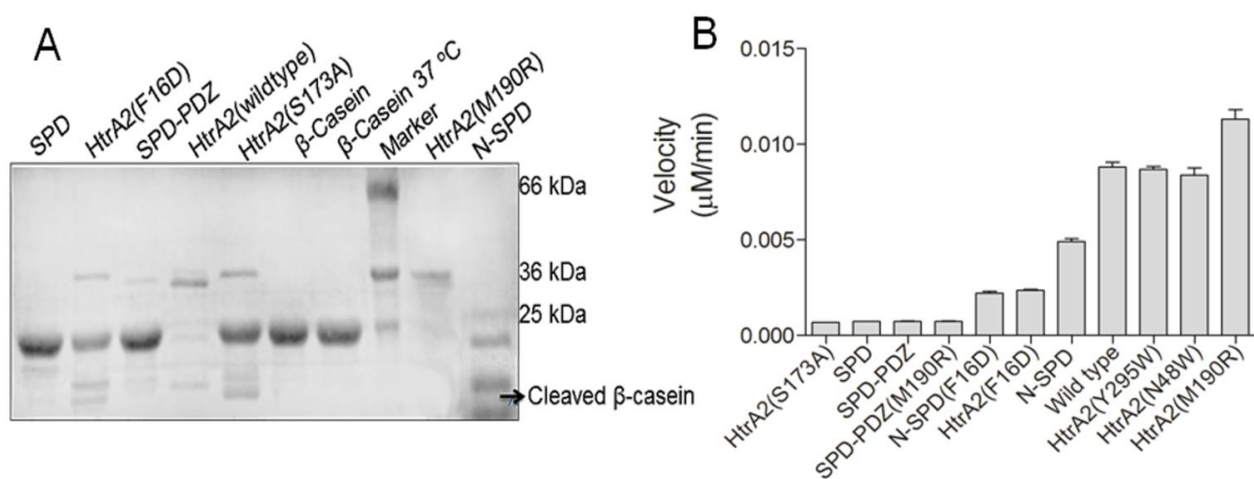
Figure 4.1.3 Comparison of proteolytic activities of HtrA2 and its variants. *A) β-casein cleavage assay for HtrA2, and its variants. β-casein was incubated with respective protein at 37 °C and reaction samples were resolved by 12% SDS-PAGE and visualized by staining with coomassie brilliant blue. B) Initial velocities (v_0) of HtrA2 and its variants calculated using FITC β-casein as substrate. The error bars represent the standard errors (SE) calculated from three independent experiments*

The above observations were correlated with kinetic parameters of HtrA2 and its mutants to delineate the role of these mutations and deletions on substrate binding and catalysis of HtrA2 (**Figure 4.1.3C and Table 4.1.2**). In N-SPD variant, slight decrease in K_m value compared to HtrA2, (3.02 and 4.6 µM) which is representative of increase in substrate affinity suggests greater substrate accessibility that might be due to absence of the surrounding PDZ domains. However, substrate turnover rate or k_{cat} ((0.004/s) and catalytic efficiency or k_{cat}/K_m (1.29×10^3 $M^{-1}s^{-1}$) were found to be 5 and ~3.5 folds less respectively than the wild-type suggesting the importance of PDZ in mediating conformational changes around the active-site that positively influences the rate of catalysis.

With an aim at understanding whether trimeric architecture is crucial for HtrA2 activation, enzymatic parameters for full length monomeric variant, HtrA2(F16D) were analyzed. In this variant, the K_m was found to be two fold higher (9.3 µM), while there is a significant decrease in turnover rate and hence catalytic efficiency (~800 and 1600 folds, respectively). This decrease in substrate binding affinity and catalysis suggests that homotrimerization is a prerequisite for HtrA2 activity and also hints toward the presence of intermolecular PDZ-protease crosstalk for HtrA2 action.

Although literature suggests that HtrA2(M190R) negatively affects packing between SPD and PDZ domains leading to PDZ collapse on SPD and subsequent loss of activity, our studies demonstrate significantly higher initial velocity for this packing mutant compared to the wild type. Comparison of K_m values (4.06 µM) show similar substrate binding affinity suggesting the active pocket is mainly unperturbed and the active-site accessibility is not limited due to this mutation. However, the turnover rate (0.0775/s and 0.02041/s respectively) as well as catalytic efficiency (19.3×10^3 $M^{-1}s^{-1}$ and 4.45×10^3 $M^{-1}s^{-1}$ respectively) are ~4 folds higher than the wild-

type suggesting presence of a more catalytically competent oxyanion hole in the former. This might be possible either by opening up the or by removing the PDZ inhibition from protease domain.

Since, SPD and SPD-PDZ were completely inactive, no kinetic parameters could be obtained. These observations emphasize the role of trimerization in protease activity and demonstrate that PDZ inhibition might not be the sole reason for protease inactivation.

HtrA2 Protein	K_m (μM)	V_{max} (M/s)	k_{cat} (1/s)	k_{cat}/K_m (1/M.s)
HtrA2(Wild type)	4.60	4.08×10^{-9}	0.020	4.5×10^3
HtrA2(M190R)	4.06	15.50×10^{-9}	0.078	19.3×10^3
HtrA2(F16D)	9.30	4.08×10^{-12}	0.000025	0.026×10^3
N-SPD	3.02	0.79×10^{-9}	0.004	1.29×10^3
SPD	–	–	–	–
SPD-PDZ	–	–	–	–

Table 4.1.2. *Steady state kinetic parameters for HtrA2 wildtype and its variants using FITC β-casein as the substrate. The data is the average of three independent experiments*

Further, to understand the rate of substrate catalysis for all monomeric mutants, protease activity was monitored with increasing concentrations (2-6 μg) of the enzyme. Increasing concentrations of SPD and SPD-PDZ did not show any activity **(Figure 4.1.4A and B),** whereas HtrA2(F16D) and N-SPD(F16D) showed activity with substrate β-casein **(Figure 4.1.4C and D).** Protease activity for HtrA2(F16D) and N-SPD(F16D) increased in a linear fashion with FITC labelled β-casein **(Figure 4.1.4E)** suggesting that with increase in protease concentration, enzyme substrate complex is more stabilised leading to enhanced substrate catalysis in variants containing the N-terminal region. This emphasizes the role of N-terminal region in formation of proper

conformation. To negate the possibility that oligomerization might occur at higher concentrations, which leads to an increase in protease activity, concentration-dependent oligomeric properties of HtrA2(F16D) and N-SPD(F16D) were studied using gel filtration chromatography, as shown in **(Figure 4.1.4F)**. Both the proteins were found to be monomeric at all protein concentrations, as expected.
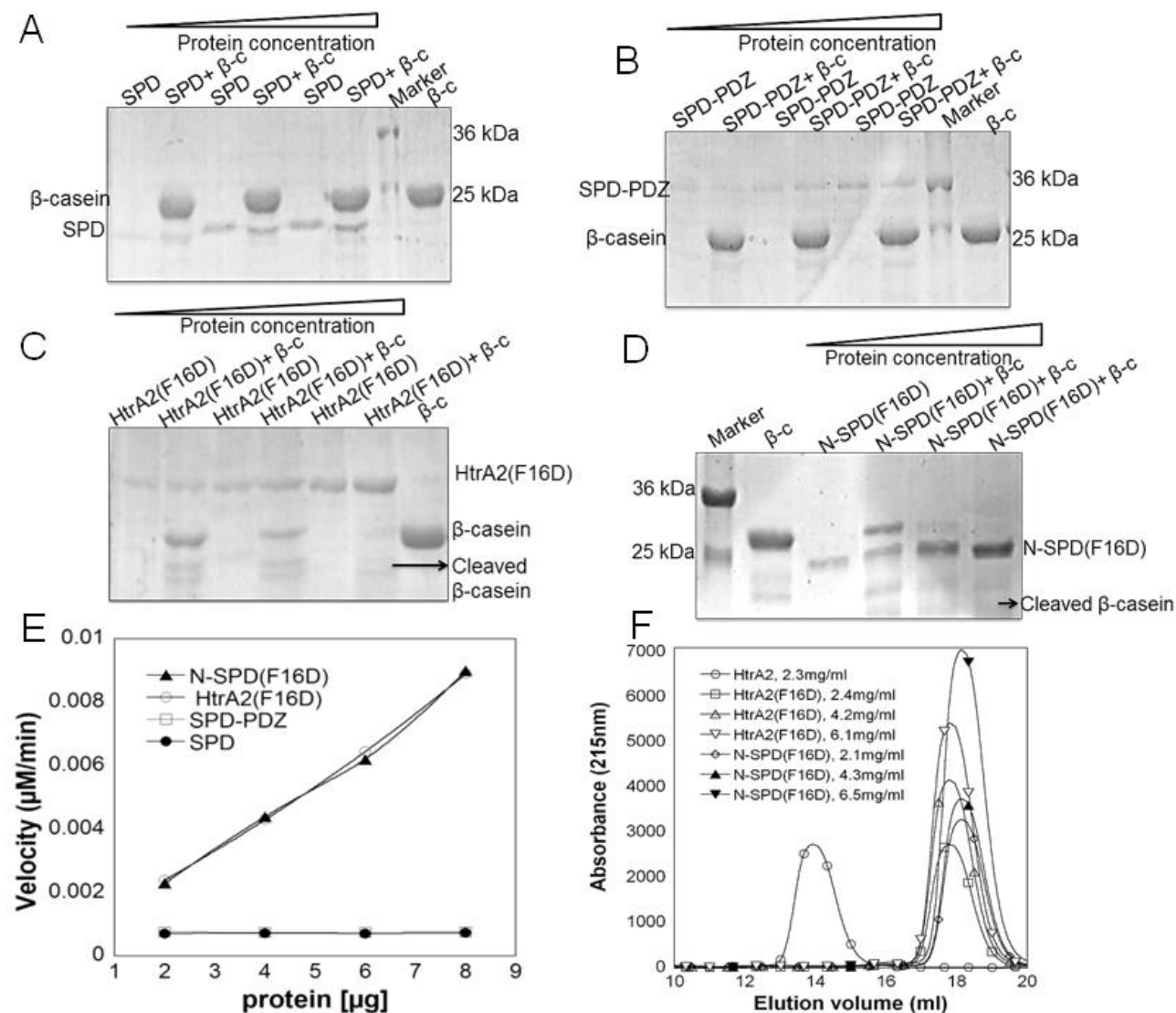
Figure 4.1.4. Proteolytic activity of HtrA2 mutants with β-casein as substrate. *In all gels β-c represents β-casein. β-casein cleavage assays with increasing concentrations (2μg, 4μg, 6μg) of A) SPD, B) SPD-PDZ domain, C) HtrA2(F16D) mutant and D) N-SPD(F16D) mutant. E) Initial velocities (v₀) with increasing concentrations (2-6μg) of SPD, SPD-PDZ, HtrA2(F16D) and N-*

SPD(F16D) using FITC β-casein as substrate. F) Elution profile with increasing concentrations of HtrA2(F16D) and N-SPD(F16D) using superdex 200 gel filtration column

4.1.2.1.4 Secondary and tertiary structural properties of HtrA2 mutants and domains

Far UV CD studies were performed to understand the effect of deletions and mutations on HtrA2 secondary structure and stability. All proteins except N-SPD and N-SPD(F16D) show similar secondary structural properties suggesting the mutations and deletions did not alter their overall secondary structure **(Figure. 4.1.5A)**. Both N-SPD and N-SPD(F16D) show decrease in total α-helical characteristics of the protease which might be due to absence of PDZ domain in these two variants. Secondary structural properties of all HtrA2 constructs harbouring either Y295W or N48W mutation are comparable to their non-tryptophan counterparts suggesting these tryptophan mutations are structurally not perturbing.

Fluorescence emission studies were performed for all tryptophan mutants (Y295W and N48W) and variants of HtrA2 to characterize the tertiary structural changes at the PDZ-protease interface, near the region as well as to understand the effect of certain mutations and deletions on the overall protein conformation. The two monomeric variants of HtrA2, HtrA2(F16D,Y295W), and SPD-PDZ(Y295W) showed red-shifted emission maxima (by 2 nm) compared to trimeric HtrA2(Y295W) **(Figure. 4.1.5B)** demonstrating that PDZ of the same molecule might not be completely collapsing on the SPD domain as suggested by the model (10). Interestingly, the packing mutant HtrA2(M190R,Y295W) showed similar red-shift implicating that this mutation did not negatively disrupt intramolecular PDZ-protease contacts as suggested earlier. This observation corroborates very well with the enzyme kinetics data discussed in the previous section. In contrast, emission maxima for HtrA2(N48W) showed slight red-shift **(Figure. 4.1.5C)** compared to the two monomeric variants suggesting that regulatory loops L1

and LD which are in the vicinity of the tryptophan might be oriented such that the tryptophan is more buried in the monomeric forms. In addition, emission maxima for trimeric N-SPD(N48W) is slightly blue-shifted (~1 nm) compared to HtrA2(N48W) which suggests PDZ domains do not influence the burial of W48 in the protease structure and the observed blue-shift in the monomeric full length HtrA2 variants might be due to rearrangements of the loops around the . Overall, these studies show that the mutants are well-folded with proper secondary and tertiary structural properties. Structural alterations and subtle conformational changes might occur with deletions and mutations respectively, which are reflected in overall protease activity.

Since protease activity of HtrA2 increased with temperature, thermal stability of the protease and secondary and tertiary structural changes in the SPD and PDZ-protease interface were monitored for different constructs. Thermal denaturation studies using CD spectroscopy demonstrate that T_m (melting temperature) of HtrA2, HtrA2(S173A), HtrA2(Y295W) and HtrA2(N48W) were ~74 °C **(Figure. 4.1.5D)** suggesting that these mutations did not have destabilizing effects on the protease. The slopes for full-length trimeric protease variants except for HtrA2(M190R) were steep demonstrating highly cooperative unfolding, whereas it was comparatively less for HtrA2(M190R) implying higher conformational flexibility (114). This might be due to the presence of more open architecture due to a greater plasticity at the PDZ-protease linker. Further, these observations corroborate with our fluorescence emission studies with tryptophan at PDZ-protease linker, where 2 nm red shifted emission maxima was observed for HtrA2(M190R) compared to wild type. T_m for N-SPD and monomeric HtrA2(F16D) were found to be ~65 °C highlighting the importance of PDZ and trimeric protease architecture in HtrA2 stability. T_m for SPD-PDZ and SPD could not be calculated because these proteins

precipitated beyond 50 $^{\circ}$C (data not shown). This suggests that N-terminal might also be very important for rendering stability to the protease.
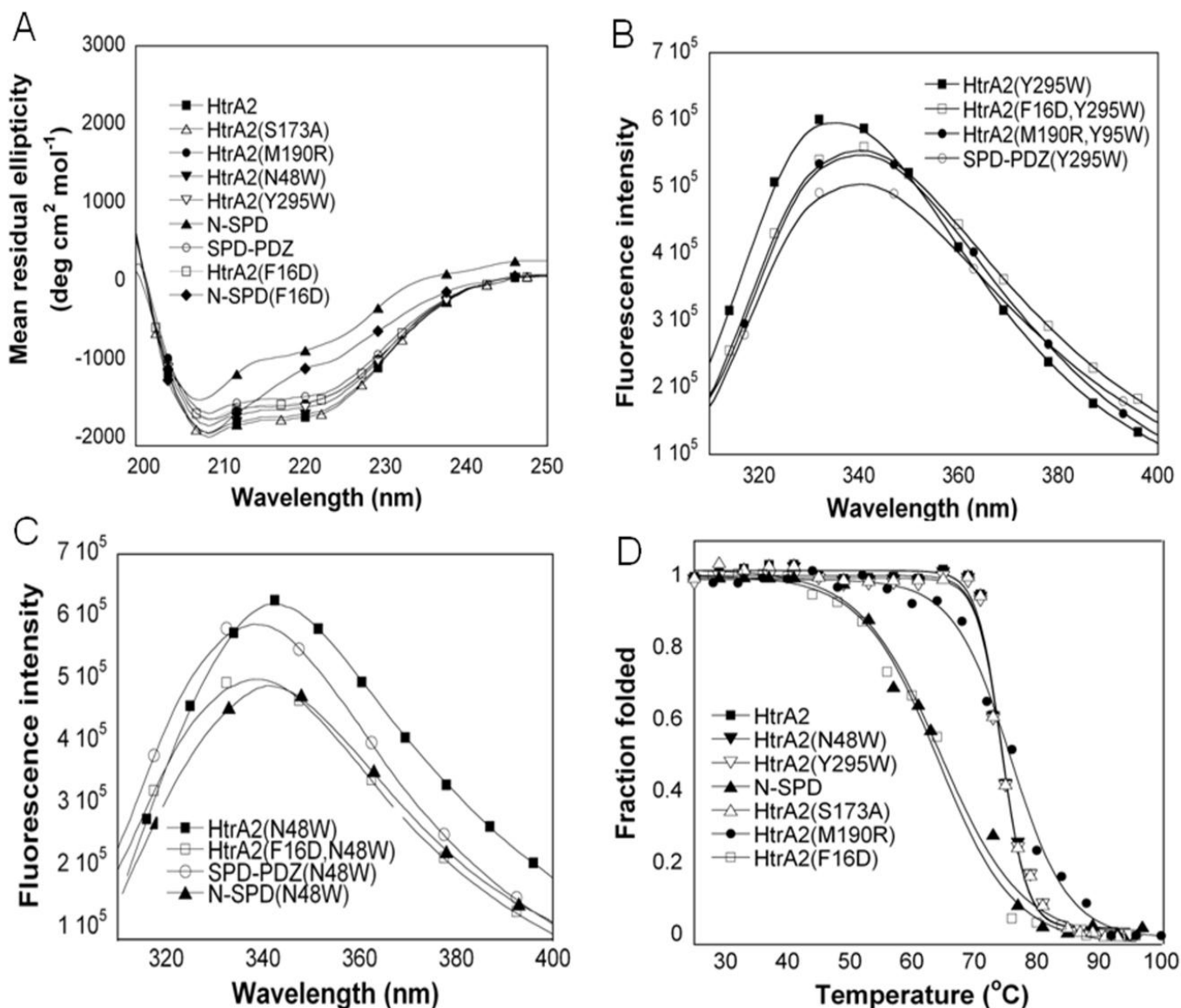
Figure 4.1.5.Comparison of secondary and tertiary structural properties of HtrA2 and its variants. *A) Far UV CD of HtrA2 and its variants at 25 $^{\circ}$C. B) Fluorescence emission spectra for different HtrA2 constructs having W295 mutation with excitation at 295 nm and emission between 310-400 nm. C) Fluorescence emission spectra of different HtrA2 having W48 mutation with excitation at 295nm and emission between 310-400 nm. D) Thermal denaturation curves for HtrA2 and its variants within the temperature range of 25 -100 $^{\circ}$C*

4.1.2.2 Role of different domain coordination, critical residues involved and interdomain dynamics in regulating substrate specificity and activity

4.1.2.2.1 Protease activity as a function of temperature

Previous studies showed that proteolytic activity of HtrA2 and its homologs increased with temperature (11, 73). Moreover, literature suggests heat activation is associated with considerable plasticity at the PDZ-protease interface similar to activation via substrate binding at PDZ (11). Thus, we performed the quantitative analysis of protease activity of HtrA2 and its variants as a function of temperature so as to understand how difference in activity correlates with conformational changes and dynamic behaviour of HtrA2. Here, we monitored the activity of HtrA2 over a wide range of temperature from 37 °C to 60 °C. Initial velocities (v_0) were calculated for HtrA2, HtrA2(F16D) and N-SPD domain using FITC β-casein as a substrate. For HtrA2, v_0 increased about 5-fold between 37 °C and 55 °C **(Figure 4.1.6)** with a subsequent decrease beyond 60 °C. The decrease might be due to protease unfolding as loss of secondary structure was also observed through spectroscopic studies at higher temperature. The marked increase might be consistent with its physiological role to serve as a quality control protein and to maintain mitochondrial homeostasis.

Identical enzymatic studies were done with trimeric N-SPD (no PDZ inhibition) and monomeric HtrA2(F16D) having intact PDZ domain. Increase in activity was observed in both although the change was not significant (~1.7 and ~1.2 fold higher than that at 37 °C) as shown in **figure 4.1.6**. Moreover, their maximum activity was found to be at ~50 °C which might be due to decrease in stability of the proteins as observed by thermal denaturation studies. These observations highlight the importance of PDZ-protease movement in increase of activity at higher temperature. N-SPD, thus without any PDZ domain does not show enhanced activity with

increase in temperature. However, the increase in protease activity that is observed in trimeric N-SPD highlights the conformational changes that occur at the N-terminal region that might also be required in concert with PDZ-protease crosstalk for HtrA2 activation. In monomeric HtrA2(F16D), although the PDZ is intact, no significant change in enzyme activity was observed suggesting the role of intermolecular PDZ-protease crosstalk in HtrA2 activation. Overall, these data reiterate the importance of N-terminal domain, PDZ domain and trimeric architecture in efficient HtrA2 activity.
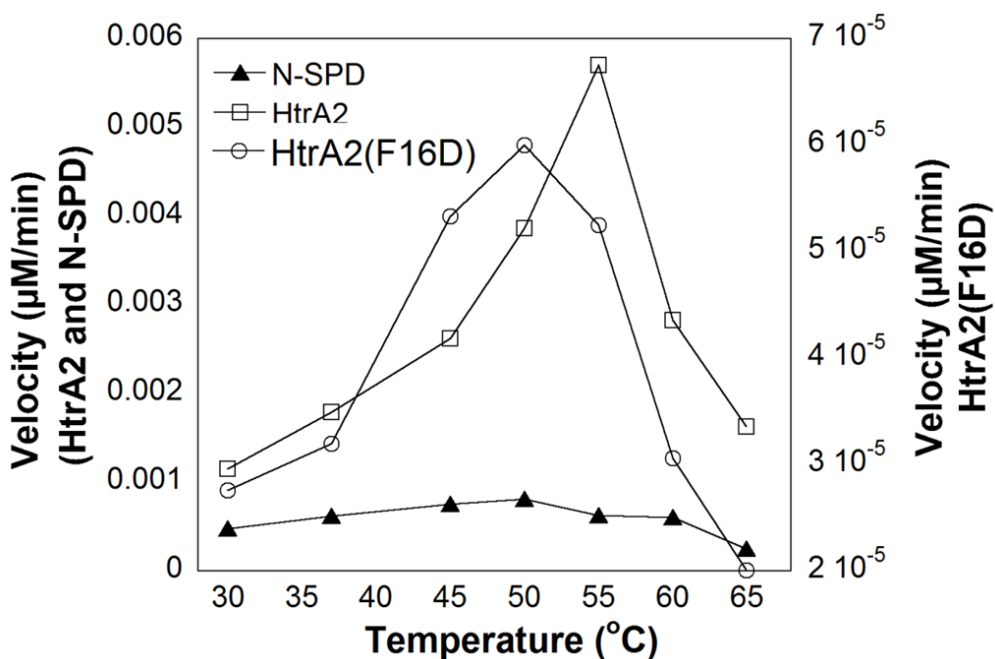
Figure 4.1.6. *Initial velocities of HtrA2 and its mutants as a function of temperature using FITC β-casein as substrate*

4.1.2.2.2 Tryptophan accessibility by fluorescence quenching studies

Fluorescence quenching studies were performed with the two tryptophan mutants that were introduced in different HtrA2 constructs to study their relative accessibility to the quencher acrylamide at 30 °C. This information would reflect the conformational dynamics at the PDZ-

protease interface and the region surrounding the active-site where these mutations are strategically placed (Y295W and N48W respectively). Since activity of substrate bound HtrA2 mimics that of thermally activated form, fluorescence quenching studies were also performed with acrylamide as a function of temperature. These studies would help to correlate the conformational plasticity with protease activity. Acrylamide, a non-polar quencher molecule quenches both the 'exposed' and 'buried' tryptophan residues primarily via collisional mechanism (115). At 30 $^{\circ}$C, the Stern Volmer constants (K_{SV}) for trimeric N48W mutants, HtrA2 and N-SPD (3.2 and 3.6 respectively) were less than their monomeric counterparts HtrA2(F16D) and SPD-PDZ (4.8 and 4.9 respectively) **(Figure 4.1.7A and Table 4.1.3).** This might be probably due to the lesser accessibility of the tryptophans in the trimeric protein architecture as the active-site is surrounded by other two HtrA2 monomers. Since W48 is near the regulatory loops L1, and LD of the active-site, difference in loop orientations might be responsible for change in K_{SV} constants which can be very well be correlated with fluorescence emission studies as well as lesser protease activity of monomeric mutants compared to the trimers.

The K_{SV} constants for HtrA2 in Y295W mutant is less compared to the different HtrA2 variants, HtrA2(M190R), HtrA2(F16D) and SPD-PDZ (4.4, 7.8, 6.5 and 6.2 respectively) **(Figure 4.1.7B and Table 4.1.4)** suggesting W295 is less accessible to the quencher in the wildtype which correlates very well with our fluorescence emission studies. Moreover, W295 is introduced in such a way that its accessibility will not be influenced structurally by the presence of other two monomers in trimeric HtrA2. In addition, it also faces the PDZ-protease interface and is in the vicinity of the substrate binding pocket (YIGV). This is supposed to reflect the environment surrounding the YIGV groove and monitor interdomain plasticity. Therefore, higher

K_{SV} constants for the above-mentioned monomeric HtrA2 variants support our enzymology and other spectroscopic data which demonstrate that PDZ from the same monomer does not collapse on the protease domain rather it might have enhanced flexibility as a consequence of absence of two other surrounding HtrA2 molecules. According to the existing HtrA2 model (10), M190R mutation on HtrA2 disrupts the packing between the PDZ and protease domains resulting in complete protease inactivation due to collapse of PDZ. With our enzymology, *in silico* and spectroscopic data, we have proved that M190R mutation does not only make the enzyme highly active but also has a more flexible and accessible active-site pocket. Higher accessibility for acrylamide in monomeric HtrA2(F16D) and SPD-PDZ is indicative of intermolecular and not intramolecular PDZ-protease interplay to be the key player in HtrA2 activation.
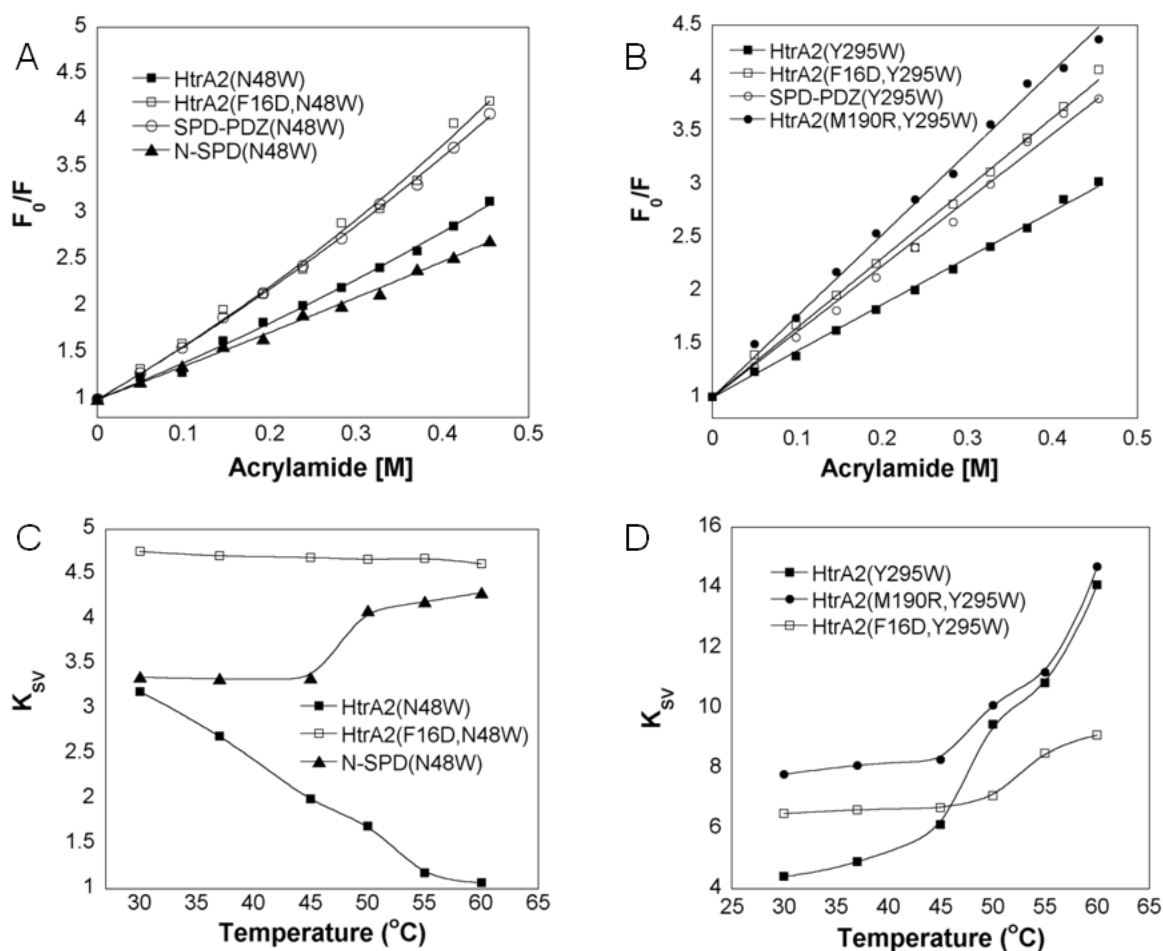
***Figure 4.1.7. Steady-state fluorescence quenching studies for tryptophan mutants of HtrA2
with Acrylamide**. A) Stern–Volmer quenching plots of the W48 mutants at 30 ^oC. B) Stern–
Volmer quenching plots of W295 mutants at 30 ^oC. C) Plot of K_{SV} versus temperature for W48
mutants. D) Plot of K_{SV} versus temperature for W295 mutants of HtrA2*

Steady-state fluorescence quenching studies with acrylamide was performed at temperatures
ranging between 30 °C and 65 °C so as to mimic the conformational changes that might occur in
an active bound protease. For all N48W mutants, both the trimeric proteins, HtrA2 and N-SPD
showed similar K_{SV} values at 30 ^oC. However, at higher temperatures, K_{SV} values for HtrA2
decreased gradually from 3.2 to 1.1 while for monomeric HtrA2(F16D) as well as trimeric N-
SPD, it remained unchanged **(Figure 4.1.7C and Table 4.1.4).** The decrease in quenching
constant for HtrA2 is indicative of rearrangement of L1 and LD loops upon activation leading to
burial of W48.   No change in quenching constant for trimeric N-SPD negates the role of PDZ
domains in influencing W48 accessibility. In case of monomeric HtrA2(F16D), no change in
K_{SV} constants with increasing temperature provide two important insights into HtrA2
mechanism. First, trimeric architecture is required for formation of a catalytically competent
enzyme and second, PDZ domain might not play critical role in active-site rearrangement for the
same protease molecule. These observations, along with enzymology data revalidate our
hypothesis of interdomain PDZ-protease crosstalk in HtrA2 activation.

In HtrA2 variants with Y295W mutation, since the tryptophan resides near the YIGV
groove and PDZ-protease linker, change in K_{SV} values are expected to depict the conformational
dynamics at and surrounding the interface as a function of temperature. For HtrA2 and
HtrA2(M190R), increase in tryptophan exposure was observed (3.2 and 1.9 folds, respectively)
with temperature till 60 ºC. This increase in K_{SV} values suggest that PDZ might be moving away
from serine protease domain and also exposing the YIGV groove, making the protease more

accessible to the substrate thus increasing the protease activity. This is further supported by the enzymatic studies where the activity was found to be maximum at ~55 ℃ (**Figure 4.1.7D and table 4.1.3).** In HtrA2(M190R), initial red shift compared to wild-type is suggestive of a more open YIGV groove and less compact PDZ-protease interface. Although the initial emission maxima is higher than wildtype in HtrA2(F16D), there is only 1.3 fold increase in K_{SV} constant with increase in temperature. This suggests that with increase in temperature, although the PDZ does not fall on the protease in the monomer, it does not move significantly away from it either. However, the slight red shift that is seen beyond 50 ℃ is indicative of increase in its activity at higher temperatures as discussed earlier. All these observations point toward requirement of trimeric architecture of the protease for structural plasticity as well as accentuate the role of intermolecular PDZ-protease interaction in regulating HtrA2 activity.

Temperature (^{o}C)	K_{SV} HtrA2(N48W)	K_{SV} HtrA2 (F16D,N48W)	K_{SV} SPD-PDZ(N48W)	K_{SV} N-SPD(N48W)
30	3.2±0.16	4.76±0.11	4.9 ±0.11	3.40±0.17
37	2.7±0.12	4.71±0.13	_	3.34±0.11
45	2.0 ±0.15	4.69±0.12	_	3.35±0.13
50	1.7±0.23	4.67±0.17	_	4.10 ±0.15
55	1.2 ±0.11	4.68±0.12	_	4.20 ±0.16
60	1.1 ±0.08	4.62±0.25	_	4.30 ±0.11

Table 4.1.3. *Stern-Volmer quenching constants (K_{SV}) for HtrA2 variants as a function of temperature with W48 as the intrinsic fluorophore. Data (average of 3 independent experiments) were fit to the Stern-Volmer equations as described in the materials and methods*

Temperature (^{o}C)	K_{SV} HtrA2(Y295W)	K_{SV} HtrA2(F16D,Y295W)	K_{SV} SPD-PDZ(Y295W)	K_{SV} HtrA2(M190R,Y295W)
30	4.41±0.11	6.5±0.08	6.2 ±0.07	7.8±0.08
37	4.90 ±0.27	6.6±0.12	–	8.1±0.19
45	6.13±0.32	6.7±0.14	–	8.3±0.22
50	9.46±0.40	7.1±0.16	–	10.1±0.30
55	10.84±0.43	8.5±0.23	–	11.2±0.28
60	14.10 ±0.23	9.1±0.27	–	14.7±0.40

Table 4.1.4. *Stern-Volmer quenching constants (K_{SV}) for HtrA2 variants as a function of temperature with W295 as the intrinsic fluorophore. Data (average of 3 independent experiments) were fit to the Stern-Volmer equations as described under materials and methods*

4.1.2.2.3 Intramolecular PDZ-protease interaction by FRET

With an aim at looking at the distance between PDZ and protease domain quantitatively so as to validate our hypothesis that intramolecular PDZ-protease collapse is not significant in HtrA2, FRET studies were performed with wild-type HtrA2 as well as its monomeric and packing mutants. Since, the donor and acceptor residues (tryptophan and IAEDANS-labelled cysteine respectively) are present in the same protein molecule, energy transfer as a function of temperature was studied. Structure-guided mutation F208C was done in the α4 of serine protease domain on HtrA2(Y295W) template. The FRET pairs were chosen such that they face each other and reside in the vicinity of the PDZ-protease linker region. This approach would provide a

comparative analysis of not only the distance between PDZ and protease in these three different HtrA constructs but will also help understand the dynamics of the interface as a function of temperature. These FRET residues although face each other in the same monomer, are far away from their pairs that are present in the adjoining molecules in the trimeric HtrA2 constructs and hence their influence on FRET transfer has been expected to be minimal. The tryptophan fluorescence and IAEDANS absorption spectra of all HtrA2 FRET mutants overlap facilitating the energy transfer **(Figure 4.1.8)**. The transfer efficiency 'E' and distance 'R' (Å) were calculated as described under Materials and Methods. Comparison of these two parameters for the three proteins at 30 ^{o}C show that HtrA2(F208C, Y295W) has a shorter C208–W295 distance compared to its M190R and F16D **(Table 4.1.5)** counterparts thus supporting our hypothesis.
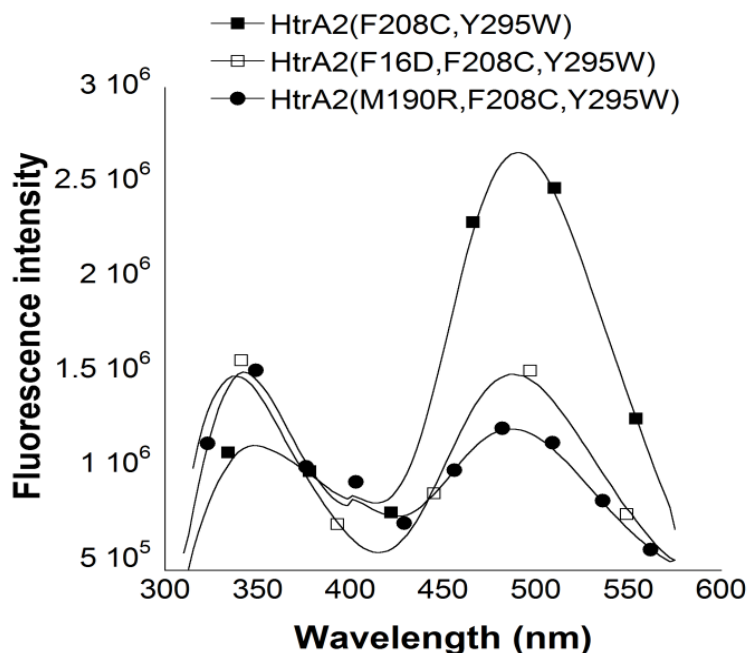
Figure 4.1.8. *FRET studies representing intramolecular PDZ-protease distance. Fluorescence emission of HtrA2 and its mutants labelled with IAEDANS. Fluorescence was excited at a wavelength of 295 nm and spectra were collected between 310-575 nm*

With increase in temperature, energy transfer efficiency for HtrA2(F208C,Y295W) and HtrA2(M190R, F208C,Y295W) initially increased and calculated distances R between the

acceptor and donor decreased from 30 $^{\circ}$C to 50 $^{\circ}$C **(Figure 4.1.19A)**. Beyond 50 $^{\circ}$C, energy transfer efficiency decreased with a subsequent increase in calculated R values. This can be explained by a model of PDZ movement where, as a function of temperature, the interface movement occurs such that PDZ moves away from SPD in a V-shaped trajectory thus bringing the two residues in vicinity to each other **(Figure 4.1.9B).** However, beyond 50 $^{\circ}$C, the gap between PDZ and protease domains increases which is reflected in increase in 'R' and concomitant decrease in 'E 'values **(Table 4.1.5)**. Consistent with fluorescence quenching studies, HtrA2(F16D, F208C, Y295W) did not show much change in distance between the FRET pairs with temperature.
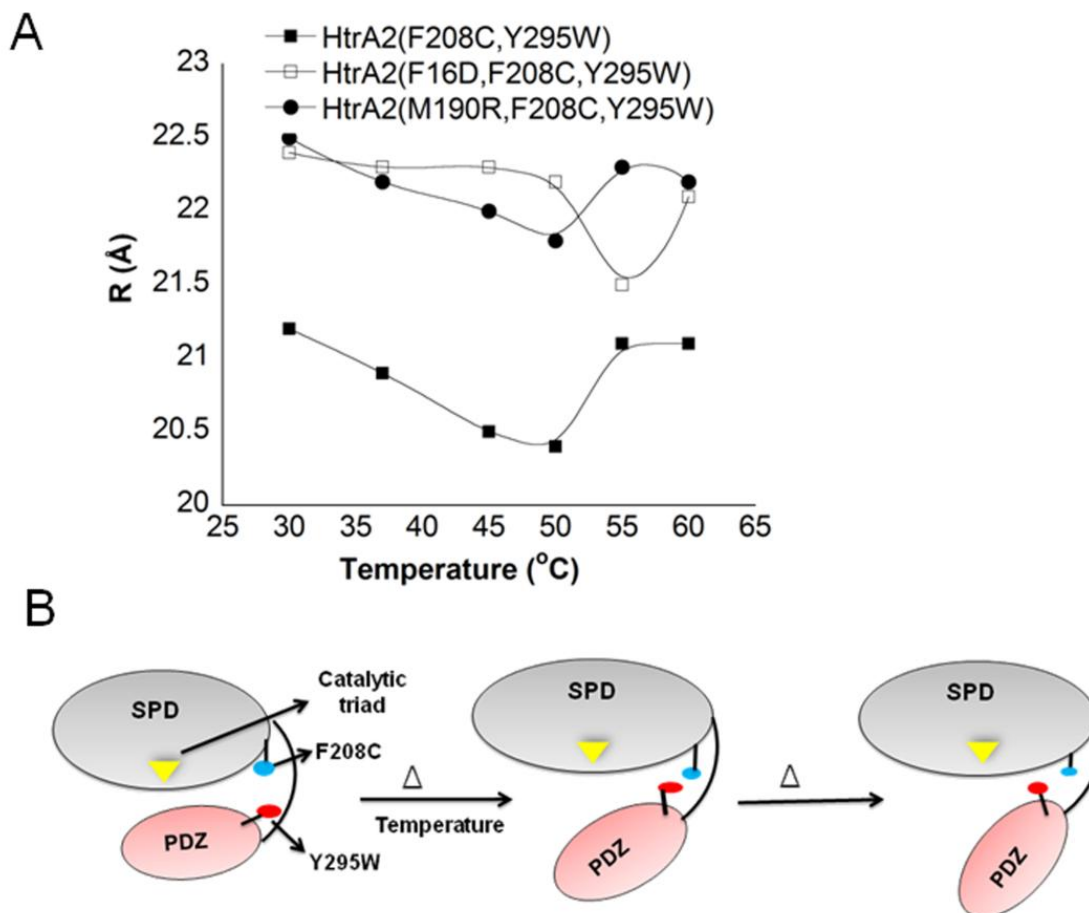
Figure 4.1.9. ***FRET studies representing dynamics at PDZ-protease interface***. *A) Calculated distance between the W295 and IAEDANS for HtrA2 mutants as function of temperature. B) Model showing the dynamics at SPD-PDZ interface as a function of temperature*

Temperature (°C)	E			R (Å)		
	HtrA2	HtrA2(M190R)	HtrA2(F16D)	HtrA2	HtrA2(M190R)	HtrA2(F16D)
30	55.3	45.2	46.75	21.2	22.5	22.4
37	57.4	47.3	47.43	20.9	22.2	22.3
45	60.0	50.0	47.67	20.5	22.0	22.3
50	61.0	51.1	48.39	20.4	21.8	22.2
55	55.9	47.9	53.24	21.1	22.3	21.5
60	55.6	47.5	48.90	21.1	22.2	22.1

Table 4.1.5. FRET parameters between IAEDANS (acceptor) and W295 (donor) for HtrA2(F208C,Y295W) and its variants as a function of temperature. 'E' is the transfer efficiency, and 'R' is the distance between two probes. E and R values were calculated from the equations as described in the methods section

4.1.3 Discussion

The goal of this study was to delineate the role of different domains, their combinations, oligomerization and critical residues in modulating HtrA2 activity and specificity with an aim at developing a model for HtrA2 mechanism of action. The importance of HtrA2 as a promising therapeutic target is reflected in a plethora of studies on its structure and functions in the past decade. This includes the crystal structure of inactive unbound form that provides a broad overview of its structural organization (10). However, these studies could not define its mode of activation which is a prerequisite for delineating its role in various biological pathways and diseases. Thus, understanding the structural correlates of HtrA2 activation will be a step forward toward designing molecules to manipulate its functions for devising therapeutic strategies (116, 117).

HtrA2 has a complex arrangement of L1, L2 and LD loops encompassing the active-site pocket and a flexible linker at the PDZ-protease interface whose relative orientations and

crosstalk with different domains might be essential for defining its functions. The crystal structure of the inactive form of the protease (S173A) proposed a model where the relative intramolecular PDZ-protease movement was considered the primary reason for regulation of HtrA2 activity. However, a part of N-terminal region, PDZ-protease linker and several critical loops were missing from the structure thus limiting its ability to demonstrate the dynamics of the mechanism of action. According to the model, the PDZ domains upon substrate binding move away from SPD making way for the substrate to access the catalytic pocket thus emphasizing intramolecular PDZ-protease crosstalk to be pivotal in protease activation. The model also hypothesized that in the monomeric HtrA2 variant, complete collapse of PDZ on protease leads to its inactivity, which can be subsequently rescued through removal of PDZ domain. Role of the short N-terminal region other than trimer formation was also not highlighted in the previous model and hence is incapable of fully explaining the intricate collaboration among different domains of HtrA2. Our data challenges this hypothesis and underlines the importance of PDZ, N-terminal region and trimerization in proper active-site formation thus providing a comprehensive illustration of mode of HtrA2 activation.

Here, with an apt combination of enzymology and biophysical studies, we have demonstrated the complexity of conformational changes and dynamics that regulate HtrA2 functions. In this study, domain-wise dissection of HtrA2 has been done to delineate their roles alone and in different combinations, including loops, crucial residues and flexible interface linker in modulating HtrA2 functions. For example, deletion of PDZ domain resulted in a trimeric HtrA2 variant without PDZ inhibition (both inter and intramolecular), whereas, monomeric SPD-PDZ and HtrA2(F16D) constructs were created to highlight the importance of both N-terminal

region and trimerization in protease activation. This unique approach clearly pinpointed the roles of each of them toward formation of a catalytically competent HtrA2 molecule.

The 18-amino-acid-long N-terminal trimerization region in HtrA2 is unique among HtrAs, It resembles Smac/DIABLO in its IAP binding ability and in promoting caspase-dependent apoptosis (3, 4, 118). Apart from these functions, its significance in structure and stability of the protease has not been characterized. Here, we show that N-terminal region plays an important role in active-site rearrangement with stabilization of the enzyme-substrate complex. Comparison of HtrA2(F16D) and SPD-PDZ establish the role of N-terminal region towards rendering stability to the protease. The C-terminal PDZ domains in HtrAs perform myriads of functions that include allosteric modulation, protein-protein interactions and higher order oligomer formation (72, 119, 120). In HtrA2, it has been hypothesized that PDZ acts as a substrate binding (via its YIGV tetrapaptide motif) as well as a regulatory domain (10, 11). Relative orientation and movement between PDZ and protease domain was considered to be the determining factor for HtrA2 activity as well as specificity. We have shown that the mechanism of HtrA2 activation, although requires PDZ-protease crosstalk, is not straightforward and using functional enzymology and quantitative biophysical approach, we re-examined and modified the existing mechanism of HtrA2 activation (10, 11). Our data demonstrate that this activation occurs in a complex, concerted manner involving movement in N-terminal region, trimerization and intermolecular PDZ-protease crosstalk, which subsequently rearrange the active-site loops and create a catalytically competent oxyanion hole.

Spectroscopic and enzymology studies as a function of temperature with different HtrA2 variants ascertain considerable rearrangement in and around loop L1 suggesting a malformed oxyanion hole in the apo-protease. These experimental studies excellently corroborate with the

recent literature report (71) where substrate binding leads to movement of α5 of PDZ* toward SPD of adjacent monomer. This subtle rearrangement leads to flipping of F170, which is a part of oxyanion hole, towards H65 of the catalytic triad thus making the protease poised for catalysis. However, L2 that harbours the substrate specificity pocket shows minimal movement further re-establishing our observations.

Interestingly, contrary to the previous literature report (10), HtrA2(M190R), a mutant that was designed to study the packing and mobility of PDZ-protease interface has been found to have significantly enhanced activity compared to the wild-type HtrA2. This might be due to the less compact structural architecture with a more open and solvent accessible active-site as well as greater plasticity at the PDZ-protease linker as observed by thermal denaturation and other spectroscopic studies. Combination of these two factors might have synergistically led toward efficient initial substrate binding as well as catalysis thus enhancing enzyme activity by several folds. Moreover, a close look at the HtrA2 structure shows that mutating a methionine to a bulkier arginine residue might lead to steric clash with leucine 233 which is perhaps prevented by opening up of the active-site pocket. Moreover, this mutation that happens to occur next to a lysine residue (K191) increases the local positive charge at the hydrophobic milieu of PDZ-protease interface which in addition to the steric effect might open up the pocket even further leading to enhanced substrate catalysis. However, additional mutational and structural studies are required to confirm this hypothesis.

 Based on all these observations and critical inferences, a comprehensive working model of HtrA2 activation has been proposed as illustrated in **Fig 4.1.10**. In full length trimeric HtrA2, initial substrate binding or increase in temperature leads to movement of PDZ* towards SPD of the adjacent molecule. This intermolecular movement along with simultaneous N-terminal

rearrangement leads to subtle reorganization of the active-site loops to form an active protease. Interestingly, the intermolecular domain plasticity concomitantly facilitates intramolecular linker movement thus indirectly aiding initial substrate binding and further protease activation. This complex yet precise synergistic coordination among different domains of the protease might be functionally important for selecting substrates under normal and diseased conditions.
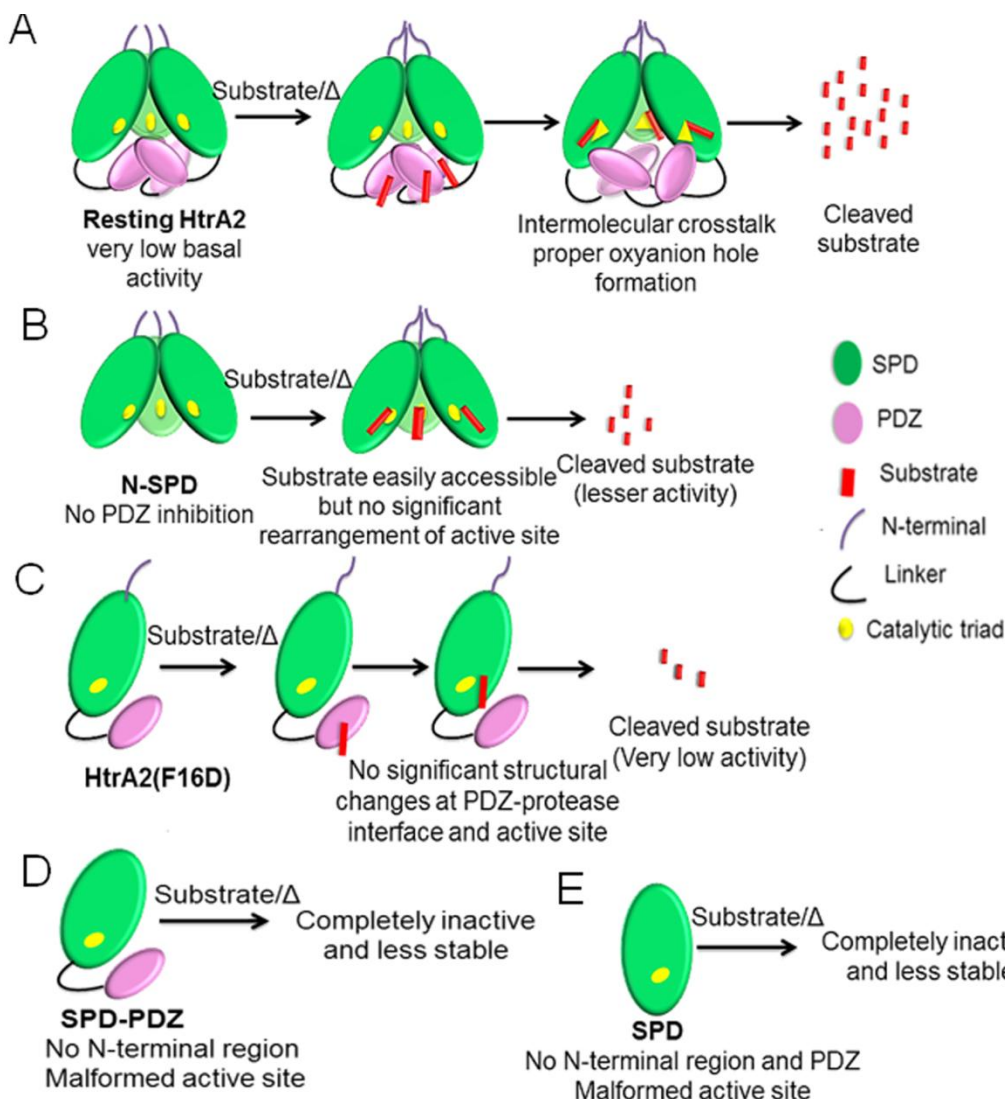
Figure 4.1.10. Proposed model representing mechanism of HtrA2 activation. *A) In full-length trimeric HtrA2, initial substrate binding or increase in temperature leads to movement of PDZ* toward SPD of adjacent molecule. This intermolecular movement along with simultaneous N-terminal rearrangement leads to subtle reorganization of the loops to form an active protease. B) In trimeric N-SPD, substrate is easily accessible to the active-site, but lack of PDZ movement*

leads to significant reduction in activity. Presence of residual activity can be attributed to partial active-site rearrangement and stabilization mediated by the N terminus. C) In the monomeric HtrA2(F16D)variant, absence of intermolecular crosstalk and subsequent loop rearrangements result in a malformed oxyanion hole, which significantly reduces the rate of catalysis. D) Monomeric SPD-PDZ with malformed active-site is completely inactive and is less stable. E) Monomeric SPD without N terminus and PDZ is completely inactive and is less stable.

Although, N-terminal mediated partial active-site reorientation and stabilization is novel among HtrA family of proteases, PDZ domains do act as modulators in most of the cases (72, 121, 122). For example, in bacterial DegS, which is a periplasmic stress sensor (72, 121, 122), inhibitory interaction of PDZ with loop L3 of SPD in the unbound state keeps the protease in its basal form. This inhibition is relieved by outer membrane protein (OMP) binding to PDZ that subsequently leads to both *cis* and *trans* protease domain rearrangement so as to form an active DegS molecule (123). Whereas, in HtrA2, we have established that very low basal activity in the apo-protease might be due to presence of a catalytically incompetent active-site pocket which requires intermolecular PDZ-protease interaction as well as additional N-terminal contacts and stabilization for formation of a fully functional trimeric ensemble. In bacterial periplasmic space, where certain amounts of unassembled OMPs are always present, stress response beyond a threshold level can therefore be readily modulated by OMP-PDZ interaction (123). However, in HtrA2, evolution might have provided an additional N-terminal regulatory switch for tighter control of its activation which might be required only during triggering of apoptotic signal. Thus, nature uses unique fusion of individual domains, loops and linkers that evolve into polypeptides with distinct functional and regulatory properties.

Chapter 4.2

To understand the interaction of HtrA2 with antiapoptotic

binding partner cum substrate—Pea15

4.2.1 Introduction

HtrA2 is involved in several critical biological functions such as protein quality control, unfolded protein response (UPR), cell growth, apoptosis, arthritis, cancer and neurodegenerative disorder (41-44). Under normal physiological conditions, it acts as regulator of mitochondrial homeostasis where its protective function switches into proapoptotic behavior in response to stress-inducing agents. HtrA2 mediates apoptosis through classical pathways via caspase activation by displacing XIAP from caspases (3, 4). There is also evidence that interaction with IAPs is not the only mechanism involved in HtrA2 induced cell death, as the propteolytic activity of HtrA2, is sufficient to promote caspase independent cell death. HtrA2, via its protease activity degrades several cellular substrates such as Pea15 (8), FLIP (7), Hax1 (9). It also cleaves cytoskeletal proteins such as Actin, vimentin, α- and β-tubulin (13). Moreover, Eukaryotic translation initiation actor-4 gamma 1 (eIF-4γ1) and Elongation factor-1 alpha (EF-1α) (13) are also substrates of HtrA2. Despite substantial evidence of involvement of HtrA2 in triggering apoptosis, little is known about its mode of regulation, substrate recognition and specificity.

Although substrate unbound form of HtrA2 provided a broad overview of its structural organization, however, it could not decipher the mechanism of action or its regulation which is a prerequisite for understanding its role in various biological pathways and diseases. Thus considering the biological relevance of HtrA2, in chapter 4 of this thesis we demonstrated the importance of intricate PDZ-protease domain coordination and conformational plasticity at PDZ-protease interface in defining its functions. It was reported that several repertoire of proteins (for e.g. GRIM 19, WARTS kinase and Presenilin) bind to the C-terminal PDZ domain of HtrA2 and stimulate the protease activity to promote cell death (43). Interestingly, in addition to the regulatory role played by PDZ domain, HtrA2 manifests an additional mode of regulation via its

---

N-terminus by binding to and cleaving IAPs. This phenomenon apparently demonstrates existence of multiple or complex mechanisms of HtrA2 activation and regulation involving PDZ as well as other regions of the protein. A clear understanding of the molecular mechanism of HtrA2 interaction with its binding partners or substrates will define ways of regulating its functions. Therefore, we performed the comprehensive binding and enzymology studies with its natural antiapoptotic substrate Pea15. These studies will help to delineate a unified model of HtrA2 activation and lead toward designing activators for HtrA2 that could modulate its functions with desired characteristics against diseases associated with it.

4.2.2 Results

4.2.2.1 HtrA2 protease domain preferably interacts with α-5 and α-6 helices of Pea15

Although it has been previously demonstrated that HtrA2 binds Pea15 to induce apoptosis (8) , the corresponding minimal binding region and critical residues involved in HtrA2 and Pea15 are not known. Therefore, pull down studies were performed with MBP fused recombinant Pea15 as bait and HtrA2 variants as prey. HtrA2 variants used for these studies were HtrA2 full length, N-SPD (PDZ deleted variant) and PDZ domain (protease domain deleted variant) as shown in **figure 4.2A**. Pull down experiments demonstrated that Pea15 interacts with the serine protease domain and not the conventional PDZ domain of HtrA2. No pull down was detectable using MBP control alone **(Figure 5.2B).**

Further to define the region responsible for the interaction in Pea15, we generated series of deletion constructs as shown in **figure 5.2A**. We then compared the ability of HtrA2 to interact with, Δα(1-3), Δα(1-4), Δα (1-5), Δα(5,6) and C-terminal (ΔDED) deletion constructs of pea15. The results showed that Δα(1-3), Δα(1-4), Δα(1-5) constructs interacted with HtrA2 with equal

affinity as full length Pea15. However, no interaction was detected with C-terminal as well as Δα(5,6) deletion constructs. This complete abrogation of interaction suggests HtrA2 protease domain might preferably interact with the α-5 and **α**-6 helices of Pea15 DED domain. Surprisingly, DED (ΔC-terminal) domain, which has a tendency to interact with several proteins (124), showed very weak interaction with HtrA2. This highlights the importance of C-terminal region in addition to DED in binding to HtrA2.
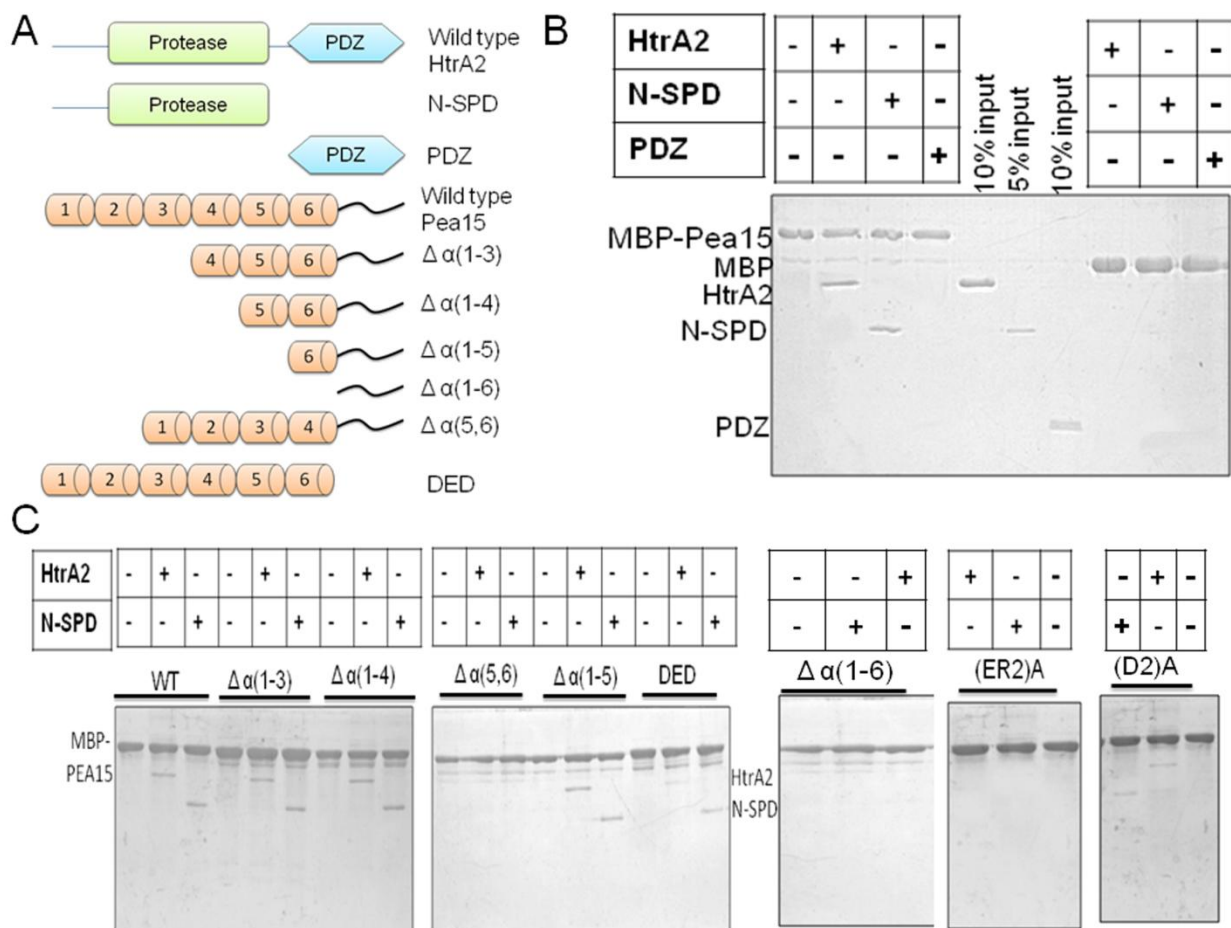
Figure 4.2.1. Pull down assay with HtrA2 variants and Pea15 constructs. *A) Schematic representation of different pea15 deletion constructs used for HtrA2-Pea15 interaction studies. B) MBP fused Pea15 lysate is used as bait and purified HtrA2 variants (HtrA2 wild type, N-SPD and PDZ) are used as prey. 10 μg of recombinant MBP-Pea15 bound to amylase resin was incubated with the recombinant 100 μg of HtrA2 for 12 hrs at 4 °C. The reaction was stopped with Laemmli buffer at 100 °C and proteins were separated by SDS-PAGE followed by coomassie blue staining. C) MBP fused Pea15 deletion and binding site mutants are used as* bait

and purified HtrA2 variants as prey. (ER2)A represents E64A, R71A, R83A and D2A represents D93A, D96A

To pin point the critical residues involved in the interaction, we performed blind docking using Cluspro software. Total 40 docked models based on electrostatic, hydrophobic, van de Waals + electrostatic and balanced interactions (10 docked conformations for each type of interaction) were generated. The structures based on the balanced type of interaction were studied, as it included electrostatic, hydrophobic and electrostatic interactions which were preferred for docking. Taking the clues from our pull down studies, we selected the best pose from balanced type of interactions, where α-5 and α-6 helices of Pea15 showed interaction with protease domain of HtrA2 **(Figure 5.2.2A)**. Detailed list of interactions generated from the *PDBsum* (111) provided in **figure 5.2.2B**. To further substantiate these docking results, several point mutations E68A (α-5 helix), R71A (in the loop between α-5 and α-6 helix), R83A (α-6 helix) of DED and D93A, D96A in C-terminal region of Pea15 were generated. We observed that substitution of residues E68, R71, R83 in combinations completely abrogated the binding of Pea15 with HtrA2 suggesting these residues might be the potential participants in mediating interaction with HtrA2. In addition to the residues in DED we also generated point mutations in C-terminal (D93A, D96A) of Pea15. Substitution of residues D93A and D96A alone did not abolish the interaction completely suggesting the involvement of DED as a primary docking site for HtrA2. However, there was partial abrogation in interaction hinting that C-terminal is also required in conjunction with DED for binding to HtrA2, thus strengthening our hypothesis.

Taken together, our study defines a bipartite mode of interaction between HtrA2 and Pea15 where protease domain of HtrA2 might interact with both DED domain as well as C-

terminal disordered region of Pea15 to suppress the ultimate outcome of the Pea15 antiapoptotic

signaling cascade in cytoplasm.
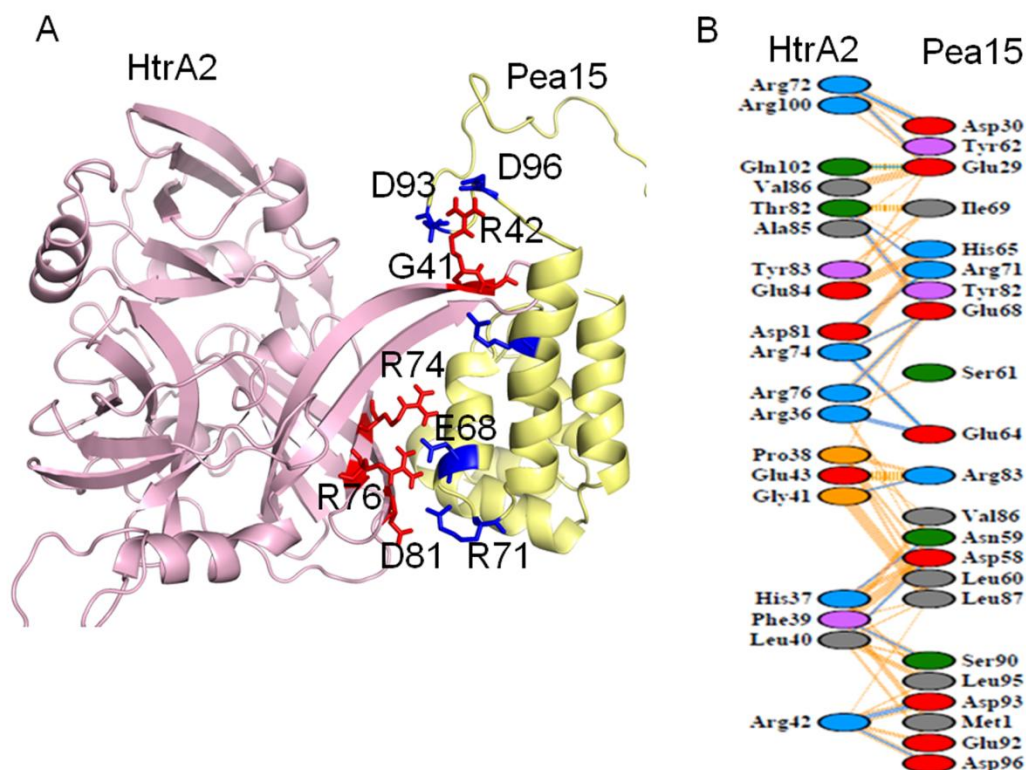
Figure 4.2.2. Cluspro docking analysis of HtrA2 (receptor) and Pea15 (ligand). A) Critical residues involved in interaction between HtrA2 and Pea15 are shown as sticks. Residues from HtrA2 are shown as red and from Pea15 as blue colors. B) Detailed list of interactions generated from PDBsum. Blue lines are hydrogen bond interactions, orange are non bonding interaction

4.2.3 Cleavage of Pea15 is independent of HtrA2 PDZ domain

To address the role of different domains in regulating HtrA2 activity and specificity, protease

activity of HtrA2 and its variants was studied using Pea15 as a substrate. In all protease activity

studies, the mutant (S173A) was used as a negative control. It was observed that PDZ deleted

variant (N-SPD) showed rapid hydrolysis of Pea15 compared to wild-type HtrA2. To quantitate

the rate of hydrolysis, intensity of proteolytically degraded Pea15 band at 7 hr was analyzed

relative to the uncleaved Pea15 using *GelQuant.NET* software. After 7 hr N-SPD cleaved 90%, while HtrA2 cleaved 30% of the pea15. Further to understand the rate of protease activity, time-based degradation of pea15 was monitored. N-SPD degraded 50% of the Pea15 in 3 hr while the same is achieved in 10 hr in the case of the wild-type HtrA2 **(Figure 4.2.3).** Overall, these results suggest that lower protease activity for HtrA2 wild-type might be due to inhibitory effect of PDZ domain on its protease activity, probably through restriction of substrate accessibility to the active-site.
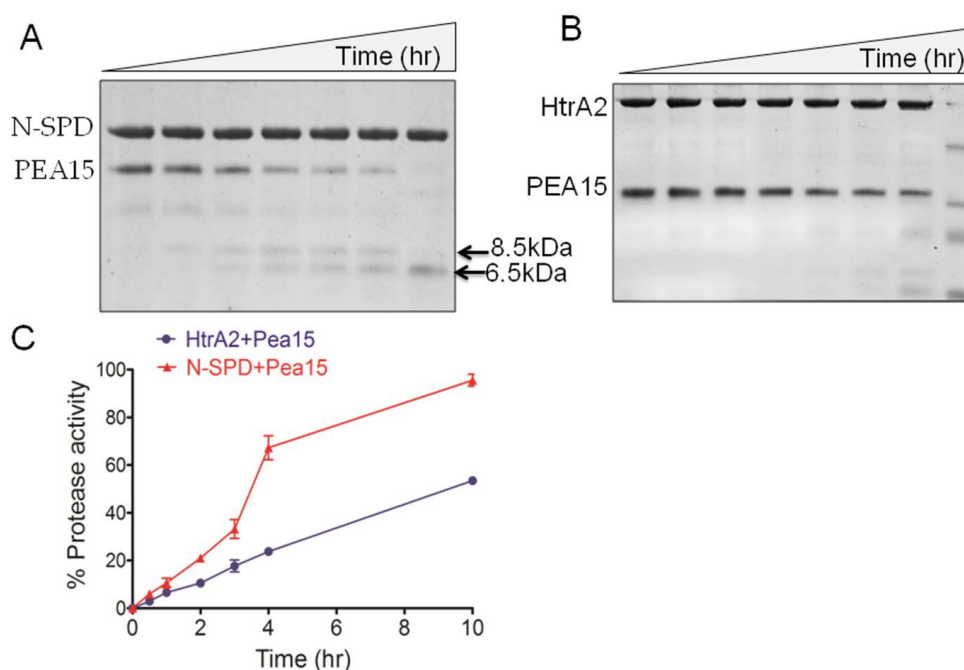
Figure 4.2.3. Time course protease assays with HtrA2 and Pea15. A) *Pea15 was incubated with A) N-SPD B) HtrA2 at 37 °C from 0-12 hrs. The reaction at each time point was stopped with Laemmli buffer at 100 °C. Proteins were separated by Tris-Tricine SDS-PAGE followed by coomassie blue staining. C) Percentage protease activity was calculated by quantifying the intensity of residual Pea15 at each time point relative to the Pea15 incubated with N-SPD at 10 hrs*

Protease assays were also done with the different deletion constructs and binding site mutants of Pea15 to validate our interaction studies. It was observed that HtrA2 and N-SPD cleaved all deletion mutants Δα(1-3), Δα(1-4), Δα(1-5) except C-terminal region and Δα(5,6) variants

(Figure 4.2.4A and B). These results very well corroborate with the pull down studies where Δα(5,6) and C-terminal region did not show any interaction with HtrA2. Moreover, HtrA2 and N-SPD cleaved DED (ΔC-terminal region) with less competence compared to full length Pea 15. This low rate of cleavage highlights the bipartite mode of interaction where, HtrA2 protease domain interacts simultaneously with both DED and C-terminal for greater binding specificity and affinity.
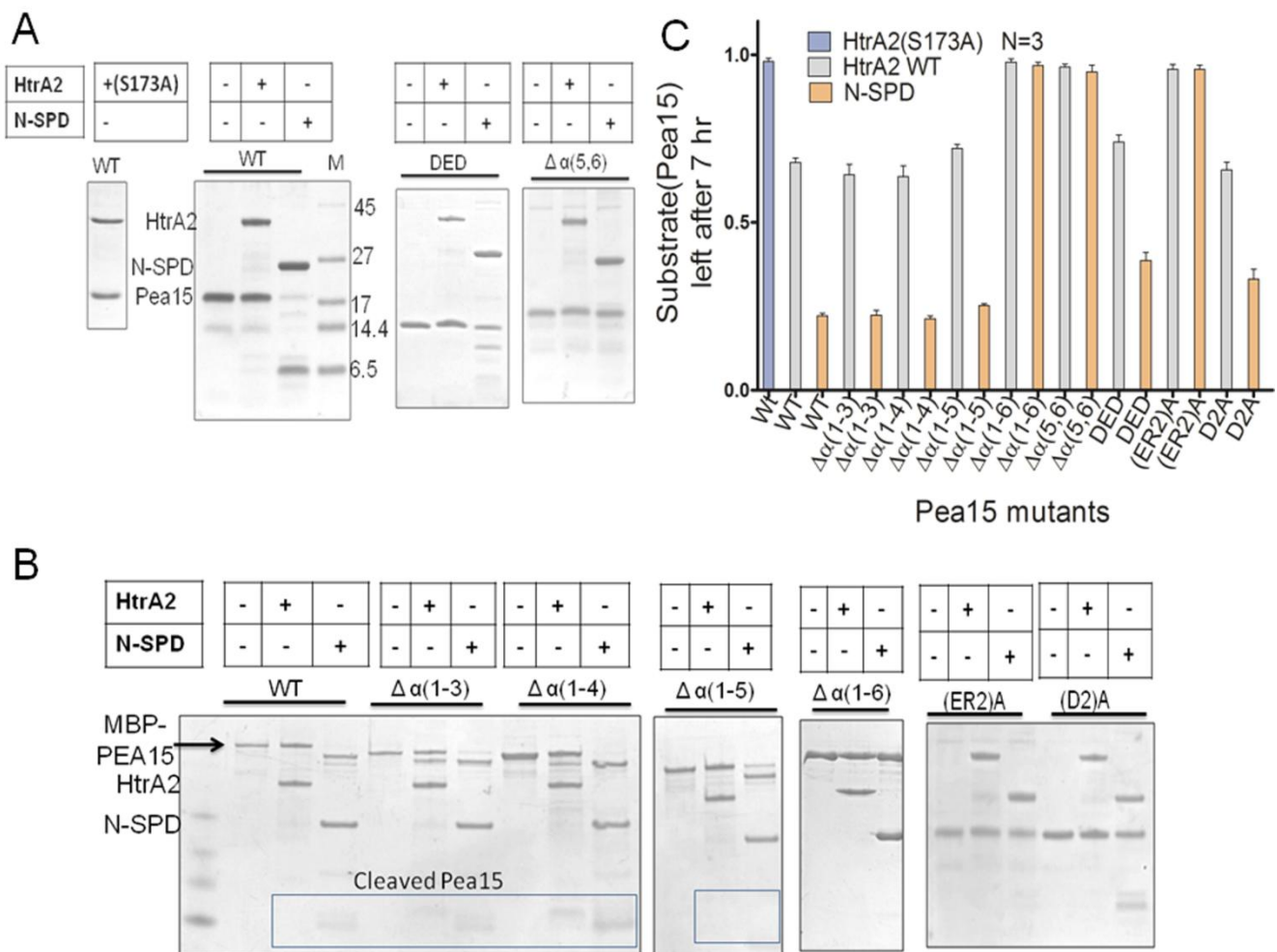
Figure 4.2.4. Proteolytic activity of HtrA2 and its variants with Pea15 as a substrate.
A) Pea15 was incubated with full length HtrA2 and N-SPD at 37 °C for 7 hrs. Reaction samples were resolved by 15% Tris-Triscine SDS-PAGE and visualized with Coomassie brilliant blue staining. For protease assays with deletion constructs, MBP fused Pea15 proteins were used. B) Semi quantitative analysis showing intensity of Pea15 remained at 7hr was calculated using GelQuantNet software

In addition Pea15 binding site mutants (E68A, R71A, R83A) did not show any proteolytic degradation with HtrA2 and N-SPD probably due to their inability to interact with these proteins. As anticipated, Pea15 C-terminal binding site mutants (D93A, D96A) showed 50% decrease in its proteolytic degradation by HtrA2 and N-SPD when compared to the full length Pea15. This decrease in proteolytic degradation validates our hypothesis that DED is the primary docking site in mediating interaction with HtrA2.

4.2.5 Secondary and tertiary structural properties

Far UV CD studies were performed to understand the effect of deletions and mutations on Pea15 and HtrA2 secondary structure. All the MBP fused Pea15 deletion constructs except DED showed decrease in their total α-helical characteristics due to the sequential deletion of helices from full length protein **(Figure 4.2.5A).** Secondary structural properties of all HtrA2 and Pea15 constructs harbouring either binding site or cleavage site mutations are comparable to their wild-type secondary structure suggesting these mutations are structurally not perturbing.

Fluorescence emission studies were performed for all the Pea15 variants with single tryptophan (W45) on the α4 helix to understand the effect of these mutations on the overall protein tertiary structure. All binding and cleavage site mutants showed similar emission maxima (~316 nm) except Δα(5,6) which showed red-shifted emission maxima (by 11 nm) compared to wild-type pea15 **(Figure 4.5B)**. The observed red shift in emission maxima might be due to the deletion of the two helices making the tryptophan more solvent exposed. This loss in the secondary structure of Δα(5,6) of pea15 might be the reason for the abrogation in binding. However, the mutations (E68A, R71A, R83A) on these helices did not affect the overall protein conformation.
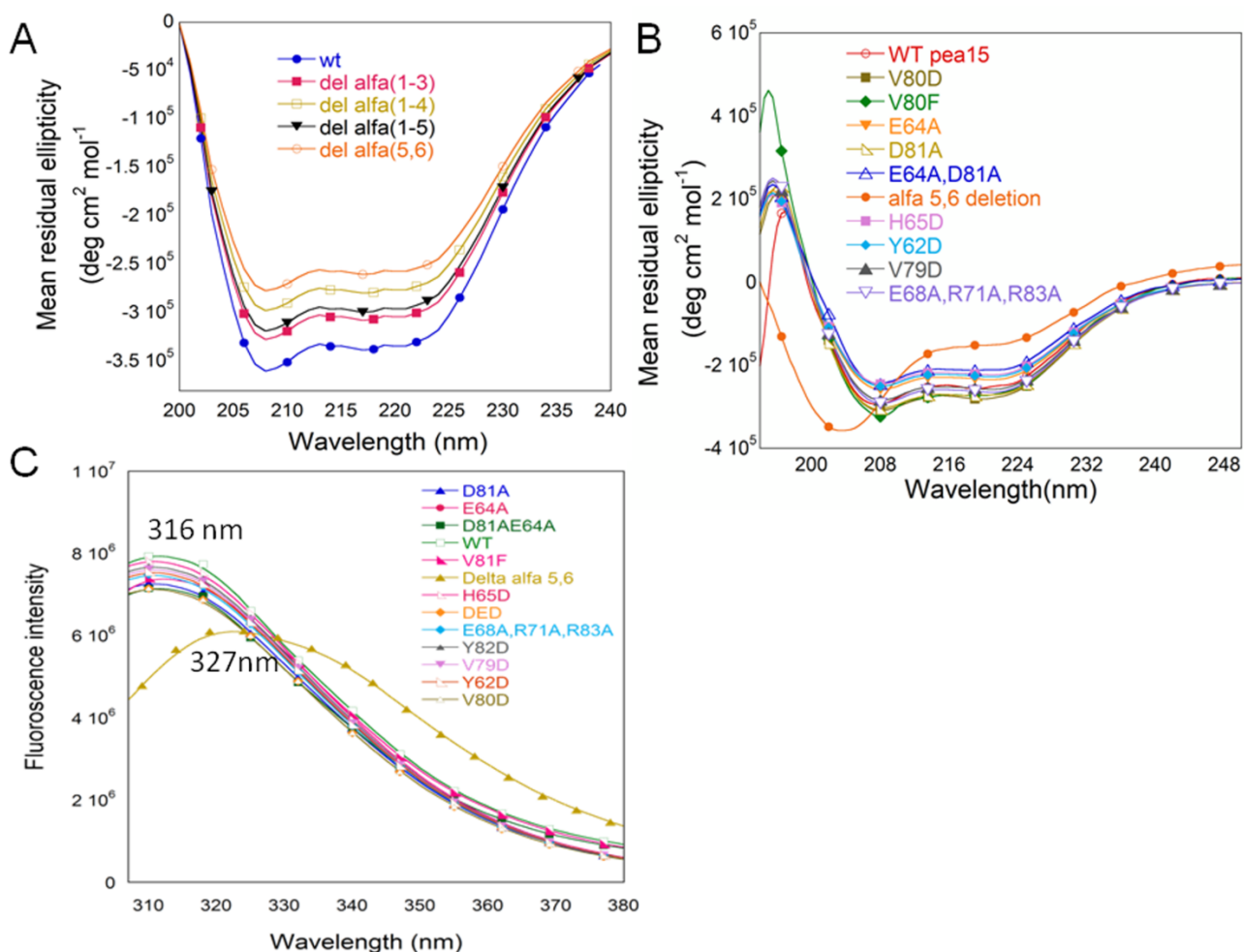
***Figure 4.2.5. Secondary and tertiary structural analysis of Pea15 constructs.** A) Far UV CD structures of MBP-fused Pea15 deletion mutants. B) Far UV CD structures of Pea15 binding and cleavage site mutants. C) Fluorescence emission studies of binding and cleavage site mutants at 295nm excitation and 305-400 nm emission wavelengths*

4.2.6 Mapping HtrA2 cleavage sites on Pea15

Time course protease degradation of Pea15 was performed to determine the cleavage pattern and also to map the cleavage sites on Pea15. From 0-7 hr incubation of pea15 with HtrA2 and N-SPD two specific fragments ~8.5 kDa and ~6.5 kDa were observed, on further incubation this 8.5 kDa fragment is degraded to 6.5 kDa. This suggests that Pea15, which is a ~17 kDa protein (including

the C-terminal His_6 and vector back bone) is degraded into two 8.5 kDa bands. While one of these bands is cleaved into 6.5 kDa fragment, and other 8.5 kDa band breaks down into very short fragments to be detected by Tris-tricine SDS-PAGE.

These Pea15 fragments (~8.5 kDa and ~6.5 kDa) generated by HtrA2 proteolysis were subjected to N-terminal sequencing by Edman degradation. Two preferred cleavage sites were identified in α-5 and α-6 helices of Pea15 DED domain respectively as shown in **figure 4.2.6A**. The preferred scissile peptide bond for the first cleavage site is between I63-E64 of -5 helix, which corresponds to the ~8.5 kDa, fragment (residues 64-130 aa). The second cleavage site is between V79-D80 of α-6 helix corresponding to the ~6.5 kDa fragment (residues 80-130 aa). It should be noted that the cleavage on Pea15 might not limited to the two mapped sites because other shorter peptides were barely detectable by coomassie blue staining.

C

MAEYGTLLQD LTNNITLEDL EQLKSACKED IPSEKSEEIT TGSAWFSFLE SHNKLDKDNL

SYI E HIFEIS RRPDLLTMV V D YRTRVLKIS EEDELDTKLT RIPSAKKYKD IIRQPSEEEI IKLAPPPKKAEF
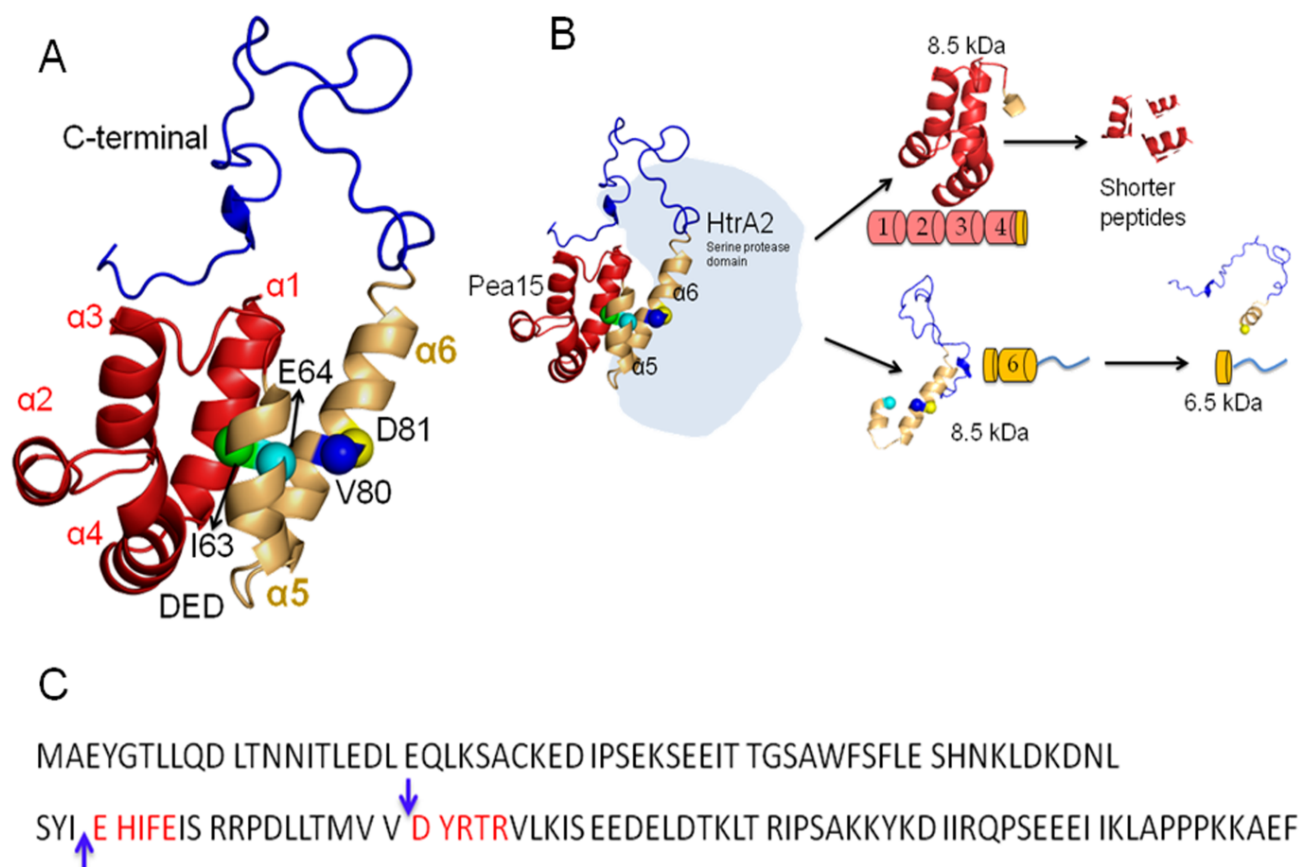
Figure 4.2.6. Representation of HtrA2 cleavage sites on Pea15. A) Ribbon diagram of the NMR structure of Pea15 (PDB accession number 1N3K). Cleavage site residues are shown in spheres. Ribbon diagram was generated using PyMOL. B) Schematic illustration of degradation pattern of Pea15. C) Residues identified using the N-terminal sequencing is highlighted as red. Two preferred scissile bonds are indicated as blue arrow

4.2.7 HtrA2 has broad specificity toward residues neighboring the peptide cleavage site

The substrate specificity of classical serine proteases is mainly defined by the residue positions at carboxyl-terminal (P1′, P2′, P3′) and amino-terminal (P1, P2, P3) to the cleavage site which are anchored by enzyme sub site residues (S3-S3′) in specificity pocket (125). Substrate specificity of HtrA2 is limited to only two published reports, which showed the strong specificity profile at the residue positions P1, P2, P1′ and P2' (11, 13). The first studies reported by Martin and co-workers focused on the determination of the primary sequence specificity of HtrA2 protease activity using combinatorial peptide library. The second report by Walle *et al.* who used a proteomic approach to identify the optimal substrate cleavage site for HtrA2 protease. To determine whether the specificity of the HtrA2 corresponds with the reported literature, we performed a sequence analysis of the identified cleavage products (~8.5 kDa and ~6.5 kDa fragments). The specificity profile for our N-terminal sequencing analysis is shown in **table 4.2.1.** The observed frequencies of amino acids in the P1 position indicated a strong preference for aliphatic residues (V and I) which is in agreement with the previous reports. Our studies demonstrated that P2 position prefers aromatic (Y) and aliphatic (V) while P3 position accommodates small hydrophobic (S, M) residues. This corroborates well with the previous published data. In contrast to the previous reports where A or S were selected at P1', our N-terminal sequencing analysis at P1' displayed preference for acidic residues (D and E). The major selectivity at P2′ is for aromatic (Y) and basic (H) residues which is in agreement with the

previous report which showed preference for aliphatic residue at this position. The observed discrepancy in cleavage site specificity between oligopeptide sequence and protein substrates might be due to conformational constraint of a potentially susceptible sequence in proteins which may be readily accommodated in substrate binding groove of protease.

Residue	8.5 kDa	6.5 kDa
P1	I	V
P2	Y	V
P3	S	M
P4	L	T
P1'	E	D
P2'	H	Y
P3'	I	R
P4'	F	T

Table 4.2.1. *Specificity of HtrA2 using Pea15 as substrate*

In order to map the other HtrA2 cleavage sites on Pea15, we mutated prime and non-prime cleavage site residues **(Figure 4.2.7)**. Since the previous reports suggested that specificity of HtrA2 primarily depends on P1, P2, P1' and P2' we focused on mutating these residues in Pea15. We expected substitution of these residues would block the cleavage at these respective sites and hence generate longer fragments which could be detected on Tris-Tricine SDS-PAGE. The P1 substrate residue is the primary determinant of specificity for serine proteases. Interestingly, although our N-terminal sequencing and previous reports displayed striking preference for

aliphatic residues at the P1 position none of the previous groups have indicated preference for polar and aromatic residues at this position. So we mutated P1 aliphatic residues (V79) in Pea15 to acidic (V79D) and aromatic (V79F). Surprisingly, mutants V79D and V79F had no affect on rate of Pea15 degradation by HtrA2 and N-SPD. Moreover the mutant (V79F) was cleaved much faster compared to the wild-type Pea15. Thus our mutational analysis of P1 cleavage site residues showed equal preference for D and stronger preference for F in addition to aliphatic residues. As our sequencing analysis at P1′ displayed preference for acidic residues, we mutated these residues to A (E64A, D80A), where previous reports suggested A is the most preferred residue at this position. We expected a profound change in the Pea15 degradation by HtrA2 strikingly, A substitution did not have any effect on its degradation. The rate of cleavage of theses mutants were similar to wild-type Pea15. The obtained specificity from our studies with regards to the P2 (Y62, H65) and P2' (Y78, V81), was mostly hydrophobic. Since none of the previous reports showed selection for acidic residues at this position, we mutated these residues to acidic (D). The observed rate of cleavage for these mutants was equal to wild-type Pea15 suggesting the equal preference for acidic (D) in addition to hydrophobic residue. Taken together these results suggest HtrA2 has a broad specificity towards the residues in the vicinity of cleavage site. The observed broad substrate specificity of HtrA2 might be due to the structural rearrangement at the substrate specificity pocket to accommodate different type of amino acids near the peptide cleavage site. This broad substrate specificity of HtrA2 might account for its various biological functions in maintaining mitochondrial homeostasis, protein quality control and apoptosis by degrading a variety of physiological substrates. However, the specificity of HtrA2 in recognizing selective substrates might hint toward the involvement of additional structural elements in the protein substrates that interact with the protease and influence its

overall topological targeting and enzymatic activity. Further to gain an insight into the structural

determinants of HtrA2 substrate recognition and specificity a high resolution crystal structure of

HtrA2 in complex with protein substrate or oligopeptide is required.
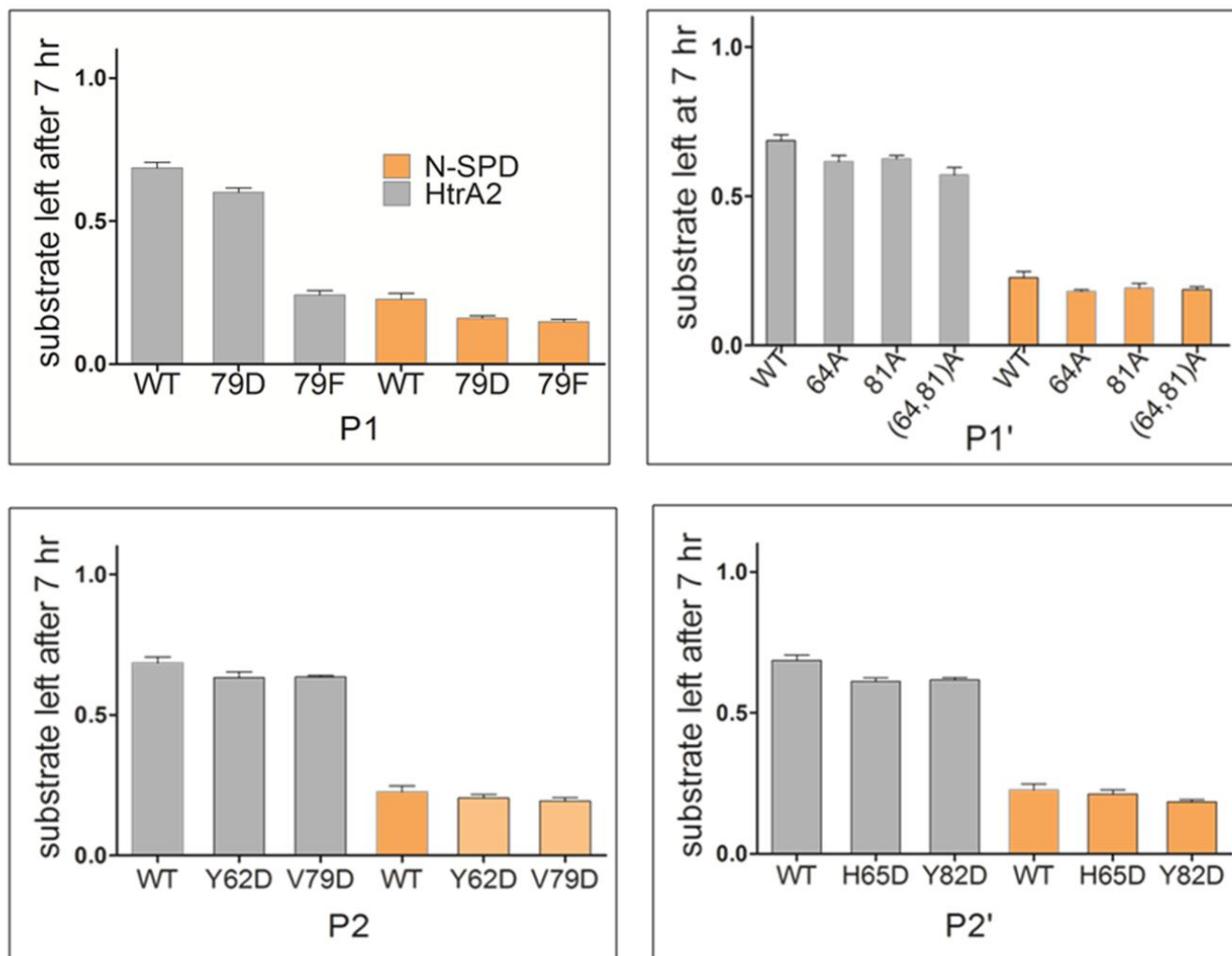
Figure 4.2.7. Cleavage site specificity profile of HtrA2 using Pea15 as a substrate. *Values represent the amount of substrate left after 7 hr of a given amino acid selected at positions carboxyl-terminal (P1', P2') and amino-terminal (P1, P2,) to the HtrA2 cleavage site and are normalized to an average value of one relative to uncleaved substrate*

4.2.3 Discussion

HtrA2 is a nuclear-encoded mitochondrial serine protease that performs several critical cellular functions in a coordinated fashion. Although, HtrA2 has primarily been identified as an IAP-binding proapoptotic protein, its other functions such as caspase-independent induction of apoptosis and serine protease activity are poorly characterized.

Despite numerous reports on HtrA2 induced apoptosis, little is known about its mode of regulation, and the mechanism of interaction with its substrates involved in mediating this function. The available crystallographic data on mature substrate unbound form of HtrA2 provided a broad overview of its structural organization. However, these studies could not define its mode of activation, which is a prerequisite for understanding its role in various biological pathways and diseases. Thus, considering the biological relevance we previously (chapter 4.1) elucidated the role of N-terminal region, oligomerization, and intermolecular PDZ-protease interaction in proper active site formation and enzyme-substrate complex stabilization in HtrA2 enzymatic functions (126). Another study elucidated the activation mechanism of HtrA2 by XIAP in a PDZ-independent yet synergistic activation mechanism via N-terminal region (11). This phenomenon emphasizes multiple modes of HtrA2 activation and regulation, the precise mechanism for which remains to be elucidated. Furthermore, delineating the basis and global mode of HtrA2 activation might give rise to therapeutic possibilities in various pathophysiological conditions such as cancer and neurodegenerative disorders.

To delineate the structural correlates of HtrA2 activation, substrate recognition and specificity, comprehensive binding studies with its interacting partners is necessary. In the present work we dissected the molecular mechanism of HtrA2 with its known antiapoptotic substrate Pea15. Although previous studies have reported that stress induced activated HtrA2

interacts with the cytosolic Pea15 and promotes its degradation which leads to cell death (8). However, the interacting region, critical residues involved in interaction and substrate specificity of HtrA2 are not known. It was well established in literature that PDZ domain of HtrA2 is involved in interacting with different cellular proteins. Our interaction studies provide a remarkable insight into the unique mechanism which involves previously unidentified region of HtrA2 in interaction with Pea15. We identified that protease domain and not the conventional PDZ domain of HtrA2 interacts with residues of α-5 and α-6 helices of Pea15 DED domain. Moreover, our mutational analysis has shown that E86, R71, and R83 of Pea 15 are essential in mediating the interaction with HtrA2. However, previously it was reported that Pea15 DED is sufficient for the interaction with HtrA2, surprisingly, our deletion mutational analysis showed C-terminal of Pea15 is also essential in mediating interaction with HtrA2. This complex bipartite mode of interaction involving both DED and C-terminal region might require for enhancing the affinity of individually weaker interactions and allows for greater binding specificity.

Enzymology studies with wild-type HtrA2 and its variant, N-SPD using substrate Pea15 delineated new regulatory mechanism of HtrA2. Interestingly, PDZ deleted variant (N-SPD) showed rapid hydrolysis of Pea15 compared to wild-type HtrA2. The lower protease activity for HtrA2 wild-type might be due to inhibitory effect of PDZ domain on its protease activity, probably through restriction of substrate accessibility to the active-site. Based on our observations, we hypothesize that in a cellular milieu, binding of proteins to PDZ domain of HtrA2 might allosterically modulates the protease thereby increasing the overall catalytic efficiency in a PDZ-dependent manner. Thus, upregulation in its protease activity in conjunction with PDZ binding proteins might promote the non-classical 'caspase-independent mechanism' and hence cell death. In agreement with this hypothesis, it has been demonstrated that the

proteolytic activity of the HtrA2 towards IAPs is enhanced several fold by protein-protein interactions, mediated by the PDZ domain of HtrA2 and the C- terminal of WARTS Kinase (127), presenilin-1 (128), GRIM-19 (129) and proliferation-associated gene product (Pag) (130). This amplified proapoptotic property resulted in elevated rate of apoptosis in HeLa, human adenocarcinoma, and kidney embryonic cells. Moreover, it has been observed that binding of peptides to the PDZ domain of HtrA2 stimulates its protease activity *in vitro* (11, 130). To data, Pea15 has been reported to be over-expressed in a number of different types of cancer, such as gliomas, squamous carcinoma, breast, lung cancer, and B cells chronic lymphocytic leukemia (131). Therefore, developing a strategy that modulates the proteolytic activity of HtrA2 towards antiapoptotic Pea15 could be a promising tool in cancer treatment.

Our primary sequence specificity based on the N-terminal sequencing and mutational analysis displayed a broad specificity for HtrA2 toward the residues in vicinity of cleavage site. Although previous reports suggest HtrA2 has preference towards aliphatic residues at P1 position, our studies indicated that polar (D) and aromatic (F) residues are also equally preferred at P1. In contrast to the literature for selectivity of A and S at P1', our results demonstrated striking preference for acidic residues (E and D) at the P1'. Previous reports suggests that P2 prefers basic (R) and aliphatic (L) residues while, P2' position displays preference for aromatic (F) residues (11). Interestingly, our data demonstrate that acidic residues (D) are also preferred at P2 and P2' positions. This apparent discrepancy in cleavage site specificity between peptide and protein substrates of HtrA2 is due to conformational constraint of a potentially susceptible sequence in proteins. Moreover, Variations in the natural frequency of occurrence of amino acids in endogenous proteins may be an additional parameter that may help explain the differences between peptide and protein cleavage site specificities. It is likely that this specificity partly

determines the choice of residues selected by HtrA2 within a target protein. However, the selection of target proteins may also be dependent on which proteins are bound to the PDZ domain or other regions of HtrA2, and thus brought into proximity with the active site region.

.

Chapter 5

Conclusions and

Future perspectives

5.1. Conclusions

Defective apoptosis or impaired apoptotic signaling is associated with development and progression of cancer (14). Over the past few decades, significant advances have been made in understanding the molecular mechanisms that regulate apoptosis and the mediators that trigger cell death. Consequently, apoptosis induction in cancer cells has emerged as one of the great hopes for the management of cancers (16, 22-27). Currently, strategies to trigger caspase activation are at the forefront of apoptosis-based drug development (28, 29). However, the complexity of cancer biology draws interest in search of new molecules that can potentially modulate the apoptotic signaling pathway. The findings that serine protease HtrA2 mediates caspase-dependent and independent cell death open new avenues in apoptosis and cancer research. Here, with a goal to understand the HtrA2 mechanism of action or its regulation, which is a prerequisite for understanding its role in various biological pathways, we characterized the structural and functional properties of HtrA2.

In the present study, using inter-disciplinary approaches such as *in silico,* enzymology and biophysical studies, we have demonstrated the complexity of conformational changes and dynamics that regulate HtrA2 functions. Here, we have done domain-wise dissection of HtrA2 to delineate their roles alone and in different combinations, including loops, crucial residues and flexible interface linker in modulating HtrA2 functions. This unique approach clearly pinpointed the role of trimerisation, N-terminal region and intermolecular PDZ-protease dynamics in a precise coordinated fashion toward formation of a catalytically competent HtrA2 molecule. These findings establish the role of PDZ domain in not only interface dynamics and initial substrate binding but also in intermolecular contacts in the trimeric protease architecture leading

to efficient substrate catalysis. This complex synergistic mechanism of action might be important for regulation of its biological functions.

We also provided the first comprehensive binding analysis of HtrA2-Pea15 interaction. Our binding studies demonstrated that serine protease domain of HtrA2 interacts with both DED domain as well as C-terminal disordered region of Pea15 in bipartite binding mode. We believe that this bipartite binding mode might be required for greater binding affinity and specificity to suppress the ultimate outcome of the Pea15 antiapoptotic signaling cascade in cytoplasm. Enzymology studies with Pea15 suggest that allosteric activation of HtrA2 might be required by adaptor proteins in the cell to relieve the inhibitory effect of PDZ domain. We speculate that HtrA2 by virtue of its ability to cleave different cellular substrates might have developed an intrinsic allosteric mechanism for precise control of its protease activity. Furthermore, our substrate specificity studies with Pea15 highlight that HtrA2 has broad substrate specificity toward the residues in the vicinity of the cleavage site. We hypothesize that this broad specificity might account for its diverse physiological functions in cells by cleaving several substrates.

Proteolytic activity of HtrA2 was shown to be critical in inducing apoptosis in prostate and ovarian cancer cells in presence of stress inducing agents (79). These studies show the possibility of targeting HtrA2 in cancer therapy. Our advancement in understanding toward HtrA2 mechanism of action will help in developing tailored allosteric effectors that enhances the proteolytic activity of HtrA2 towards its substrates. This could be a promising tool in cancer treatment in combination with other chemotherapeutic agents such as cisplatin and paclitaxel (132).

5.2 Future perspective

Although our observations redefine the existing activation model and provide new insights into HtrA2 structure, function, and dynamics, several intricate questions still remain unanswered. Despite the structural similarity between DegS, HtrA1 and HtrA2, there are striking mechanistic differences both in protein dynamics as well as PDZ-protease interactions. Literature suggests in bacterial DegS, ligand binding to PDZ leads to both *cis* and *trans* protease domain rearrangement so as to form an active DegS molecule. Our studies so far suggest role of *trans* PDZ-protease crosstalk (intermolecular) to play primary role in allosteric activation of HtrA2. Interestingly, HtrA1 is regulated by a conformational selection and does not depend on allosteric ligands as seen in HtrA2. Moreover, it has also been observed that HtrA2 can be activated through its N-terminal tetrapeptide (AVPS) motif. Therefore, to understand the allosteric mechanism of HtrA2 in molecular detail, it becomes necessary to dissect the trimeric protease structure so as to delineate the roles of individual PDZ domains, the N-terminal region and conserved critical amino acids mediating allosteric propagation of HtrA2. Identification of the control switch regulating the protease activity will provide intricate details of its association with myriads of cellular substrates and their mechanism of cleavage. Furthermore, it will provide an idea of how HtrA2 might be activated *in vivo* in presence of different stimuli.

HtrA2-Pea15 binding studies suggest that HtrA2 requires Pea15 DED for interaction. Indeed, a truncated protein, lacking the entire DED, does not interact with HtrA2. It would be interesting to look into the interaction of HtrA2 with other DED containing proteins. This interaction studies will indicate the specificity of HtrA2 toward Pea15. Furthermore, it would be important to address how the relative endogenous expression levels of HtrA2 and Pea15 regulate

apoptosis in tumor cell. This complex interplay between these proteins might provide a crucial role in cellular fate determination.

HtrA2 has a broad specificity toward the residues in the vicinity of cleavage site. A high resolution crystal structure of HtrA2 in complex with protein substrate or oligopeptide will provide an insight into the structural determinants of HtrA2 substrate specificity. Moreover, knowledge of HtrA2 substrate specificity might provide a clue for identification of new substrates.

References

1. Lipinska, B., Fayet, O., Baird, L., and Georgopoulos, C. (1989) Identification, characterization, and mapping of the Escherichia coli htrA gene, whose product is essential for bacterial growth only at elevated temperatures. *J Bacteriol* **171**, 1574-1584.

2. Wu, G., Chai, J., Suber, T. L., Wu, J.-W., Du, C., Wang, X., and Shi, Y. (2000) Structural basis of IAP recognition by Smac/DIABLO. *Nature* **408**, 1008-1012

3. Suzuki, Y., Imai, Y., Nakayama, H., Takahashi, K., Takio, K., and Takahashi, R. (2001) A serine protease, HtrA2, is released from the mitochondria and interacts with XIAP, inducing cell death. *Mol. Cell.* **8**, 613-621.

4. Hegde, R., Srinivasula, S., Zhang, Z., Wassell, R., Mukattash, R., Cilenti, L., DuBois, G., Lazebnik, Y., Zervos, A., Fernandes-Alnemri, T., and Alnemri, E. (2002) Identification of Omi/HtrA2 as a mitochondrial apoptotic serine protease that disrupts inhibitor of apoptosis protein-caspase interaction. *J Biol Chem* **277**, 432-438.

5. Martins, L., Iaccarino, I., Tenev, T., Gschmeissner, S., Totty, N., Lemoine, N., Savopoulos, J., Gray, C., Creasy, C., Dingwall, C., and Downward, J. (2002) The serine protease Omi/HtrA2 regulates apoptosis by binding XIAP through a reaper-like motif. *J Biol Chem* **277**, 439-444.

6. Verhagen, A., Silke, J., Ekert, P., Pakusch, M., Kaufmann, H., Connolly, L., Day, C., Tikoo, A., Burke, R., Wrobel, C., Moritz, R., Simpson, R., and Vaux, D. (2002) HtrA2 promotes cell death through its serine protease activity and its ability to antagonize inhibitor of apoptosis proteins. *J Biol Chem* **277**, 445-454.

7. Bhuiyan, M. S., and Fukunaga, K. (2007) Inhibition of HtrA2/Omi ameliorates heart dysfunction following ischemia/reperfusion injury in rat heart in vivo. *European Journal of Pharmacology* **557**, 168-177

8.   Trencia, A., Fiory, F., Maitan, M., Vito, P., Barbagallo, A., Perfetti, A., Miele, C., Ungaro, P., Oriente, F., Cilenti, L., Zervos, A., Formisano, P., and Beguinot, F. (2004) Omi/HtrA2 promotes cell death by binding and degrading the anti-apoptotic protein ped/pea-15. *J Biol Chem.* **279**, 46566-46572.

9.   Cilenti, L., Soundarapandian, M., Kyriazis, G., Stratico, V., Singh, S., Gupta, S., Bonventre, J., Alnemri, E., ., and AS., Z. (2004) Regulation of HAX-1 anti-apoptotic protein by Omi/HtrA2 protease during cell death. *J Biol Chem.* **279**, 50295-50301.

10.   Li, W., Srinivasula, S., Chai, J., Li, P., Wu, J., Zhang, Z., Alnemri, E., and Shi, Y. (2002) Structural insights into the pro-apoptotic function of mitochondrial serine protease HtrA2/Omi. *Nat. Struct. Biol.* **9**, 436-441.

11.   Martins, L., Turk, B., Cowling, V., Borg, A., Jarrell, E., Cantley, L., and Downward, J. (2003) Binding specificity and regulation of the serine protease and PDZ domains of HtrA2/Omi. *J Biol Chem.* **278**, 49417-49427.

12.   Hill, J., Vaidyanathan, H., Ramos, J., Ginsberg, M., and Werner, M. (2002) Recognition of ERK MAP kinase by PEA-15 reveals a common docking site within the death domain and death effector domain. *EMBO J.* **21**, 6494-6504.

13.   Vande Walle, L., Van Damme, P., Lamkanfi, M., Saelens, X., Vandekerckhove, J., Gevaert, K., and Vandenabeele, P. (2007) Proteome-wide Identification of HtrA2/Omi Substrates. *Journal of Proteome Research* **6**, 1006-1015

14.   Duque-Parra, J. (2005) Note on the origin and history of the term "apoptosis". *Anat Rec B New Anat* **283**, 2-4.

15.   Lawen, A. (2003) Apoptosis-an introduction. *Bioessays* **25**, 888-896.

16.   Ozoren, N., and El-Deiry, W. (2003) Cell surface Death Receptor signaling in normal and cancer cells. *Semin Cancer Biol* **13**, 135-147.

17.   Thorburn, A. (2004) Death receptor-induced cell killing. *Cell Signal* **16**, 139-144.

18.   Peter, M., and Krammer, P. (1998) Mechanisms of CD95 (APO-1/Fas)-mediated apoptosis. *Curr Opin Immunol* **10**, 545-551.

19.   Strasser, A., O'Connor, L., and Dixit, V. (2000) Apoptosis signaling. *Annu Rev Biochem* **69**, 217-245.

20.   Degli Esposti, M. (1999) To die or not to die—The quest of the TRAIL receptors. *J Leukoc Biol* **65**, 535-542.

21.   Abe, K., Kurakin, A., Mohseni-Maybodi, M., Kay, B., and Khosravi-Far, R. (2000) The complexity of TNFrelated apoptosis-inducing ligand. *Ann N Y Acad Sci* **926**, 52-63.

22.   Zornig, M., Hueber, A., Baum, W., Evan, G., and 1551:F1-37. (2001) Apoptosis regulators and their role in tumorigenesis. *Biochim Biophys Acta* **1551**, F1-37.

23.   Daniel, P., Wieder, T., Sturm, I., and Schulze-Osthoff, K. (2001) The kiss of death: promises and failures of death receptors and ligands in cancer therapy. *Leukemia* **15**, 1022-1032.

24.   Green, D., and Evan, G. (2002) A matter of life and death. *Cancer Cell* **1**, 19-30.

25.   Thompson, C. (1995) Apoptosis in the pathogenesis and treatment of disease. *Science* **267**, 1456-1462.

26.   Sheikh, M., and Huang, Y. (2004) Death receptors as targets of cancer therapeutics. *Curr Cancer Drug Targets* **4**, 97-104.

27.   Burns, T., and el-Deiry, W. (2003) Cell death signaling in maligancy. *Cancer Treat Res* **115**, 319-343.

28. Lushnikov, E. F., and Zagrebin, V. M. (1987) [Cellular apoptosis: its morphology, biological role and the mechanisms of its development]. *Arkh Patol* **49**, 84-89

29. Wyllie, A. H., Kerr, J. F., and Currie, A. R. (1980) Cell death: the significance of apoptosis. *Int Rev Cytol* **68**, 251-306

30. McIlwain, D. R., Berger, T., and Mak, T. W. (2013) Caspase Functions in Cell Death and Disease. *Cold Spring Harbor Perspectives in Biology* **5**

31. Philchenkov, A. (2004) Caspases: potential targets for regulating cell death. *J Cell Mol Med* **8**, 432-444

32. Faccio, L., Fusco, C., Chen, A., Martinotti, S., Bonventre, J., and Zervos, A. (2000) Characterization of a Novel Human Serine Protease That Has Extensive Homology to Bacterial Heat Shock Endoprotease HtrA and Is Regulated by Kidney Ischemia. *J Biol Chem.* **275**, 2581-2588

33. Chien, J., Aletti G Fau - Baldi, A., Baldi A Fau - Catalano, V., Catalano V Fau - Muretto, P., Muretto P Fau - Keeney, G. L., Keeney Gl Fau - Kalli, K. R., Kalli Kr Fau - Staub, J., Staub J Fau - Ehrmann, M., Ehrmann M Fau - Cliby, W. A., Cliby Wa Fau - Lee, Y. K., Lee Yk Fau - Bible, K. C., Bible Kc Fau - Hartmann, L. C., Hartmann Lc Fau - Kaufmann, S. H., Kaufmann Sh Fau - Shridhar, V., and Shridhar, V. (2006) Serine protease HtrA1 modulates chemotherapy-induced cytotoxicity. *J Clin Invest.* **7**, 1994-2004

34. Clausen, T., Kaiser, M., Huber, R., and Ehrmann, M. (2011) HTRA proteases: regulated proteolysis in protein quality control. *Nat Rev Mol Cell Biol* **12**, 152-162.

35. Chien, J., Campioni, M., Shridhar, V., and Baldi, A. (2009) HtrA serine proteases as potential therapeutic targets in cancer. *Curr Cancer Drug Targets* **9**, 451-468.

36. He, X., Khurana A Fau - Maguire, J. L., Maguire Jl Fau - Chien, J., Chien J Fau - Shridhar, V., and Shridhar, V. (2012) HtrA1 sensitizes ovarian cancer cells to cisplatin-induced cytotoxicity by targeting XIAP for degradation. *Int J Cancer* **5**, 10295-10235

37. Akhurst, R. J., and Derynck, R. (2001) TGF-beta signaling in cancer--a double-edged sword. *Trends Cell Biol* **11**, s44-51

38. Gray, C., Ward, R., Karran, E., Turconi, S., Rowles, A., Viglienghi, D., Southan, C., Barton, A., Fantom, K., West, A., Savopoulos, J., Hassan, N., Clinkenbeard, H., Hanning, C., Amegadzie, B., Davis, J., Dingwall, C., Livi, G., and Creasy, C. (2000) Characterization of human HtrA2, a novel serine protease involved in the mammalian cellular stress response. *Eur. J. Biochem.* **267**, 5699-5710.

39. Oka, C., Tsujimoto R Fau - Kajikawa, M., Kajikawa M Fau - Koshiba-Takeuchi, K., Koshiba-Takeuchi K Fau - Ina, J., Ina J Fau - Yano, M., Yano M Fau - Tsuchiya, A., Tsuchiya A Fau - Ueta, Y., Ueta Y Fau - Soma, A., Soma A Fau - Kanda, H., Kanda H Fau - Matsumoto, M., Matsumoto M Fau - Kawaichi, M., and Kawaichi, M. (2004) HtrA1 serine protease inhibits signaling mediated by Tgfbeta family proteins. *Development* **5**, 1041-1053

40. Clausen, T., Southan, C., and Ehrmann, M. (2002) The HtrA family of proteases: implications for protein composition and cell fate. *Mol. Cell.* **10**, 443-455.

41. Suzuki, Y. T.-N., K., Akagi, T., Hashikawa, T., and Takahashi, R. (2004) Mitochondrial protease Omi/HtrA2 enhances caspase activation through multiple pathways. *Cell Death Differ.* **11**, 208-216.

42. Meltzer, M., Hasenbein, S., Mamant, N., Merdanovic, M., Poepsel, S., Hauske, P., Kaiser, M., Huber, R., Krojer, T., Clausen, T., and Ehrmann, M. (2009) Structure,

function and regulation of the conserved serine proteases DegP and DegS of Escherichia coli. *Res Microbiol* **160**, 660-666.

43. Zurawa-Janicka, D., Skorko-Glonek, J., and Lipinska, B. (2010) HtrA proteins as targets in therapy of cancer and other diseases. *Expert Opin Ther Targets* **14**, 665-679.

44. Polur, I., Lee, P., Servais, J., Xu, L., and Li, Y. (2010) Role of HTRA1, a serine protease, in the progression of articular cartilage degeneration. *Histol Histopathol* **25**, 599-608.

45. Jones, J. M., Datta P Fau - Srinivasula, S. M., Srinivasula Sm Fau - Ji, W., Ji W Fau - Gupta, S., Gupta S Fau - Zhang, Z., Zhang Z Fau - Davies, E., Davies E Fau - Hajnoczky, G., Hajnoczky G Fau - Saunders, T. L., Saunders Tl Fau - Van Keuren, M. L., Van Keuren Ml Fau - Fernandes-Alnemri, T., Fernandes-Alnemri T Fau - Meisler, M. H., Meisler Mh Fau - Alnemri, E. S., and Alnemri, E. S. (2003) Loss of Omi mitochondrial protease activity causes the neuromuscular disorder of mnd2 mutant mice. *Nature.* **6959**, 721-727

46. Krick, S., Shi S Fau - Ju, W., Ju W Fau - Faul, C., Faul C Fau - Tsai, S.-y., Tsai Sy Fau - Mundel, P., Mundel P Fau - Bottinger, E. P., and Bottinger, E. P. (2008) Mpv17l protects against mitochondrial oxidative stress and apoptosis by activation of Omi/HtrA2 protease. *Proc Natl Acad Sci U S A.* **37**, 14106-14111

47. Raff, M. (1998) Cell suicide for beginners. *Nature* **396**, 119-122.

48. Nikoletopoulou, V., Markaki, M., Palikaras, K., and Tavernarakis, N. (2013) Crosstalk between apoptosis, necrosis and autophagy. *Biochimica et Biophysica Acta (BBA) - Molecular Cell Research* **1833**, 3448-3459

49. Kasibhatla, S., and Tseng, B. (2003) Why Target Apoptosis in Cancer Treatment? *Molecular Cancer Therapeutics* **2**, 573-580

50. Jin, Z., and El-Deiry, W. S. (2005) Overview of cell death signaling pathways. *Cancer Biol Ther* **4**, 139-163

51. Schultz, D. R., and Harrington, W. J., Jr. (2003) Apoptosis: programmed cell death at a molecular level. *Semin Arthritis Rheum* **32**, 345-369

52. Naismith, J. H., and Sprang, S. R. (1998) Modularity in the TNF-receptor family. *Trends Biochem Sci* **23**, 74-79

53. Schneider, P., and Tschopp, J. (2000) Apoptosis induced by death receptors. *Pharm Acta Helv* **74**, 281-286

54. Askkenazi, A., and Dixit, V. (1999) Apoptosis control by death and decoy receptors. *Curr Opin Cell Biol* **11**, 255-260.

55. Park, H. H., Lo, Y.-C., Lin, S.-C., Wang, L., Yang, J. K., and Wu, H. (2007) The Death Domain Superfamily in Intracellular Signaling of Apoptosis and Inflammation. *Annual review of immunology* **25**, 561-586

56. Sessler, T., Healy, S., Samali, A., and Szegezdi, E. (2013) Structural determinants of DISC function: new insights into death receptor-mediated apoptosis signalling. *Pharmacol Ther* **140**, 186-199

57. Yan, Q., McDonald, J. M., Zhou, T., and Song, Y. (2013) Structural insight for the roles of fas death domain binding to FADD and oligomerization degree of the Fas-FADD complex in the death-inducing signaling complex formation: a computational study. *Proteins* **81**, 377-385

58. Wang, L., Yang, J. K., Kabaleeswaran, V., Rice, A. J., Cruz, A. C., Park, A. Y., Yin, Q., Damko, E., Jang, S. B., Raunser, S., Robinson, C. V., Siegel, R. M., Walz, T., and Wu,

H. (2010) The Fas-FADD death domain complex structure reveals the basis of DISC assembly and disease mutations. *Nat Struct Mol Biol* **17**, 1324-1329

59.   Salvesen, G. S., and Dixit, V. M. (1999) Caspase activation: the induced-proximity model. *Proc Natl Acad Sci U S A* **96**, 10964-10967

60.   Kroemer, G. (2003) Mitochondrial control of apoptosis: an introduction. *Biochem Biophys Res Commun* **304**, 433-435

61.   Acehan, D., Jiang, X., Morgan, D. G., Heuser, J. E., Wang, X., and Akey, C. W. (2002) Three-dimensional structure of the apoptosome: implications for assembly, procaspase-9 binding, and activation. *Mol Cell* **9**, 423-432

62.   Zou, H., Li, Y., Liu, X., and Wang, X. (1999) An APAF-1.cytochrome c multimeric complex is a functional apoptosome that activates procaspase-9. *J Biol Chem* **274**, 11549-11556

63.   Li, H., Zhu, H., Xu, C. J., and Yuan, J. (1998) Cleavage of BID by caspase 8 mediates the mitochondrial damage in the Fas pathway of apoptosis. *Cell* **94**, 491-501

64.   Luo, X., Budihardjo, I., Zou, H., Slaughter, C., and Wang, X. (1998) Bid, a Bcl2 interacting protein, mediates cytochrome c release from mitochondria in response to activation of cell surface death receptors. *Cell* **94**, 481-490

65.   Bhuiyan, M. S., and Fukunaga, K. (2008) Activation of HtrA2, a Mitochondrial Serine Protease Mediates Apoptosis: Current Knowledge on HtrA2 Mediated Myocardial Ischemia/Reperfusion Injury. *Cardiovascular Therapeutics* **26**, 224-232

66.   Spiess, C., Beil, A., and Ehrmann, M. (1999) A temperature-dependent switch from chaperone to protease in a widely conserved heat shock protein. *Cell* **97**, 339-347.

67.   Faccio, L., Fusco, C., Viel, A., and Zervos, A. S. (2000) Tissue-Specific Splicing of Omi Stress-Regulated Endoprotease Leads to an Inactive Protease with a Modified PDZ Motif. *Genomics* **68**, 343-347

68.   Kadomatsu, T., Mori M Fau - Terada, K., and Terada, K. (2007) Mitochondrial import of Omi: the definitive role of the putative transmembrane region and multiple processing sites in the amino-terminal segment. *Biochem Biophys Res Commun* **2**, 516-521

69.   Murwantoko., Yano, M., Ueta, Y., Murasaki, A., Kanda, H., Oka, C., and Kawaichi, M. (2004) Binding of proteins to the PDZ domain regulates proteolytic activity of HtrA1 serine protease. *Biochem J* **381**, 895-904.

70.   Lee, H.-J., and Zheng, J. J. (2010) PDZ domains and their binding partners: structure, specificity, and modification. *Cell Communication and Signaling : CCS* **8**, 8-8

71.   Bejugam , P. R., Kuppili , R. R., Singh , N., Gadewal, N., Chaganti, L. K., Sastry, G. M., and Bose, K. (2012) Allosteric regulation of serine protease HtrA2 through novel non-canonical substrate binding pocket. *Plos one* **8**

72.   Krojer, T., Sawa, J., Huber, R., and Clausen, T. (2010) HtrA proteases have a conserved activation mechanism that can be triggered by distinct molecular cues. *Nat Struct Mol Biol* **17**, 844-852.

73.   Zhang, X., and Z., C. (2004) Temperature dependent protease activity and structural properties of human HtrA2 protease. *Biochemistry* **69**, 687-692.

74.   Kraut, J. (1977) Serine Proteases: Structure and Mechanism of Catalysis. *Annual Review of Biochemistry* **46**, 331-358

75. Yang, Q., Church-Hajduk, R., Ren, J., Newton, M., and Du, C. (2003) Omi/HtrA2 catalytic cleavage of inhibitor of apoptosis (IAP) irreversibly inactivates IAPs and facilitates caspase activity in apoptosis. *Genes Dev.* **17**, 1487-1496.

76. Srinivasula, S. M., Gupta S Fau - Datta, P., Datta P Fau - Zhang, Z., Zhang Z Fau - Hegde, R., Hegde R Fau - Cheong, N., Cheong N Fau - Fernandes-Alnemri, T., Fernandes-Alnemri T Fau - Alnemri, E. S., and Alnemri, E. S. (2003) Inhibitor of apoptosis proteins are substrates for the mitochondrial serine protease Omi/HtrA2. *J Biol Chem* **34**, 31469-31472

77. Marabese, M., Mazzoletti M Fau - Vikhanskaya, F., Vikhanskaya F Fau - Broggini, M., and Broggini, M. (2008) HtrA2 enhances the apoptotic functions of p73 on bax. *Cell Death Differ* **5**, 849-858

78. Hartkamp, J., Carpenter, B., and Roberts, S. G. E. (2010) The Wilms' Tumor Suppressor Protein WT1 Is Processed by the Serine Protease HtrA2/Omi. *Molecular Cell* **37**, 159-171

79. Yamauchi, S., Hou, Y. Y., Guo, A. K., Hirata, H., Nakajima, W., Yip, A. K., Yu, C.-h., Harada, I., Chiam, K.-H., Sawada, Y., Tanaka, N., and Kawauchi, K. (2014) p53-mediated activation of the mitochondrial protease HtrA2/Omi prevents cell invasion. *The Journal of Cell Biology* **204**, 1191-1207

80. Martins, L. M., Morrison A Fau - Klupsch, K., Klupsch K Fau - Fedele, V., Fedele V Fau - Moisoi, N., Moisoi N Fau - Teismann, P., Teismann P Fau - Abuin, A., Abuin A Fau - Grau, E., Grau E Fau - Geppert, M., Geppert M Fau - Livi, G. P., Livi Gp Fau - Creasy, C. L., Creasy Cl Fau - Martin, A., Martin A Fau - Hargreaves, I., Hargreaves I Fau - Heales, S. J., Heales Sj Fau - Okada, H., Okada H Fau - Brandner, S., Brandner S Fau -

Schulz, J. B., Schulz Jb Fau - Mak, T., Mak T Fau - Downward, J., and Downward, J. (2004) Neuroprotective role of the Reaper-related serine protease HtrA2/Omi revealed by targeted deletion in mice. *Mol Cell Biol* **22**, 9848-9862

81.   Plun-Favreau, H., Klupsch, K., Moisoi, N., Gandhi, S., Kjaer, S., Frith, D., Harvey, K., Deas, E., Harvey, R. J., McDonald, N., Wood, N. W., Martins, L. M., and Downward, J. (2007) The mitochondrial protease HtrA2 is regulated by Parkinson's disease-associated kinase PINK1. *Nat Cell Biol* **9**, 1243-1252

82.   Unal Gulsuner, H., Gulsuner, S., Mercan, F. N., Onat, O. E., Walsh, T., Shahin, H., Lee, M. K., Dogu, O., Kansu, T., Topaloglu, H., Elibol, B., Akbostanci, C., King, M.-C., Ozcelik, T., and Tekinay, A. B. (2014) Mitochondrial serine protease HTRA2 p.G399S in a kindred with essential tremor and Parkinson disease. *Proceedings of the National Academy of Sciences* **111**, 18285-18290

83.   Strauss, K. M., Martins, L. M., Plun-Favreau, H., Marx, F. P., Kautzmann, S., Berg, D., Gasser, T., Wszolek, Z., Müller, T., Bornemann, A., Wolburg, H., Downward, J., Riess, O., Schulz, J. B., and Krüger, R. (2005) Loss of function mutations in the gene encoding Omi/HtrA2 in Parkinson's disease. *Human Molecular Genetics* **14**, 2099-2111

84.   Kooistra, J., Milojevic J Fau - Melacini, G., Melacini G Fau - Ortega, J., and Ortega, J. (2008) A new function of human HtrA2 as an amyloid-beta oligomerization inhibitor. *J Alzheimers Dis* **2**, 281-294

85.   Huttunen, H. J., Guénette, S. Y., Peach, C., Greco, C., Xia, W., Kim, D. Y., Barren, C., Tanzi, R. E., and Kovacs, D. M. (2007) HtrA2 Regulates β-Amyloid Precursor Protein (APP) Metabolism through Endoplasmic Reticulum-associated Degradation. *Journal of Biological Chemistry* **282**, 28285-28295

86. Cilenti, L., Ambivero, C. T., Ward, N., Alnemri, E. S., Germain, D., and Zervos, A. S. (2014) Inactivation of Omi/HtrA2 protease leads to the deregulation of mitochondrial Mulan E3 ubiquitin ligase and increased mitophagy. **1843**, 1295-1307

87. Narkiewicz, J., Klasa-Mazurkiewicz, D., Zurawa-Janicka, D., Skorko-Glonek, J., Emerich, J., and Lipinska, B. (2008) Changes in mRNA and protein levels of human HtrA1, HtrA2 and HtrA3 in ovarian cancer. *Clinical Biochemistry* **41**, 561-569

88. Gmeiner, W. H., Boyacioglu, O., Stuart, C. H., Jennings-Gee, J., and Balaji, K. C. (2015) The cytotoxic and pro-apoptotic activities of the novel fluoropyrimidine F10 towards prostate cancer cells are enhanced by Zn2+-chelation and inhibiting the serine protease Omi/HtrA2. *The Prostate* **75**, 360-369

89. Zhu, Z.-H., Yu, Y. P., Zheng, Z.-L., Song, Y., Xiang, G.-S., Nelson, J., Michalopoulos, G., and Luo, J.-H. (2010) Integrin Alpha 7 Interacts with High Temperature Requirement A2 (HtrA2) to Induce Prostate Cancer Cell Death. *The American Journal of Pathology* **177**, 1176-1186

90. Hartkamp, J., and Roberts, S. G. E. (2010) HtrA2, taming the oncogenic activities of WT1. *Cell Cycle* **9**, 2508-2514

91. Danziger, N., Yokoyama, M., Jay, T., Cordier, J., Glowinski, J., and Chneiweiss, H. (1995) Cellular Expression, Developmental Regulation, and Phylogenic Conservation of PEA-15, the Astrocytic Major Phosphoprotein and Protein Kinase C Substrate. *Journal of Neurochemistry* **64**, 1016-1025

92. Araujo, H., Danziger, N., Cordier, J., Glowinski, J., and Chneiweiss, H. (1993) Characterization of PEA-15, a major substrate for protein kinase C in astrocytes. *Journal of Biological Chemistry* **268**, 5911-5920

93.   Fiory, F., Formisano, P., Perruolo, G., and Beguinot, F. (2009) *Frontiers: PED/PEA-15, a multifunctional protein controlling cell survival and glucose metabolism* Vol. 297

94.   Sulzmaier, F. J., Opoku-Ansah, J., and Ramos, J. W. (2012) Phosphorylation is the switch that turns PEA-15 from tumor suppressor to tumor promoter. *Small GTPases* **3**, 173-177

95.   Formstecher, E., Ramos, J. W., Fauquet, M., Calderwood, D. A., Hsieh, J.-C., Canton, B., Nguyen, X.-T., Barnier, J.-V., Camonis, J., Ginsberg, M. H., and Chneiweiss, H. (2001) PEA-15 Mediates Cytoplasmic Sequestration of ERK MAP Kinase. *Developmental Cell* **1**, 239-250

96.   Hill, J. M., Vaidyanathan, H., Ramos, J. W., Ginsberg, M. H., and Werner, M. H. (2002) Recognition of ERK MAP kinase by PEA-15 reveals a common docking site within the death domain and death effector domain. *The EMBO Journal* **21**, 6494-6504

97.   Ashkenazi, A., and Dixit, V. M. (1998) Death Receptors: Signaling and Modulation. *Science* **281**, 1305-1308

98.   Kubes, M., Cordier, J., Glowinski, J., Girault, J.-A., and Chneiweiss, H. (1998) Endothelin Induces a Calcium-Dependent Phosphorylation of PEA-15 in Intact Astrocytes: Identification of Ser104 and Ser116 Phosphorylated, Respectively, by Protein Kinase C and Calcium/Calmodulin Kinase II In Vitro. *Journal of Neurochemistry* **71**, 1307-1314

99.   Estellés, A., Yokoyama, M., Nothias, F., Vincent, J.-D., Glowinski, J., Vernier, P., and Chneiweiss, H. (1996) The Major Astrocytic Phosphoprotein PEA-15 Is Encoded by Two mRNAs Conserved on Their Full Length in Mouse and Human. *Journal of Biological Chemistry* **271**, 14800-14806

100. Callaway, K., Abramczyk, O., Martin, L., and Dalby, K. N. (2007) The Anti-Apoptotic Protein PEA-15 Is a Tight Binding Inhibitor of ERK1 and ERK2, Which Blocks Docking Interactions at the D-Recruitment Site†. *Biochemistry* **46**, 9187-9198

101. Renault, F., Formstecher, E., Callebaut, I., Junier, M.-P., and Chneiweiss, H. (2003) The multifunctional protein PEA-15 is involved in the control of apoptosis and cell cycle in astrocytes. *Biochemical Pharmacology* **66**, 1581-1588

102. Kischkel, F. C., Hellbardt, S., Behrmann, I., Germer, M., Pawlita, M., Krammer, P. H., and Peter, M. E. (1995) Cytotoxicity-dependent APO-1 (Fas/CD95)-associated proteins form a death-inducing signaling complex (DISC) with the receptor. *The EMBO Journal* **14**, 5579-5588

103. Viparelli, F., Cassese, A., Doti, N., Paturzo, F., Marasco, D., Dathan, N. A., Monti, S. M., Basile, G., Ungaro, P., Sabatella, M., Miele, C., Teperino, R., Consiglio, E., Pedone, C., Beguinot, F., Formisano, P., and Ruvo, M. (2008) Targeting of PED/PEA-15 Molecular Interaction with Phospholipase D1 Enhances Insulin Sensitivity in Skeletal Muscle Cells. *Journal of Biological Chemistry* **283**, 21769-21778

104. Bradford, M. M. (1976) A rapid and sensitive method for the quantitation of microgram quantities of protein utilizing the principle of protein-dye binding. *Analytical Biochemistry* **72**, 248-254

105. Edelhoch, H. (1967) Spectroscopic Determination of Tryptophan and Tyrosine in Proteins*. *Biochemistry* **6**, 1948-1954

106. Kelly, S. M., Jess, T. J., and Price, N. C. (2005) How to study proteins by circular dichroism. In *Biochim Biophys Acta* Vol. 1751 pp. 119–139

107. Ef tink , M. R., and Ghiron , C. A. (1981) on the analysis of the temperature and viscosity dependence of fl uorescence-quenching reactions with proteins,. *Arch. Biochem.Biophys* **209**, 706– 709

108. Wang, C. K., and Cheung, H. C (1986) Proximity relationship in the binary complex formed between troponin I and troponin C. *J. Mol. Biol.* **191**, 509-521

109. Lakowicz, J. (2006) In *Principles of fluorescence spectroscopy* (Geddes, C. D., ed) Vol. 6 pp. 443-468., Springer-Verlag, New York

110. Mottarella, S. E., Beglov, D., Beglova, N., Nugent, M. A., Kozakov, D., and Vajda, S. (2014) Docking Server for the Identification of Heparin Binding Sites on Proteins. *Journal of Chemical Information and Modeling* **54**, 2068-2078

111. Laskowski, R. A. (2009) PDBsum new things. *Nucleic Acids Research* **37**, D355-D359

112. Doyle, D., Lee, A., Lewis, J., Kim, E., Sheng, M., and MacKinnon, R. (1996) Crystal structures of a complexed and peptide-free membrane protein-binding domain: molecular basis of peptide recognition by PDZ. *Cell* **85**, 1067-1076.

113. Bhuiyan, M., and Fukunaga, K. (2009) Mitochondrial serine protease HtrA2/Omi as a potential therapeutic target. *Curr Drug Targets* **10**, 372-383

114. Roy, S., and Hecht, M. (2000) Cooperative thermal denaturation of proteins designed by binary patterning of polar and nonpolar amino acids. *Biochemistry* **39**, 4603-4607

115. Tallmadge, D. H., HuEbnert, J. S., and Borkman, R. F. (1989) ACRYLAMIDE QUENCHING OF TRYPTOPHAN PHOTOCHEMISTRY AND PHOTOPHYSICS. *Photochemistry and Photobiology* **49**, 381-386

116. Wang, W., Takimoto, R., Rastinejad, F., and El-Deiry, W. S. (2003.) Stabilization of p53 by CP-31398 inhibits ubiquitination without altering phos-phorylation at serine 15 or 20 or MDM2 binding. :. *Mol Cell Biol* **23**, 2171-2181

117. Gavathiotis, E., Reyna , D. E., Bellairs, J. A., Leshchiner, E. S., and Walensky, L. D. (2012) Direct and selective small-molecule activation of proapoptotic BAX. *NATURE CHEMICAL BIOLOGY* **8**, 639–645

118. Wu, G., Chai, J., Suber, T., Wu, J., Du, C., Wang, X., and Shi, Y. (2000) Structural basis of IAP recognition by Smac/DIABLO. *Nature* **408**, 1008-1012.

119. Merdanovic, M., Mamant, N., Meltzer, M., Poepsel, S., Auckenthaler, A., Melgaard, R., Hauske, P., Nagel-Steger, L., Clarke, A., Kaiser, M., R., H., and Ehrmann, M. (2010) Determinants of structural and functional plasticity of a widely conserved protease chaperone complex. *Nat Struct Mol Biol* **17**, 837-843.

120. Wrase, R., Scott, H., Hilgenfeld, R., and Hansen, G. (2011) The Legionella HtrA homologue DegQ is a self-compartmentizing protease that forms large 12-meric assemblies. *Proc Natl Acad Sci USA* **108**, 10490-10495.

121. Sohn, J., Grant, R., and Sauer, R. (2009) OMP peptides activate the DegS stress-sensor protease by a relief of inhibition mechanism. *Structure* **17**, 1411-1421.

122. Sohn, J., and Sauer, R. (2009) OMP peptides modulate the activity of DegS protease by differential binding to active and inactive conformations. *Mol Cell* **33**, 64-74.

123. Mauldin, R., and Sauer, R. (2013) Allosteric regulation of DegS protease subunits through a shared energy landscape. *Nat Chem Biol* **9**, 90-96

124. Tibbetts, M. D., Zheng, L., and Lenardo, M. J. (2003) The death effector domain protein family: regulators of cellular homeostasis. *Nat Immunol* **4**, 404-409

125. Schechter, I., and Berger, A. (1967) On the size of the active site in proteases. I. Papain. *Biochemical and Biophysical Research Communications* **27**, 157-162

126. Chaganti, L. K., Kuppili Rr Fau - Bose, K., and Bose, K. (2013) Intricate structural coordination and domain plasticity regulate activity of serine protease HtrA2. *FASEB J* **8**, 3054-3066

127. Kuninaka, S., Nomura M Fau - Hirota, T., Hirota T Fau - Iida, S.-I., Iida S Fau - Hara, T., Hara T Fau - Honda, S., Honda S Fau - Kunitoku, N., Kunitoku N Fau - Sasayama, T., Sasayama T Fau - Arima, Y., Arima Y Fau - Marumoto, T., Marumoto T Fau - Koja, K., Koja K Fau - Yonehara, S., Yonehara S Fau - Saya, H., and Saya, H. (2005) The tumor suppressor WARTS activates the Omi / HtrA2-dependent pathway of cell death. *Oncogene* **34**, 5287-5298

128. Gupta, S., Singh, R., Datta, P., Zhang, Z., Orr, C., Lu, Z., DuBois, G., Zervos, A. S., Meisler, M. H., Srinivasula, S. M., Fernandes-Alnemri, T., and Alnemri, E. S. (2004) The C-terminal Tail of Presenilin Regulates Omi/HtrA2 Protease Activity. *Journal of Biological Chemistry* **279**, 45844-45854

129. Ma, X., Kalakonda, S., Srinivasula, S. M., Reddy, S. P., Platanias, L. C., and Kalvakolanu, D. V. (2007) GRIM-19 associates with the serine protease HtrA2 for promoting cell death. *Oncogene* **26**, 4842-4849

130. Hong, S.-K., Cha, M.-K., and Kim, I.-H. (2006) Specific protein interaction of human Pag with Omi/HtrA2 and the activation of the protease activity of Omi/HtrA2. *Free Rad. Biol. and Med.* **40**, 275-284.

131. Quintavalle, C., Costanzo, S. D., Zanca, C., Tasset, I., Fraldi, A., Incoronato, M., Mirabelli, P., Monti, M., Ballabio, A., Pucci, P., Cuervo, A. M., and Condorelli, G.

(2014) Hsc70 binds and directs the non-phosphorylated tumor-suppressor form of PED to Chaperone-Mediated Autophagy (CMA) degradation in lung cancer. *Journal of cellular physiology* **229**, 1359-1368

132.   Zurawa-Janicka, D., Skorko-Glonek, J., and Lipinska, B. (2010) HtrA proteins as targets in therapy of cancer and other diseases. *Expert Opin Ther Targets* **14**, 665-679

Publications

Intricate structural coordination and domain plasticity regulate activity of serine protease HtrA2

Lalith K. Chaganti, Raja Reddy Kuppili, and Kakoli Bose[1]

Advanced Centre for Treatment, Research, and Education in Cancer (ACTREC), Tata Memorial Centre, Navi Mumbai, India

ABSTRACT   HtrA2, a complex trimeric pyramidal mitochondrial serine protease that regulates critical biological functions and diseases, including apoptosis and cancer, is a promising therapeutic target. It promotes apoptosis through multiple pathways, complex mechanisms of which are still elusive. The existing model of activation that emphasizes relative intramolecular movements between C-terminal PDZ and protease domains (PDZ-protease collapse in inactive and resting states) has not been able to unambiguously demonstrate dynamics of its actions. Using structure-guided design, molecular biology and protein biochemistry, we obtained various combinations of HtrA2 domains and mutants. Conformational changes and stability were characterized using molecular dynamics simulation and spectroscopic tools while functional enzymology delineated their roles in regulating enzyme catalysis. Quantitative Förster resonance energy transfer showed lesser intramolecular PDZ-protease distance in trimeric HtrA2 compared to its inactive monomeric counterpart (~21 and ~22.3 Å, respectively, at 37°C). Our findings highlight importance of N-terminal region, oligomerization, and intricate intermolecular PDZ-protease interaction in proper active-site formation, enzyme-substrate complex stabilization, and hence HtrA2 functions. These observations redefine the existing activation model and showcase a unique example of how precise interdomain coordination, plasticity, and intermolecular contacts lead to distinct functional properties and hence provide new insights into HtrA2 structure, function, and dynamics.—Chaganti, L. K., Kuppili, R. R., Bose, K. Intricate structural coordination and domain plasticity regulate activity of serine protease HtrA2. *FASEB J.* 27, 3054–3066 (2013). www.fasebj.org

Key Words: PDZ · serine protease domain · dynamics

H<small>IGH-TEMPERATURE REQUIREMENT PROTEASE</small> A2 (HtrA2), a unique mitochondrial proapoptotic protein, belongs to a large family of serine proteases (S1, chymotrypsin family) that are conserved from prokaryotes to humans. HtrA proteins are known for their complex structural organization, which is reflected in their multitasking ability and involvement in several critical biological functions, as well as pathogenicity, such as protein quality control, unfolded protein response, cell growth, apoptosis, arthritis, cancer, and metabolism of amyloid precursor proteins (1–4). Interestingly, despite diversity in functions and low sequence identity, their overall structural integrity is evolutionarily maintained, which comprises a serine protease domain and one or more C-terminal PDZ [postsynaptic density protein (PSD95), *Drosophila* disc large tumor suppressor (Dlg1), and zonula occludens-1 protein (zo-1)] or protein-protein interaction domains (5) arranged in a complex pyramidal oligomeric assembly ranging from trimeric to 24-meric architecture (6–8). While bacterial DegP is the most elaborately studied protein that has dual temperature-dependent chaperone-protease activity (9), not much information is available on human HtrAs except for HtrA2 and HtrA1 (10, 11). Although HtrAs share an overall common polypeptide fold with an active site containing a catalytic triad, oxyanion hole, and substrate-specificity pocket, subtle conformational variations provide the basis for their specificity and functional diversity (12). For example, the N-terminal tetrapeptide AVPS is unique in mature HtrA2 (10, 13) which makes it the only inhibitor of apoptosis (IAP) binding protein in the human homologues. Apart from deactivating IAPs, complex structural organization and domain plasticity in HtrA2 has enabled it to promote apoptosis through various caspase-mediated and independent pathways (14) *via* its serine protease activity, the complex mechanisms of which are still elusive. Thus, understanding the structural basis of

---

HtrA2 activation and specificity requires intricate dissection of its domains and deciphering the underlying dynamics that regulate its functions.

Crystallographic data (15) on the mature unbound form of HtrA2 provide a broad overview of overall structural organization of the inactive protease. Mature HtrA2 with 7 α-helices and 19 β-sheets forms well-defined domains. The trimeric protease has a pyramidal architecture with the short N-terminal region holding the oligomer together through extensive intermolecular hydrophobic and Van der Waals interactions involving 3 aromatic residues (Y14, F16, and F123). The core serine protease domains (SPDs) are surrounded by C-terminal PDZ domains, which, along with the trimeric architecture, restrict entry of the substrates to the active site, leading to a low basal activity. PDZ is attached covalently to the SPD through a flexible interface linker sequence (residues 211–226), and it has been believed that the PDZ-protease dynamics and their relative orientation modulate HtrA2 activity and hence functions. These observations led to development of an activation model that highlights the role of PDZ in substrate binding and subsequent protease activation (15). The model states that on substrate binding, PDZ that otherwise falls on the protease domain opens up, allowing the substrate to enter the binding pocket, whereas in the monomeric mutant of HtrA2, PDZ completely collapses on SPD, restricting substrate entry to the active site, thus rendering it inactive. Although the model provides a basic understanding of HtrA2 activation, it could neither satisfactorily define the roles of trimerization and N-terminal domain in HtrA2 functions nor decipher the dynamics of PDZ-protease crosstalk, as electron density for both the linker and part of N-terminal is unavailable in the structural data. Unlike other HtrAs, the substrate binding YIGV (GLGF motif) groove of the PDZ domain is buried deep within the protein interior and is blocked by Pro225 and Val226 of SPD in the closed protease conformation (15, 16). Therefore, either initial binding at the YIGV pocket would demand an extremely stringent structural signature, such as partial substrate unfolding, or there might be an alternative mechanism. With a closer look at different biological roles of HtrA2, its wide substrate specificity, and putative binding sites on its known available substrates, the former possibility seems unlikely (17). Alternatively, we have shown earlier that activation of HtrA2 occurs allosterically, where the signal is relayed *via* a distal noncanonical substrate binding site with subsequent opening up of the YIGV pocket (18).

Here, with an aim at understanding the subtle structural reorganizations and intrinsic conformational dynamics that lead to HtrA2 activation, we dissected its various domains to decipher their roles individually as well as in combination in mediating HtrA2 specificity and functions. Our studies highlight the importance of N-terminal domain, oligomerization, and intricate intermolecular PDZ-pro-

tease interaction in proper active-site formation, stabilization of the enzyme-substrate complex, and hence HtrA2 functions. It establishes the role of the PDZ domain in not only interface dynamics and initial substrate binding but also in intermolecular contacts in the trimeric protease architecture leading to efficient substrate catalysis.

MATERIALS AND METHODS

Plasmid construction

Clone of mature HtrA2 construct (Δ133) comprising residues 134–458 in bacterial expression vector (pET-20b) with a C-terminal his$_6$ tag was obtained from Addgene (Cambridge, MA, USA). Different HtrA2 domains were subcloned between Nde-1 and Xho-1 restriction sites of pET-20b vector. Primers used for SPD were 5′-CATatgGatgtggtggagaagac-3′ and 5′-CTCGAGAAACTCTCGAAGACG-3′, and for SPD + PDZ domain (SPD-PDZ) were 5′-CATATGGATGTGGTGGAGAC-3′ and 5′-CTCGAGCTCaggggtcac-3′. N terminus and SPD (N-SPD) was cloned between Nde-1 and *Eco*RI site of pMAL-c5E vector (New England Biolabs, Ipswich, USA); primers used were 5′-CATATGGCCGTCCCTAGCCCG-3′ and 5′-GAATTCT-CAAACTCTCGAAG-3′. Several mutants of HtrA2 were generated using site-directed mutagenesis (Stratagene, Cedar Creek, TX, USA). The forward primers for the mutants Y295W, N48W, F16D, M190R, F208C, and S173A, respectively, are 5′-GAAGATGTTTGGGAAGCTGTTCG-3′, 5′-CCTATCT-CGTGGGGCTCAGGATTC-3′, 5′-GTCAGTACAACGAC-ATCGCAGATGTG-3′, 5′-GAACACCAGGAAGGTCACAGC-3′, 5′-TCTTCGAGAGTGTCTGCATCGTG-3′, and 5′-CAGCTATT-GATTTTGGAAACTCT-3′. For all these mutants, the reverse primer was the complementary sequence. All HtrA2 variants were confirmed by sequencing.

Protein purification

*E. coli*BL21(DE3)pLysS cells transformed with expression plasmids and HtrA2 variants were purified as described previously (18). Briefly, proteins with a C-terminal his$_6$ tag in the pET-20b vector were purified by affinity chromatography using Ni-IDA columns, while N-SPD with N-terminal maltose binding protein (MBP) fusion tag was purified using amylose resin. All purified proteins were >95% pure, as estimated by SDS-PAGE.

Size-exclusion chromatography

Molecular mass of HtrA2 variants was estimated by size-exclusion chromatography. Aliquots (1 ml) of samples were run on a Superdex 200 10/300 HR column (GE Healthcare, Uppsala, Sweden) preequilibrated with buffer composed of 20 mM Na$_2$HPO$_4$/NaH$_2$PO$_4$ and 100 mM NaCl, pH 8 (buffer SP). Proteins were eluted with the same buffer at a flow rate of 0.5 ml/min. The standards used for calibration were alcohol dehydrogenase (ADH), bovine serum albumen (BSA), lysozyme, and MBP. All standards except for MBP, which was laboratory purified, were purchased from Sigma (St. Louis, MO, USA). Elution volume (V_e)/void volume (V_0) *vs.* log of molecular masses of standards was plotted to generate the calibration curve from which molecular masses of HtrA2 variants were calculated.

Enzyme activity assay

Protease activity of different HtrA2 constructs was determined using substrate β-casein (Sigma). For each 30-μl reaction mixture, 2 μg of respective protein was incubated with 6 μg of β-casein in buffer SP at 37°C for 2.5 h, and results were analyzed by SDS-PAGE. For all quantitative studies, fluorescein isothiocyanate (FITC) β-casein (Sigma) was used, and assays were performed as described previously (18). Protease activity was also determined over a temperature range 30–65°C with 5°C intervals. For each 200 μl of reaction mixture, 0.5 μM protein was incubated with 0.6 μM of FITC β-casein substrate in buffer SP. Enzyme was preincubated at each respective temperature for 15 min, and proteolytic cleavage was monitored using a Fluorolog-3 spectrofluorometer (Horiba Scientific, Edison, NJ, USA) with excitation at 485 nm followed by 535 nm emission. Initial velocities were calculated at each respective temperature using linear regression analysis.

Molecular dynamics simulation (MDS)

M190R mutation was performed on HtrA2 structure [Protein Data Bank (PDB) ID: 1LCY; ref. 15] using the Build Mutants protocol of Discovery Studio 2.5 (Accelrys, San Diego, CA, USA). This mutant structure was optimized and minimized using CHARMM (19) force field and steepest method in Discovery Studio 2.5 (20). Minimized HtrA2 and HtrA2(M190R) mutant structures were subjected to 3 ns MDS using the GROMACS 4.5.1 package (21), and the coordinates were saved for every 2-ps time interval. In MD quality analysis, potential energy (PE) of the protein and total energy of the entire system were calculated. The energy minimum structure was obtained from the root mean square deviation (RMSD) plot. The lowest PE conformations were then used for comparative structural analysis of HtrA2 and HtrA2 (M190R). To further understand the intricacy, relative movement of residues F170 of the oxyanion hole and H65 of the catalytic triad was also plotted across the timescale of trajectory for HtrA2 (M190R) using Xmgrace (21). All the ribbon models were generated using PyMOL (DeLano Scientific, Palo Alto, CA, USA).

Fluorescence emission and far-UV CD spectroscopy

Fluorescence emission was measured with protein solutions (2 μM) in buffer SP with 295-nm excitation followed by emission between 310 and 400 nm. Far-UV CD data were collected between 190 and 250 nm with 10 μM protein solutions in buffer SP in a Jasco J-815 spectropolarimeter (Jasco, Easton, MD, USA). For thermal denaturation studies, far-UV CD experiments were performed between 25 and 100°C at 2°C intervals. The mean residue ellipticity was calculated as described previously (22).

Fluorescence quenching

Fluorescence quenching experiments were performed between 30 and 65°C at 5°C intervals using 5 M acrylamide as an external quencher over a concentration range of 0–500 mM. Protein was preincubated for 15 min at each respective temperature, and fluorescence emission scans were taken after addition of quencher with excitation at 295 nm. The values of fluorescence were corrected for dilution effects, residual emission, and Raman scattering (23), and data were then analyzed using the Stern-Volmer relationship (Eq. 1):

$$F_0/F = 1 + K_{SV}[Q] \qquad (1)$$

For a graph with upward curvature, a modified Stern-Volmer relationship (Eq. 2) was used:

$$F_0/F = 1 + K_D[Q]\exp([Q]VN/1000) \qquad (2)$$

where F_0 and F are fluorescence intensity in the absence and presence of quencher, respectively; $[Q]$ is concentration of quencher (molar); K_{SV} is the Stern-Volmer quenching constant; K_D is the dynamic quenching constant; V is volume of the sphere; and N is Avogadro's number.

Förster resonance energy transfer (FRET) studies

For FRET studies, single tryptophan (Y295W) and cysteine mutants (F208C) were used. To 50 μM protein solutions in buffer SP, 5-fold molar excess of 5-((((2-iodoacetyl) amino) ethyl) amino) naphthalene-1-sulfonic acid (IAEDANS; Sigma) was added and incubated in dark for 16 h at 4°C. To remove unbound label, protein was passed through an Ni-IDA affinity column and eluted using imidazole. Labeling efficiency was assessed as described previously (24). Fluorescence emission was measured over a temperature range of 30–65°C at 5°C intervals. Then 2 μM protein was excited at 295 nm, and emission was measured over a wavelength range 310–575 nm. Fluorescence resonance energy transfer efficiency was calculated using Eq. 3 (25):

$$E = 1 - F_{DA} - F_D(1 - F_A)/F_Df_A \qquad (3)$$

where E is the calculated efficiency; F_{DA} and F_D are emission of donor (tryptophan) in the presence and absence of acceptor (IAEDANS), respectively, and f_A is fractional occupancy of the acceptor site. Donor-acceptor (D-A) separation was obtained using Eq. 4:

$$R = (E^{-1} - 1)^{1/6}R_0 \qquad (4)$$

where R is the D-A separation, and R_0 is the Förster critical distance. The value for R_0 was taken as 22 Å (26).

RESULTS

Different HtrA2 domains and variants

Different mutants and variants of HtrA2 were generated to understand the role of critical residues and contributions from different domain combinations in maintaining its overall structural integrity and functions (**Fig. 1A**). It was reported in the literature (15) that N-terminal aromatic residues are crucial for maintaining its trimeric architecture through intermolecular Van der Waals interactions. One such residue (F16) when mutated to aspartate was found to disrupt these interactions and render the protein monomeric (15). We made the same mutation for our studies to understand the role of trimerization in HtrA2 structure and function. At the same time, this mutant, along with the N-terminal deleted SPD-PDZ variant, was thought to be helpful in understanding the contribution of N-terminal region in structure, stability, and active site formation. Similarly, a trimeric N-SPD variant was also generated that was expected to retain its oligomeric property (intact N-terminal trimerization domain) but with no PDZ interference. M190R mutation at the PDZ-protease interface has been implicated as having a detrimental effect on PDZ plasticity due to negative intersubunit packing (15) and was created to demonstrate its role in relative PDZ-protease orientation and interdomain contacts, and its
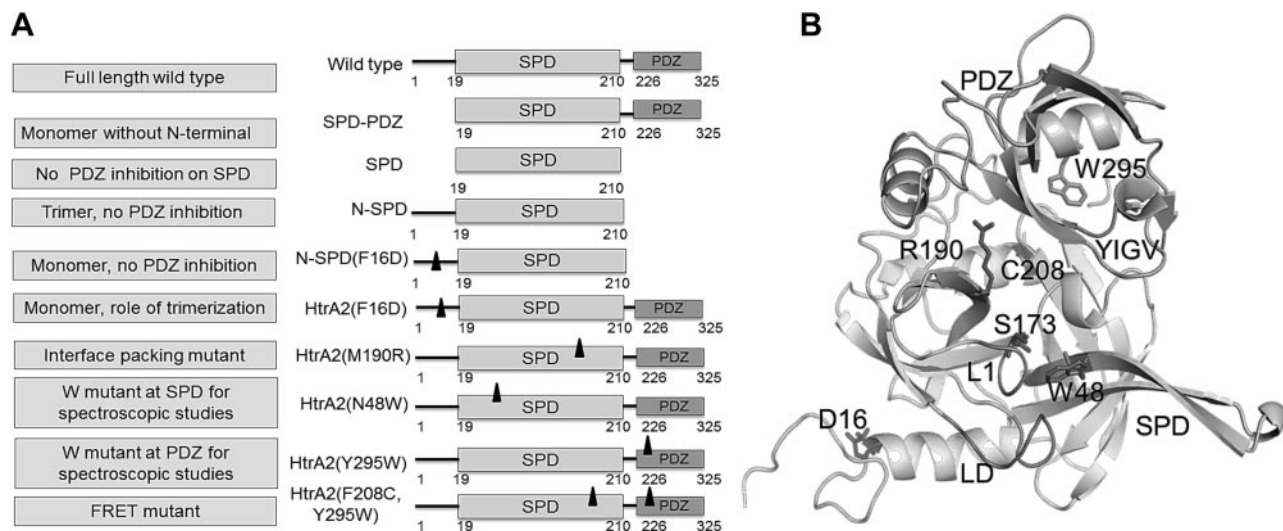
Figure 1. Representation of different domains and mutants of HtrA2. *A*) Schematic representations of different HtrA2 constructs generated for the present study. Light gray boxes indicate protease domain (19–210 residues); dark gray boxes indicate PDZ domain (226–325 residues); solid lines indicate N-terminal region (1–18 residues) and linker region (211–225 residues); triangles indicate positions of mutations on the respective domains. *B*) Ribbon diagram of the crystal structure of HtrA2 (PDB accession number 1LCY). Amino acid substitutions in HtrA2 protease and PDZ domains are shown in stick models. Ribbon diagram was generated using PyMOL.

subsequent effect on HtrA2 activity. A monomeric version of N-SPD, N-SPD(F16D), was generated to understand the importance of the N terminus in HtrA2 structure and stability. This protein, on comparison with N-SPD, mature HtrA2, SPD-PDZ, and HtrA2(F16D), would highlight the importance of PDZ in the trimeric HtrA2 structure and the role of interdomain interaction if any. SPD was cloned and purified separately to understand the roles of the N-terminal region and PDZ domain in proper active site formation, protein stability, and maintenance of structural integrity. The experiment would also demonstrate whether PDZ inhibition might be the sole reason for HtrA2 inactivation.

Since HtrA2 is devoid of tryptophans, single-tryptophan mutants were strategically generated in the SPD and PDZ domain (N48W and Y295W, respectively) so as to understand and compare the environments surrounding the active site and PDZ-protease interface spectroscopically (Fig. 1*B*). N48W was introduced on the β2 strand of SPD, in the vicinity of the L1 and LD regulatory loops in the active site region. This tryptophan was found to be in proximity to F170 of SPD, which is an important component of an oxyanion hole. The position of W48 was chosen in such a way that it reflected the environment of the active site and its surrounding regulatory loops. This tryptophan mutant was thus expected to delineate subtle conformational changes near the active site region and interdomain crosstalk during HtrA2 activation. Y295W was introduced on α7 of PDZ at the interface between SPD and the PDZ domain such that this tryptophan faces SPD of the same monomer and is very close to the canonical peptide binding (YIGV) groove. It is also in the vicinity of the intersubunit linker and is positioned in such a way that PDZ movement away from SPD would expose the tryptophan, leading to red-shifted emission max-

ima. Thus, these tryptophans would aid in understanding the conformational changes at the active-site and PDZ-protease interface. A cysteine mutation was introduced at SPD, HtrA2(F208C) (Fig. 1*B*), to examine the distance between PDZ and protease domains by pairing with W295 residue using FRET studies.

Role of N-terminal region in oligomerization

Molecular masses of HtrA2 variants were estimated by gel filtration chromatography to understand the role of the N-terminal region, mainly F16, in maintaining its trimeric architecture. The predicted molecular masses of the proteins are shown in **Table 1**, which demonstrates that HtrA2 (wild type), 2 tryptophan mutants of

TABLE 1. *Oligomeric properties of different HtrA2 constructs*

Protein	Theoretical molecular mass (kDa)	V_e/V_0	Calculated molecular mass (kDa)
ADH	141	2.04	
BSA	66	2.53	
MBP	43	2.63	
Lysozyme	14.4	3.22	
HtrA2(F16D)	36.2	2.73	37.10
N-SPD	70.3	2.40	73.62
SPD-PDZ	34.2	2.72	36.90
N-SPD(F16D)	23	2.81	24.1
HtrA2 wild type	109.6	2.20	108.8
HtrA2(N48W)	109.6	2.20	108.8
HtrA2(Y295W)	109.6	2.20	108.8

Molecular masses of HtrA2 and its variants were calculated from calibration curves generated using different standard protein molecules (ADH, BSA, MBP, and lysozyme) as described in Materials and Methods.
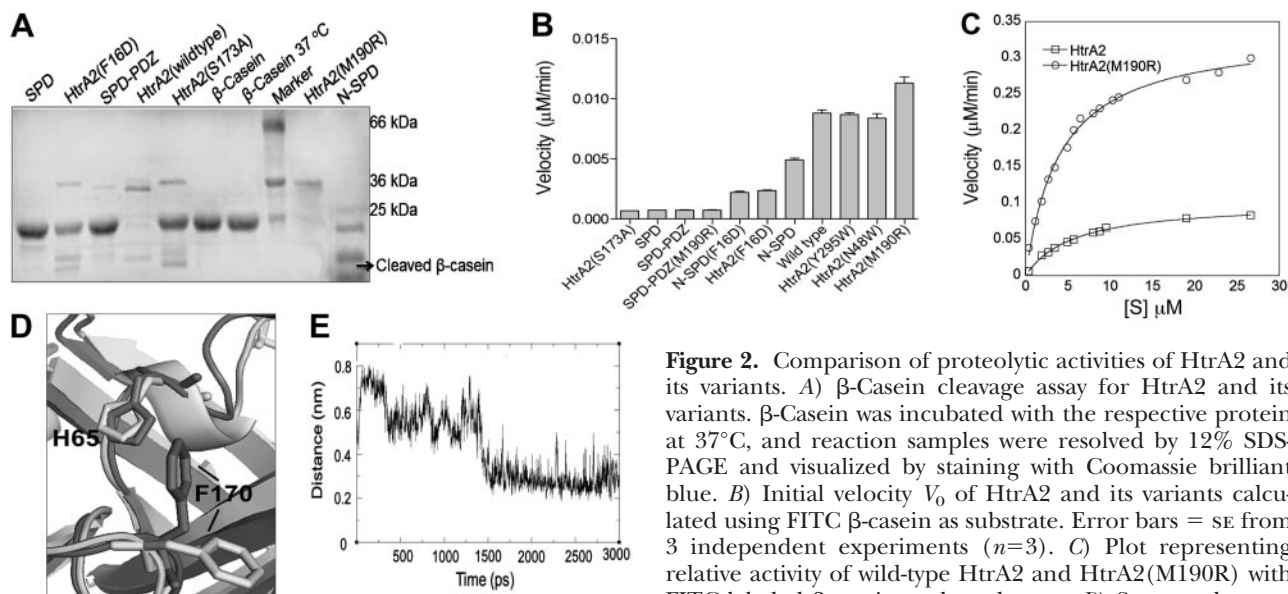
Figure 2. Comparison of proteolytic activities of HtrA2 and its variants. A) β-Casein cleavage assay for HtrA2 and its variants. β-Casein was incubated with the respective protein at 37°C, and reaction samples were resolved by 12% SDS-PAGE and visualized by staining with Coomassie brilliant blue. B) Initial velocity V_0 of HtrA2 and its variants calculated using FITC β-casein as substrate. Error bars = SE from 3 independent experiments ($n=3$). C) Plot representing relative activity of wild-type HtrA2 and HtrA2(M190R) with FITC labeled β-casein as the substrate. D) Structural superposition of wild-type HtrA2 (light gray) and HtrA2(M190R) (dark gray) after MD simulations shows F170 moves closer to H65 of the catalytic triad in the latter. E) Graphical representation of the distance between residues F170 and H65 for the 3-ns MDS trajectory on HtrA2(M190R). Graph shows movement of the residues toward each other along the trajectory.

HtrA2 (Y295W and N48W), and N-SPD are trimers with intact N-terminal regions. HtrA2(F16D) and SPD-PDZ represent monomers, reiterating the importance of N-terminal F16 in homotrimerization, as suggested by the literature (15, 27).

Role of oligomerization and different domains in protease activity

Protease activity of HtrA2, its variants and mutants was studied to understand the role of different domains and critical residues in regulating HtrA2 activity and specificity using a generic serine protease substrate, β-casein, in both gel and fluorescence-based assays. These studies have been designed to reflect protease activity as a consequence of conformational changes due to initial substrate (here β-casein) binding at the PDZ domain. In all protease activity studies, the active site mutant, HtrA2(S173A), was used as a negative control. It was observed that HtrA2, N-SPD, and HtrA2 (M190R) cleaved β-casein, but monomeric HtrA2 (F16D) showed much less β-casein cleavage, and other monomeric variants, SPD and SPD-PDZ variants without an N-terminal region, did not show any protease activity (**Fig. 2A**), highlighting the importance of trimerization and the N-terminal region in HtrA2 activity. For more

quantitative analysis, enzyme kinetics was studied fluorometrically with FITC-labeled β-casein as a substrate, and V_0 was calculated. Monomeric mutants and variants, such as HtrA2(F16D), SPD, N-SPD(F16D), and SPD-PDZ, showed much less activity compared to wild type (Fig. 2B). Tryptophan mutants, HtrA2(Y295W) and HtrA2(N48W), have enzyme activity comparable to the wild type, suggesting that the mutations did not affect the active conformation of the protease. Interestingly, contrary to the existing literature report (15), SPD was found to be completely inactive, while HtrA2(M190R) was enzymatically more active than the wild type, although this mutation was expected to negatively affect SPD-PDZ packing, leading to PDZ collapse on SPD and subsequent loss of activity. However, although higher activity was observed in M190R mutant in the trimeric HtrA2, introduction of the same mutation in the monomeric inactive SPD-PDZ did not show any activity, suggesting that oligomerization is a prerequisite for active enzyme formation.

To correlate these observations with substrate binding and catalysis, kinetic parameters were determined and compared with HtrA2 (Fig. 2C and **Table 2**). Comparison of K_m values of HtrA2(M190R) with HtrA2 show similar substrate binding affinity, suggesting that binding pocket is mainly unperturbed and the active

TABLE 2. *Steady state kinetic parameters for HtrA2 wild type and its variants, with FITC β-casein as the substrate*

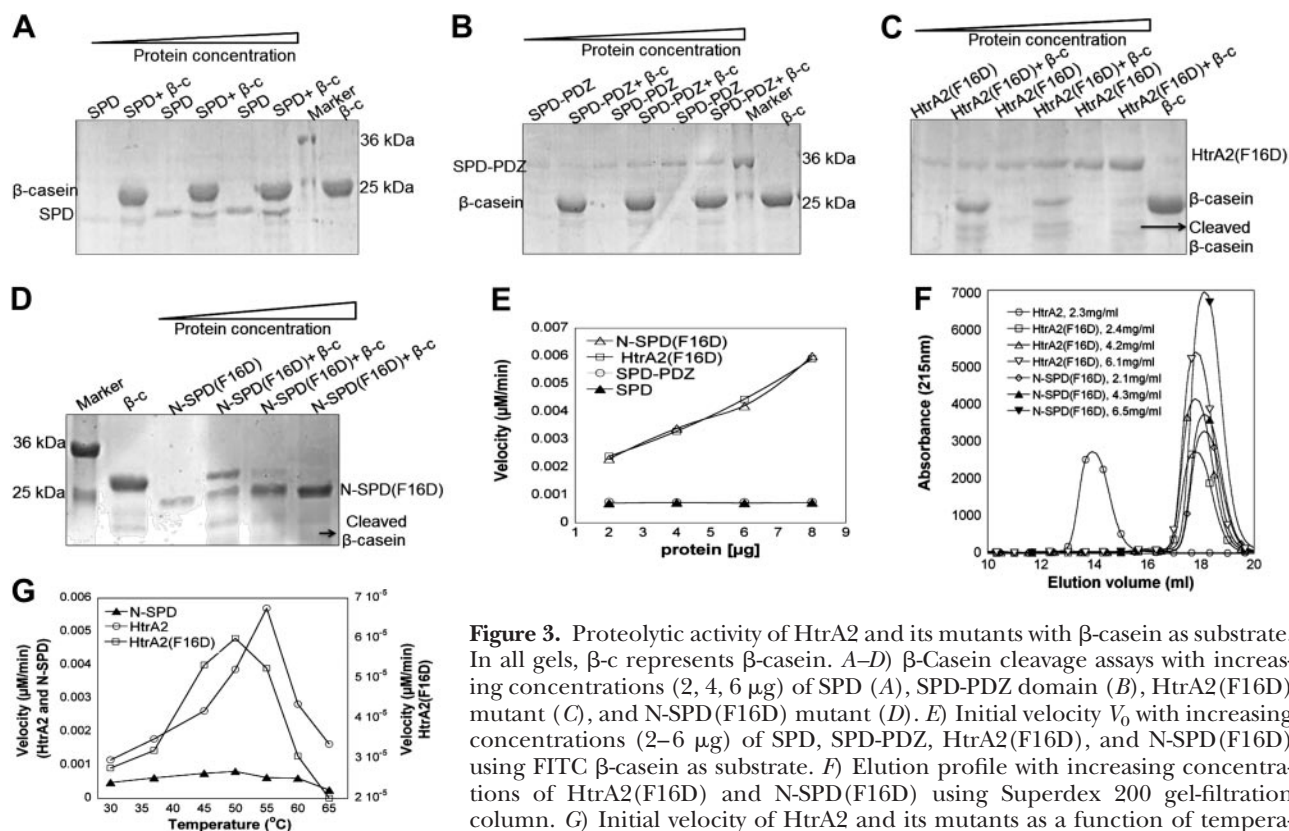| HtrA2 protein	K_m (μm)	V_{max} (M/s)	k_{cat} (s^{-1})	k_{cat}/K_m (M^{-1}s^{-1})
HtrA2 wild type	4.60 ± 0.5	4.08×10^{-9}	0.0204 ± 0.004	4.5×10^3
HtrA2(M190R)	4.06 ± 0.4	15.50×10^{-9}	0.0775 ± 0.006	19.3×10^3
SPD	–	–	–	–
SPD-PDZ	–	–	–	–

Data are averages of 3 independent experiments.

site accessibility is not limited due to this mutation (Fig. 2*C* and Table 2). However, turnover rate and catalytic efficiency were ~4-fold higher than the wild type, suggesting presence of a more catalytically competent oxyanion hole in the former. Modeling and MDS with this mutant shows subtle conformational changes in and around the active site compared to the wild type. On structural analyses, F170, which is part of the oxyanion hole, was observed to move closer to H65 of the catalytic triad so as to accommodate the LD loop and form a catalytically competent oxyanion hole (Fig. 2*D*, *E*), thus leading to higher proteolytic activity. These rearrangements result in a catalytically competent HtrA2 conformation with a proper oxyanion hole. Since SPD and SPD-PDZ were completely inactive, no kinetic parameters could be obtained. These data emphasize the role of trimerization in protein activity and demonstrate that PDZ inhibition might not be the sole reason for protease inactivation. Earlier reports from our laboratory on trimeric N-SPD and monomeric HtrA2(F16D) provide crucial insights into structural correlates of HtrA2 functions (18). Lower substrate turnover rates, as well as catalytic efficiency (5- and 3.5-fold, respectively), compared to the wild type suggested the presence of a malformed oxyanion hole in N-SPD. It also highlighted the role of PDZ in mediating conformational changes around the active site that positively influence the rate of catalysis. However, in monomeric full-length HtrA2(F16D), lesser substrate binding affinity and significant decrease in catalytic efficiency (~1600-fold) underlines the importance of

trimerization and hints at the presence of intermolecular PDZ-protease crosstalk in active-site formation and stabilization.

Further, to understand the rate of substrate catalysis for all monomeric mutants, protease activity was monitored with increasing concentrations (2–6 μg) of the enzyme. Increasing concentrations of SPD and SPD-PDZ did not show any activity (**Fig. 3***A*, *B*) whereas HtrA2(F16D) and N-SPD(F16D) showed activity with substrate β-casein (Fig. 3*C*, *D*). Protease activity for HtrA2(F16D) and N-SPD(F16D) increased in a linear fashion (Fig. 3*E*), suggesting that with increase in protease concentration, enzyme substrate complex is more stabilized, leading to enhanced substrate catalysis in variants containing the N-terminal region. This emphasizes the role of the N terminus in the formation of proper active site conformation and stabilization of the enzyme substrate complex for catalysis. To negate the possibility of oligomerization at higher concentrations, concentration-dependent oligomeric properties of HtrA2(F16D) and N-SPD(F16D) were studied using gel filtration chromatography, as shown in Fig. 3*F*. Both the proteins were found to be monomeric at all protein concentrations, as expected.

HtrA2 and its homologs have been found to show increase in activity with temperature (28). Moreover, reports in the literature suggest that heat activation is associated with considerable plasticity at the PDZ-protease interface, similar to activation *via* substrate binding at PDZ (29). Thus, quantitative analysis of activity of HtrA2 and its variants was performed as a function of

Figure 3. Proteolytic activity of HtrA2 and its mutants with β-casein as substrate. In all gels, β-c represents β-casein. *A–D*) β-Casein cleavage assays with increasing concentrations (2, 4, 6 μg) of SPD (*A*), SPD-PDZ domain (*B*), HtrA2(F16D) mutant (*C*), and N-SPD(F16D) mutant (*D*). *E*) Initial velocity V_0 with increasing concentrations (2–6 μg) of SPD, SPD-PDZ, HtrA2(F16D), and N-SPD(F16D) using FITC β-casein as substrate. *F*) Elution profile with increasing concentrations of HtrA2(F16D) and N-SPD(F16D) using Superdex 200 gel-filtration column. *G*) Initial velocity of HtrA2 and its mutants as a function of temperature using FITC β-casein as substrate.

temperature as well, to understand how change in activity correlates with conformational changes and dynamic behavior of HtrA2. V_0 was calculated for HtrA2, HtrA2(F16D), and N-SPD domain using FITC β-casein as substrate. For HtrA2, V_0 increased linearly up to 55°C. Activity of HtrA2 was ~5-fold higher at 55°C than that at 37°C (Fig. 3G) with a subsequent decrease beyond 60°C that might be due to protease unfolding as loss of secondary and tertiary structure was also observed through spectroscopic studies at higher temperature (data not shown). The marked increase might be consistent with its physiological role to serve as a quality control protein and to maintain mitochondrial homeostasis (30). Identical enzymatic studies were done with trimeric N-SPD (no PDZ inhibition) and monomeric HtrA2(F16D) having an intact PDZ domain. Increase in activity was observed in both, although the change was not significant (~1.7- and ~1.2-fold higher than that at 37°C) as shown in Fig. 3F. Moreover, their maximum activity was found to be ~50°C, which might be due to a decrease in stability of the proteins as observed by thermal denaturation studies. These observations suggest that N-SPD, whose basal activity is much less than that of the wild type, lacks the PDZ-protease dynamics preventing the rearrangement of the active site to form a more catalytically competent enzyme as observed in the wild-type protease. However, the slight increase in protease activity that is observed in N-SPD highlights the conformational changes that occur at the N-terminal region in the trimeric ensemble that might also be required in concert with PDZ-protease crosstalk for HtrA2 activation. In monomeric HtrA2(F16D), although the PDZ is intact, no significant change in enzyme activity was observed, suggesting the role of intermolecular PDZ-protease crosstalk in HtrA2 activation. Overall, these data reiterate the importance of N-terminal domain, PDZ domain, and intermolecular crosstalk (trimeric architecture) in efficient HtrA2 activity.

Secondary and tertiary structural properties of HtrA2 mutants and domains

Far-UV CD studies were performed to understand the effect of deletions and mutations on HtrA2 secondary structure and stability. All proteins except N-SPD and N-SPD(F16D) show similar secondary structural properties, suggesting that the mutations and deletions did not alter their overall secondary structure (**Fig. 4A**). Both N-SPD and N-SPD(F16D) show a decrease in total α-helical characteristics of the protease, which might be due to absence of PDZ domain in these variants. Secondary structural properties of all HtrA2 constructs harboring either Y295W or N48W mutation are comparable to their nontryptophan counterparts suggesting these tryptophan mutations are structurally not perturbing (data not shown).

Fluorescence emission studies were performed for all tryptophan mutants (Y295W and N48W) and variants of HtrA2 to characterize the tertiary structural changes at the PDZ-protease interface, near the active site region as well as to understand the effect of certain mutations and deletions on the overall protein conformation. The 2 monomeric variants of HtrA2, HtrA2 (F16D, Y295W), and SPD-PDZ(Y295W), showed redshifted emission maxima (by 2 nm) compared to trimeric HtrA2(Y295W) (Fig. 4B), demonstrating that PDZ of the same molecule might not be completely collapsing on the SPD domain as suggested by the model (15). Interestingly, the packing mutant HtrA2(M190R, Y295W) showed similar redshift implicating that this mutation did not negatively disrupt intramolecular PDZ-protease contacts as suggested earlier, and it has been found to be in accordance with the enzymology
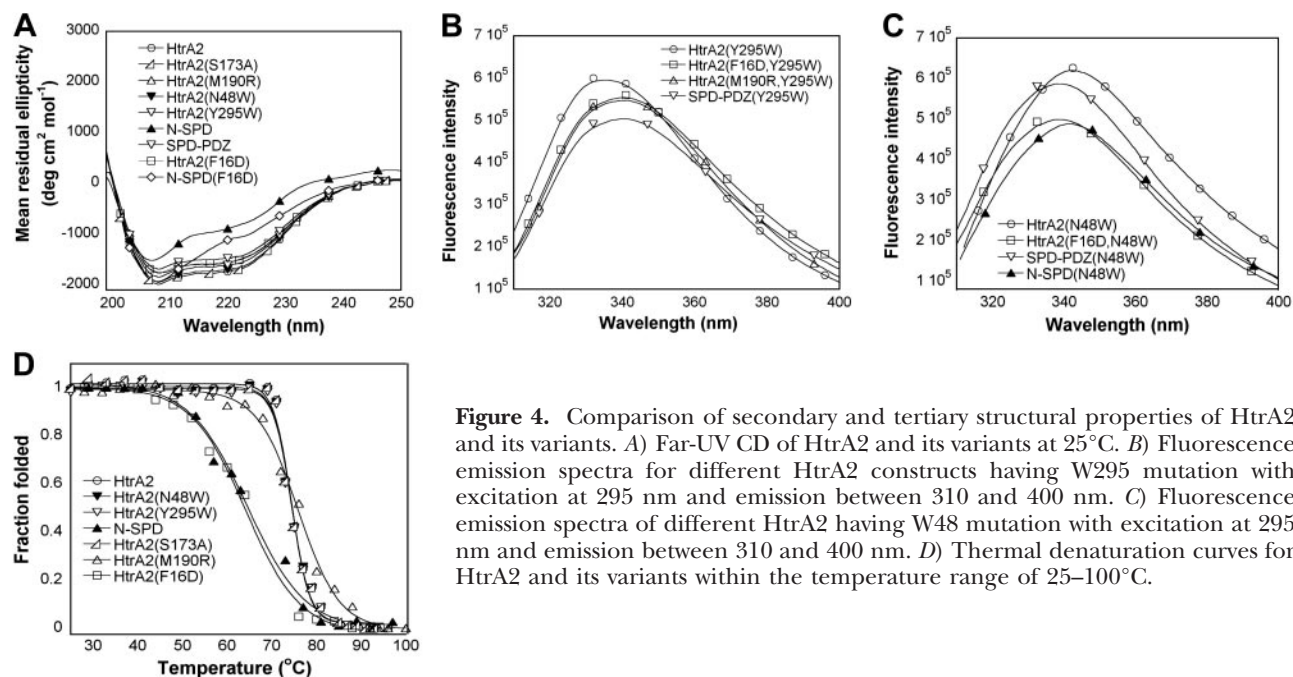

Figure 4. Comparison of secondary and tertiary structural properties of HtrA2 and its variants. A) Far-UV CD of HtrA2 and its variants at 25°C. B) Fluorescence emission spectra for different HtrA2 constructs having W295 mutation with excitation at 295 nm and emission between 310 and 400 nm. C) Fluorescence emission spectra of different HtrA2 having W48 mutation with excitation at 295 nm and emission between 310 and 400 nm. D) Thermal denaturation curves for HtrA2 and its variants within the temperature range of 25–100°C.

data discussed in the previous section. In contrast, emission maxima for HtrA2(N48W) showed slight red-shift (Fig. 4C) compared to the 2 monomeric variants, suggesting that regulatory loops L1 and LD, which are in the vicinity of the tryptophan, might be oriented such that the tryptophan is more buried in the monomeric forms. In addition, emission maxima for trimeric N-SPD(N48W) is slightly blueshifted (~1 nm) compared to HtrA2(N48W), which suggests that PDZ domains do not influence the burial of W48 in the protease structure, and the observed blueshift in the monomeric full-length HtrA2 variants might be due to rearrangements of the loops around the active site. Overall, these studies show that the mutants are well folded with proper secondary and tertiary structural properties. Structural alterations and subtle conformational changes might occur with deletions and mutations, respectively, which are reflected in overall protease activity.

Since protease activity of HtrA2 increased with temperature, thermal stability of the protease and secondary and tertiary structural changes in the SPD and PDZ-protease interface were monitored for different constructs. Thermal denaturation studies using CD spectroscopy demonstrate that melting temperature (T_m) of HtrA2, HtrA2(S173A), HtrA2(Y295W), and HtrA2(N48W) was ~74°C (Fig. 4D) suggesting that the mutations did not have destabilizing effects on the protease. The slopes for full-length trimeric protease variants, except for HtrA2(M190R), were steep, demonstrating highly cooperative unfolding, whereas the slope was less for HtrA2(M190R), implying higher conformational flexibility, which might be due to presence of a more open active site architecture (31). T_m for N-SPD and monomeric HtrA2(F16D) was found to be ~65°C, highlighting the importance of PDZ and trimeric protease architecture in HtrA2 stability. T_m for SPD-PDZ and SPD could not be calculated because these proteins precipitated beyond 50°C. This suggests that the N terminus might also be very important for rendering stability to the protease.

Tryptophan accessibility by fluorescence quenching studies

Fluorescence quenching studies were performed with the 2 tryptophan mutants in different HtrA2 constructs to determine their relative accessibility to acrylamide (32) between 30 and 65°C. Since activity of substrate-bound HtrA2 mimics that of thermally activated form, this information would thus reflect conformational dynamics at the PDZ-protease interface and the region surrounding the active site where these mutations are strategically placed (29). At 30°C, K_{SV} values for trimeric N48W mutants, HtrA2 and N-SPD (3.2 and 3.4, respectively), were less than for their monomeric counterparts HtrA2(F16D) and SPD-PDZ (4.8 and 4.9, respectively; **Table 3**). Since W48 is near the regulatory loops L1 and LD, difference in their orientations might also be responsible for change in K_{SV}, which can be very well correlated with fluorescence emission studies, as well as lesser protease activity of monomeric mutants compared to the trimers.

The K_{SV} constants for HtrA2(Y295W) are lower compared to other HtrA2 variants, HtrA2(M190R), HtrA2(F16D), and SPD-PDZ (4.4, 7.8, 6.5, and 6.2, respectively; Table 3) suggesting that W295 is less accessible to the quencher in the wild type, which correlates very well with our fluorescence emission studies. Moreover, W295 is introduced in such a way that its accessibility will not be influenced structurally by the presence of the other 2 monomers in trimeric HtrA2. In addition, it also faces the PDZ-protease interface and is in the vicinity of the substrate binding pocket (YIGV). This is supposed to reflect the environment surrounding the YIGV groove and monitor interdomain plasticity. Therefore, higher K_{SV} constants for the above-mentioned monomeric HtrA2 variants support our enzymology and other spectroscopic data that demonstrate that PDZ from the same monomer does not collapse on SPD; rather, it might have enhanced flexibility as a consequence of absence of 2 other surrounding HtrA2 molecules. According to the existing HtrA2 model (15), M190R mutation disrupts the packing between PDZ and protease domains, resulting in complete protease inactivation due to collapse of PDZ. With

TABLE 3. *Stern-Volmer quenching constants (K_{SV}) for HtrA2 variants as a function of temperature with W48 and W 295 as the intrinsic fluorophore*

HtrA2 construct	K_{SV}					
	30°C	37°C	45°C	50°C	55°C	60°C
HtrA2(N48W)	3.2 ± 0.16	2.7 ± 0.12	2.0 ± 0.15	1.7 ± 0.23	1.2 ± 0.11	1.1 ± 0.08
HtrA2(F16D, N48W)	4.76 ± 0.11	4.71 ± 0.13	4.69 ± 0.12	4.67 ± 0.17	4.68 ± 0.12	4.62 ± 0.25
SPD-PDZ(N48W)	4.9 ± 0.11	−	−	−	−	−
N-SPD(N48W)	3.40 ± 0.17	3.34 ± 0.11	3.35 ± 0.13	4.10 ± 0.15	4.20 ± 0.16	4.30 ± 0.11
HtrA2(Y295W)	4.41 ± 0.11	4.90 ± 0.27	6.13 ± 0.32	9.46 ± 0.40	10.84 ± 0.43	14.10 ± 0.23
HtrA2(F16D, Y295W)	6.5 ± 0.08	6.6 ± 0.12	6.7 ± 0.14	7.1 ± 0.16	8.5 ± 0.23	9.1 ± 0.27
SPD-PDZ(Y295W)	6.2 ± 0.07	−	−	−	−	−
HtrA2(M190R, Y295W)	7.8 ± 0.08	8.1 ± 0.19	8.3 ± 0.22	10.1 ± 0.30	11.2 ± 0.28	14.7 ± 0.40

Data (averages ± SD of 3 independent experiments) were fitted to the Stern-Volmer equations (Eqs. 1 and 2) as described in Materials and Methods.

our enzymology, *in silico*, and spectroscopic data, we have proved that M190R mutation does not only make the enzyme highly active but also has a more flexible and accessible active site pocket.

However, at higher temperatures, K_{SV} values for HtrA2 decreased gradually from 3.2 to 1.1, while for monomeric HtrA2(F16D), as well as trimeric N-SPD, they remained unchanged (Table 3). The decrease in quenching constant for HtrA2 is indicative of rearrangement of L1 and LD loops on activation, leading to burial of W48. No change in quenching constant for trimeric N-SPD suggests that loop reorientations might be dynamically coupled to PDZ movement. In monomeric HtrA2(F16D), no change in K_{SV} constants with temperature provides two important insights into the HtrA2 mechanism: first, trimeric architecture is required for formation of a catalytically competent enzyme; second, the PDZ domain might not play a critical role in active site rearrangement for the same protease molecule. These observations, along with enzymology data, revalidate our hypothesis of interdomain PDZ-protease crosstalk in HtrA2 activation.

For HtrA2 and HtrA2(M190R), with Y295W mutation, increase in tryptophan exposure was observed (3.2- and 1.9-fold, respectively) with temperature till 60°C. This increase in K_{SV} values suggests that PDZ might be moving away from SPD and also exposing the YIGV groove, making the protease more accessible to the substrate, thus increasing protease activity. This is further supported by the enzymatic studies where the activity was found to be maximum at ~55°C (Table 3). In HtrA2(M190R), initial redshift compared to wild type is suggestive of a more open YIGV groove and less compact PDZ-protease interface. Although the initial emission maxima are higher than for wild type in HtrA2(F16D), there is only a 1.3-fold increase in the K_{SV} constant, demonstrating that PDZ does not move significantly away from SPD with increase in temperature. This might be due to absence of intermolecular PDZ-SPD movement, which otherwise indirectly modulates PDZ-protease plasticity within the same monomer. All these observations point toward requirement of

trimeric architecture of the protease for structural plasticity and accentuate the role of intermolecular PDZ-protease interaction in regulating HtrA2 activity. Overall, these temperature-dependent structural changes near the catalytic triad and interface of serine protease-PDZ domain of trimeric full-length HtrA2 might be the reason for the higher fold increase in enzyme activity.

Intramolecular PDZ-protease interaction by FRET

With an aim at looking at the distance between PDZ and protease domain quantitatively, FRET studies were performed with wild-type HtrA2 as well as its monomeric and packing mutants as a function of temperature. Structure-guided F208C mutation was done in α4 of SPD on the HtrA2(Y295W) template. The FRET pairs were chosen such that they face each other and reside in the vicinity of the PDZ-protease linker region. This approach would provide a comparative analysis of not only the distance between PDZ and protease in these 3 different HtrA constructs but would also help understand the dynamics of the interface as a function of temperature. These FRET residues that face each other in the same monomer are far away from their pairs in the adjoining molecules in trimeric HtrA2, and hence influence from other molecules on FRET transfer has been expected to be minimal. The tryptophan fluorescence and IAEDANS absorption spectra of all HtrA2 FRET mutants overlap, facilitating efficient energy transfer (**Fig. 5A**). Comparison of transfer efficiency E and distance R (Å) at 30°C shows that HtrA2(F208C, Y295W) has a shorter C208−W295 distance compared to its M190R and F16D counterparts (**Table 4**), thus supporting our hypothesis.

With increase in temperature, energy transfer efficiency for HtrA2(F208C, Y295W) and HtrA2(M190R, F208C, Y295W) initially increased, and calculated distances R between the acceptor and donor decreased from 30 to 50°C. Beyond 50°C, energy transfer efficiency decreased with subsequent increase in R values. However, consistent redshift (2.5 and 1.5 nm, respectively) in fluorescence emission maxima between 30
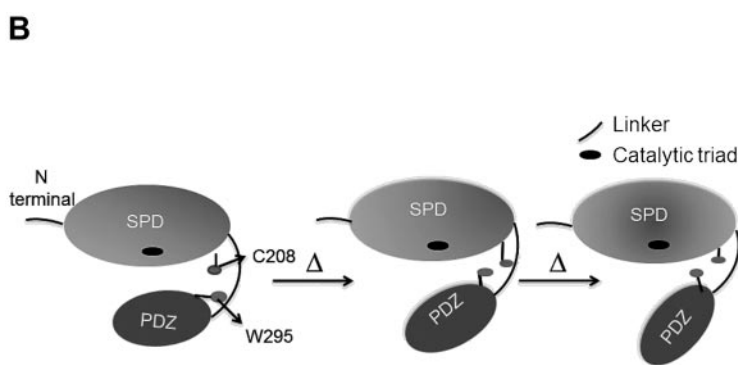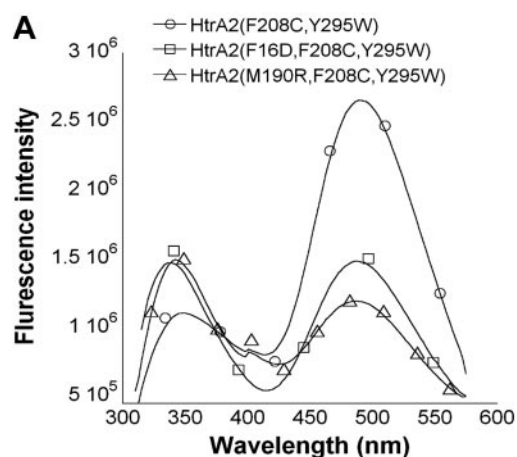

Figure 5. FRET studies representing intramolecular PDZ-protease distance. *A*) Fluorescence emission of HtrA2 and its mutants labeled with IAEDANS. Fluorescence was excited at a wavelength of 295 nm and spectra were collected between 310 and 575 nm. *B*) Model showing the dynamics at SPD-PDZ interface as a function of temperature.

TABLE 4. *FRET parameters between IAEDANS (acceptor) and W295 (donor) for HtrA2 (F208C, Y295W) and its variants as a function of temperature*

Temperature (°C)	E			R (Å)		
	HtrA2	HtrA2(M190R)	HtrA2(F16D)	HtrA2	HtrA2(M190R)	HtrA2(F16D)
30	55.3	45.2	46.75	21.2	22.5	22.4
37	57.4	47.3	47.43	20.9	22.2	22.3
45	60.0	50.0	47.67	20.5	22.0	22.3
50	61.0	51.1	48.39	20.4	21.8	22.2
55	55.9	47.9	53.24	21.1	22.3	21.5
60	55.6	47.5	48.90	21.1	22.2	22.1

E is the transfer efficiency; *R* is the distance between 2 probes. *E* and *R* values were calculated from Eqs. 3 and 4 as described in Materials and Methods.

and 50°C was observed with these 2 mutants (data not shown). This apparent anomaly can be explained by a model where, as a function of temperature, the interface movement occurs such that the PDZ moves away from SPD in a V-shaped trajectory thus bringing the 2 residues in vicinity of each other (Fig. 5*B*). However, beyond 50°C, the gap between PDZ and protease domains increases more, which is reflected in increase in *R* values (Table 4). Consistent with fluorescence quenching studies, HtrA2(F16D, F208C, Y295W) did not show much change in distance between the FRET pairs with temperature.

DISCUSSION

The goal of this study was to delineate the role of different domains, their combinations, oligomerization, and critical residues in modulating HtrA2 activity and specificity with an aim at developing a model for HtrA2 mechanism of action. The importance of HtrA2 as a promising therapeutic target is reflected in a plethora of studies on its structure and functions in the past decade. This includes the crystal structure of inactive unbound form that provides a broad overview of its overall structural organization (15). However, none of these studies could unambiguously define its mode of activation, which is a prerequisite for delineating its role in various biological pathways and diseases. Thus, understanding the structural correlates of HtrA2 activation will be a step forward toward designing molecules to manipulate its functions for devising therapeutic strategies (33, 35).

HtrA2 has a complex arrangement of L1, L2, and LD loops encompassing the active site pocket and a flexible linker at the PDZ-protease interface whose relative orientations and crosstalk with different domains might be essential for defining its functions. The crystal structure of the inactive form of the protease (S173A; ref. 15) proposed a model where the relative intramolecular PDZ-protease movement was considered the primary reason for regulation of HtrA2 activity. However, a part of the N-terminal region, PDZ-protease linker, and several critical loops were missing from the structure, thus limiting its ability to demonstrate the

dynamics of the mechanism of action. According to the model, the PDZ domains on substrate binding move away from SPD, making way for the substrate to access the catalytic pocket thus emphasizing intramolecular PDZ-protease crosstalk to be pivotal in protease activation. The model also hypothesized that in the monomeric HtrA2 variant, complete collapse of PDZ on protease leads to its inactivity, which can be subsequently rescued through removal of PDZ domain. The role of the short N-terminal region other than trimer formation was also not highlighted in the previous model and hence is incapable of fully explaining the intricate collaboration among different domains in HtrA2. Our data challenge this hypothesis and underline the importance of PDZ, the N-terminal region, and trimerization in proper active-site formation, thus providing a comprehensive illustration of mode of HtrA2 activation.

Here, with an apt combination of *in silico*, enzymological, and biophysical studies, we have demonstrated the complexity of conformational changes and dynamics that regulate HtrA2 functions. In this study, domain-wise dissection of HtrA2 has been done to delineate their roles alone and in different combinations, including loops, crucial residues, and flexible interface linker in modulating HtrA2 functions. For example, deletion of PDZ domain resulted in a trimeric HtrA2 variant without PDZ inhibition (both inter- and intramolecular), whereas monomeric SPD-PDZ and HtrA2(F16D) constructs were created to highlight the importance of both N-terminal region and trimerization in protease activation. This unique approach clearly pinpointed the roles of each of them toward formation of a catalytically competent HtrA2 molecule.

The 19-aa N-terminal trimerization region in HtrA2 is unique among HtrAs. It resembles Smac/DIABLO in its IAP binding ability and in promoting caspase-dependent apoptosis (10, 13, 35). Apart from these functions, its significance in structure and stability of the protease has not been characterized. Here we show that N-terminal region plays an important role in active site rearrangement with stabilization of the enzyme-substrate complex. Comparison of HtrA2(F16D) with SPD-PDZ establishes the role of the N-terminal region toward rendering stability to the protease. The C-termi-

nal PDZ domains in HtrAs perform myriads of functions that include allosteric modulation, protein-protein interactions, and higher-order oligomer formation (36–38). In HtrA2, it has been hypothesized that PDZ acts as a substrate binding (*via* its YIGV tetrapeptide motif) as well as a regulatory domain (15). Relative orientation and movement between PDZ and protease domain was considered to be the determining factor for HtrA2 activity as well as specificity. We have shown that the mechanism of HtrA2 activation, although requires PDZ-protease crosstalk, is not straightforward, and using functional enzymology and a quantitative biophysical approach, we reexamined and modified the existing mechanism (15). Our data demonstrate an inability to form a proper active site as the main reason for lower basal activity in HtrA2 rather than inaccessibility of the active site due to shielding by the PDZ domain from the same molecule. This rearrangement occurs in a complex, concerted manner involving trimerization, the N-terminal region, and intermolecular PDZ-protease crosstalk, which subsequently rearranges the active-site loops and creates catalytically competent oxyanion hole.

Spectroscopic and enzymology studies as a function of temperature with different HtrA2 variants ascertain considerable rearrangement in and around the L1 loop, suggesting a malformed oxyanion hole in the apo-protease. These experimental studies excellently corroborate with a recent literature report (18) where substrate binding leads to movement of α5 of PDZ* toward SPD of adjacent monomer thus flipping F170 of the oxyanion hole near H65 of the catalytic triad making the protease poised for catalysis. However, L2, which harbors the substrate specificity pocket, shows minimal movement, reestablishing our observations.

Interestingly, contrary to the previous literature report (15), HtrA2(M190R), a mutant that was designed to study the packing and mobility of the PDZ-protease interface, has been found to have significantly enhanced activity compared to the wild-type HtrA2. It might be due to the less compact structural architecture with a more open and solvent accessible active site as well as greater plasticity at the PDZ-protease linker as observed by thermal denaturation and other spectroscopic studies. Combination of these 2 factors might have synergistically led toward efficient initial substrate binding as well as catalysis thus enhancing enzyme activity by severalfold. A close look at the HtrA2 structure (15) shows that mutating a methionine to a bulkier arginine residue might lead to steric clash with leucine 233, which is perhaps prevented by opening up of the active-site pocket. Moreover, this mutation that happens to occur next to a lysine residue (K191) increases the local positive charge at the hydrophobic milieu of the PDZ-protease interface, which in addition to the steric effect might open up the pocket even further leading to enhanced substrate catalysis. However, additional mutational and structural studies are required to confirm this hypothesis.

Based on all these observations and critical infer-

ences, a comprehensive working model of HtrA2 activation has been proposed, as illustrated in **Fig. 6**. In full-length trimeric HtrA2, initial substrate binding or increase in temperature leads to movement of PDZ* toward the SPD of an adjacent molecule. This intermolecular movement along with simultaneous N-terminal rearrangement leads to subtle reorganization of the active-site loops to form an active protease. Interestingly, the intermolecular domain plasticity concomitantly facilitates intramolecular linker movement thus indirectly aiding initial substrate binding and further protease activation. This complex yet precise synergistic coordination among different domains of the protease might be functionally important for selecting substrates under normal and diseased conditions.

Although N-terminal-mediated partial active-site reorientation and stabilization is novel among the HtrA family of proteases, PDZ domains do act as modulators in most of the cases (36, 39, 40). For example, in bacterial DegS, which is a periplasmic stress sensor
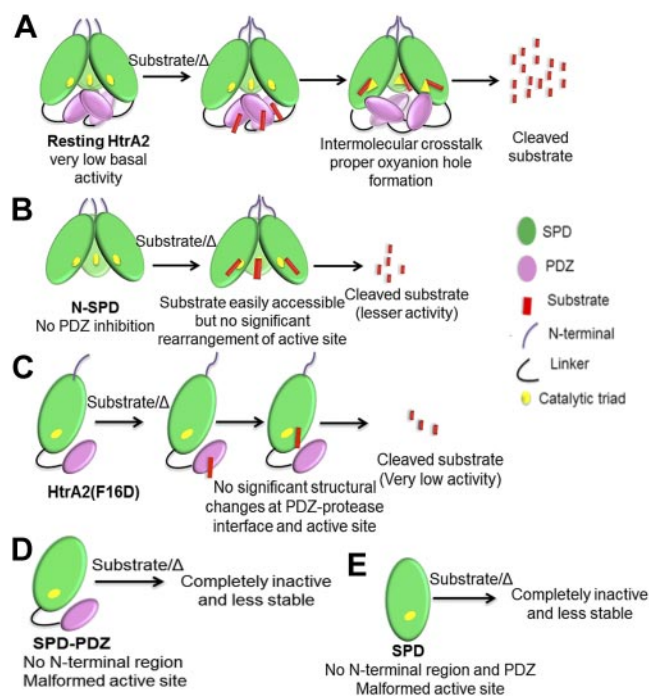

Figure 6. Proposed model representing mechanism of HtrA2 activation. *A*) In full-length trimeric HtrA2, initial substrate binding or increase in temperature leads to movement of PDZ* toward SPD of adjacent molecule. This intermolecular movement along with simultaneous N-terminal rearrangement leads to subtle reorganization of the active-site loops to form an active protease. *B*) In trimeric N-SPD, substrate is easily accessible to the active site, but lack of PDZ movement leads to significant reduction in activity. Presence of residual activity can be attributed to partial active site rearrangement and stabilization mediated by the N terminus. *C*) In the monomeric HtrA2(F16D) variant, absence of intermolecular crosstalk and subsequent loop rearrangements result in a malformed oxyanion hole, which significantly reduces the rate of catalysis. *D*) Monomeric SPD-PDZ with malformed active site is completely inactive and is less stable. *E*) Monomeric SPD without N terminus and PDZ is completely inactive and is less stable.

(41–43), inhibitory interaction of PDZ with loop L3 of SPD in the unbound state keeps the protease in its basal form. This inhibition is relieved by outer membrane protein (OMP) binding to PDZ that subsequently leads to both cis and *trans* protease domain rearrangement so as to form an active DegS molecule (44). On the other hand, in HtrA2, we have established that very low basal activity in the apo-protease might be due to presence of a catalytically incompetent active-site pocket which requires intermolecular PDZ-protease interaction as well as additional N-terminal contacts and stabilization for formation of a fully functional trimeric ensemble. In bacterial periplasmic space, where certain amounts of unassembled OMPs are always present, stress response beyond a threshold level can therefore be readily modulated by OMP-PDZ interaction (44). However, in HtrA2, evolution has possibly provided an additional N-terminal regulatory switch for tighter control of its activation, which might be required only during triggering of apoptotic signal. Thus, nature uses unique fusion of individual domains, loops, and linkers that evolve into polypeptides with distinct functional and regulatory properties. [FJ]

REFERENCES

1. Suzuki, Y. Takahashi-Niki, K., Akagi, T., Hashikawa, T., and Takahashi, R. (2004) Mitochondrial protease Omi/HtrA2 enhances caspase activation through multiple pathways. *Cell Death Differ.* **11,** 208–216

2. Meltzer, M., Hasenbein, S., Mamant, N., Merdanovic, M., Poepsel, S., Hauske, P., Kaiser, M., Huber, R., Krojer, T., Clausen, T., and Ehrmann, M. (2009) Structure, function and regulation of the conserved serine proteases DegP and DegS of *Escherichia coli*. *Res. Microbiol.* **160,** 660–666

3. Zurawa-Janicka, D., Skorko-Glonek, J., and Lipinska, B. (2010) HtrA proteins as targets in therapy of cancer and other diseases. *Expert Opin. Ther. Targets* **14,** 665–679

4. Polur, I., Lee, P., Servais, J., Xu, L., and Li, Y. (2010) Role of HTRA1, a serine protease, in the progression of articular cartilage degeneration. *Histol. Histopathol.* **25,** 599–608

5. Clausen, T., Kaiser, M., Huber, R., and Ehrmann, M. (2011) HTRA proteases: regulated proteolysis in protein quality control. *Nat. Rev. Mol. Cell Biol.* **12,** 152–162

6. Jiang, J., Zhang, X., Chen, Y., Wu, Y., Zhou, Z., Chang, Z., and Sui, S. (2008) Activation of DegP chaperone-protease via formation of large cage-like oligomers upon binding to substrate proteins. *Proc. Natl. Acad. Sci. U. S. A.* **105,** 11939–11944

7. Krojer, T., Garrido-Franco, M., Huber, R., Ehrmann, M., and Clausen, T. (2002) Crystal structure of DegP (HtrA) reveals a new protease-chaperone machine. *Nature* **416,** 455–459

8. Krojer, T., Pangerl, K., Kurt, J., Sawa, J., Stingl, C., Mechtler, K., Huber, R., Ehrmann, M., and Clausen, T. (2008) Interplay of PDZ and protease domain of DegP ensures efficient elimination of misfolded proteins. *Proc. Natl. Acad. Sci. U. S. A.* **105,** 7702–7707

9. Lipinska, B., Fayet, O., Baird, L., and Georgopoulos, C. (1989) Identification, characterization, and mapping of the *Escherichia coli* htrA gene, whose product is essential for bacterial growth only at elevated temperatures. *J. Bacteriol.* **171,** 1574–1584

10. Hegde, R., Srinivasula, S., Zhang, Z., Wassell, R., Mukattash, R., Cilenti, L., DuBois, G., Lazebnik, Y., Zervos, A., Fernandes-Alnemri, T., and Alnemri, E. (2002) Identification of Omi/HtrA2 as a mitochondrial apoptotic serine protease that disrupts inhibitor of apoptosis protein-caspase interaction. *J. Biol. Chem.* **277,** 432–438

11. Zumbrun, J., and Trueb, B. (1996) Primary structure of putative serine protease specific for IGF-binding. *FEBS Lett.* **398,** 187–192

12. Singh, N., Kuppili, R., and Bose, K. (2011) The structural basis of mode of activation and functional diversity: a case study with HtrA family of serine protease. *Arch. Biochem. Biophys.* **516,** 85–96

13. Suzuki, Y., Imai, Y., Nakayama, H., Takahashi, K., Takio, K., and Takahashi, R. (2001) A serine protease, HtrA2, is released from the mitochondria and interacts with. XIAP, inducing cell death. *Mol. Cell* **8,** 613–621

14. Suzuki, Y., Nakabayashi, Y., Nakata, K., Reed, J., and Takahashi, R. (2001) X-linked inhibitor of apoptosis protein (XIAP) inhibits caspase-3 and -7 in distinct modes. *J. Biol. Chem.* **276,** 27058–27063

15. Li, W., Srinivasula, S., Chai, J., Li, P., Wu, J., Zhang, Z., Alnemri, E., and Shi, Y. (2002) Structural insights into the pro-apoptotic function of mitochondrial serine protease HtrA2/Omi. *Nat. Struct. Biol.* **9,** 436–441

16. Doyle, D., Lee, A., Lewis, J., Kim, E., Sheng, M., and MacKinnon, R. (1996) Crystal structures of a complexed and peptide-free membrane protein-binding domain: molecular basis of peptide recognition by PDZ. *Cell* **85,** 1067–1076

17. Bhuiyan, M., and Fukunaga, K. (2009) Mitochondrial serine protease HtrA2/Omi as a potential therapeutic target. *Curr. Drug Targets* **10,** 372–383

18. Bejugam, P. R., Kuppili, R. R., Singh, N., Gadewal, N., Chaganti, L. K., Sastry, G. M., and Bose, K (2012) Allosteric regulation of serine protease HtrA2 through novel non-canonical substrate binding pocket. *PloS ONE* **8,** e55416

19. Brooks, B. R., Brooks, C. L., III, Mackerell, A. D., Jr., Nilsson, L., Petrella, R. J., Roux, B., Won, Y., Archontis, G., Bartels, C., Boresch, S., Caflisch, A., Caves, L., Cui, Q., Dinner, A. R., Feig, M., Fischer, S., Gao, J., Hodoscek, M., Im, W., Kuczera, K., Lazaridis, T., Ma, J., Ovchinnikov, V., Paci, E., Pastor, R. W., Post, C. B., Pu, J. Z., Schaefer, M., Tidor, B., Venable, R. M., Woodcock, H. L., Wu, X., Yang, W., York, D. M., and Karplus, M. (2009) CHARMM: the biomolecular simulation program. *J. Comput. Chem.* **30,** 1545–1614

20. Baldi, A., Mottolese, M., Vincenzi, B., Campioni, M., Mellone, P., Di Marino, M., di Crescenzo, V., Visca, P., Menegozzo, S., Spugnini, E., Citro, G., Ceribelli, A., Mirri, A., Chien, J., Shridhar, V., Ehrmann, M., Santini, M., and Facciolo, F. (2008) The serine protease HtrA1 is a novel prognostic factor for human mesothelioma. *Pharmacogenomics* **9,** 1069–1077

21. Hess, B., Kutzner, C., van der Spoel, D., and Lindahl, E. (2008) GROMACS 4: Algorithms for highly efficient, load-balanced, and scalable molecular simulation. *J. Chem Theory Comput.* **4,** 435–447

22. Kelly, S. M., Jess, T. J., and Price, N. C. (2005) How to study proteins by circular dichroism. *Biochim Biophys Acta.* **1751,** 119–139

23. Eftink, M. R., and Ghiron, C. A. (1981) on the analysis of the temperature and viscosity dependence of fluorescence-quenching reactions with proteins. *Arch. Biochem. Biophys.* **209,** 706–709

24. Liang, J. J., and Liu, B.-F. (2006) Fluorescence resonance energy transfer study of subunit exchange in human lens crystallins and congenital cataract crystallin mutants. *Protein Sci.* **15,** 1619–1627

25. Wang, C. K., and Cheung, H. C (1986) Proximity relationship in the binary complex formed between troponin I and troponin C. *J. Mol. Biol.* **191,** 509–521

26. Lakowicz, J. (2006) Energy transfer. In *Principles of Fluorescence Spectroscopy*, Vol. 6 (Geddes, C. D., ed) pp. 443–468, Springer-Verlag, New York

27. Nam, M., Seong, Y., Park, H., Choi, J., Kang, S., and Rhim, H. (2006) The homotrimeric structure of HtrA2 is indispensable for executing its serine protease activity. *Exp. Mol. Med.* **38,** 36–43

28. Zhang, X., and Z., C. (2004) Temperature dependent protease activity and structural properties of human HtrA2 protease. *Biochemistry* **69,** 687–692

29. Martins, L., Turk, B., Cowling, V., Borg, A., Jarrell, E., Cantley, L., and Downward, J. (2003) Binding specificity and regulation of the serine protease and PDZ domains of HtrA2/Omi. *J. Biol. Chem.* **278,** 49417–49427

30. Castro, I. P. d., Miguel Martins, L., and Loh, S. H. Y. (2011) Mitochondrial quality control and Parkinson's Disease: a pathway unfolds. *Mol. Neurobiol.* **43,** 80–86

31. Roy, S., and Hecht, M. (2000) Cooperative thermal denaturation of proteins designed by binary patterning of polar and nonpolar amino acids. *Biochemistry* **39,** 4603–4607

32. Calhoun, D. B., Vanderkooi, J. M. G., Woodrow, G. V., III, and Englander, S. W. (1983) Penetration of dioxygen into proteins studied by quenching of phosphorescence and fluorescence. *Biochemistry* **22,** 1526–1532

33. Wang, W., Takimoto, R., Rastinejad, F., and El-Deiry, W. S. (2003) Stabilization of p53 by CP-31398 inhibits ubiquitination without altering phos-phorylation at serine 15 or 20 or MDM2 binding. *Mol. Cell. Biol.* **23,** 2171–2181

34. Gavathiotis, E., Reyna, D. E., Bellairs, J. A., Leshchiner, E. S., and Walensky, L. D. (2012) Direct and selective small-molecule activation of proapoptotic BAX. *Nat. Chem. Biol.* **8,** 639–645

35. Wu, G., Chai, J., Suber, T., Wu, J., Du, C., Wang, X., and Shi, Y. (2000) Structural basis of IAP recognition by Smac/DIABLO. *Nature* **408,** 1008–1012

36. Krojer, T., Sawa, J., Huber, R., and Clausen, T. (2010) HtrA proteases have a conserved activation mechanism that can be triggered by distinct molecular cues. *Nat. Struct. Mol. Biol.* **17,** 844–852

37. Merdanovic, M., Mamant, N., Meltzer, M., Poepsel, S., Auckenthaler, A., Melgaard, R., Hauske, P., Nagel-Steger, L., Clarke, A., Kaiser, M., R., H., and Ehrmann, M. (2010) Determinants of structural and functional plasticity of a widely conserved protease chaperone complex. *Nat. Struct. Mol. Biol.* **17,** 837–843

38. Wrase, R., Scott, H., Hilgenfeld, R., and Hansen, G. (2011) The Legionella HtrA homologue DegQ is a self-compartmentizing protease that forms large 12-meric assemblies. *Proc. Natl. Acad. Sci. U. S. A.* **108,** 10490–10495

39. Sohn, J., Grant, R., and Sauer, R. (2009) OMP peptides activate the DegS stress-sensor protease by a relief of inhibition mechanism. *Structure* **17,** 1411–1421

40. Sohn, J., and Sauer, R. (2009) OMP peptides modulate the activity of DegS protease by differential binding to active and inactive conformations. *Mol. Cell* **33,** 64–74

41. Sohn, J., Grant, R., and Sauer, R. (2007) Allosteric activation of DegS, a stress sensor PDZ protease. *Cell* **131,** 572–583

42. Walsh, N., Alba, B., Bose, B., Gross, C., and Sauer, R. (2003) OMP peptide signals initiate the envelope-stress response by activating DegS protease via relief of inhibition mediated by its PDZ domain. *Cell* **13,** 61–71

43. Hasenbein, S., Meltzer, M., Hauske, P., Kaiser, M., Huber, R., Clausen, T., and Ehrmann, M. (2010) Conversion of a regulatory into a degradative protease. *J. Mol. Biol.* **397,** 957–966

44. Mauldin, R., and Sauer, R. (2012) Allosteric regulation of DegS protease subunits through a shared energy landscape. *Nat. Chem. Biol.* **9,** 90–96

Allosteric Regulation of Serine Protease HtrA2 through Novel Non-Canonical Substrate Binding Pocket

Pruthvi Raj Bejugam[1][9], Raja R. Kuppili[1][9], Nitu Singh[1], Nikhil Gadewal[1], Lalith K. Chaganti[1], G. Madhavi Sastry[2], Kakoli Bose[1]*

1 Advanced Centre for Treatment, Research and Education in Cancer (ACTREC), Tata Memorial Centre, Kharghar, Navi Mumbai, India, 2 Schrödinger, Sanali Infopark, Banjara Hills, Hyderabad, India

Abstract

HtrA2, a trimeric proapoptotic serine protease is involved in several diseases including cancer and neurodegenerative disorders. Its unique ability to mediate apoptosis via multiple pathways makes it an important therapeutic target. In HtrA2, C-terminal PDZ domain upon substrate binding regulates its functions through coordinated conformational changes the mechanism of which is yet to be elucidated. Although allostery has been found in some of its homologs, it has not been characterized in HtrA2 so far. Here, with an *in silico* and biochemical approach we have shown that allostery does regulate HtrA2 activity. Our studies identified a novel non-canonical selective binding pocket in HtrA2 which initiates signal propagation to the distal active site through a complex allosteric mechanism. This non-classical binding pocket is unique among HtrA family proteins and thus unfolds a novel mechanism of regulation of HtrA2 activity and hence apoptosis.

Introduction

Multidomain proteins due to their structural complexity require different levels of regulatory mechanisms for executing cellular functions efficiently within a specified time period. Allosteric modulation of conformations is one such mechanism which often helps a protein to regulate a functional behaviour such as for an enzyme to attain an active functional state upon ligand or substrate binding. In allostery, sometimes there are large conformational changes that require significant rotations and translations of individual domains at the timescales of microsecond to millisecond. While in some other cases, minimal structural perturbation helps in propagation of the signal in an energy efficient way to the functional domain where movement is mainly restricted to the side chains, loops and linker regions and which occur within picosecond to nanosecond timescales [1]. PDZ (post-synaptic density-95/discs large/zonula occludens-1) domains that are involved in myriads of protein-protein interactions [2,3] exhibit minimal structural changes during allosteric propagation. These domains have multiple ligand docking sites and are known to possess unique dynamics that regulate conformation of the functional site from a distal region.

HtrA2 (High temperature requirement protease A2), a PDZ bearing protein, is a mitochondrial trimeric pyramidal proapoptotic serine protease with complex domain architecture whose activity is likely regulated by interdomain crosstalk and structural plasticity [4]. Mature HtrA2 comprises 325 amino acids with residues S173, D95 and H65 forming the catalytic triad which is buried 25 Å above the base of the pyramid suggesting requirement of conformational changes for its activation. Apart from PDZ, this multidomain protein has a short N-terminal region, a serine protease domain and a non-conserved flexible linker at the PDZ-protease interface [4]. HtrA2 is involved in both caspase dependent as well as caspase independent apoptotic pathways [5,6,7]. Literature suggests it might have chaperoning functions as well and recently has been found to be associated with several neurodegenerative disorders [8,9,10]. Based on information from literature [4,11], this multitasking ability of HtrA2 can be attributed to its serine protease activity which is intricately coordinated by its unique substrate binding process, complex trimeric structure, interdomain networking and conformational plasticity. However, the unbound inactive form of the crystal structure with partially missing active site loops and flexible PDZ-protease linker has been unable to unambiguously determine the role of dynamics and allostery if any in HtrA2 activation and specificity. Therefore, to understand the molecular details of its mechanism of action, dynamics study at the substrate binding site and active site pocket becomes imperative.

HtrA2 belongs to a serine protease family that is conserved from prokaryotes to humans [12] where allostery is a common mechanism for protease activation in some of its homologs. DegS, a bacterial counterpart of HtrA2, allosterically stabilizes the active site pocket upon substrate binding at the distal PDZ domain [13]. DegP, the most extensively studied protein of the family, has a cage-like hexameric structure whose activation is regulated by allostery and oligomerization. Peptide binding to distal PDZ1

domain leads to rearrangement of the catalytic pocket into enzymatically competent form that readily oligomerizes and renders stability to the active conformation [14].

With an aim at understanding the conformational changes and structural plasticity that govern HtrA2 activity and specificity, we took an *in silico* approach to study the movements of flexible regions of the protein upon ligand binding. The PDZ domain of HtrA2 has a known hydrophobic substrate binding YIGV pocket (similar to GLGF motif) which is deeply embedded within the trimeric protein structure with P225 and V226 from the serine protease domain occupying the groove [4,15]. This structural arrangement makes it impossible for substrate protein to bind without significant conformational changes. Thus, to examine whether allosteric modulation through an alternative site is involved in substrate binding and catalysis of HtrA2, molecular dynamics simulation (MDS) approach with a bound peptide activator was used to look into the structural rearrangements that occur in nanosecond time scale. Although the information usually obtained from MDS is restricted primarily to movements in the accessible and flexible regions of a protein, it nonetheless contributes significantly towards understanding of the overall structural rearrangement and dynamics during its allosteric activation. In our study, we modelled the entire mature protease by filling in the missing regions using Prime 3.0 [16], followed by energy minimization with GRoningen MAchine for Chemical Simulation or GROMACS [17]. Identification of the putative binding site(s) on HtrA2 was done using SiteMap 2.5 [18] and the selective binding pocket (SBP) for the ligand was chosen based on optimum energy parameters. Peptides at SBP were docked from our peptide library that was generated based on available literature reports [19,20,21] and structural complementarities. MDS of the docked structures was done using Desmond 2010 [22] which provided critical information on loop and linker movements in HtrA2. These results combined with mutational and enzymology studies show that upon activator binding at the novel allosteric pocket, SBP, the linker at the PDZ-protease interface and loops L1, LA and LD around the catalytic groove undergo rearrangements in a coordinated manner so as to form an efficient active site pocket. Moreover, the PDZ domains mediate intersubunit interactions which stabilize the oxyanion hole. These observations highlight the importance of allostery which might be an important prerequisite for an active conformation of the trimeric protease.

Results

Identification of Selective Binding Pocket (SBP)

The high resolution crystal structure of HtrA2 [4] (Figure 1a) that lacked flexible loops, linkers and some N-terminal residues was the target protein for our studies. These regions were modelled and energy minimised as described under Methods section. Comparison of refined model with unrefined structure showed significant movements of the loops defining new binding sites on the protein surface. The linker at SPD-PDZ interface moved towards α7 of PDZ domain whereas the linker in the protease domain moved closer to the SPD-PDZ linker so as to form a groove (Figure 1b).

Among the five possible putative binding sites that were identified, Site2 or SBP (Figure 1c) that encompasses the groove generated by SPD-PDZ linker, protease and PDZ domains attained the best score (Table 1). The site score takes into account parameters such as volume, density, solvent exposure, hydrophilic and hydrophobic nature of residues and donor to acceptor ratio and hence is a comprehensive representation of the possibility of it being a binding site.

SBP has optimum volume and contacts available including maximum hydrogen donor and acceptor groups that are crucial for interacting with peptides. The size of the site is very important since the binding peptides have 6–7 residues and the site needs to be large enough to accommodate them. It also has highest hydrophobicity which makes it the best interaction site and hence used in our studies. Although sites 1 and 3 have scores closer to that of SBP, taking into account all the above-mentioned parameters, SBP was chosen for further docking and MDS studies.

Peptide Docking Show Similar Interacting Residues

Here, we have used a holistic approach in designing activator peptides where different techniques were applied in parallel so as to conduct a comprehensive search for a signature pattern that would dock at SBP. In one method, replicas for functional groups were chosen based on sequence and structural complementarities with hydrophobic SBP which were used for generating small molecular fragments. Scores obtained from docking these small molecules (Table S1) provided the framework for designing different combinations of tetrapeptides as shown in Table S2. With leads from literature and *in silico* structure-guided design, Gly and Val residues were added at N- and C-termini respectively of some peptides which subsequently increased the docking scores from −6 to −10 kcal/mol.

Similarly, two peptides previously reported in the literature as well peptides designed from the putative binding sites in pea-15 and Hax-1 also interacted well with SBP. Analysis of docking results with all these different peptides show interaction with similar residues of SBP as observed in ligplot (Figure S1). However, the control peptide KNNPNNAHQN, which has quite a few asparagine residues, is an ideal sequence to act as negative peptide for the pocket due to its stereochemical properties [19], did not bind to SBP demonstrating the specificity of designed peptides.

From the above extensive docking analysis, N216, S217, S219, E292 and E296 in SBP were found to be common for most of the peptide interactions (Figures 2a–b). Of these residues, N216, S217, S219 belong to the linker region while E292 and E296 to the PDZ domain that were either involved in hydrogen bond formation or Van der Waals interaction with the peptides. This result suggests that SBP might be the possible binding site and therefore a prospective putative allosteric site.

The role of some of these important residues in allostery if any and its subsequent effect on catalytic activity and substrate turnover was further probed by enzymology studies as described later in the text.

MDS Analyses of HtrA2 and HtrA2– Peptide Complexes

The peptides GSAWFSF was chosen for MDS studies as it gave the best XP and E-model scores (Table 2). GQYYFV has been reported to be a well known activator of HtrA2 [19] and hence used as another representative peptide for simulation studies. Moreover, the two peptides were chosen such that one is a designed peptide (GQYYFV) while the other is a part of a well-known HtrA2 binding protein Pea-15 (GSAWFSF). In addition to this, GQYYFV with docking score lesser than GSAWFSF was chosen for MDS analysis to understand whether different affinity for the substrate results in similar movements in the protease. MDS analyses of HtrA2-GQYYFV and HtrA2-GSAWFSF complexes demonstrated significant difference in conformation as well as dynamics when compared with unbound HtrA2. Visual inspection of the domain wise movements in peptide bound HtrA2 indicated large fluctuations in hinge/linker region (211–226) as shown in Figures 3a and b. Although these
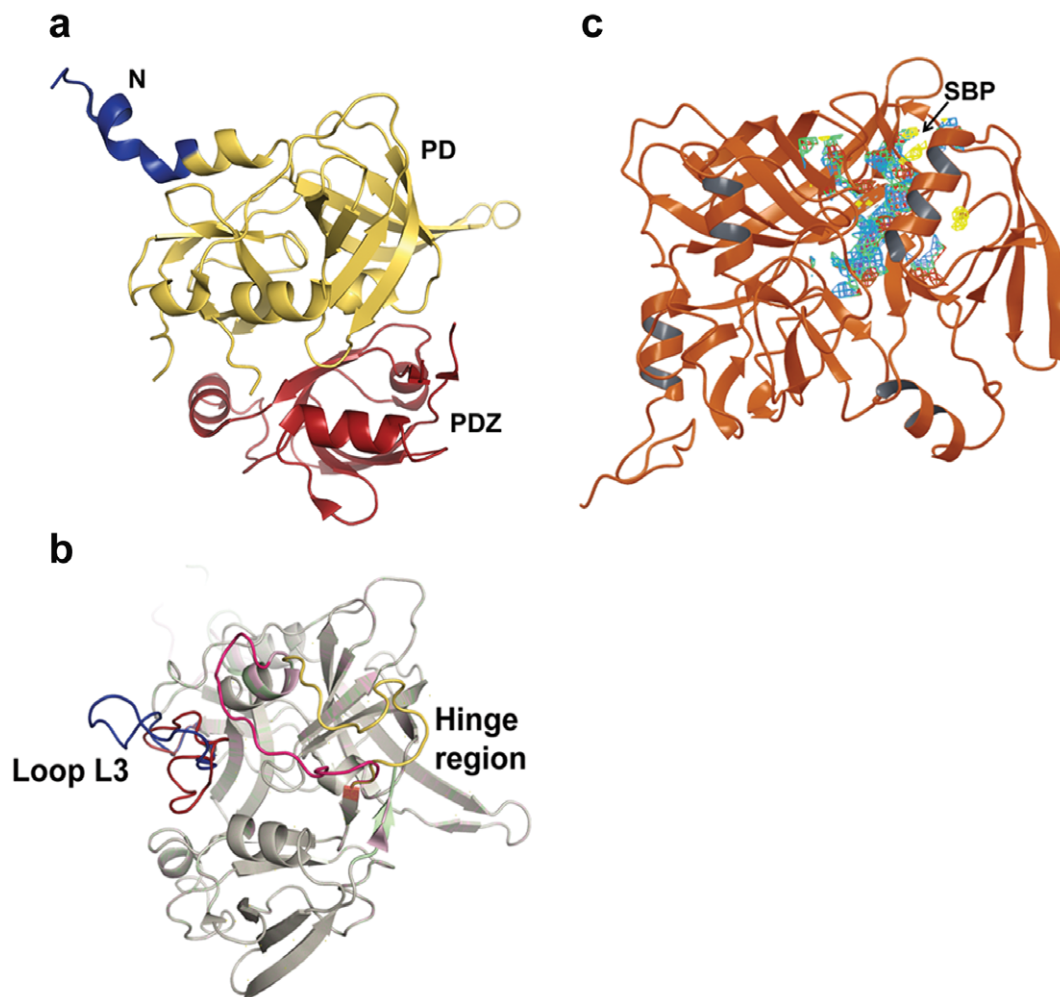
Figure 1. Ribbon model of HtrA2 structures (PDB ID: 1LCY). a. Domain organization of HtrA2 protease which comprises N-terminal region (blue), protease domain denoted as PD (yellow) and PDZ domain (red) at C-terminal end. b. Structural alignment of loop refined (light magenta) and unrefined (light green) structures of HtrA2 protein with modelled N-terminal AVPS, loop L3 (residues 142–162) and hinge region (residues 211–225) built with Prime (Schrödinger 2011). On refinement, loop L3 and hinge region are reorganized so as to define new regions at the protease and PDZ domain interface. c. Selective binding pocket (SBP) on HtrA2. The energy minimised structure of HtrA2 after modelling flexible regions in the protein is represented as a ribbon model. The binding site designated as SBP, selected on the basis of the Sitemap score and residue analyses, is located at the interface of PDZ and protease domain and shown as a multi-coloured mesh.
doi:10.1371/journal.pone.0055416.g001

movements were larger for GSAWFSF than GQYYFV bound complex, the movement pattern remained similar in these two peptides. Enhanced dynamic movement in the former complex could be attributed to the peptide length (heptameric as compared to hexameric in the latter). Domain wise RMSD analysis of these trajectories provided quantitative output of deviations with respect to time. The trajectory graphs (Figures 3c–e) show that along the entire sequence, hinge region $(211-226)$ has RMSD of 2.5 Å for

Table 1. Putative binding sites in HtrA2 identified by SiteMap tool.

Site Number from SiteMap	Residues present in the site	Site score
Site 2	K214, K215, N216,S217,S219, R226, R227, Y228, I229, G230,V231,M232,M233, L234, T235, L236, S237, S239, I240, E243, H256, K262, I264,Q289, N290, A291,E292, Y295,E 296, R299, S302	1.092716
Site 1	H65, D69, R71, A89, V90, P92, D95,T324	0.957142
Site 3	N48, H65, D169, S173,K191, M232, H261,L265	0.936056
Site 4	V192, F251	0.807891
Site 5	I33,L34,D35,R36,V73,R74	0.673032

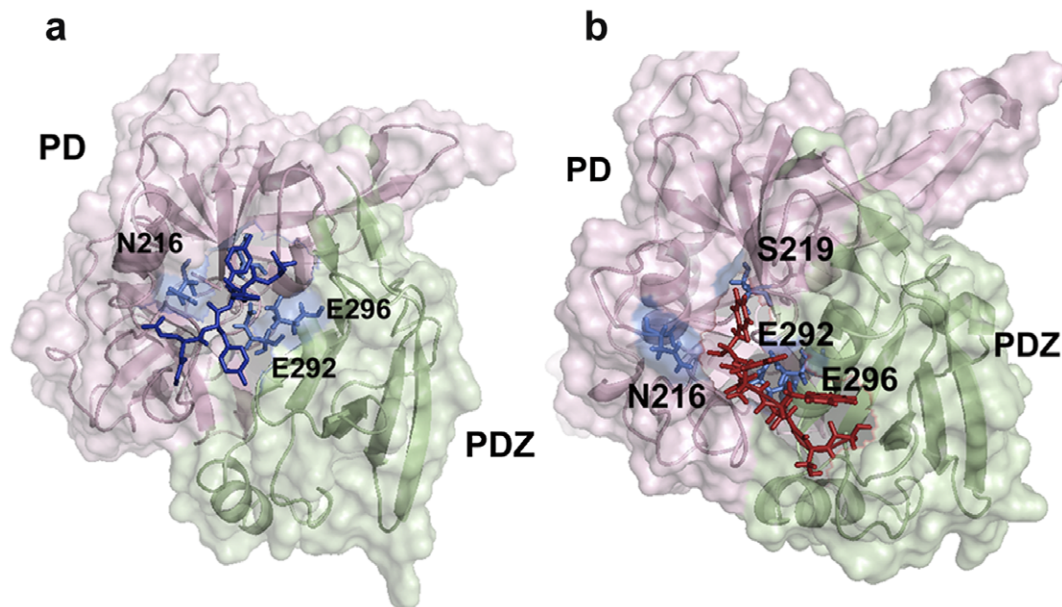doi:10.1371/journal.pone.0055416.t001

Figure 2. Representative surface structures of peptide activator docked HtrA2. a. Peptide GSAWFSF -HtrA2 complex and b. Peptide GQYYFV-HtrA2 complex. The former peptide represents putative SBP binding peptide in Pea-15 and the latter is a peptide obtained from the literature. The common interacting residues from SBP for both the peptides are labelled and are shown as blue sticks. PD denotes serine protease domain in both the Figures.
doi:10.1371/journal.pone.0055416.g002

the peptide GSAWFSF and 1.5 Å for GQYYFV from the starting unbound form.

The RMSF of these trajectories were comparable with rmsd values showing higher relative fluctuations in and around the hinge region. Representative RMSF plots for GQYYFV and GSAWFSF bound HtrA2 complexes depict these large fluctuations for residues 190–225 as shown in Figures 4b and C respectively. All structural alignment comparisons and relative fluctuation analyses post MDS emphasize distinct significant conformational change in the hinge (211–226) region upon peptide binding. In addition to this, binding of peptides led to dynamic movements in many functionally important regions distal to SBP such as helices α5 and α7 in PDZ domain.

Conformational Transitions in Flexible Regions and at the Active Site

Further detailed analyses of the effect that local subtle structural changes at SBP had on distal regions of the protease especially at the active site and its vicinity revealed the possibility of SBP being a putative allosteric site. Functional active site formation and its accessibility along with a well formed oxyanion hole are important prerequisites for the activity of an enzyme.

Structural comparison of the MD simulated peptide bound structure of HtrA2 with the unbound form show movements in different domains and linker regions. The PDZ-protease linker that covers the peptide binding groove in the PDZ domain moves away from it thus increasing it accessibility. The peptide bound HtrA2 complex show relative movements in the active site triad residues compared to the unbound form. Atomic distance analysis of both the forms revealed that distances between nitrogen (ε) atom of H65 and oxygen (γ) atom of S173 increased in peptide bound complexes while that between nitrogen (δ) atom of H65 and oxygen (δ) of D95 decreased when compared with the unbound HtrA2 structure (Table 3). This pattern being consistent with both

the peptides suggests that interaction of peptide activator with SBP leads to opening up of the active site cleft.

Apart from active site triad, changes were also observed in the orientation of mechanistically important L1, LD and LA loops in the peptide bound complex (Figures 4d–e). Their orientations with respect to the active site determine proper oxyanion hole formation, accessibility of the active site, formation of catalytic triad and hence enzyme activity. MDS analyses for these regions showed significant deviations upon peptide binding. Structural alignment of GSAWFSF bound HtrA2 complex with the unbound form demonstrated breaking of Van der Waals contacts between loop LD and β2 strand of protease domain which facilitates LD movement towards α1 of protease domain and bringing P130 of the former in proximity to A25 of the latter. Similarly, S50 in β2 of protease domain establishes interactions with G171 of L1 (oxyanion hole residue) while breaking contacts with A132 of LD loop due to movement or tilt in the L1 loop. As a result of this reorganization, LD which was closer to L1 in the unbound HtrA2 moves sharply away from it upon peptide binding. These positional rearrangements also lead to disruption of interaction between D165 of L1 and G195 of L2 loops. All these movements coordinate to bring LD closer to the proximal region of protease domain thereby opening up the catalytic site. For GQYYFV peptide, movements of all these loops were subtle as compared to that for GSAWFSF except for the LA loop which exhibited larger deviation in the former. The other significant flexible region movement is in loop L3 which, in concert with linker region, assists in accommodating the peptide at SBP.

The relative reorientation of these loops along with catalytic triad residues seems to be assisting formation of a more open structure near the active site. However, loop L2 that harbors the specificity pocket remains mostly unchanged suggesting presence of a well formed binding pocket in the unbound form whose accessibility is limited compared to the substrate bound form. In context with trimeric HtrA2, more open conformation might be

Table 2. Peptide docking of HtrA2 and identification of interacting residues.

Peptides Used in Our study	Interacting Residues		Glide score in Kcal.mole^{-1}
	H bond Interactions	**Vdw Interactions**	
PEA 15 (GSAWFSF)	Glu 292, Glu 296, Asp 293, Ile 283, Met 287	Gln 286, Ala 297, Ser 222	−10.564
Designed (VKSDSG)	Asn 216, Leu 152, Glu 296, Glu 292	Ala 89, Ile 221, ser 218,	−10.394
Designed (GRTDSV)	Glu 296, Glu 292, Asn 216, Ser 217	Asp 293	−10.037
Designed (GRDTSV)	Ser 219, Glu 292	Ser 239, Gln 286	−9.57
Designed (GRDTYV)	Asp 293, Asn 216, Ser 217, Ser 219	Glu 296, Arg 299,	−9.54
Phosphatase (PAEWTRY)	Asp 117, Ala 149, Arg 150, Lys 215, Gln 146	Pro 148, Leu 152, Lys 214, Gln 156, Val 159, Ser 239	−9.481
HAX-1 (TKPDIGV)	Glu 292, Glu 296, Ser 219, Ile 221, Arg 299	Asn 216, Ser 222	−8.486
Connexin (ARKSEWV)	Asp 293/426, Asn 290/423, Gln 156/289	Glu 292, Pro 155, Gln 289, Met 287, His 256, Glu 255, pro 238	−8.165
Presenilin (AFHQFYI)	Leu 152, Asn 216, Ser 217, Glu 292, Glu 296	Pro 155, Arg 211, ser 218, Ser 219	−8.063
IL-EBF (AGYTGFV)	Asn 216, Ser 217, Glu 292, Arg 150/, Leu 152	Ser 219, Gly 153, pro 155	−7.903
Yes Protein (ESFLTWL)	Asn 216, Leu 152, Glu 296, Asp 293, Gln 289, Ser 237	Gln 156, Pro 238, Pro 155, Ser 218, Glu 292, Gln 286	−7.722
Cathepsin SVSSIFV	Glu 296, Asn 216, Ile 283/416,	Glu 292, Leu 152, Gly 153, Ala 297	−7.524
Warts Protein Kinase (NRDLVYV)	Lys 214, Lys215, Ala 149, Glu 207, Arg150, Gln 146	Leu 152, Gln 156, Val 159	−7.321
GQYYFV[6]	Glu 292, Glu 296, Asn 216, Ile 221, Leu 152	Ser 219, Gly 153, Arg 299	−7.163
GGIRRV[6]	Glu 292, Glu 296, Asn 216, Ser 217, Ser 219	Arg 211, Gly 153	−6.785
Tuberin (EDFTEFV)	Arg 211, Asn 216, Ser 219	Ala 89, Ile 221, ser 218, Arg 299, Glu 296, Glu 292, Gly 153	−1.883
Control Peptide (KNNPNNAHQN)		**Did not dock with HtrA2**	

The possible residues which are involved in hydrogen bonding and Vander Waal's interactions along with Glide scores are mentioned.
doi:10.1371/journal.pone.0055416.t002

significant as it enhances the accessibility of the substrate and thereby might contribute positively toward the rate of enzyme catalysis.

Influence of SBP on HtrA2 Activity and Role of PDZ Domain

To determine whether critical SBP residues (N216, S219, E292 and E296) are important for mediating allosteric propagation in HtrA2, site directed mutagenesis to alanine were done. Mutation of a conserved YIGV residue (G230A) was also done to understand the role of canonical YIGV groove in this complex signal propagation pathway. Moreover, since the protein is found to be active in its trimeric form [4] and also that SBP encompasses a major part of PDZ, we used trimeric and monomeric HtrA2 variants, N-SPD and F16D respectively to understand the role of PDZ in intra and inter-molecular cross-talk.

To negate the role of overall conformational changes if any due to these mutations, MDS and secondary structural analyses were done on the mutant proteins. Similar active site conformations were observed in both the wildtype and mutants. Moreover, the overall secondary structure and thermal stability remained unperturbed due to the mutations (data not shown). Enzymology studies with different SBP mutants were done using β-casein, a well-established generic substrate of serine proteases [23]. β-casein has a putative SBP binding site (GPFPIIV) which has been found to interact with the similar residues at SBP by our docking studies (Table 2) and hence expected to mimic the allosteric modulation mediated by SBP binding if any. The kinetic

parameters for wild type, N-SPD domain, F16D and other mutants were determined using fluorescent β-casein (Figure 5). The catalytic efficiency (k_{cat}/K_m) for the double mutant N216A/S219A and single mutant E292A showed ∼2.4 fold decrease in enzyme activity as compared to wild type whereas enzymatic parameters remained mostly unchanged for E296A. K_m values for the mutants were not significantly higher compared to the wild type, suggesting that the specificity pocket might be mostly intact with some subtle alterations. However, there was a marked decrease in V_{max} and in substrate turnover (k_{cat}) rates for N216A/S219A and E292A suggesting presence of a malformed oxyanion hole in the SBP mutants. These results demonstrate that N216/S219 and E292 of SBP are important for mediating allosteric activation of HtrA2 upon activator binding. This is strengthened by the observation that SBP mutants did not interact with the activating peptides as seen by isothermal calorimetric studies and a representative figure is shown in the supplementary material (Figure S3). In addition, the ligplot of the peptide showing the detailed interaction with HtrA2 is also depicted in figure S1.

In our in silico studies, YIGV has been found to be a part of the greater SBP mesh (Table 1) and since docking with small molecular fragments (∼35–100 Da) showed direct binding with YIGV residues (Table S1), we wanted to understand the effect of YIGV mutation on HtrA2 activity as well. Enzymology studies with G230A demonstrated increase in K_m value compared to the wild type highlighting the involvement of YIGV in this intricate allosteric mechanism. Protein turnover rate was also much lower in G230A as compared to the wild type reiterating the importance of oxyanion hole formation upon activator binding at SBP. Thus,
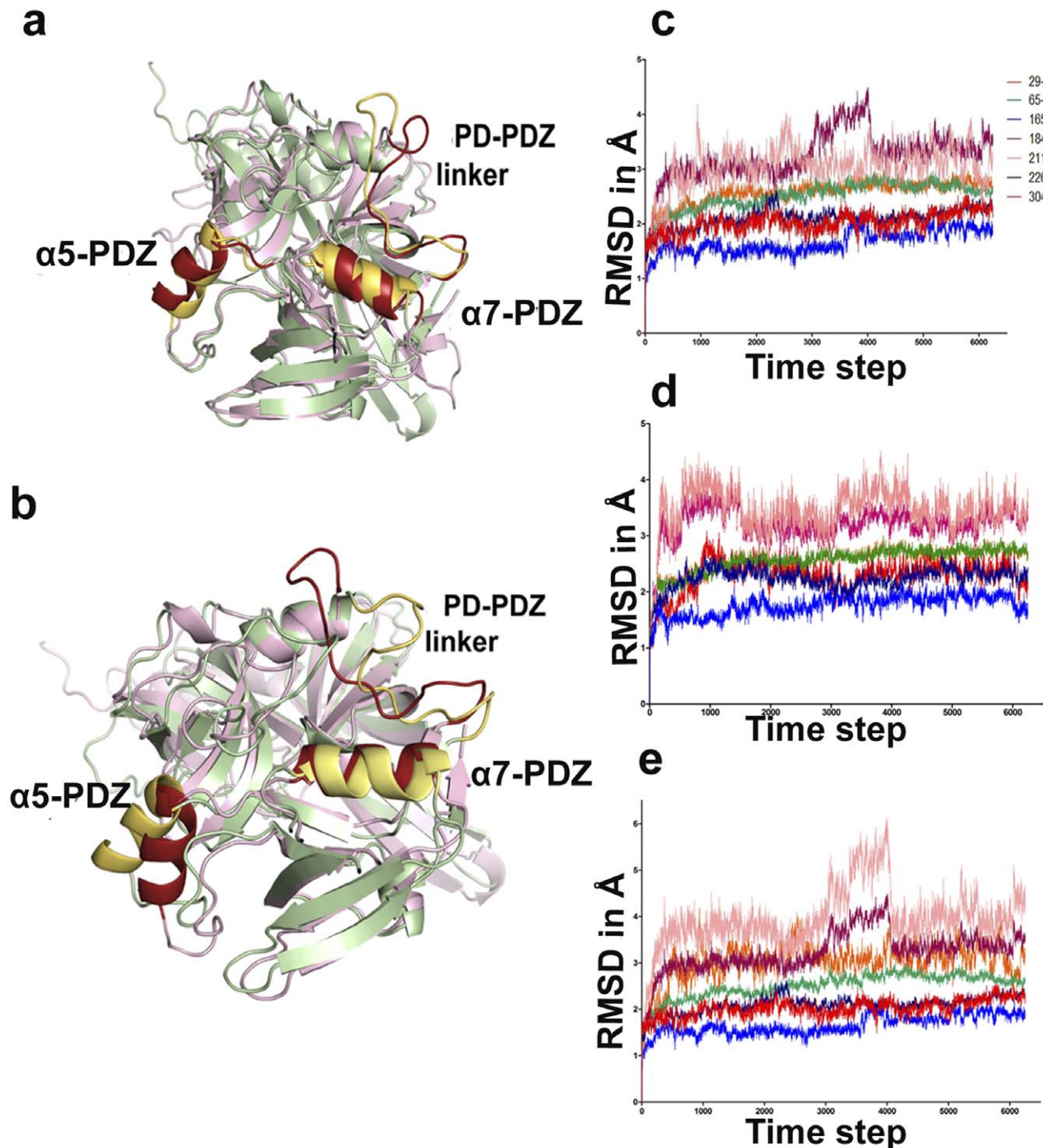
Figure 3. Domain wise conformational changes induced on peptide binding at SBP. a. The structural alignment of minimum energy structure of the peptide bound GQYYFV-HtrA2 complex (light pink) and unbound structure (green) displays orientation of the movement of the hinge region and the α-helices of PDZ. b. The structural alignment of GSAWFSF-HtrA2 complex (light pink) and unbound structure (green). Graphical representations of the RMSD for the 30 ns MDS trajectory of the following: c. HtrA2–GQYYFV complex. d. unbound HtrA2 (negative control). e. HtrA2–GSAWFSF complex. The stretch of residues selected for each set of RMSD calculations are shown on the right of panel c.
doi:10.1371/journal.pone.0055416.g003

inaccessibility of the canonical PDZ binding pocket YIGV, in the trimeric protease structure might have adjured presence of exposed SBP which is dynamically coupled to YIGV groove for efficient allosteric signal propagation to the distal active site. Direct binding of small molecules at YIGV supports this hypothesis as they could be accommodated in the classical binding groove

without requirement of any initial conformational change as it might be with the larger peptide activators.

Interestingly, although catalytic efficiency for N-SPD has been found to be 3.4 fold less as compared to the wildtype, its K_m value suggests slight increase in substrate affinity for the enzyme (Table 4). This increase in substrate affinity might be due to
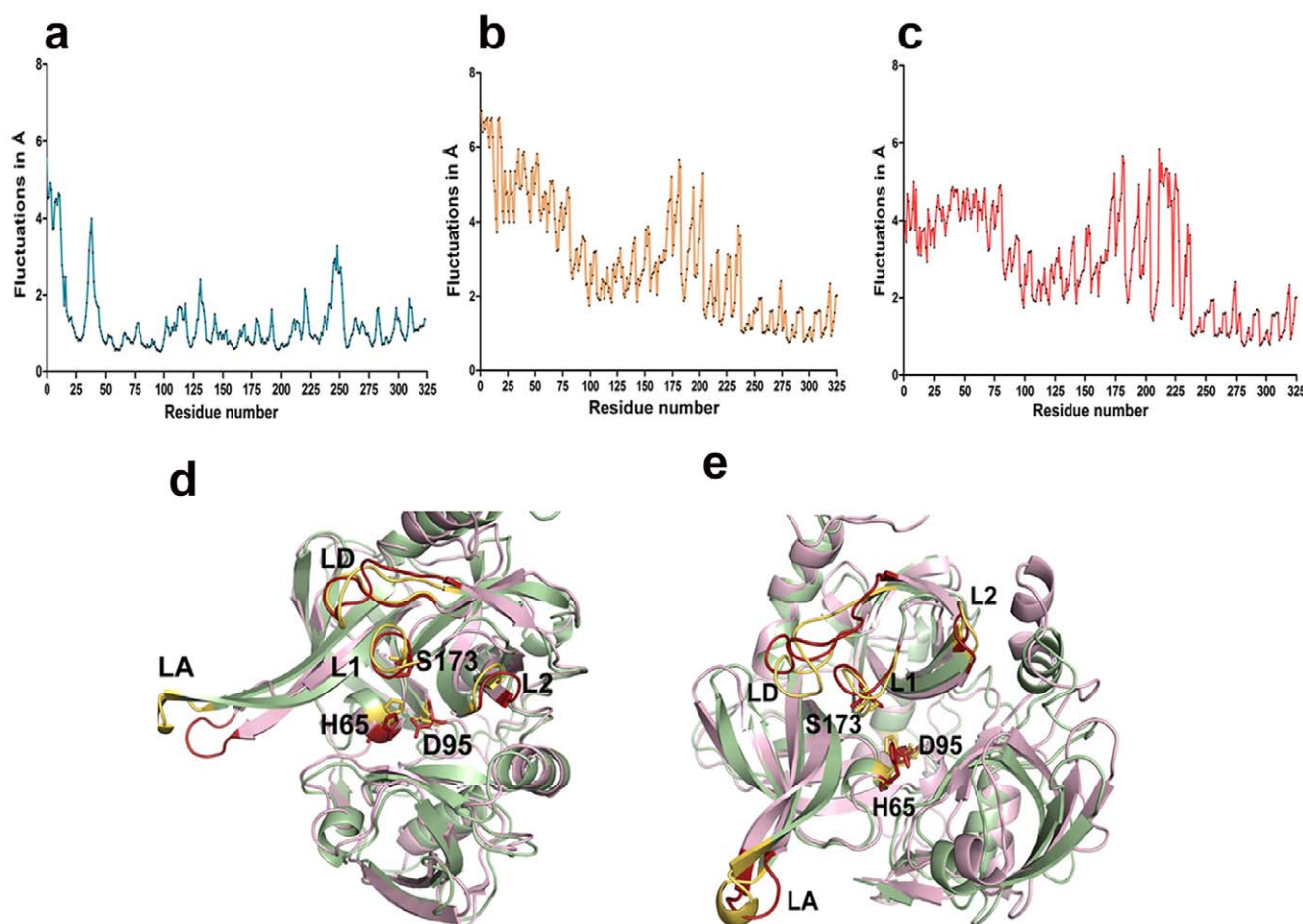
Figure 4. Graphical representation of root mean square fluctuation (RMSF) and loop movements upon peptide binding. a. MD simulation trajectory for unbound HtrA2. b. RMSF graph for GQYYFV bound HtrA2. c. RMSF graph for GSAWFSF bound HtrA2. d. Comparison of fluctuations in loops LA, L1, L2 and LD in the GQYYFV peptide bound (pink) and unbound structure (green). The loops in the bound and unbound forms are displayed in red and yellow respectively. e. Comparison of fluctuations in loops LA, L1, L2 and LD in the GSAWFSF peptide bound (pink) and unbound structure (green). The loops in the bound and unbound forms are displayed in red and yellow respectively. The catalytic triad residues are shown in both panels d. and e.
doi:10.1371/journal.pone.0055416.g004

absence of PDZ surrounding the active site region resulting in greater substrate accessibility. However in N-SPD, k_{cat} was found to be 5 fold less than that of wild type highlighting the role of PDZ in initiating conformational changes near the active site pocket as well as in the oxyanion hole so as to increase overall enzyme stability. However, in the full length monomeric mutant of HtrA2 (F16D), there is a two fold increase in K_m with significant decrease in turnover rate and hence catalytic efficiency (Table 4) which

Table 3. Comparison of distances between atoms of the catalytic triad in the peptide bound and unbound forms of HtrA2.

Protein Complex	NE2 (His) – OG (Ser)		ND1 (His) – OD1(Asp)	
	Bound	**Unbound**	**Bound**	**Unbound**
HtrA2 (GSAWFSF)	5.2	4.1	2.6	2.9
HtrA2 (GQYYFV)	5.5	4.1	2.7	2.9

doi:10.1371/journal.pone.0055416.t003

emphasizes importance of intermolecular crosstalk between PDZ and protease domains in trimeric HtrA2 structure.

The importance of intermolecular interaction between PDZ* and SPD has also been manifested in our MD studies where structural analyses show binding of peptide activator (GQYYFV) at the SBP alters PDZ orientation and brings α5 helix of PDZ from one subunit in close proximity to the protease domain of the adjacent subunit. The helix moves towards LD loop of the protease domain, thereby shifting the orientation of the phenyl ring of F170 which is a part of oxyanion hole towards H65 of the catalytic triad (Figure 6a) so as to accommodate the loop. These rearrangements result in a more stable and catalytically competent HtrA2 formation with a proper oxyanion hole. Thus the full length trimeric HtrA2 is more active than trimeric N-SPD, where the activation pocket is not stable in absence of PDZ.

Discussion

Our aim was to understand the structural dynamics that regulates activation and specificity of HtrA2. This multidomain trimeric protease has unique proapoptotic properties as it is associated with both caspase-dependent and independent cell
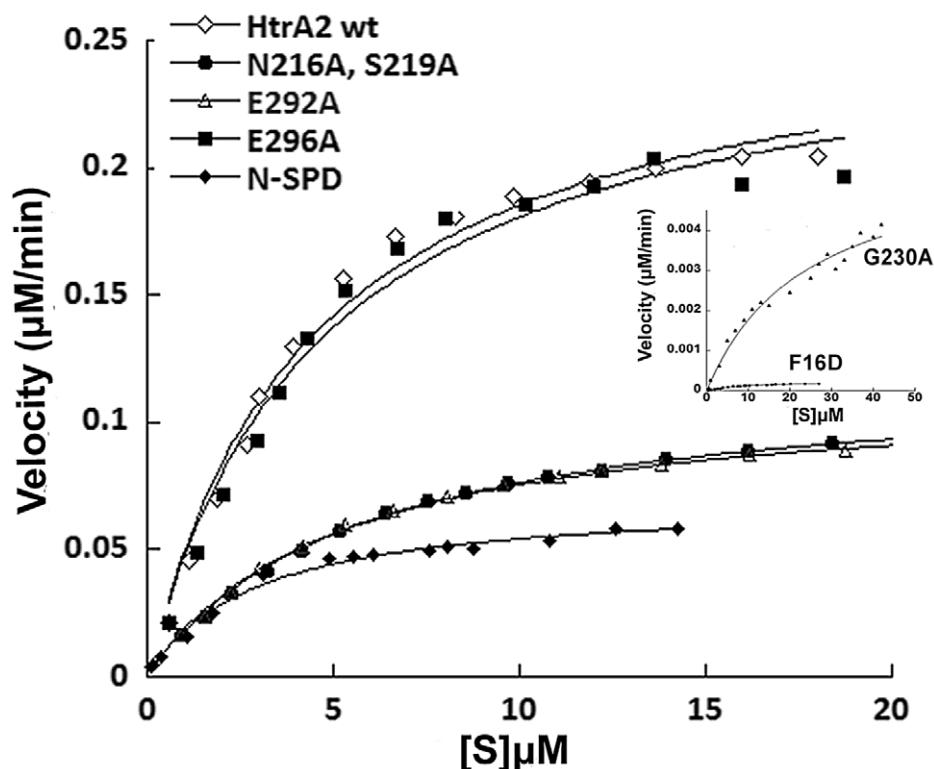
Figure 5. Steady state kinetic parameters of HtrA2. Graph representing relative activity of wild type HtrA2 and its mutants and variants with FITC labelled β-casein as the substrate. The graph for two mutants (F16D and G230A) is shown in inset.
doi:10.1371/journal.pone.0055416.g005

death pathways through its serine protease activity [5,12]. Association of HtrA2 with cancer and neurodegenerative disorders makes it a promising therapeutic target. For example, over-expression of HtrA2 substrates such as IAPs and the Wilms's tumor suppressor protein WT1 in several cancers suggests modulation of HtrA2 protease activity can effectively regulate their relative levels in the cells [24,25,26,27]. Out of several approaches that can be used to regulate HtrA2 activity, allosteric modulation is one of the simplest and most efficient ways. However, modulating HtrA2 functions with desired characteristics for disease intervention will require a detailed understanding of its mode of activation and the underlying conformational plasticity that controls it.

Table 4. Steady state kinetic parameters for HtrA2 wild type, variants and mutants with β-casein as the substrate.

HtrA2 Proteins	K_m (μM)	V_{max} (M/s)	k_{cat} (1/s)	k_{cat}/K_m (1/M.s)
Wild type	4.59	4.083×10^{-9}	0.02041	4.452×10^3
N216A, S219A	5.43	1.937×10^{-9}	0.00968	1.788×10^3
E292A	5.15	1.903×10^{-9}	0.00951	1.849×10^3
E296A	4.68	3.734×10^{-9}	0.01868	3.995×10^3
N-SPD	3.02	0.7851×10^{-9}	0.0039	1.29×10^3
F16D	9.3	4.08×10^{-12}	0.000025	0.0026×10^3
G230A	9.32	1.03×10^{-9}	0.0051	0.54×10^3

doi:10.1371/journal.pone.0055416.t004

Peptide design using site complementarity followed by MDS of the docked peptide-macromolecular complex is an extremely useful tool to study subtle conformational changes and protein dynamics. HtrA2 has a complex network of flexible loops surrounding the active site pocket and a linker at the PDZ-protease interface whose relative orientations and crosstalk with different domains might be critical in defining HtrA2 functions. With partially missing loops and the flexible linker region, the solved structure of HtrA2 [4] could not fully explain the dynamics and allostery that regulate its activity and specificity. Here, with an *in silico* and biochemical approach, we have shown that like few other HtrA family proteins, allosteric propagation does regulate HtrA2 activity.

In this study, peptide binding to SBP showed conformational changes in the distal flexible regions of HtrA2 such as the PDZ-protease interface, loops L1, LD and LA that rearrange to form a more catalytically efficient active site thus establishing the role of SBP as an allosteric site in HtrA2. A close look at and around the active site pocket shows that in the bound form, the N atom of Gly (−2 position) faces the oxyanion hole to form an H-bond whereas in the unbound form it flips in the opposite direction to form a malformed oxyanion hole [12,28]. Moreover, keeping in trend with other HtrA proteases, the phenylalanine ring of −3 position moves closer to the imidazole ring of His65 while in the unbound form, it moves outward as observed from Figures 6b–c and Movie S1. All these subtle structural rearrangements along with making and breaking of bonds at sites away from the active site might stabilize the peptide bound form such that it shifts the equilibrium toward catalysis.

Enzymology studies with β-casein that has a putative SBP binding sequence (GPFPIIV) as shown in Table 4 show significant
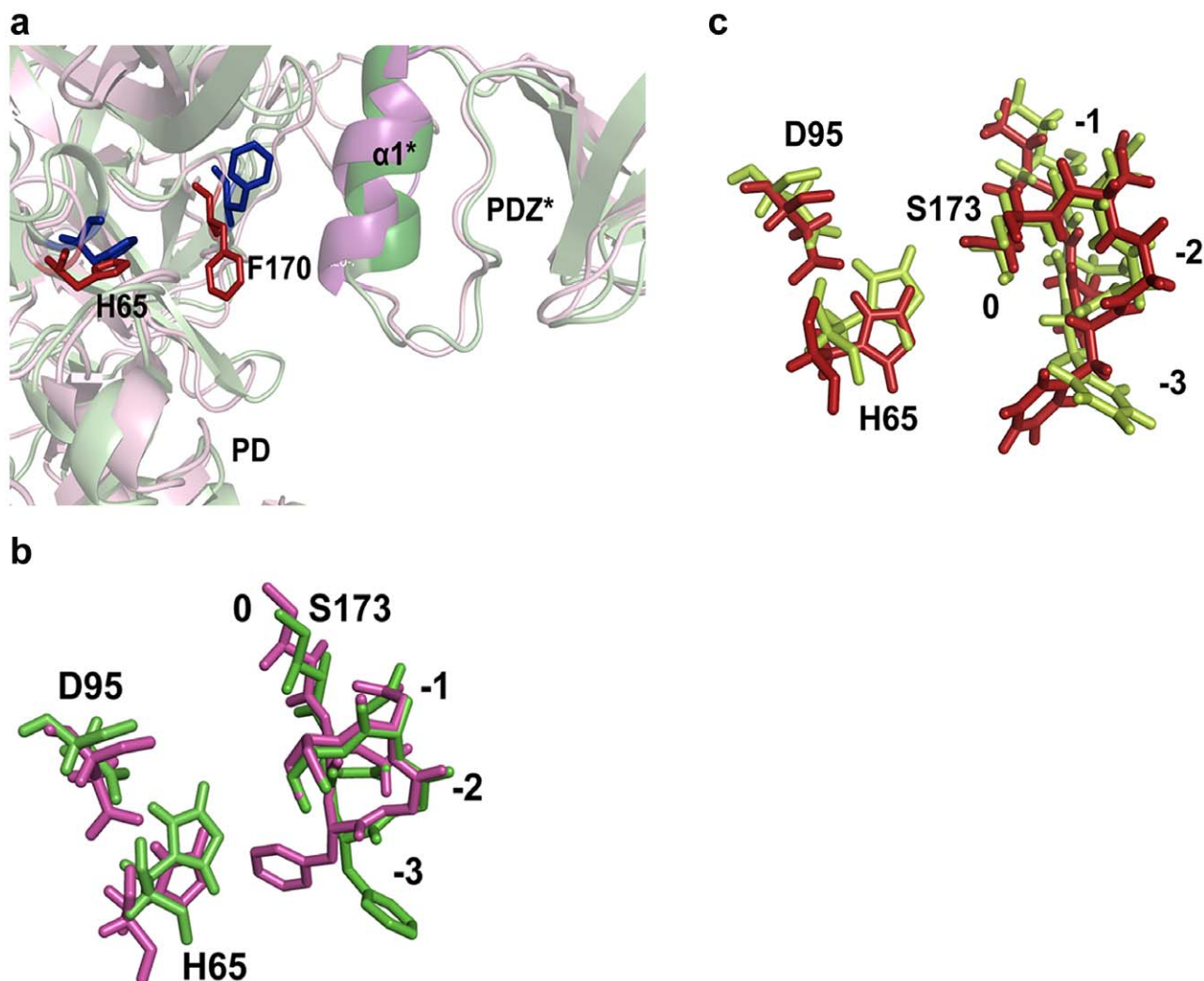
Figure 6. Structural changes at the oxyanion hole and YIGV groove upon peptide binding. a. Overlay of the oxyanion hole and catalytic triad residues represented as sticks for peptide GQYYFV bound (magenta) and unbound (green) structures. PD denotes serine protease domain of HtrA2. b. Overlay of the oxyanion hole and catalytic triad residues represented as sticks for peptide GSAWFSF bound (red) and unbound (limon green) structures. c. Role of PDZ in the formation of proper active site formation. The structural superposition of GQYYFV bound (pink) and unbound (green) structures shows α5 helix of PDZ of one subunit moves towards the LD loop and oxyanion hole of the adjacent subunit. The positions of the residues in the oxyanion hole are denoted as 0, −1, −2 and −3.
doi:10.1371/journal.pone.0055416.g006

decrease in catalytic efficiency in SBP mutants. This observation suggests interaction of substrate protein with SBP brings about rearrangement around the active site of the enzyme by positively influencing its activity thus behaving as an allosteric regulator. The SBP mutants (N216A/S219A and E292A) show apparent decrease in V_{max} without significantly altering the apparent K_m (with L2 specificity pocket mostly unaltered) and hence follow the 'V system' of allosteric modulation [29]. In this system, both the relaxed (R) and the tensed (T) states bind the substrate at the active site with similar affinity while the peptide (activator) at SBP binds the R and T states with different affinity. This differential affinity of the peptide towards SBP along with R state stabilization shifts the equilibrium towards R state thus positively influencing its turnover rate and hence catalytic efficiency which has been observed in case of HtrA2.

In N-SPD, where the PDZ domain is absent, apparent decrease in K_m can be attributed to greater accessibility of the substrate to the active site. However, since the change in binding affinity is not

large, the specificity pocket might be mostly unaltered compared to the wild type which is confirmed through our MD studies where the loop L2 remains mostly unaltered. Interestingly, k_{cat} value in N-SPD has been found to decrease significantly which is suggestive of either a malformed oxyanion hole and/or decrease in overall protein stability which might be due to absence of supporting PDZ domain. However, similar studies with F16D (monomeric full length HtrA2 mutant) also show significant decrease in turnover rate and catalytic efficiency which accentuates the importance of intermolecular and not intramolecular PDZ-protease crosstalk in trimeric HtrA2. Our MDS supports this observation by demonstrating that in the peptide bound form of HtrA2, α5* of PDZ* moves towards LD loop of protease domain of adjacent subunit thus pushing phenyl ring of F170 of the oxyanion hole towards H65 of the catalytic triad (Figure 6a). This reorientation in the oxyanion hole makes the protease poised for catalysis as seen in other HtrA family members as well [12] thus significantly enhancing the turnover rate. Therefore, intermolecular crosstalk

stabilizes the active site and makes it catalytically competent establishing the requirement of complex trimeric architecture of the protease.

The GLGF motif (YIGV in HtrA2) is the canonical peptide binding site [2,4] in PDZ domains. However, in HtrA2, it is deeply embedded within a hydrophobic groove where the residues are intertwined with each other through several intramolecular interactions making the site highly inaccessible to the binding of peptide [4]. Thus, peptide binding to YIGV is only possible upon certain structural rearrangements at that site. Given the property of PDZ domains of having multiple docking sites and the fact that HtrA2 requires huge conformational changes for proper active site formation, we hypothesized presence of a relatively exposed pocket where peptide binding occurs prior to interaction with the buried YIGV groove. In our studies, we have found a novel surface exposed region (SBP) around PDZ domain which is easily accessible to the peptide. With an aim at understanding the allosteric mechanism in HtrA2 and whether the binding site is structurally conserved, we did a side-by-side comparison with the peptide-bound PDZ structure of its bacterial counterpart DegS that is known to exhibit allostery [30]. The structural overlay of peptide bound forms of these two proteins show striking structural similarity in the regions of binding (Figure 7a) with the GLGF groove (YIGV in HtrA2 and YIGI in DegS) oriented differently. Since the YIGV motif is buried in HtrA2 structure, its inaccessibility might be the reason for the peptide to initially bind to another relatively accessible region with similar hydrophobic milieu. However, in DegS, the YIGI groove is already exposed to accommodate the peptide easily and hence this kind of initial interaction is not required.

Our MDS studies show that peptide binding at SBP leads to subtle structural changes in the region adjoining YIGV leading to opening up of the pocket. The last β strand of PDZ domain which lies on one side of YIGV groove moves away from it. The YIGV and the loop spanning residues 67–73 move away from each other while the loop comprising residues 263–277 of the β-α-β motif also drifts at an angle away from the YIGV making it more solvent exposed (Figure 7b). Therefore, upon SBP binding, the relative movements of the loops in vicinity of the hydrophobic YIGV pocket might confer it with the kind of exposure that is required for interaction with peptides. These observations along with our enzymology studies with SBP and YIGV mutants, led to defining a model (Figure 8) for allosteric propagation in HtrA2. The model suggests that initial binding of the peptide activator at SBP leads to structural fluctuations which result in subtle rearrangement at and around the YIGV groove (a part of greater SBP mesh as identified by Sitemap) thus exposing it. Opening up of the deeply embedded YIGV pocket makes it accessible to the substrate molecule which consequently leads to allosteric signal propagation at the active site in the serine protease domain.

This alternative non-canonical PDZ binding site though novel in HtrA family of proteins, is not unprecedented in literature. It has been observed that PDZ7 of the scaffold protein Glutamate receptor interacting protein 1 (GRIP1) has an alternative exposed hydrophobic pocket that binds its substrate GRASP-1 since the canonical binding site is deeply embedded within the protein [31]. Overlay of the PDZ from HtrA2 and PDZ7 of GRIP1 show striking structural similarity including the classical peptide binding groove and the novel non-canonical pocket (Figure S2). Thus, in these two proteins, perturbations at the alternative distal binding sites might be coupled dynamically to the classical binding groove by a complex mechanism that includes fast (ps–ns) timescale dynamics which consequently leads to allosteric signal propagation to the active site.

In the recent past, allosteric modulators have evolved into important drug targets due to several advantages they have over
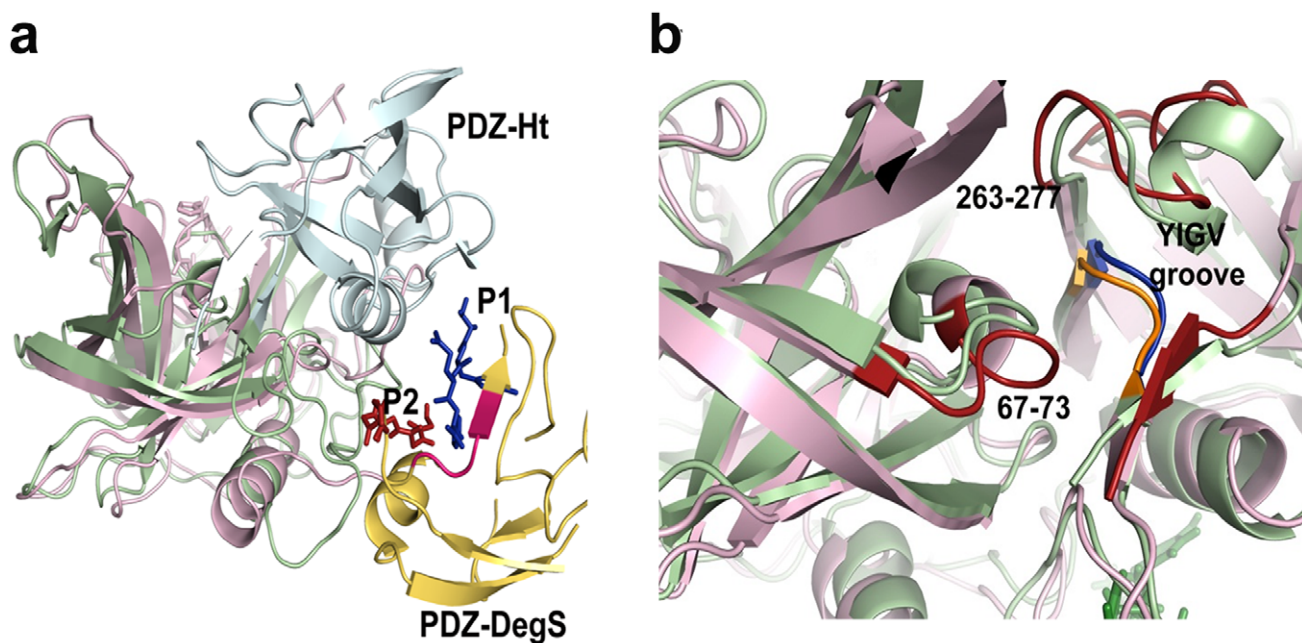

Figure 7. Structural comparison of PDZ domain orientation. a. Structural alignment of *E.coli* DegS (PDB ID: 1SOZ) and the peptide bound HtrA2 showing PDZ domains for both the proteins (represented in blue and yellow respectively) are oriented differently but the peptides, P1 (blue) and P2 (pink) represented as sticks for the respective proteins seem to bind to a structurally similar region. The GLGF substrate binding motif is exposed for DegS while buried for HtrA2 as shown in pink and blue respectively. b. Alignment of the peptide bound (pink) and unbound (green) structures at the region around the YIGV groove shows outward movement of the loops spanning residues 67–73 and 263–277 shown in red for the bound structures which leads to opening up of the YIGV groove.
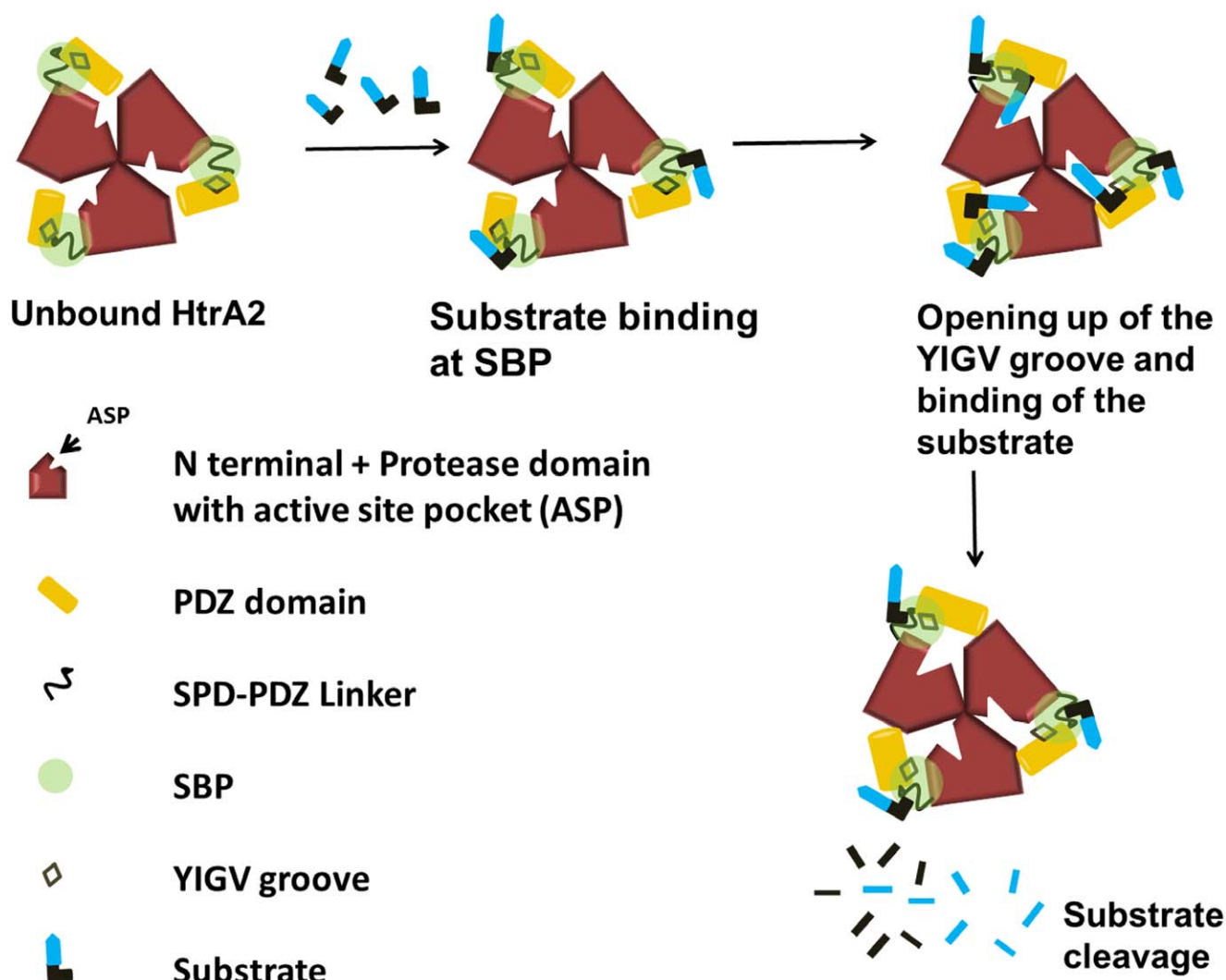doi:10.1371/journal.pone.0055416.g007

Figure 8. Allosteric model for HtrA2 protease activity. The substrate protein binds to relatively exposed part of SBP due to inaccessibility of the YIGV groove which triggers opening up of the PDZ domain. This reorientation makes the YIGV groove accessible for substrate interaction and the PDZ of a subunit moves closer to the protease domain of the adjacent subunit leading to formation of a proper active site and oxyanion hole. This complex allosteric signal propagation leads to subsequent substrate binding and catalysis at the active site pocket. Thus structural perturbations at these two distant sites (SBP and catalytic pocket) might be dynamically coupled to the canonical peptide binding groove through a complex allosteric mechanism.
doi:10.1371/journal.pone.0055416.g008

orthosteric ligands that include more diversity, less toxicity and absolute subtype selectivity [32,33]. Therefore, designing suitable SBP binding peptides or peptidomimetics of HtrA2 might be an excellent approach to modulate HtrA2 functions for devising therapeutic strategies against various diseases it is associated with.

Materials and Methods

Loop Modeling and Site Prediction

Crystal structure of HtrA2 (PDB ID: 1LCY) [4] obtained from Protein Data Bank [34] has missing N-terminal residues (AVPSP) and two flexible regions ([211]RGEKKNSSSGISGSQ [225] and [149]ARDLGLPQT [157]). These missing structures were modelled and loops were refined using Prime 3.0 (Schrödinger, LLC, New York, 2011). which was later subjected to molecular dynamics simulation for 5 ns with GROMACS, version 4.5.1 [17] to obtain the lowest energy structure of HtrA2. The binding sites were then predicted using SiteMap 2.5 (Schrödinger, LLC, New York, 2011).

Out of 5 pockets predicted, the site that scored the best based on its size, hydrophobic and hydrophilic characters, degree to which ligand might donate or accept hydrogen bonds and exposure to solvent was selected for further analysis. This site selective binding pocket (SBP) encompasses PDZ-protease interface with the involvement of hinge region and a part of PDZ domain (Table 1).

Peptide Designing and Molecular Docking

Based on properties of amino acids lining the binding site, fragment docking (Glide XP, Schrödinger, LLC, New York, 2011) [35] approach was used to dock 20 amino acids and 8 functional group replicas (N-methylacetamide, methanol, phenol, benzene, propane, acetate ion, methylammonium, methylguanidinium) at SBP [36]. Based on properties of the amino acids that form SBP, replicas were chosen and were used for generating fragments in combinations of four as shown in Table S1. Combine Fragment tool (Schrödinger, LLC, New York, 2011) was used to join the

fragments which were docked at SBP with three major filtering options (bond angle deviation 5 degrees, atom-atom distance 1 Å and fragment centroid distance 2.0). The set of replica functional groups that displayed the best docking scores were used to build the peptide. The amino acids Arg, Ser, Gln, Glu, Asp, Asn, Thr, Lys and their positions in tetrapeptide combination were chosen based on the functional groups they resembled. Subsequently all possible peptide combination of these amino acids with respect to their relative positions were generated. The predicted tetrameric peptides (Table S2) were selected and docked again with SBP.

In parallel, another mode of designing was used by identifying signature peptides from literature which bind HtrA2 [19]. Initially two peptides were chosen (GQYYFV and GGIRRV) and based on the sequence similarity and hydrophobicity, stretches of putative binding residues from two known binding partners of HtrA2 were identified (GPFPIIV from C-terminal region of β-casein and GSAWFSF, an internal motif of antiapoptotic Pea-15) [37]. A putative HtrA2 binding pattern was designed based on phage display library [21] which along with the earlier four sequences was used to generate all possible peptide combinations. Considering structural complementarity and three dimensional arrangements of amino acids at SBP, Gly and Val residues were added at N- and C-termini of some peptides to increase the stability of the docked complex. A 10 mer peptide having the sequence KNNPNNAHQN that does not match the consensus SBP binding peptide pattern was used as a negative control. These combinations were used for searching all possible sequences of known and potential HtrA2 binding partners [38].

All designed peptides were built *in silico* using BREED (Schrödinger, LLC, New York, 2011) and Combine Fragments tools which were then prepared for docking using LigPrep 2.5 (Schrödinger, LLC, New York, 2011). After ligand preparation, Confgen 2.3 (Schrödinger, LLC, New York, 2011) was used to generate all possible energetically minimum conformers of the designed peptides which were then docked using Glide [39,40].

In the modeled HtrA2 structure, energy minimization was done using Protein Preparation Wizard 2.2 (Epik Version 2.2, Schrödinger, LLC, New York, 2011) after addition of H-atoms. Molecular Docking was initiated by preparing Grid file (input file) which contains receptor (protein structure) and binding site information (Prime output). All three precision methods which include high throughput virtual screening (HTVS), standard precision (SP) and extra precision (XP) [35] of Glide [39,40] were used for docking these peptides on SBP. This series of docking methods were used to filter out energetically less favorable peptide conformers and get a subset of best possible peptides for further studies.

MD Simulation (MDS) and Analysis

After analyzing the docking results, best HtrA2-peptide complexes based on Glide XP score and E-model value were used for Molecular Dynamic Simulation which was performed using Desmond 2010 [22] software package. Optimized Potentials for Liquid Simulations (OPLS) [41] all-atom force field was used to analyze model stability. The protein structures were solvated with Monte Carlo simulated TIP3P [42] water model with a 10 Å buffer space from the protein edges in an orthorhombic box and the system was then neutralized by replacing water molecules with sodium and chloride counter ions. Similarly, unbound HtrA2 system was also developed as a control. Neutralization of systems was done by adding 2 Na^+ ions in unbound HtrA2 and 4 Na^+ ions for peptide bound complexes. The particle-mesh Ewald method (PME) [43] was used to calculate long-range electrostatic interactions with a grid spacing of 0.8 Å. Van der Waals and

short range electrostatic interactions were smoothly truncated at 9.0 Å. Nose–Hoover thermostats were utilized to maintain the constant simulation temperature and the Martina–Tobias–Klein method was used to control the pressure [44]. The equations of motion were integrated using the multistep RESPA integrator [45] with an inner time step of 2.0 fs for bonded interactions and non-bonded interactions within the short range cut-off. An outer time step of 6.0 fs was used for non-bonded interactions beyond the cut-off. These periodic boundary conditions were applied throughout the system.

These prepared systems were equilibrated with the default Desmond protocol that comprises a series of restrained minimizations and MDS. Two rounds of steepest descent minimization were performed with a maximum of 2000 steps and a harmonic restraint of 50 kcal/mol/per $Å^2$ on all solute atoms followed by a series of four MDS. The first simulation was run for 12 ps at a temperature of 10 K in the NVT (constant number of particles, volume, and temperature) ensemble with solute heavy atoms restrained with force constant of 50 kcal/mol/$Å^2$. The second simulation was similar to the first except it was run in the NPT (constant number of particles, pressure, and temperature) ensemble. A 24 ps simulation followed with the temperature raised to 300 K in the NPT ensemble and with the force constant retained. The last one was a 24 ps simulation at 300 K in the NPT ensemble with all restraints removed. This default equilibration was followed by a 5000 ps NPT simulation to equilibrate the system. A 30 ns NPT production simulation was then run and coordinates were saved in every 2 ps of time intervals.

The total trajectory of MD simulation was 30 ns. MD Simulation was analyzed using the analytical tools in the Desmond package. In MD quality analysis, potential energy of the protein as well as total energy of the entire system was calculated. The lowest potential energy conformations were then used for comparative analysis of peptide bound and unbound structures. Trajectories of peptide bound complexes and unbound HtrA2 were then compared based on their overall calculated RMSD (root mean square deviation), domain wise RMSD and RMSF (root mean square fluctuation) values and were plotted using GraphPad Prism 5.0 (GraphPad Software, San Diego, CA, USA).

Production of Recombinant HtrA2 Wild Type, its Mutants and Domains

Mature (Δ133 HtrA2) with C-terminal his6-tag in pET-20b (Addgene, Cambridge, MA) was expressed in *E. coli* strain BL21 (DE3) pLysS. N-SPD, comprising N-terminal and serine protease domains (residues 1–210) of HtrA2 was sub cloned into pMALc5E-TEV using appropriate primers. Point mutations were introduced into pET-20b Δ133 HtrA2 by PCR using primer sets that included mutations for residues N216A, S219A, E292A, E296A and F16D. N-SPD clone and these mutants were confirmed by DNA sequencing. Protein expression was induced by culturing cells at 18°C for 20 h in presence of 0.2 mM isopropyl-1-thio-D-galactopyranoside. Cells were lysed by sonication and the centrifuged supernatants for HtrA2 and its mutants were incubated with pre-equilibrated nickel-IDA beads for 1 h at room temperature. Protein purification was done using Ni-affinity chromatography as described earlier [19]. Eluted protein was further purified using gel permeation chromatography. N-SPD was purified using amylose resin where the bound protein was eluted using 10 mM maltose and was subjected to TEV protease cleavage [46] to remove maltose binding protein (MBP). N-SPD was further separated from MBP by gel filtration using Superdex 75 column. All purified proteins were analyzed by SDS-PAGE for

purity. The fractions with >95% purity were stored in aliquots at −80°C until use.

FITC-β-Casein Cleavage Assay

The proteolytic activity of wild type and the mutants were determined using FITC-labelled β-casein cleavage assay [47]. Fluorescent substrate cleavage was determined by incubating 200 nM of enzymes with increasing concentration (0–25 μM) of β-casein at 37°C in cleavage buffer (20 mM Na_2HPO_4/NaH_2PO_4, pH 8.0, 100 mM NaCl, 0.1 mM DTT). Fluorescence was monitored in a multi-well plate reader (Berthold Technologies) using excitation wavelength of 485 nm and emission at 545 nm. Reaction rates v_0 (μM/min) were determined by linear regression analysis corresponding to the maximum reaction rates for individual assay condition. Assays are representative of at least three independent experiments done in triplicate. The steady-state kinetic parameters were obtained from the reaction rates by fitting data to Michaelis-Menten equation using nonlinear least squares subroutine in KaleidaGraph program (Synergy software).

Supporting Information

Figure S1 Interaction of peptides with HtrA2. a. Ligplot for GSAWFSF with HtrA2 which represents residues involved and the nature of interactions. b. Ligplot for GQYYFV interaction pattern with HtrA2. c. Ligplot for GPFPIIV with HtrA2 which represents residues involved and the nature of interactions. d. Ligplot for SEHRRHFPNCFFV peptide with HtrA2 which represents residues involved and the nature of interactions. The residues of peptides and HtrA2 involved in interaction are shown in blue and red respectively.
(TIF)

Figure S2 Comparison of SBP and allosteric pocket of GRIP-1 protein. Structural overlay of the protein GRIP-1(green) bearing PDB ID 1M5Z and GQYYFV bound HtrA2 (pink) shows striking resemblance of the orientation of buried GLGF motif shown in yellow and blue respectively. The α helix denoted as αB (green) for GRIP-1, known to be involved in formation of allosteric pocket overlays very well with the one involved in SBP formation (orange) in GQYYFV (red sticks) - HtrA2 complex.
(TIF)

Figure S3 ITC studies for activating peptide with HtrA2 and the SBP double mutant. The peptide used was 13mer SEHRRHFPNCFFV, which has similar consensus sequence as

defined for PDZ peptide groove binding substrate. The peptide was better in terms of solubility as compared to other activating peptides and binding studies were done using Isothermal titration calorimetry. The titrations were carried out using Micro Cal ITC200 (GE Healthcare) with the calorimetry cell containing 200 μl of wild type or N216A/S219A mutant HtrA2 in 20 mM Na_2HPO_4/NaH_2PO_4 buffer, 100 mM NaCl, pH 7.8. The concentration of protein was in range from 20 to 50 μM and was titrated with 1.5 μl injections of a solution containing 0.4 mM activator peptide reconstituted in the same buffer. To correct the effect of heat of dilution, a blank injection was made under identical conditions. All experiments were performed at 25°C and the data was analyzed using the manufacture provided MicroCal software with the integrated heat peaks fitted to a one site-binding model. Simulated ITC raw data for the protein with the activating peptide is represented in the upper panel and the integrated data in the lower panel. The dissociation constant was calculated to be 7.5 μM for wild type (left panel) and no significant heat change was observed for the SBP double mutant (right panel).
(TIF)

Table S1 Docking analysis of replica fragments with HtrA2. The fragments have been arranged according to their docking scores.
(DOC)

Table S2 Designed peptide fragments. Fragments of peptide combinations generated based on functional group studies have been enlisted.
(DOC)

Movie S1 Orientation of active site triad and oxyanion hole formation during MD simulation of HtrA2-peptide complex. From this visual representation of HtrA2 peptide (GSAWFSF) complex during MD simulation it can be seen that the catalytic triad residues H65, D95, S173 reorient to form an active conformation along with oxyanion hole residues (N172, G171 and F170). All the residues involved are represented as sticks. This movie shows proper active site and oxyanion hole formation.
(AVI)

Author Contributions

Conceived and designed the experiments: KB. Performed the experiments: PRB RRK NG NS LKC. Analyzed the data: KB PRB RRK GMS. Wrote the paper: KB PRB RRK.

References

1. Ma B, Tsai C, Haliloglu T, Nussinov R (2011) Dynamic Allostery: Linkers Are Not Merely Flexible. Structure 19: 907–917.

2. Jeleń F, Oleksy A, Śmietana K, Otlewski J (2003) PDZ domains common players in the cell signaling. Acta Biochim Pol 50: 985–1017.

3. Hung A, Morgan S (2002) PDZ Domains: Structural Modules for Protein Complex Assembly. J Biol Chem 277: 5699–5702.

4. Li W, Srinivasula S, Chai J, Li P, Wu J, et al. (2002) Structural insights into the pro-apoptotic function of mitochondrial serine protease HtrA2/Omi. Nat Struct Biol 9: 436–441.

5. Suzuki Y, Takahashi-Niki K, Akagi T, Hashikawa T, Takahashi R (2004) Mitochondrial protease Omi/HtrA2 enhances caspase activation through multiple pathways. Cell Death Differ 11: 208–216.

6. Martins L, Iaccarino I, Tenev T, Gschmeissner S, Totty N, et al. (2002) The serine protease Omi/HtrA2 regulates apoptosis by binding XIAP through a reaper-like motif. J Biol Chem 277: 439–444.

7. Verhagen A, Silke J, Ekert P, Pakusch M, Kaufmann H, et al. (2002) HtrA2 promotes cell death through its serine protease activity and its ability to antagonize inhibitor of apoptosis proteins. J Biol Chem 277: 445–454.

8. Kooistraa J, Milojevicb J, Melacinia G, Ortegaa J (2009) A new function of human HtrA2 as an amyloid-beta oligomerization inhibitor. J Alzheimers Dis 17: 281–294.

9. Johnson F, Kaplitt M (2009) Novel mitochondrial substrates of omi indicate a new regulatory role in neurodegenerative disorders. PLoS One 4: e7100.

10. Lin C, Chen M, Chen G, Tai C, Wu R (2011) Novel variant Pro143Ala in HTRA2 contributes to Parkinson's disease by inducing hyperphosphorylation of HTRA2 protein in mitochondria. Hum Genet 130: 817–827.

11. Nam M, Seong Y, Park H, Choi J, Kang S, et al. (2006) The homotrimeric structure of HtrA2 is indispensable for executing its serine protease activity. Exp Mol Med 38: 36–43.

12. Singh N, Kuppili R, Bose K (2011) The structural basis of mode of activation and functional diversity: A case study with HtrA family of serine protease. Arch Biochem Biophys 516: 85–96.

13. Sohn J, Grant RA, Sauer RT (2010) Allostery is an intrinsic property of the protease domain of DegS: implications for enzyme function and evolution. J Biol Chem 285: 34039–34047.

14. Merdanovic M, Mamant N, Meltzer M, Poepsel S, Auckenthaler A, et al. (2010) Determinants of structural and functional plasticity of a widely conserved protease chaperone complex. Nat Struct Mol Biol 17: 837–843.

15. Beuming T, Farid R, Sherman W (2009) High-energy water sites determine peptide binding affinity and specificity of PDZ domains. Protein Sci 18: 1609–1619.

16. Sherman W, Day T, Jacobson M, Friesner R, Farid R (2006) Novel procedure for modeling ligand/receptor induced fit effects. J Med Chem 49: 534–553.
17. Van Der Spoel D, Lindahl E, Hess B, Groenhof G, Mark A, et al. (2005) GROMACS: fast, flexible, and free. J Comput Chem 26: 1701–1718.
18. Halgren T (2007) New method for fast and accurate binding-site identification and analysis. 69: 146–148.
19. Martins L, Turk B, Cowling V, Borg A, Jarrell E, et al. (2003) Binding specificity and regulation of the serine protease and PDZ domains of HtrA2/Omi. J Biol Chem 278: 49417–49427.
20. Ma S, Song E, Gao S, Tian R, Gao Y (2007) Rapid characterization of the binding property of HtrA2/Omi PDZ domain by validation screening of PDZ ligand library. Sci China C Life Sci 50: 412–422.
21. Zhang Y, Appleton B, Wu P, Wiesmann C, Sidhu S (2007) Structural and functional analysis of the ligand specificity of the HtrA2/Omi PDZ domain. Protein Sci 16: 2454–2471.
22. Bowers K, Chow E, Xu H, Ron O, Eastwood M, et al. (2006) Scalable Algorithms for Molecular Dynamics Simulations on Commodity Clusters; Florida.
23. Savopoulos J, Carter P, Turconi S, Pettman G, Karran E, et al. (2000) Expression, Purification, and Functional Analysis of the Human Serine Protease HtrA2. Protein Expr Purif 19: 227–234.
24. Ibrahim A, Mansour I, Wilson M, Mokhtar D, Helal A, et al. (2012) Study of survivin and X-linked inhibitor of apoptosis protein (XIAP) genes in acute myeloid leukemia (AML). Lab Hematol 18: 1–10.
25. Nagata M, Nakayama H, Tanaka T, Yoshida R, Yoshitake Y, et al. (2011) Overexpression of cIAP2 contributes to 5-FU resistance and a poor prognosis in oral squamous cell carcinoma. Br J Cancer 105: 1322–1330.
26. Navakanit R, Graidist P, Leeanansaksiri W, Dechsukum C (2007) Growth inhibition of breast cancer cell line MCF-7 by siRNA silencing of Wilms tumor 1 gene. J Med Assoc Thai 90: 2416–2421.
27. Sugiyama H (1998) Wilms tumor gene (WT1) as a new marker for the detection of minimal residual disease in leukemia. Leuk Lymphoma 30: 55–61.
28. Kraut J (1977) Serine proteases: structure and mechanism of catalysis. Annu Rev Biochem 46: 331–358.
29. Mazat J, Patte J (1976) Lysine-sensitive aspartokinase of Escherichia coli K12. Synergy and autosynergy in an allosteric V system. Biochemistry 15: 4053–4058.
30. Sohn J, Sauer R (2009) OMP peptides modulate the activity of DegS protease by differential binding to active and inactive conformations. Mol Cell 33: 64–74.
31. Feng W, Fan J, Jiang M, Shi Y, Zhang M (2002) PDZ7 of glutamate receptor interacting protein binds to its target via a novel hydrophobic surface area. J Biol Chem 277: 41140–41146.
32. Christopoulos A, May LT, Avlani VA, Sexton PM (2004) G protein-coupled receptor allosterism: the promise and the problem(s). Biochem Soc Trans 32: 873–877.
33. May L, Leach K, Sexton P, Christopoulos A (2007) Allosteric modulation of G protein-coupled receptors. Annu Rev Pharmacol Toxicol 47: 1–51.
34. Berman H, Westbrook J, Feng Z, Gilliland G, Bhat T, et al. (2000) The Protein Data Bank. Nucleic Acids Res 28: 235–242.
35. Friesner R, Murphy R, Repasky M, Frye L, Greenwood J, et al. (2006) Extra precision glide: docking and scoring incorporating a model of hydrophobic enclosure for protein-ligand complexes. J Med Chem 49: 6177–6196.
36. Zeng J, Treutlein H (1999) A method for computational combinatorial peptide design of inhibitors of Ras protein. Protein Eng 12: 457–468.
37. Trencia A, Fiory F, Maitan M, Vito P, Barbagallo A, et al. (2004) Omi/HtrA2 promotes cell death by binding and degrading the anti-apoptotic protein ped/pea-15. J Biol Chem 279: 46566–46572.
38. Ma S, Song E, Gao S, Tian R, Gao Y (2007) Rapid characterization of the binding property of HtrA2/Omi PDZ domain by validation screening of PDZ ligand library. Sci China C Life Sci 50: 412–422.
39. Halgren T, Murphy R, Friesner R, Beard H, Frye L, et al. (2004) Glide: a new approach for rapid, accurate docking and scoring. 2. Enrichment factors in database screening. J Med Chem 47: 1750–1759.
40. Friesner R, Banks J, Murphy R, Halgren T, Klicic J, et al. (2004) Glide: a new approach for rapid, accurate docking and scoring. 1. Method and assessment of docking accuracy. J Med Chem 47: 1739–1749.
41. Jorgensen W, Maxwell D, Tirado-Rives J (1996) Development and Testing of the OPLS All-Atom Force Field on Conformational Energetics and Properties of Organic Liquids. J Am Chem Soc 118 11225–11236.
42. Jorgensen W, Chandrasekhar J, Madura J, Impey R, Klein M (1983) Comparison of simple potential functions for simulating liquid water. J Chem Phys 79: 926–935.
43. Darden T, York D, Pedersen L (1993) Particle mesh Ewald: An N-log(N) method for Ewald sums in large systems J Chem Phys 98: 10089–10093.
44. Martyna G, Tobias D, Klein M (1994) Constant pressure molecular dynamics algorithms. J Chem Phys 101: 4177–4189.
45. Humphreys D, Friesner R, Berne B (1994) A Multiple-Time-Step Molecular Dynamics Algorithm for Macromolecules. J Phys Chem 98 6885–6892.
46. Nallamsetty S, Kapust R, Tözsér J, Cherry S, Tropea J, et al. (2004) Efficient site-specific processing of fusion proteins by tobacco vein mottling virus protease in vivo and in vitro. Protein Expr Purif 38: 108–115.
47. Twining S (1984) Fluorescein isothiocyanate-labeled casein assay for proteolytic enzymes. Anal Biochem 143: 30–34.